ProQuest LLC.
789 East Eisenhower Parkway
P.O. Box 1346
Ann Arbor, MI 48106 – 1346

Understanding Molecular Interactions in the Precipitation and Dissolution of Silica and Silicates under Ambient Conditions

GRAHAM EDWARD TILBUREY

A thesis submitted in partial fulfilment of the
requirements of Nottingham Trent University
for the Degree of Doctor of Philosophy

June 2007

Acknowledgements

I would like to acknowledge and thank my supervisor Professor Carole Perry for giving me the opportunity to undertake a PhD in her laboratory and for her support, encouragement and for the scientific freedom she has given me during this project. This has enabled me to produce a PhD that truly reflects my interest in the field of (bio)silicification, silica formation *in vitro* and materials science.

Special thanks are due to Dr Siddharth Patwardhan (Sid) who has been a mentor and close friend throughout my PhD and inspired me in times of need, and to Dr Dave Belton (Mr B) who I have discussed many good and bad ideas with and for providing unconditional help whenever it was needed.

Thanks also to the entire Biomolecular and Materials Interface Group who have provided an exceptional working and social environment. Thanks in particular are due to my close friends, Claudius Kischka, Tamar Saison, Maria Pietat Casado and Michael Hörenz who have encouraged, supported and inspired me during the PhD and writing of this thesis.

I would like to thank my loving family who have always been there in times of joy and despair, without whom this thesis would not have been possible.

Finally, I would like to acknowledge Air Force office of Scientific Research for funding.

Abstract

The bio-geo-chemical silicon cycle provided the inspiration for investigations to be carried out into the formation and dissolution of silica. This thesis is concerned with understanding the molecular interactions occurring between silicon species and small organic molecules with emphasis on the dissolution and formation of silica *in vitro*. Three model systems have been employed to investigate molecular interactions occurring during silica formation; two supersaturated orthosilicic acid containing solutions generated from dipotassium tris(1,2-benzenediolato-*O,O*)silicate (KSiCat), an unbuffered tetramethoxysilane (TMOS) system and globally undersaturated silicon systems. The later two were developed in this thesis. These model systems enabled use to investigate the molecular interactions between bioinspired additives and different silicon species. Bioinspired polyelectrolytes and small organic molecules were investigated and shown to interact in a completely differently manner with similar silicon species.

The role of hydroxyl groups in silica formation was investigated using alkanediols. It has been hypothesised in the literature that Si-O-C bonds may template silica formation *in vivo*. Investigation into the interactions between hydroxyl functionalised molecules and supersaturated solutions of orthosilicic acid. No evidence was found for the formation of Si-O-C bonds and it was found that hydrogen bonding does not have a significant effect on the formation of silica.

Finally, an investigation was carried out into the effect of azamacrocyclic molecules in silica formation. Two supersaturated silica forming systems which utilised; KSiCat and TMOS were used. Inorganic-organic hybrid needle-like tetragonal prisms were formed when KSiCat was used which was shown to be a displacement reaction of the potassium ions by cyclam to form a 1:1 cyclam:SiCat layer like structure. In the unbuffered TMOS system azamacrocyclic molecules with ≥14 atoms were found to have a significant effect on the kinetics of silica formation. Through the control of pH, mono-dispersed solutions of silica spheres of different sizes could be stabilised through a charge neutralisation mechanism.

Table of Contents

Chapter 2 – Experimental Methods

Part I: Instrumentation and operating procedure.

Part II: A comparative study between dipotassium tris(1,2-benzenediolate-*O,O'*)silicate and tetramethoxysilane and the effect of counter ions on the formation of silica.

Chapter 3 - The Role of Organic Molecules in the Stability of Silicon Species in an Undersaturated System: *Implications for biological and bioinspired silicification.*

Chapter 4 - Are hydroxyl containing biomolecules important in (bio)silicification? A model study.

Chapter 5 – Using Azamacrocyclic Molecules to Control the Formation of Silica.

Part I: The Formation of Inorganic-Organic Hybrid Needle-like Tetragonal Prism.

Chapter 6 – Conclusions and Further work.

List of Figures

Chapter 1

Chapter 2

Chapter 3

Chapter 4

Chapter 5

List of Tables

Table

List of Abbreviations

SDV	Silica deposition vesicle
HEP's	Hydrogen flouride extractable proteins
ORF	Open read frame
TEOS	Tetraethylorthosilicate
PAMAM	Polyamidoamine dendrimers
PPI	Polypropylenimine
PLL	Poly(L-lysine)
PAH	Poly(allylamine hydrochloride)
PEI	Polyethyleneimine
TMOS	Tetramethoxyorthsilicate
TSPP	tetrakis(4-sulfonylphenyl)porphyrin
TEOG	tetraethoxygermane
ICP	Inductively coupled plasma spectroscopy
ppm	part per million
METOL	4-methylaminophenol
FTIR	Fourier Transform Infrared spectroscopy
KBr	Potassium bromide
PCS	Photon correlation spectroscopy
DLS	Dynamic light scattering
TGA	Thermal Gravimetric Analysis
SEM	Scanning Electron Microscopy
TEM	Transmission Electron Microscopy
KSiCat	Dipotassium tris(1,2-benzenediolato-*O,O'*)silicate
DSS	2,2-Dimethyk-2-silapentane-5-sulfonic acid
dd water	Deionised and distilled water
k_{3rd}	Third order rate constant
k_{+}	First order forward rate constant
k_{-}	First order reverse rate constant
LCPA	Long chain polyamines

DAE	Diaminoethane
DETA	Diethylenetriamine
TETA	Triethylenetetramine
TEPA	Tetraethylenepentamine
PEHA	Pentaethylenehexamine
N3	Dipropylenetriamine
N5	Tetrapropylenepentamine
1,10 DA	Diaminodecane
LCMS	Liquid Chromatography Mass Spectroscopy
1,2 Diol	1,2-ethanediol
1,3 Diol	1,3-propanediol
1,4 Diol	1,4-butnaediol
1,5 Diol	1,5-pentanediol
1,6 Diol	1,6-hexanediol
1,7 Diol	1,7-heptanediol
ATR-FTIR	Attenuated Total Reflection Fourier Transform Infrared Spectroscopy
EDS	Energy Dispersive Spectroscopy
3NC	1,4,7-triazacyclononane
4N2	1,4,7,10-tetraazacyclododecane
Cyclam	1,4,8,11-tetraazacyclotetradecane
2MC	1,8 dimethyl 1,4,8,11-tetraazacyclodecane
4MC	1,4,8,11 tetramethyl 1,4,8,11-tetraazacyclodecane
6NC	1,8 dimethyl 1,4,8,11-tetraazacyclodecane
12C4	12-crown-4
18C6	18-crown-6
KGeCat	Dipotassium tris(1,2-benzenediolato-*O,O'*)germanate
4MEDAE	*N,N,N',N'*-tetramethylethylenediamine
4MEDAB	*N,N,N',N'*-tetramethyl-1,4-butanediamine
4MEDAH	*N,N,N',N'*-tetramethyl-1,6-hexanediamine

Chapter 1 – Literature Survey: The Fundamentals of Silicon Chemistry, (Bio)silicification, Bioinspired and Biomimetic Routes to Controlling Silica Formation.

1. General Introduction

Silicon is the second most abundant element in the Earth's crust,[1] it is not found naturally in its elemental form, but usually occurs in combination with oxygen to form silica and other elements to form silicates. In its pure oxide form silica occurs naturally in three different crystalline forms, namely; quartz, tridymite and cristobalite.[1] Silicates account for an estimated 90 % of the Earth's minerals including rocks and melts,[2] where it occurs in combination with a number of other elements including potassium and aluminium to form orthoclase feldspar, with iron and magnesium to form olivine and pyroxenes and with calcium and magnesium to form hornblende. Silica occurs as a major component of the Earth's crust as well as in the Earth's aqueous reservoirs in its monomeric form called mono or orthosilicic acid.[1] The dissolution of silica into aqueous solution involves a chemical reaction in an excess of water, known as hydrolysis. In contrast to the dissolution reaction the formation of silica can be considered as a dehydration reaction or sometimes termed as a condensation reaction.[1]

$$2SiO_x + 2H_2O \rightarrow (SiO_2)_{x-1} + Si(OH)_4 \qquad (1.1)$$

Equation 1.1 is catalyzed by OH^- ions and as such, silica is highly soluble in alkaline conditions. The solubility of silica in an aqueous solution depends primarily on the form of the bulk silica. For massive amorphous silica the equilibrium concentration of $Si(OH)_4$ at 25 °C is *ca.* 70 ppm as SiO_2.[1] When considering the solubility of amorphous hydrated silica, which usually consists of nano particles or porous aggregates as well as

surface Si-OH groups, the solubility is significantly different. The presence of the OH group aids the solubility of the silica, with most powders and gels having a solubility of 100-130 ppm.[1] The solubility of crystalline silica such as quartz is comparatively low at *ca.* 6 ppm (SiO_2) due to its highly unreactive surface.[1] The occurrence of silicates throughout the natural environment and their solubility in water accounts for the ubiquitous occurrence of orthosilicic acid in fresh and salty water. The source of silica and ultimately silicic acid in aquatic systems comes from the weathering of minerals and through suspended clays and not through the dissolution of quartz, commonly known as "sand" which is only soluble to a few ppm.[3] Silicic acid is present in river waters at 5 to 35 ppm (SiO_2) and upon entry into the sea at between 5 to 15 ppm.[1] The oceans and seas of the Earth vary greatly in the concentration of silicic acid from 2-14 ppm where the presence of multivalent metal ions such as iron, aluminum and magnesium have been shown to limit the solubility of amorphous silica to less than 10 ppm.[1] The availability of dissolved silicates can have a dramatic affect on the structure, health and productivity of a terrestrial ecosystem. For some organisms such as diatoms and radiolarian, silicon in the form of silicic acid is essential.[4, 5] These organisms utilize the soluble form of silica found in aqueous environments to accumulate and deposit intricate nano-patterned hydrated amorphous silica through a genetically controlled process called biosilicification. This process is summarized in Equation 1.2.

$$Si(OH)_4 + Si(OH)_4 \rightarrow Si(OH)_3OSi(OH)_3 + H_2O \qquad (1.2)$$

Other silicic acid molecules may react with any one of the hydroxyl groups on the new dimeric species in a similar fashion. If condensation were able to go to completion a generic SiO_2 polymer would be formed. The organisms use biosilica as a structural component in their cell walls. The amount of biosilica produced from monosilicic acid by plankton and other single celled organisms such as diatoms is estimated to be around 6.7 Gtons per annum which represents 0.16 % of the available silica.[6] The oceans are assumed to consist of two internally homogeneous reservoirs of silica, the first is monosilicic acid, and the second is the biosiliceous sediment, that is created through the death of diatoms and other silica accumulating organisms which escapes dissolution.

The overall concepts of this thesis can be related to the silicon cycle shown in Figure 1.1, where each part of the diagram has been studied to some degree to give an insight into developing new materials or understanding. The overall aim is to control the properties of silica materials so tailor made silicas can be made for a specific application.

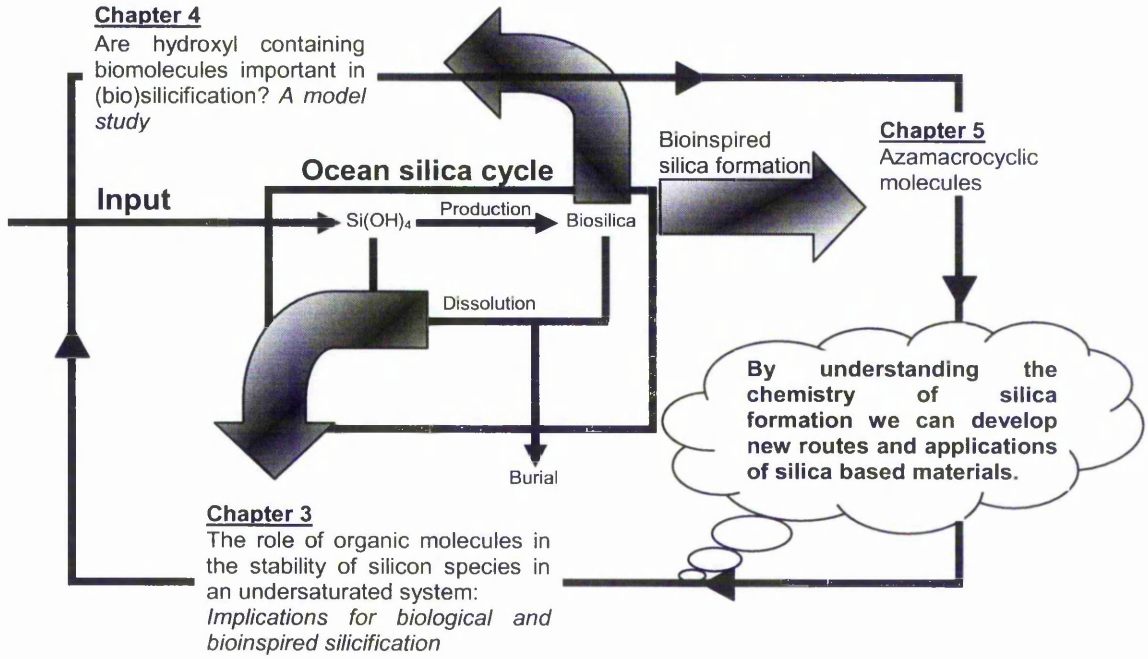

Figure 1.1 – The schematic diagram representing the ocean silica cycle and relationship between that and this thesis.

Having established the concepts that will be dealt with in this thesis, the fundamentals of silicon chemistry will now be examined as well as the approaches we and other research groups are employing to understand and control the formation of silica.

1.1. The fundamentals of silicon chemistry and the formation of silica.

Silicon is found in group four of the periodic table and shares many of the characteristics of carbon. The outer shell electronic configuration is $3s^2\ 3p^2$ and as such silicon requires four further electrons to reach the stable noble gas configuration of argon. The four valence electrons are most commonly supplied by oxygen in a tetrahedral geometry which forms the majority of silicate materials and minerals. The occurrence of

hypervalent five and six coordinate silicon in nature is rare.[7] In silicate minerals penta coordinated silicon is unknown and hexa coordinated centres only occur in high pressure phases e.g. stishovite.[7] In the laboratory, silicon coordinated by five oxygen containing ligands was completely unknown until recently when penta and hexa coordinated species were reported in solutions of ethylene glycol in the presence of alkali-metal base[8] and more recently using aliphatic polyhydroxy alcohols[7] and aliphatic acid carbohydrates[9] in aqueous solutions. In a computational study by Sahai *et al* it was proposed that these species are not favoured in aqueous solutions.[10] However, silicon has been known to occur in a hexaoxo-centre for sometime in which the silicon centre is chelated by catechol forming tris(1,2-benzenediolato-*O,O'*)silicate as well as other related compounds.[7]

The simplest soluble form of silica is orthosilicic acid, it is essentially four hydroxyl groups tetrahedrally coordinated to a central silicon atom; $Si(OH)_4$ (N.B. this has never been isolated). Silicic acid has a pK_a of 9.8 and is stable in water up to concentrations of *ca.* 100 ppm.[1] Above the solubility of the amorphous phase 100-200 ppm, silicic acid spontaneous undergoes autopolymerization reactions to form silica. This process has been reported by many authors and can be characterized by three distinct process;[1, 11]

- Polymerization of monomers to form stable nuclei of a critical size (typically 1-2 nm),
- Growth of nuclei to form particles,
- Aggregation of particles to from particles, branched networks or structural motifs.

Silicic acid condenses to form silica typically by two mechanisms (Equations 1.3 and 1.4) which occur simultaneously in a supersaturated solution of silicic acid. The first mechanism involves the condensation of two silicic acid molecules with the release of water. In this process no charged species are generated from the condensation and hence no net pH change of the solution is observed. The second mechanism involves an ionised and a unionised silicic acid molecule in a bimolecular collision (Equation 1.4).

$$Si(OH)_4 + Si(OH)_4 \rightleftharpoons (HO)_3Si{-}O{-}Si(OH)_3 + H_2O \qquad (1.3)$$

$$Si(OH)_4 + Si(OH)_3O^- \rightleftharpoons (HO)_3Si{-}O{-}Si(OH)_3 + OH^- \quad (1.4)$$

The negatively charged oxygen atom attacks the electropositive silicon centre (nucleophilic attack; favored of the two mechanisms) generating an unstable five coordinate species, which decomposes to yield a hydroxyl ion. The hydroxide ion quickly extracts a proton from a silicic acid molecule resulting in no net change in pH and a charged silicate species is generated for further reaction *via* this mechanism. The continued growth of oligomers results in the pK_a of the silanol group decreasing (*ca.* 9.8 to *ca.* 6.8), thus generating more ionised species for reaction *via* this mechanism.

Silicic acid condenses first to dimers, further reactions produce trimers and subsequent reactions generate cyclic oligomers containing between 3 and 6 silicon atoms linked with siloxane bonds.[12] The cyclic species continue to grow through preferential reaction with orthosilicic acid creating larger cyclic species with internal condensation minimizing the size of the molecule and hydroxyl groups at the external surfaces, maximizing the solubility. These larger cyclic structures are in fact the species that form the basis of the larger particles that form later *via* further condensation polymerization reactions. Ostwald ripening also occurs where smaller more soluble particles dissolve and release silicic acid that re-deposits onto the larger particles.[1] The progressive increase in the size of the particles results in a decrease in the pK_a for the removal of a proton from a silanol group, thus particles with a diameter of 1 nm will be negatively charged at circumneutral pH. In the absence of salts these particles will continue to grow in an isolated way forming a sol. The presence of salts results in surface charge neutralization and allows aggregation to occur resulting in the growth of a network of silica spheres and gelation. Figure 1.1.1 from Iler describes the formation of silica under different conditions and the structure of the silica produced under these conditions.[1]

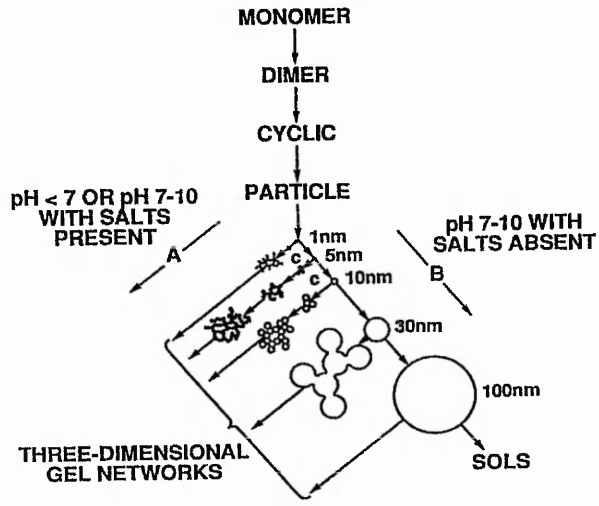

Figure 1.1.1 – Summary of the condensation polymerization reaction leading to the formation of different silica species depending on the conditions condensation occurs in.

The process of aggregation and gelation in a silica system is unique because the solid phase remains completely amorphous and appreciably soluble in water as it is in dynamic equilibrium with orthosilicic acid. The conversion of a sol to a gel occurs through the aggregation of particles and cannot be seen as the density and refractive index of the forming gel are the same as the sol. Hence, only small increases in viscosity can be detected up to the gel point where the viscosity increases rapidly and the gel becomes solid.[1]

1.2. The applications of silica

The global specialty silicas industry was estimated to be worth around two billion dollars in 2000, where relatively simple processing, dramatically increases its value from $20 per ton in the form of sand, to thousands of dollars per ton as fumed silica with comparatively little processing costs.[13] Industrial silicas are produced in a variety of different ways, from the continuous high temperature hydrolysis of silicon tetrachloride ($SiCl_4$) in a hydrogen oxygen flame to form fumed silica, to the precipitation of silica from sodium silicate solutions which have been neutralized with sulfuric acid to form a slurry of precipitated silica and a solution of sodium sulfate.[13] Silica can also be produced *via* non aqueous routes such as the low temperature sol-gel process.[14, 15] Silica is used in a large

diversity of industrial applications. Fumed silicas are used in a wide range of applications such as adhesives, sealants, coatings, greases, cosmetics and personal health care products.[16] Many of the applications make use of silica's ability to provide thixotropy to rubbers, polymers and composite systems. Silica is used to aid suspension in aerosols and nail vanishes and furthermore it can also be used to control the rheology and viscosity of products such as lipsticks, creams and in toothpaste where is also serves as an abrasive to provide optimal cleaning properties.[13] Silicone rubbers can also be reinforced with fumed silica to provide improved mechanical properties.[13] Precipitated silicas are used to reinforce tyres where adding silica significantly extends the life time of a tyre, which in these energy conscious times is invaluable. To mention just a few more applications; silica can be found in paints as a flattening agent, silica gels can be used as desiccants and also in more highly specialized applications such as catalyst supports and in chromatography where high surface areas and excellent particle size control and porosity characteristics can be utilized to separate compounds or can be functionalized to provide an excellent stationary phase support.[13] Whatever the eventual use of silica, it is its structure that determines its properties and this can be controlled and tuned to a particular application by controlling the formation of silica from an atomic length scale right through to the size of the final structure.[12] The key to providing the level of control required to produce tailor made materials for a specific application is through understanding the molecular interactions that occur during silica formation and then using another species to influence or direct the reaction towards a desired structure. An emerging application of silica is in the health food market. It has long been known that silica and in particular the bio-available form of silica, silicic acid, has a role to play in biological organisms, however in humans there is no proven link between the presence of silicon in the body and any improvement in human health. What is known is that exclusion of silicon from the diet of some animals proves detrimental to their health, for example in 1972 Schwarz *et al.* published the effect on rats[17] and almost simultaneously Carlisle *et al.* published an effect on chicks where collagenous connectivity tissue was found to be defective and bone structure also was effected.[18] Since that time a number of silicon dietary supplements have been developed for human consumption and although no proven link has been established there is a significant demand for such a product.[19]

1.3. The presence of silica in biological organisms

As mentioned previously the soluble form of silica; silicic acid is ubiquitously present in the Earths aquatic reservoirs.[1, 3] A number of specialized species have developed mechanisms for the selective uptake of silicic acid from the environment around them and are able to transport, control the formation and deposit of silica in a controlled manner. Biological organisms such as diatoms, sponges and higher plants have all developed mechanisms to incorporate and utilize the properties of silica within their structures in a process known as biomineralisation of which biosilicification is specific for silica accumulating organisms.[20] The structure of the deposited silica has attracted much interest in the scientific community as the species specific structures exhibited by diatoms in particular are excellent examples of intricate nano-patterned silica. Furthermore the silica produced by biological organisms is formed under benign condition, where temperatures rarely exceed 25 °C with ambient pressures. In times where technological improvement is being balanced against environmental impact these nano-patterned materials are also produced in an aqueous environment. Scientists have investigated biological organisms with a view to understanding how nano-patterned silica can be produced so that natures technology can be utilised to produce silica which surpasses the structures currently available by conventional industrial techniques. The controlled formation of silica will allow the development of new technologies which exploit nano-patterned silica materials.

1.3.1. Single cell silica accumulating organisms – The isolation of organic molecules and their role in (bio)silicification.

There are several types of single celled organisms that accumulate silica which can be collectively termed protozoa, they can be further subdivided into Phaeodaria, Choanoflagellates and Silicoflagellates, which are single cell organisms that accumulate silica as opal or as amorphous hydrated silica.[21] The most extensive studies of (bio)silicification have been undertaken in the field of diatoms; unicellular organisms that are usually classified as algae. Diatoms have been subdivided into two groups; the centrate diatoms which are usually radially symmetrical and pinnate diatoms which

usually show a bilateral symmetry. Together there are more than 250 genera and more than 100,000 species of which the intricately designed cell wall (frustule) is unique to each species. The frustule can be likened to a petri dish where one half is slightly larger than the other. The two halves of the petri dish are called valves, each with its specific name; the upper half, or top, of the petri dish is called the epitheca which overlaps the lower half the hypotheca and is joined by girdle bands. The epitheca is perforated with many nano-meter sized holes which allow transport of material into and out of the cell. Diatoms reproduce primarily by cell division which occurs inside the "parent cell" which means that the new cell inherits a frustule slightly smaller than its parent. Fortunately diatoms can also reproduce sexually which overcomes this size problem and allows the diatoms species to return to its normal size. Asexual reproduction results in the formation of two daughter cells, where by each daughter retains half the parent frustule. The newly forming valves are created in the silica deposition vesicles (SDV) that are bound by the silicalemma membrane, the exact nature of which is unknown since neither the SDV or the silicalemma have been exclusively isolated to date.

The aquatic reservoirs of the Earth contain billions of tons of orthosilicic acid so diatoms and other aquatic organisms that accumulate silica do not have a problem sourcing orthosilicic acid for silica formation. However, when one considers the concentration of silicic acid in the aquatic reservoirs of the Earth (*ca.* 15 ppm) it becomes clear that silica accumulating organisms are highly adept at selectively uptaking silicic acid at low concentrations from their environment. Research interest has focused on the way in which diatoms transport orthosilicic acid into the cell[22] and how the intricate nano-patterned frustule is formed.[21]

1.3.2. The transport mechanism of orthosilicic acid into diatoms

The first stage of frustule formation and (bio)silicification in diatoms is the transport of silicic acid into the cell itself. Lewin first showed that diatoms take up silicon from an aquatic environment in the 1950's,[23, 24] and this was confirmed to be in the form of orthosilicic acid by Del Amo *et al.* in 1999,[25] which unsurprisingly is the dominant form

found in sea water (*ca.* pH 8), although it should be noted that *Phaeodactylum tricornutum* can also transport the ionised form $Si(OH)_3O^-$.[25, 26] The mechanism of orthosilicic acid uptake has been shown to be proportionally coupled (1Si:1Na) to the transport of sodium ions into the cell in a process that has been shown to saturable,[27] which indicates a carrier mediated process.[28, 29] Sullivan showed in one species of diatom that silicic acid transport was not a continuous process and occurred during a distinct phase of diatom reproduction which could also be correlated to an increase in protein abundance and composition.[30] The silicon transporter gene in *Cylindrotheca fusiformis* was first cloned in 1997 by Hildebrand *et al.* and termed *SIT1*,[31] this cDNA was then used as a probe to identify other copies of the *SIT* genes in *C.Fusifromis* where it was found that a family of five *SIT* genes existed.[22, 31] The *SIT* gene family were characterised and found to have 10 highly conserved hydrophobic regions predicted to be membrane spanning segments and a long hydrophilic C-terminus,[31] which had a high probability to form a coiled-coil structure and was thus hypothesised to interact with other proteins.[32] The *SIT* gene family were found to differ significantly when the long hydrophilic C-termini were compared which lead to the hypothesis that the activity of the *SIT* protein might differ which may indicate that the proteins could be located at specific domains in diatoms.

In most diatom species silicic acid transport has been shown to temporarily coincide with cell wall silica deposition,[33] although some exceptions have been shown. In species where this statement holds true, kinetic measurements have identified a process known as "internally controlled uptake" that requires a feed back mechanism and was proposed by Conway and Harrison.[34] Silicic acid uptake was suggested to be independent of external concentration and limited by the saturation or near saturation of the intracellular pool which is dependent on the rate of utilisation or cell wall deposition. More recently, Hildebrand proposed that the regulation and uptake of orthosilicic acid might not be associated with the absolute concentration of orthosilicic acid in the intracellular pools, but by a relative ratio of bound orthosilicic acid to unbound silicic acid.[32] The literature provides some evidence for this hypothesis. Azam *et al.* showed that intracellular orthosilicic acid might be bound to some cellular component,[28] perhaps as a means of maintaining supersaturated levels of the precursor for cell wall deposition.[32]

Interestingly, this hypothesis has been indirectly backed up by attempts to measure the concentration of silicon inside diatoms where reliable estimates by Hildebrand *et al.* have shown intracellular concentrations of silicic acid to be between 19 and 340 mM despite problems estimating volumes of water in the cell[35]. Reviews with further details on the biochemistry involved in orthosilicic acid transport are available.[29, 35, 36] In the context of this thesis, which is concerned with controlling silica formation and the inter-molecular interactions occurring during this process no further detail will be discussed on the transport of orthosilicic acid in diatoms. Except to say that, in a materials context, if one could stabilise a specific silicon species using an organic component, perhaps in a similar manner to diatoms, this might provide a route to the production of materials with specific properties. Focus will now be directed towards biomolecules that have been extracted from the biosilica of silica accumulating organisms such as diatoms, sponges and higher plants and their role in controlling silica formation.

1.3.3. Biomolecules tightly associated with biosilica found in diatoms

The SDV in diatoms is widely acknowledged to be the environment in which silica deposition occurs and as such it can be hypothesise that if the structure and composition of the membrane could be elucidated then at least part, or all of the mystery surrounding how diatoms form intricately nano-patterned silica, could be solved. To date, the SDV has not been exclusively isolated because it becomes exocytosed after valve completion to form part of the mature diatom cell wall and thus its structure and composition remain largely unknown. Vrieling *et al.*[37] were able to facilitate the accumulation of a dye inside the SDV which indicated that the SDV is *ca.* pH 5 which would favour the formation of three dimensional silica gel formation.[1] Other molecules inside the SDV other than orthosilicic acid remain unknown, however the production of other species specific biominerals *e.g.* $CaCO_3$ and Fe_3O_4 usually involves regulatory biomolecules such as proteins and carbohydrates.[38] Identification of the regulatory biomolecules associated with the formation of nano-patterned silica in diatoms was first established when Coombs *et al.*[39] observed an increase in the concentration of protein in cells during silica deposition with carbohydrate incorporation only occurring after silica deposition. Although the SDV has not be isolated, researchers have found other ways to investigate

the regulatory biomolecules, most of which have focused on isolating diatom cell wall proteins based on the assumption that the regulatory biomolecules for silica formation remain closely associated with the newly formed frustule. Hecky *et al.* isolated organic material from the cell walls of lysed diatoms.[40] The cell walls were then subjected to specific hydrolysis conditions in order to selectively remove the carbohydrates and amino acids from organic material coating the cell wall. The results indicated the presence of a large number of hydroxyl fuctionalised amino acids, the significance, and model proposed from these results, is discussed and investigated in chapter 3. Swift and Wheeler approached the problem from a slightly different prospective,[41] where instead of simply isolating the diatom cell walls and analysing the remaining organic material, they envisaged that organic material could be entrapped within the biosilica cell wall. Subsequent treatment of the cell walls with NaOCl to remove the organic coating, followed by treatment with HF/NH_4F to digest the cell walls, resulted in the isolation of phosphorylated glycoproteins with relatively high amounts of glycine and serine.[41]

More recently Kröger *et al.* have extracted a number of biomolecules from *Cylindrotheca fusiformis*[21] namely Frustulins, which are involved in forming a protective coating around the diatom and will not be discussed further.[42, 43] Hydrogen fluoride extractable proteins (HEP's[44]) or Pleuralins are localised where the epitheca overlaps the hypotheca and have been shown not to be associated with silica formation.[43] Finally two other types of biomolecules were isolated from *C. fusiformis* and shown to have a marked effect on the precipitation of silica *in vitro*, these are; silaffins,[21] (a low molecular weight protein isolated from two diatoms species, and long chain polyamines (LCPA) isolated from a number of diatom species).[45]

A significant advance was made in isolating diatom biomolecules in 1999 when Kröger *et al.* isolated a group of highly cationically charged polypeptides, named silaffins, which were extracted from the cell walls of *C. fusiformis* using anhydrous HF.[46] The biomolecules extracted were shown to have molecular weights of 4, 8 kDa (silaffins 1A and 1B) and 17 kDa (silaffins 2). Silaffins 1A and 1B were shown to be highly homogeneous from amino acid sequencing data obtained from the NH_2-terminus, which lead to the identification of a 795-base pair open reading frame (ORF) *sil1*. The *sil1* ORF

encoded a polypeptide which consisted of 265 amino acid residues containing a typical signalling sequence of 19 amino acids followed by a highly acidic region and seven highly homologous regions named R1-7. The repeating units are dominated by basic amino acids, where the lysine residues in silaffin 1A have been shown to be post-translationally modified with a long chain *N*-methyl-propylamine consisting of between 4-9 repeat units,[47] ϵ-*N,N*-dimethyl-lysine or ϵ-*N,N,N*-trimethyl-*δ*-hydroxylysine. The full structure was not elucidated until milder extraction techniques were used.[48] The use of ammonium fluoride, instead of anhydrous HF, provided evidence that the serine residues were also modified with a phosphate group. The full characterization of the silaffins is shown in Figure 1.3.3.1 where the nomenclature has changed according to the extraction procedure used. Ammonium fluoride was used to extract native silaffins which have provided the most comprehensive structural information.[48]

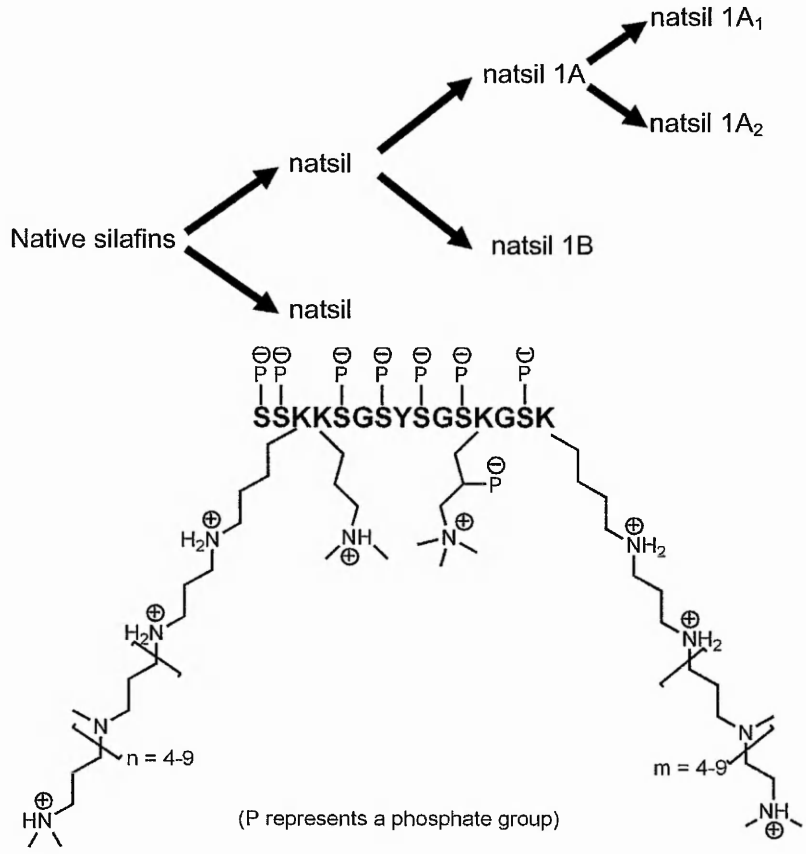

Figure 1.3.3.1 – The separation procedure leading to full structure of natSil-1A_1.

Characterisation of natSil-2 was published later by Poulsen *et al.* where it was found that natsil-2 is a glycoprotein bearing a high negative charge imparted on it by the phosphorylation, sulphonation and the carbohydrate moieties.[49] These moieties were removed previously because the original extraction was made using anhydrous HF.[46] Amino acid sequencing of natSil-2 was not possible because of the extremely high number of modifications. Thus far the structure is characterised as being highly hydroxylated as in natSil-1A and the lysine residues were once again found to be post-translationally modified. However, one distinction was the presence of significant amounts of methionine and leucine in natSil-2. Interestingly, silaffins have also been identified in *Thalassiosira pseudanana*,[48] although they are not homologous to those identified in *C. fusiformis* and exhibit no repeating sequence domains and yet there were some striking similarities as well. Both sets of silaffins identified are rich in hydroxyamino acids as well as lysine residues and both sets of lysine residue are highly post-translationally modified. It has been suggested that it is the characteristic of the domains that are important in the silaffins and post-translational modifications are important in order to precipitate silica and not the conservation of amino acid sequences. [50] More recently silaffins extracted from *Eucampia zodiacus* were found to contain a novel lysine residue and a quaternary ammonium group.[51]

The final class of molecules that were extracted from diatoms are LCPA which have been shown to be species specific and the major organic component of diatom biosilica. [52] A range of diatom species have been shown to contain a cocktail of LCPA which vary in overall chain length, degree of methylation, position of the secondary amino functionalities and finally the site specific incorporation of a quaternary ammonium ion. [53, 54] Instead of being attached to a polypeptide backbone as found in silaffins, the LCPA are attached to putrescine or a putrescine derivative. The LCPA are to the author's knowledge the longest found in nature and the species specificity is thought to be due to the functional role of the LCPA.

1.3.4. The silica precipitating characteristics of biomolecules extracted from diatoms.

The silica precipitating ability of each of the silaffins has been investigated thoroughly and yet there still remains some confusion over the exact role each of the functionalities exhibited by the silaffins. This will be demonstrated later where a description is given of the bioinspired studies preformed using the *R5* peptide. Silaffins were first shown to precipitate silica from a prehydrolysed solution of TMOS by Kröger *et al.*[46], where silaffin-1A precipitated a network of silica spheres with a diameters between 500 to 700 nm and a mixture of silaffins precipitated much smaller silica spheres with a diameter of <50 nm. In early work it was hypothesised that the silica precipitating ability of the silaffins was thought to arise because of the post-translationally modified lysine residues[46, 47], however what was overlooked at the time was that the phosphate buffer used in the silica synthesis played a critical role in the ability of silaffins to precipitate silica and due to the extraction procedure at the time the serine residues present in silaffins were dephosphorylated during extraction. This was later acknowledged when so called native silaffins were extracted using a milder extraction technique and the role of phosphate was investigated[55].

LCPA extracted from diatoms were also shown to precipitate silica spheres under similar condition to the silaffins. The species specific LCPA from *N.* angularis[45] were investigated were it was found that the molecular weight of the LCPA dictated the size of the silica spheres precipitated. The effect of pH was also investigated on the natural mixture of LCPA extracted from *N. angularis*, where it was found that with increasing pH the size of the precipitated silica spheres decreased. Silaffins also extracted from the same diatom species produced silica blocks composed of <50 nm irregular shaped silica particles a completely different structure from silicas precipitated by the LCPA. The complete organic cocktail of silaffins and LCPA was also investigated and found to produce a hybrid silica structure which can be a likened to silica blocks formed using the silaffins but now the silica blocks are composed of silica particles which the authors suggest represents a synergistic effect of the LCPA and the silaffins on the morphology of the precipitating silica.[45] LCPA extracted from *Stephanopyxis turris*[45] have been shown to precipitate silica spheres *via* the formation of micro emulsions in the presence

of phosphate and other multivalent anions. Furthermore the size of the silica spheres precipitated can be controlled by varying the concentration of the anion.[45]

As previously reported, the use of a combination of silaffins in precipitating silica produce markedly different silica morphologies. This work was continued when the role of natSil-2 was investigated.[49] NatSil-2 was unable to precipitate silica *in vitro*, probably due to its anionic character. However, when combined with extracted LCPA the effect was that silica could be precipitated under conditions where neither of the organic components alone showed any silica precipitation ability. The activating effect of natSil-2 on LCPA was hypothesised to occur because of an electrostatic interaction between the anionic natSil-2 and the positive charge held by the LCPA and increasing the concentrations of natsil-2 had an inhibitory effect on silica precipitation indicating electrostatic shielding above a critical concentration. A similar effect was observed when natSil-1A was combined with natSil-2 although in this instance the effect was immediate. The silica precipitated from this combinatorial approach yielded silica blocks with numerous irregularly shaped pores.[49] A similar approach was utilised in examining the roles of silaffins and LCPA extracted from *T.Pseudonana* where LCPA are shown to be an essential part in the silica forming machinery in *T.Pseudonana* despite the co-existence of silaffins. Instead it is hypothesised that the silaffins present help to direct the synthesis of biologically relevant structures which are not produced with LCPA alone in the formation of silica *in vitro*.[50]

Sumper proposed a phase separation model that was used to hypothesise the pattern formation in diatoms, envisaged as hexagonal networks on a varying length scale.[56] In this model it was proposed that LCPA phase separate to form microdroplets. The microdroplets were then proposed to self assemble into a monolayer of hexagonal close packed spheres' on the surface of the SDV membrane were silica formation at the aqueous interface would cause a proportion of the LCPA to be consumed by co-precipitation with the newly formed silica. This was assumed to cause a dispersion of the original LCPA microdroplets which then can reform into a similar arrangement as previously described but with a reduction in microdroplet size, thus causing an iterative decrease in the hexagonal framework as exhibited in diatoms.[56]

1.3.5. Silica deposition in demosponges

A second major type of silica accumulating organism exists in the aquatic reservoirs of the Earth, namely the sponges (phylum Porifera) of which there are three classes. The most widespread spread class is that of the demosponges which can be found in both shallow waters and to depth of over 300 m.[57] Demosponges accumulate silica in the form of siliceous spicules which are intimately associated with proteinaceous fibres which constitute the skeleton that shapes the sponge's growth. The organic mesophyl consists of a well defined system of interconnected channels and chambers which allow the sponge to process its own volume of water in *ca.* 5 seconds allowing the organism to filter the desired nutrients from the surrounding aquatic environment. Silicon is thought to enter the organism through these channels in the form of orthosilicic acid.[58] The transport of silicic acid through the organism is again largely unknown although there is no evidence to suggest transport through vesicles as proposed by and hence the transport of silicic acid is thought to occur through a simple diffusion mechanism.[59]

The siliceous spicules in demosponges are secreted in a membrane bound compartment and have an axial filament of protein around which the silicified spicule forms. Spicules vary in size and shape and have been categorised into microsclere and megasclere depending on their size, shape and skeleton function.[58] Megascleres clearly have a structural role and can vary in size from a few microns in length but there are instances when truly huge structures have been reported for instance by Levi *et al.* a spicule was reported to be 8 mm in diameter and 3 m in length.[60] The microscleres are usually significantly smaller and their role is more difficult to ascertain. The spicules are usually covered in a collogen-like protein called spongin which serves to cement the whole structure together. The formation of spicules in demosponges has been reviewed recently where details can be found on the biological aspects of silica formation which will not be discussed here.[57, 61]

The polymerisation of silicic acid around the central filament was reviewed more than two decades ago by Garrone *et al.*[62] demosponges usually have a central core called the axial canal which when intact has an axial proteinaceous filament running down the

centre of it which has been extracted and characterised by Shimizu *et al.*,[63] *Cha et al.*[64] and Krasko *et al.*[65] revealed the function and molecular characteristics that promote silica deposition.

1.3.6. Extraction and characterisation of the central axial filament of protein - silicateins

The central axial filament of protein was first extracted and characterised from *Tethya aurantia* by Shimizu *et al.*.[63] The protein extracted was given the name silicatein (for silica protein) and was found to be composed of three highly homologous fractions; α (26 kDa), β (27 kDa) and γ (28 kDa) with relative abundances of 12:6:1. The sequence of silicatein α was obtained where it was found that silicatein α is a novel member of the cathepsin L sub family of papain-like cysteine proteases.[63] Comparing the two proteins found that 45 % of the amino acid sequence was identical, with 75 % of the amino acids were found to have identical or structually similar side chains. *Cathepsin L* is a typical lysosomal proteolytic enzyme in both humans and sponges. Silicatein α is presumably localized in the silicalemma, which is a membrane enclosed vesicle where silica deposition occurs.[63] A similar protein from another sponge, *Suberites domuncula* was isolated by Krasko *et al.*[65] which when compared to silicatein α were found to possess 70 % identical and 79 % similar amino acid sequences. The silicatein proteins have distinct hydrophobic domains on its surface and the macroscopic domains are thought to cause the self assembly of the silicatein subunits into filaments. One further distinct feature of silicateins is the grouping of hydroxyl amino acids which strengthens the idea that silicateins are templates for biosilicification. The catalytic activity of silicatein has also been tested in silicification studies *in vitro*. It was found that silicateins are able to catalyse the hydrolysis of tetraethoxysilane (TEOS) and subsequent condensation reactions to form silica at neutral pH and ambient temperature. The silicatein filaments were found to catalytically hydrolyse TEOS as well as act as a template for silica deposition were silica nanospheres were deposited on the surface of the silicatein filaments.[66] The measurement of catalytic activity was made by quantifying the amount of silica precipitated which may not be indicative of the catalysis of condensation reaction but simply the promotion of aggregation known to occur by the addition of cations. Thermal denaturation showed that the catalytic activity of silicatein was

dependent on the presence of the proteins tertiary structure.[66] The hydrolysis of an alkoxysilane such as TEOS usually requires either acidic or basic conditions. Silicatein as mentioned previously is highly analogous to a group of hydrolytic enzymes, the ability of silicatein to catalyse a hydrolysis reaction is not so surprising especially when one considers that 2 of the 3 active amino acid residues found in cathepsin L are conserved in silicatein and the third; a cysteine residue is replaced by a serine residue.[63]

Silicatein α subunits have been prepared using genetic engineering in which a recombinant DNA template has been cloned in bacteria.[65-67] Zhou *et al.* showed through site directed mutagenesis, that replacement of either the serine[26] or histidine[165] the reduced the catalytic activity of silicatein α by an order of magnitude. A mechanism was suggested for the catalytic hydrolyisis of TEOS using silicatein α which centres around the serine and histidine residues replaced in the mutagenesis studies shown in Figure 1.3.6.1.[66]

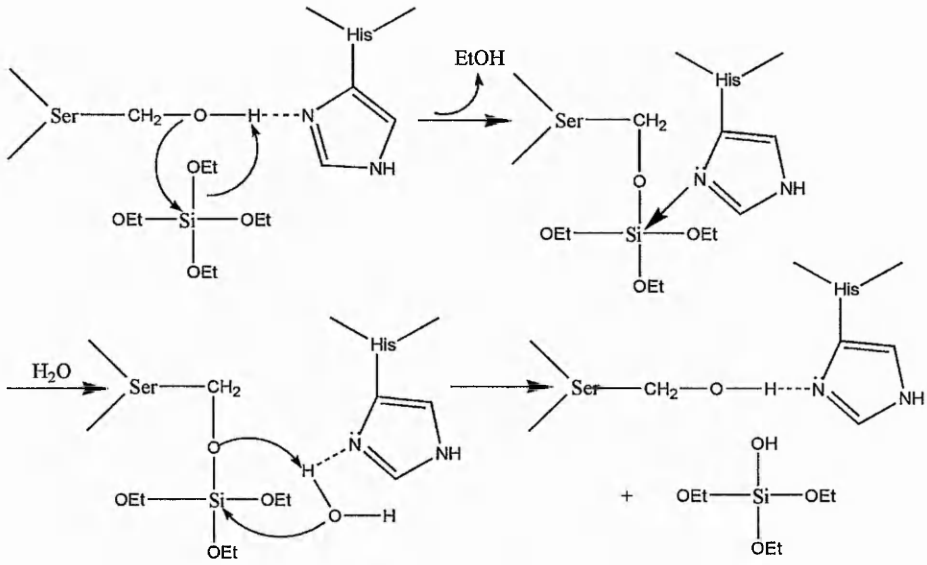

Figure 1.3.6.1 – Proposed mechanism for catalysis of TEOS to silica using silicatein.

It was suggested that the formation of a hydrogen bond between the imidazole side group and the hydroxyl side chain on the serine molecule activates the residues and promotes nucleophilic attack on the silicon centre to form a protein-silicon intermediate state with a Si-O-C bond.[66] Hydrolysis of the intermediate state regenerates the original co-operative hydrogen bond between the serine and imidazole groups with the elimination of one of

the four ethoxy groups on TEOS. This reaction may well be taking place *in vitro* however, it has no biological relevance because alkoxysilanes are not found in nature.

The isolation and characterization of silicateins found in sponges is a significant step forward in research associated with the formation of siliceous spicules in sponges. However, there are many issues that still need to be addressed when considering the complete synthesis of such ornate spicules since a central filament is unlikely to influence the deposition of silica after a complete monolayer has been deposited. Pisera suggested that the role of membranes which surround the growing filament as well as other organic molecules must be involved in determining the precise structure of the final spicule.[68]

1.3.7. The role of silica in higher plants.

Silicon is almost universally present in soil, but as we have seen in all silica accumulating organisms it is the bioavailability of silica that allows organisms to utilise its properties in their structures. The concentration of bioavailable silica (orthosilicic acid) in soils is between 0.1 and 0.6 mM.[69, 70] Higher plants differ in their ability to take and accumulate silica and it is notable that despite the ubiquitous occurrence of orthosilicic acid in aqueous environments and soils it is quite amazing that all plants are not silicified. The amount of silicon in a plant is expressed as a percentage of its dry mass which can vary from 0.1-10 %.[71] Silicon is not included in minerals that are typically essential for a plant to complete its life cycle but can be found in all plants shoots. Silicon accumulating plants are described as having a silicon content greater than 1 % on the tips of their leaves and a Si:Ca molar ratio of greater than 1.[72] Non-silicon accumulating plants are plants having less than 0.5% of silicon on the tips of their leaves and a Si:Ca ratio of 0.5. Silica has also been shown to be deposited in the stems, hulls, shells and in the hairs and spines of stinging plants such as nettles.[73] Although the presence of silica may not directly benefit the plant its inclusion in stems undoubtedly stiffens and strengthens plants as well being able to stimulate photosynthesis and reduce the amount of water lost through transpiration.[72] The uptake of orthosilicic acid by plants has also been shown to play an important role in a plants susceptibility to toxic metals and disease resistance.[70] Electron dispersive analysis has shown that in many plants insoluble silica contributes to the local

cell wall reinforcement at the site of fungal attack, and that this process is linked to the production of a highly cationic protein rich in proline PRP1 in cucumbers[74].

1.3.8. The extraction of bipolymers from *Equisetum* and their effect on silica formation

Equisetum typically accumulates silica at 10 % of its dry mass.[73] The silica has been shown to be deposited in long fibres within the epidermal membrane, extruded at the surface of the plant in a specific pattern and deposited around the stomata as shown in Figure 1.3.8.1

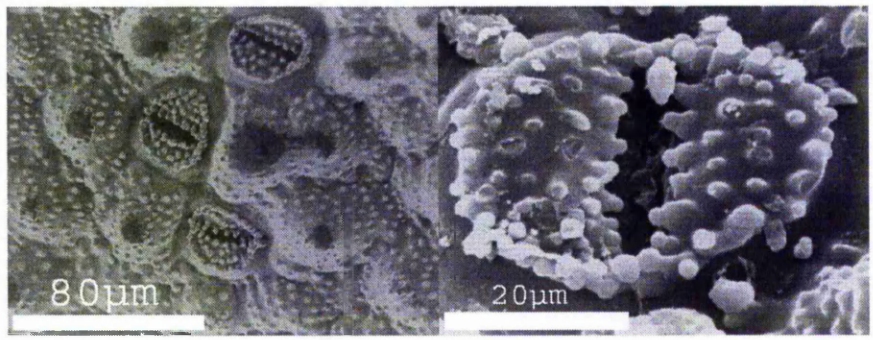

Figure 1.3.8.1 – Silica desposited at the surface of *Equisetum arvense*; left surface of plant leaf, right silica deposition around the stomata.

The organic matrix associated with biosilica in plants is largely confined to the outside of the siliceous phase, however, as with diatoms and sponges there is a small amount of organic material that is entrapped within the biosilica. Bioploymers were extracted from *Phalaris canariensis* hairs, *Equisetum telmateia* and leaves of *Phragmites* by Harrison *et al.* (formerly Perry). The extracts were made using strong oxidising acids to remove the the organic material associated with the external surface of the silica, followed by dissolution of the remaining siliceous material using buffered 1-3 % HF in 3 % NH_4F at pH 5. The soluble fraction was dialysed against dd water, lypholised and analysed for amino acid and carbohydrate content.[75] This work was continued in *Equisetum telmateia* and *arvense* when a similar technique was used to isolate the biopolymer fraction, silicification studies using a 50 mM solution of dipotassium tris(1,2-benzenediolato-*O*,*O'*)silicate which at physiological pH dissociates to form orthosilicic acid.[76] The silicification studies showed that the biopolymers extracted from *Equisetum telmateia*

increased the rate of trimer formation by *ca.* 25 %. Purification of the extracts using tangential flow results in an increase 150 % in the formation of trimers.[73] Electron microscopy revealed the presence of lath-like structures that were composed of 1-2 nm primary particles after 1 h and after 48 h the material exhibited order over 600 nm. When analysed using electron diffraction *d*-spacings observed were comparable to quartz.[73, 77]

1.3.9. From "biointeresting" to "biouseful"

The literature review presented above highlights what the research community now knows about how biological organisms use organic molecules to produce silicified structures. There is still much work to be carried out if scientists are truly going to understand the remarkable manner in which organisms can accumulate and control silica formation. For instance, almost nothing is known about how organisms store and transport silicon from its source whether that be from water or soil to the place of deposition. The research community assumes that organisms simply must accumulate silicon in some form. When required the reserves of silicon can be called upon to form a supersaturated silicon environment which promotes condensation reactions to form silica and that moreover the morphology and structure of the forming silica is controlled. The biological studies have lead to the development of three new research areas. Biological organisms have provided the research community with biomolecules and proteins from which recombinant structure can be synthesised through genetic engineering. This has lead to the development of research utilising these molecules to produce new materials and the deposition of these materials in a particular manner so they may be used to develop new technologies. The other two areas of research are bioinspired and biomimetic research. Bimimetic research is defined in this thesis as utilising a structural aspect observed in a biologically relevant molecule and exploring its molecular characteristics to gain an understanding of its function in biology. Bioinspired research is very similar; the key difference is that although the molecule being studied may be biologically inspired the way it is processed or used has no biological relevance. For instance, silicatein is known to hydrolyse TEOS in a catalytic manner but the mechanism proposed can not be claimed to be biomimetic simply because the precursor used is TEOS, an alkoxysilane, does not occur in a biological environment. Secondly the

mechanism utilises a Si-O-C bond to catalytically hydrolyse TEOS. To date there is no evidence to suggest a Si-O-C bond can be formed in a biological environment under ambient conditions, but there is no evidence to suggest this mechanism is not occurring *in vitro* and thus the research is termed bioinspired instead of biomimetic. The task facing scientists now is to utilise the technology we have learnt from biology to control silica formation *in vitro* in such a way that the properties, morphology, and structure can be controlled to surpass the materials currently available. The development of such materials will almost certainly allow silica to be used in a variety of new applications in the future. Moreover because it can be synthesised from renewable precursors, without the need for organic solvents, this environmentally friendly approach is certain to become more significant in the coming years.[78, 79]

1.3.10. The inspiration for bioinspired and biomimetic approaches to the controlled formation of silica *in vitro*.

The molecules extracted from biogenic silica have provided the inspiration for the approaches now being employed to develop new routes to silica with controlled structures. Silaffins are a typical example where characterisation of the biomolecules molecular structure has enabled scientist to develop new approaches to form silica with a controlled structure.[49] For instance, the molecular structure of silaffins encompasses a peptide backbone with posttranslationally modified lysine residues. Closer inspection of posttranslational modifications showed that amine functionality is commonly employed. This has directed scientists to investigate an enormous range of additives containing amine functionality, peptides, amino acids, carbohydrates and derivatives as well as recombinant proteins that mimic the biomolecules extracted from the biological organisms themselves. More recently, an exceptional approach has been employed to develop what promises to be a fascinating area of materials research. Chimeric proteins have been synthesised with peptide sequences from biological organisms that have been genetically engineered together to form a recombinant protein, collected the desirable properties of both peptide moieties (in this case diatoms silica and spiders silk) to form inorganic-organic hybrid materials. It has been suggested that these chimeric proteins

could be used to form other materials in which different processing techniques can be employed.[80]

1.3.11. The role of bioinspired additives in the formation of silica.

The role of additives in silica formation has been recently reviewed,[81, 82] however the aim of this section is to identify the different approaches to controlling silica formation *in vitro* and to provide a critical appraisal of these approaches and the understanding gained from them from a materials chemist point of view. Patwardhan *et al.*[81] characterised the effect of additives in silica formation into three categories. It was suggested that additives can act as a scaffold for silica formation, catalyse the formation of silica *in vitro* and promote aggregation of silica species. It was also suggested that although there are three distinct categories an additive could also appear in multiple categories. Categorising additives in this way does not complete the story from a materials chemist's point of view. As will be seen later in this thesis, additives can also be categorised by their molecular weight, which also seems to be somewhat indicative of the mechanism by which they effect silica formation in an aqueous environment.

The role of organic additives in silica formation was comprehensively document in Iler[1] and since then a variety of shapes have been reported.[83-85] In recent years bioinspired silica formation has progressed significantly, where organic molecules are used to control the structure of the silica formed in an aqueous environment under ambient conditions. The structure of this review of the use of additives will tend from simple "small molecules" (<1 kDa) to larger more complex molecules such as polyelectrolytes and will discuss the control applied to the formation of silica and, where possible, the mechanisms involved in the controlled formation of silica. Finally, a section will be devoted to the progress that has been achieved using biologically relevant peptides and proteins to form new materials.

Polyamines have been known to be flocculating agents for many years.[1] Bioinspired routes involving polyamines were first investigated by Mizutani *et al.*[90] who investigated a significant number of short chain polyamines and amine containing polyelectrolytes on

the effect of silica condensation at pH 8.5. He observed significant increases in polymerisation rates using the molybdenum blue method and showed that inorganic-organic hybrid materials were formed by inclusion of the amine into the silica structures. Interestingly, it was shown that molecules as small as 1,3-diaminopropane were capable of having a significant effect on the formation of silica as well as larger amine containing polelectrolytes.[86, 87] This work was subsequently followed up and extended to incorporate a bioinspired approach following the work published on silaffins[46] were lysine residues have been shown to be posttranslationally modified with polyamines. Polyamines and amine containing polyelectrolytes have now been extensively studied and a number of mechanisms have been proposed for the catalysis and increased aggregation effects exhibited by polyamines on the formation of silica. In accordance with the overview set out above initially the small polyamine containing molecules will be discussed first, whilst amine contain polyelectrolytes will be discussed later.

Belton *et al.* have systematic studies on diaminoalkanes[88] and ethyleneimines[89] with increasing number of amine functional groups from 2-6. The work has yielded several mechanisms and is discussed later in chapter 3, however, for completeness a brief mention will be made here to aid future discussion and introduce the effects of small molecules on silica formation. The systematic study of increasing hydrophobicity in diaminoalkanes on the effect of silica formation gave rise to a step change in the 3rd order rate constant as well as dramatic increases in the rate of aggregation of silica. The increases in 3rd order rate constant followed by a plateau in behaviour were proposed to be due to the hydrophobic effect, deduced because quite simply this was the only significant change in the molecule's structure which could cause a incremental increase followed by a plateau caused by the formation of micelle like structure which cause a rearrangement in the water molecules effectively making silicic acid more reactive.[88] The increase in the rate of aggregation was proposed because of the electrostatic effect which in short chain diaminoalkanes was due to surface neutralisation however, further increases in carbon chain length show a step change between 4 and 6 carbon atoms which is proposed result from the diaminoalkanes being able to bridge the particle double layer.[88] Menzel *et al.*[90] synthesised a number of different of polyamines with C2 and C3 spacings and investigated not only the ability of the molecules to precipitate silica but

also the acid base characteristics of the molecules. They found that polyamines have a significant buffering effect and that during protonation the amine would acquire charge on alternate amine groups to minimise electrostatic repulsions, which was later used by Belton *et al.* to propose a mechanism for the catalysis of condensation reactions involving polyethyeneimines.[89] Menzel *et al.*[90] found that the effect of polyamines on the condensation of orthosilicic acid is dependent on the architecture of the polyamine, (branched or linear) and also the degree of methylation. Furthermore, it is was proposed that nature (in the case of silaffins extracted from *C. fusiformis*) does not utilise the most effective molecules for the production of biosilica found *in vitro* to be linear polyethyleneimines and polypropyleneimenes but uses a methylated derivative probably to allow more time to assemble the intricate nano-patterned structures. Importantly it should be noted here that single molecular species where not used during Menzel *et al.* investigations, which therefore meant that only general conclusions can be drawn.[90]

Belton *et al.*[89] continued their studies on simple amine functionalised molecules through a bioinspired approach using spermine and spermidine which are naturally occurring polyamines and polyethyleneimine molecules containing 2-6 nitrogen atoms. In this study glassy silicas were produced using pentaethylenehexamine in which a mechanism for catalysis of condensation reactions using the polyamine in which the accumulation of charge on alternate nitrogen atoms is thought to be crucial in the catalytic mechanism proposed where a polyamine is electrostatically associated with a silica surface and catalyses the condensation of silicic acid at the surface of a silica particle[89]. Interesting, this mechanism contradicts mechanism proposed by Kröger *et al.*[91] who proposed the role of the posttranslationally modified propyleneimines in silaffins to catalyse the condensation of two molecules of silicic acid. The work on short chain polyamines is being continued by Perry and co-workers through the synthesis of polypropyleneimes with varying degrees of methylation and chain length,[92] although we await mechanistic details for the role of propyleneimines in silica formation and complete characterisation of the silica produced.

A bioinspired approach was preformed by Coradin *et al.* where the effect of amino acids was first studied.[93] A small range of amino acids were studied in a monomeric and

polypeptide form. The interactions of the amino acids were found to be greater in a polymeric form and it was concluded that the interactions with silica were probably due to electrostatic and hydrogen bonding effects.[93] Belton *et al.*[94] drew inspiration from the amino acid sequences observed in silaffins and expanded this study to encompass a complete range of amino acids that would be predominantly positively, negatively charged or neutral at *ca.* pH 7. Furthermore, they incrementally increased the number of amino acids to study homopeptides of lysine (1-5 and 150 amino acids) and glycine (1, 4, 5 amino acids). Conclusions were made with respect to the electrostatic interactions between positively charged amino acids which were shown to increase the rate of aggregation and kinetics of silica formation, which resulted in the formation of granular materials.[94]

The role of positively charged molecules in silica formation had been well documented prior to the approach adopted by Knecht and co-workers which was to apply a greater level of control to the molecules templating silica formation.[95] They chose to use polyamines in the form of dendrimers (PAMAM and PPI) to template the formation of silica in the presence of a phosphate buffer and interestingly no silica was formed in the absence of a phosphate buffer. The dendrimer templates have been shown to precipitate discrete silica nano-particles[95] where surface charge neutralisation with cations binding to the charged silanol groups prevents necking and aggregation of the silica spheres. It has been shown that the size of the metal cation can be linked with the eventual size of the nano-particle; where smaller cations such as Li, Na and K allow large silica sphere to be produced (235 nm) and larger cations Rb and Cs produce silica nano-particles with a diameter of 210 and 195 nm.[96] The authors suggest that the smaller ions (Li, Na and K) bind with a single silanol group and promote charge neutralisation, where as the larger cation bind with multiple silanol groups which leave numerous negatively charged silanol groups exposed. The increase in surface charge leads to greater interparticle repulsions and causes a smaller particle size.[96] The same group have shown that dendrimers are incorporated into the silica spheres and when used in conjunction with CdS, Au[97] and enzymes, the dendrimers can facilitate their encapsulation inside the silica nano-particles.[98]

The challenge for scientists having gained some insight into the role of small molecules in silica formation is to now take this technology and apply it to some of the challenges that will enable bioinspired silica to be used in an industrial context in developing new and replacing old silica technologies. One biomimetic approach has been developed by Morse *et al.*[99] where a study of bifunctional small molecules was shown to catalyse the formation of silica from TEOS solution. Furthermore, for cysteamine the most successful biomimetic catalyst was used to encapsulate firefly luciferase, green and blue fluorescent protein and *Escherichia coli* cells expressing GFP in silica mixtures.[99] The link between this section on small molecules and the previous section on the biomolecules extracted from biological organisms has probably only come about in the last decade or so through the development of phage display peptide library technologies. The biomolecules extracted from biological organisms exhibit many structural characteristics which unfortunately makes discovering the precise function of each structural moiety very difficult. It is also important to realise that even if an understanding of a particular moiety has been gained, the role of the moiety in the native biomolecule and in the biological organism itself. One must consider, what seems like an infinite number of parameters in order to gain a complete understanding of biomineralisation. The scientific community continues to develop new strategies to simplify this problem and phage display peptide libraries are one of the most promising upcoming areas. The technology involves a selection technique in which random peptides from a library are expressed as a fusion with a phage coat protein, resulting in the display of the fused protein on the surface of the phage particle.[100] Libraries usually consist of roughly a billion peptides and through a process called "biopanning" specific peptides can be isolated for their binding characteristics to a particular surface or mineral.[100] This technique offers a way to identify the binding function of short peptides sequence and through this approach perhaps an understanding of peptide sequence expressed in proteins can be gained where hundred and often thousands of peptides interact in a specific manner to control, influence and achieve a specific function. The technique was first used to identify silica binding peptides by Naik *et al.*[100] where a number of silica binding peptide were isolated and their silica precipitating characteristics investigated.[100] A similar techniques has been employed by Sano *et al.* in which a phage library was used to identify titanium binding peptides,[101] in particular 1 peptide named TBP1 was identified and site directed

mutagenesis of the TBP-1 peptide resulted in the identification of a peptide which consisted of only 6 amino acids that were essential for the peptide to bind to titania.[101] Furthermore, when the binding characteristics of the peptide were investigated on other surfaces it was found that the peptide sequence was capable of binding Si and Ag particles as well as titania.[102] Since the surface properties of these materials are very different it was concluded that TBP-1 must recognise an unknown common subnanometric structure in each of the other three surfaces.[102]

The work started by Coradin on polypeptides has lead to an enormous amount of work being carried out on polypeptides which in some cases can also be described as cationically charged polyelectrolytes. Patwardhan *et al.* have conducted a number of studies on polypeptides including poly(L-lysine) (PLL),[103] poly(L-Arginine),[104] poly(L-Histidine)[105] and a number of synthetic polyamines such as poly(allylamine hydrochloride) (PAH),[106] polyethyleneimine (PEI)[107] and poly(1-vinylimidazole).[108] The use of these polypeptides and polyeletrolytes in general induced the formation of silica spheres from a solution of prehydrolysed TMOS. The effect of varying process parameters as well the buffer used to maintain circumneutral pH was studied.[109, 110] The main criticism for most of this work which was carried out in a remarkably short period of time is the lack of mechanistic and chemical understanding that was gained from these studies. It does not seem a coincidence that poly(L-lysine) which is the amino acid known to be posttranslationally modified in silaffins produced novel silica structures including a hexagonal plate morphology.[111] Since that time a number of groups have undertaken work related to poly(L-lysine) in which the chain length,[94, 112, 113] secondary structure[114] and buffer were all shown to have a significant effect on the form of the silica produced. Poly(L-lysine) molecules with polymer chain length of less than 100 units were shown to form silica spheres, in polymers greater than 100 units the silica morphology was shown to form hexagonal plates.[112] Investigations involving secondary structure showed that silica particles with different pore sizes could be prepared.[114] However, it was at pH 9-11.2 and instead of using a buffer to keep the pH constant, sodium hydroxide was added drop wise to maintain the pH mentioned previously. Poly(L-lysine) was also shown to be able to hydrolyse TEOS at neutral pH.[115] This was then utilised to from silica sols where nano-particles of 5-8 nm formed by varying the

silicon to water ratio. These nano-particles were then used in solution to dip-coated silica films with a thickness between 100-250 nm.[116] It was left to the original authors to provide the most comprehensive study of poly(L-lysine) and to explain the mechanism and characterise the formation of silica hexagonal plates[117] although other authors had alluded to the mechanism previously.[112] Patwardhan *et al.*[117] showed that the shape of the precipitated silica was dependant on the secondary structure of the poly(L-lysine) and it was shown that hexagonal plate formation was independent of both the chirality and silica precursor. In fact it was shown that the formation of hexagonal plates was dependent on the poly(L-lysine) being able to adopt a helical structure which then self assembled into hexagonal close packed arrangement in the presence of phosphate.[117]

The remarkable self assembly of poly(L-lysine) in phosphate solutions perhaps could have been utilised in an early study of block copolypeptides by Morse and co-workers. However, Morse *et al.*[118] were inspired by silicatein and conducted a series of experiments using homopeptides where they found that only L-cysteine produced silica from a solution of TEOS at pH 7, it was concluded that simple homopeptides did not express enough complexity in their structure to mimic the activity of silicatein. The study was continued when amphiphilic block copolypeptides involving poly L-alanine, L-lysine, L-serine, L-glutamine, L-tyrosine and L-cysteine residues were synthesised. It was found that cationic block copolymers showed more activity than the corresponding anionic copolymers and L-glutamate completely inhibited the ability of L-cysteine blocks to produce silica, which the authors suggested supported Mizutani's hypothesis that polycations are important for interaction between negatively charged silicate molecules.[86] This is perhaps not surprising as the glutamate portion of the copolymer contained 15 times more residues than the cysteine portion. Copolymers containing lysine residues all showed some activity but only the cysteine and serine residues were able to produce silica with a controlled morphology. Copolymers of lysine and cysteine were found to precipitate silica with a spherical morphology with a diameter of hundred of microns. Furthermore, the oxidative ability of the cysteine copolymer to form disulphide bonds allowed a column-like silica morphology to be produced.[118] This study which was certainly the first of its kind involving silica formation, perhaps its only downfall in my opinion was the use of TEOS, in the context of silicatein this approach was justified, but

in a bioinspired approach to silica formation perhaps a silicic acid containing solution might have produced even more remarkable results. Furthermore the study utilised a Tris-HCl buffer, perhaps if a phosphate buffer was used which might have allowed the poly(L-lysine) to self assemble as demonstrated by Tomcsak *et al.*[112] and Patwardhan *et al.*.[117] Certainly this work should be revisited bearing in mind the understanding gained from the studies of poly(L-lysine).

Amine functionalised polyelectrolytes have been used to simulate the post translational modifications on the lysine residues found in silaffins. The main advantage of these molecules over the polyaminoacids is they are significantly cheaper and are already used for example in water treatment.[119] Patwardhan *et al.* first reported the use of PAH in the synthesis of silica structures using a variety of processing conditions and in combination with other polyelectrolytes.[106, 107, 109, 110, 120-122]

Sumper and co-workers have shown that LCPA extracted from *S. turis* form silica spheres when investigated in pre-hydrolysed solutions of TMOS, furthermore it was shown that the concentration of phosphate buffer ions controlled the particle size.[123] This approach was continued when PAH was used instead of the LCPA.[124] Interestingly, microscopic phase separation also occurred in this system creating droplets which templates the formation of silica. The droplets were said to form through electrostatic interaction and/or hydrogen bonds between the negatively charged phosphate ions and the positively charged PAH molecules. It was also shown that other multivalent ions were also capable of inducing phase separation,[124] and that a second parameter, pH, could also be adjusted to dictate the size of the phase separated droplets.[125] Interestingly, a completely different behaviour was observed when the polyamine concentration was doubled or halved, causing a stabilised polyamine silica sol. When the polyamine stabilised sol was used as a source of silica and added to a phase separated polyamine/phosphate droplet solution a skeletal silica framework was produced. It was proposed that this mechanism could be employed in diatoms where firstly a polyamine stabilised sol of silica particles could be employed to allow silica to be accumulated in a controlled manner in the SDV and secondly to template the formation of the intricate diatom frustules through the self assembly of LCPA and phosphate into hexagonally

close packed droplets. The authors hypothesise that self-assembly of the phosphate/polyamine droplets on the SDV membrane could produce the intricately nano-patterned biosilica exhibited by diatoms.[126, 127]

Until now we have focused on the work that has been carried out using polyamines, however, work has also been carried out using molecules that exhibit hydroxyl functionality. Since the proposal by Hecky *et al.*[40] that carbohydrate molecule might act as a template for silica formation through the formation of Si-O-C bonds there have been a number of theoretical and experimental investigations that have attempted to justify the existence of an Si-O-C bond in nature which are reviewed in Chapter 3. It is interesting to note that cellulose has been found to regulate and stabilise primary particles[128].

In a combinatorial approach, Zollfrank *et al.*[129] took a rigid cellulose backbone which was functionalised with dipropylenetriamine, this molecule was then used to template the formation of tubular silica. Interestingly, this is study showed the formation of short range ordered silica which was calculated to be 3.5 nm which corresponds to approximately ten layers of $(SiO_2)_8$ which were found to align parallel to the tube axis, with lattice spacings similar to the (101) lattice distance of α and β-quartz. The outer layers of the tube were found to be amorphous which is consistent with deposition in an uncontrolled manner which is consistent with a central filament core, once silica deposition extends past the influence of the filament it can no longer be controlled.[129]

In other template work involving crystalline materials to template silica formation, Jin *et al.*[133,134] have conducted a number of studies based upon novel polyethyleneimines (PEI) with porphyrin cores which they synthesised in house. Incidentally, this group have also used TMOS which was not hydrolysed prior to the addition of the crystalline PEI. Whilst the authors have demonstrated that a number of different silica morphologies can be produced by varying the ratio of water to methanol (termed methanol modulation) the PEI is dissolved in, the simple fact remains that this work is not based on controlling silica formation but rather templating silica formation through the preparation of crystalline PEI in slightly different morphological forms and since the pH at which the experiments were carried out is not mentioned the mechanism is probably simple

hydrolysis of TMOS under basic conditions caused by PEI followed by silicic acid condensation at the surface of the PEI crystals.[130, 131] The work has been continued through the synthesis of linear PEI,[132] PEI with a benzene core[133] were once again methanol modulation produces a variety of structures. The work with the PEI with a benzene core was combined with tetrakis(4-sulfonylphenyl)porphyrin (TSPP) which was shown to incorporate into the PEI structure around which silica could be deposited.[133] Furthermore, when PEI was used it was found that it could effectively reduce $PtCl_4^{2-}$ to deposit Pt nanoparticles inside the silica nanotubes creating a nanowire-like morphology once the PEI was removed by calcinations.[134] The metallurgical work was continued using monovalent, divalent and trivalent metal ions into a linear PEI system prior to silicification which resulted in three valance dependent morphologies; in particular, 2D disc-like and globular respectively, with the silica was deposited around.[135]

In a new approach to silica formation the role of nano-confinement has been introduced where silica formation has been carried out in distinct confined regions of various phases. The concept has recently been shown to have a quite remarkable effect on the formation of mesoporous silica structures via the sol-gel processing route. The results show that by varying the tube diameter in which the reaction takes place different silica structure can be produced from identical starting reagents.[136] Interestingly the concept has moved into biomimetic silica formation where an onion phase has been shown to produce individual nano-particles stacked between the preserved multilamellar structures of the onion phase.[137] Coradin and co-workers have also shown the synthesis of tubular silica that is formed inside the pore of a polycarbonate membrane[138], which can then be dissolved away to yield the silica tubes. One might expect a simple templating mechanism of the silica on the walls of the membrane, however the authors have shown that the silica tube dimensions are not dependent on the pore size but instead they suggest the silica is formed through interfacial interactions with the pore surface. However, it was found that the size of the pore did dictate the size of the primary nano-particle which the authors suggest indicates an effect of confinement on the diffusion-limited growth of silica.[138] This area represents one of many parameters that might control the nano-patterning of silica in a biological organism and it would be interesting to see what effect confinement had on the self assembly of phase separated polyamine micro emulsions. Of course one

might expect that small droplets formed by one LCPA might interact differently from large droplets formed by a different LCPA in a confined medium. One thing is for sure in the bioinspired and biomimetic formation of silica there are many new ideas and interesting hypotheses that need to be considered in the future.

1.3.12. The characterisation and use of protein molecules extracted from diatoms and sponges

The role of additives in silica formation has been detailed above, from small molecules right through to large polyelectrolytes in which the reoccurring theme is of a cationic charge with interacts with anionic silicon species often in a controlled manor to direct silica formation. However, whilst some researchers continue to search for biomimetic and bioinspired routes to novel structures there are others that continue to study the interactions of the molecules extracted from biological organisms and their synthetic analogues. Nature is exceptional at producing these nano-patterned materials so it is understandable to ask the question, "why try to improve on perfection?". Naturally the answer is biological molecules currently are extracted using the very solvents and chemicals we are trying to avoid using to produce nano-patterned silica and their synthetic analogues are currently extremely expensive and time consuming. Technological advances will continue to reduce the cost of producing synthetic analogues of biological molecules and by continuing to investigate the interactions of these molecules in silica formation will undoubtedly lead to refinements in bioinspired and biomimetic models of silica formation *in vitro*. To this end researchers have utilised the Sil1 gene from *C. fusiformis* which encompasses seven highly homologous repeating domains R1-R7. The peptide sequence denoted *R5* (SSKKSGSYSGSKGSKRRIL-COOH) exhibited by silaffins extracted from *C. fusiformis* has been studied in silica formation.[46, 122] The study revealed that silica spheres of *ca.* 300 nm could be precipitated from a phosphate-citrate buffered prehydrolysed solution of TMOS at pH7. In contrast to the suggestion by Kröger *et al.*[46] it was found that the posttranslational modifications exhibited by native silaffins were not required for silica formation. Naik *et al.* also found that the morphology of the silica produced could be tailored by applying different mechanical and electrical stresses to the precipitating silica solution.[139, 140] The

function of the amino acid sequence was investigated by Knecht *et al.*[141] using site-directed mutagenesis where they found that the arginine-arginine-isoleucine-leucine motif (RRIL) was essential to maintain a significant effect on the formation of silica *in vitro*.[142] Finally, with regard to silica, *R5* has been used to template the formation of a silica beads on a holographic bed, which resulted in an unusual composite inorganic-organic device that exhibited improved optical performance[141].

Biomimetic routes to other metal oxides have also used *R5*, which shows that we can apply the knowledge we gain from biosilicification to produce other materials in a bioinspired manner. Wright *et al.*[143] showed that titania particles of a specific diameter can be formed using *R5* and titanium(IV) bis(ammonium lactato)-dihydroxide (TBALDH) which could be converted from the anatase phase to rutile at 700 °C. It was further shown that the (RRIL) motif which was shown to be essential in the formation of silica was indeed also essential for titania precipitation.[143] Similar results were obtained when using PAH and PLL.[143,144] Kröger *et al.* adopted a slightly different approach and used recombinant silaffins instead of *R5* where the rutile phase of titania was produced under ambient conditions.[145] With regard to other oxides that can be synthesised in a biomimetic manner, Patwardhan *et al.* showed that germania can also be precipitated from tetraethoxygermane (TEOG)[146].

Patterning and especially on a nanometer scale is widely accepted in the scientific community to be pivotal in the successful development of new materials such as highly efficient optoelectronic materials and low-loss coupling to silicon semiconductors.[78, 79] Silicatein from *Suberites domuncula* has recently been immobilised on a surface using a novel linker molecule NTA alkanethiol which binds through a nickel containing molecule to a histidine tagged recombinant silicatein molecule.[147] Silica was then deposited on the surface using TEOS; silicatein has successfully been shown to catalyse the hydrolysis *in vitro*.[63, 66] This technique of protein immobilisation and subsequent deposition of a mineral could facilitate nano-patterning on a surface through the molecular patterning of the alkanethiol on the surface. The hydrolytic ability of silicatein was first shown to be non-specific by Morse *et al.*[148] when as with *R5*, silicatein was shown to be able to catalyse the formation of anatase from TBALDH *in vitro* and as silicatein has now been

shown to retain its activity when immobilised on a surface, Tahir *et al.* showed that silicatein could also catalyse the formation of titania on a surface, moreover, the repertoire of materials for which silicatein can catalyse the formation of was expanded to include zirconia.[149] Silicatein has also been shown to reduce $AuCl_4^-$ to gold nano-particles both in solution and when immobilised. Titania nano-wires have been functionalised as previously described with immobilised silicatein and then incubated in the presence of $AuCl_4^-$ gold nano-particles where found to form at the surface of the titania nano-wire.[150]

The literature reviewed in this section has been focused on the mechanisms and molecular interactions that occur in biological organisms that enable them to selectively up take, stabilise and deposit silica in a genetically controlled manner. The extraction and characterisation of biomolecules associated with biosilica has enabled researchers to develop biomimetic and bioinspired approaches to the formation of silica *in vitro*. Systematic studies of additives, where a single molecular feature such as hydrophobicity, polymer chain length and protein conformation, scientists have been able to develop a detailed understanding of the molecular interactions that control silica formation. However, thus far the morphology of the materials produced *in vitro* are still vastly inferior to those produced by biological organisms. Therefore, the main aim of this thesis is to further enhance the knowledge of molecular interactions that control the formation of silica *in vitro* through the development of new model systems. The model systems will enable us to understanding of the molecular interactions occurring during silica synthesis in the presence of new and established additives. The investigations carried out during this thesis have been inspired by the geochemical silica cycle shown in Figure 1.1 where the formation and dissolution of biosilica are critical to maintain a balanced system. Once a comprehensive understanding has been gained of these processes it is perceived that this knowledge will enable scientists to develop new materials and applications. The main advantages of this approach over other methods used to synthesise silica is the uses of aqueous based system, benign condition and renewable precursors. In light of the importance now being placed on the impact industrial processes have on the environment the development of "green" processes to synthesise materials is essential to satisfy the needs of today's society.

References

1. R. K. Iler, *The Chemistry of Silica* John Wiley & Sons, New York, 1979.
2. P. M. Dove, J. J. DeToreo and S. Weiner., *Biomineralization*, Mineralogical society of America, Washington, 2003.
3. P. Treguer, D. M. Nelson, A. J. Vanbennekom, D. J. Demaster, A. Leynaert and B. Queguiner, *Science*, 1995, **268**, 375-379.
4. R. Atkin, V. S. J. Craig, E. J. Wanless and S. Biggs, *J. Colloid Interface Sci.*, 2003, **266**, 236-244.
5. M. A. Brzezinski, R. J. Olson and S. W. Chisholm, *Marine Ecology-Progress Series*, 1990, **67**, 83-96.
6. R. Tacke, *Angew. Chem. Int. Ed.*, 1999, **38**, 3015-3018.
7. S. D. Kinrade, J. W. Del Nin, A. S. Schach, T. A. Sloan, K. L. Wilson and C. T. G. Knight, *Science*, 1999, **285**, 1542-1545.
8. R. M. Laine, K. Y. Blohowiak, T. R. Robinson, M. L. Hoppe, P. Nardi, J. Kampf and J. Uhm, *Nature*, 1991, **353**, 642-644.
9. S. D. Kinrade, R. J. Hamilton, A. S. Schach and C. T. G. Knight, *J. Chem. Soc., Dalton Trans.* 2001, 961-963.
10. N. Sahai and J. A. Tossell, *Inorg. Chem.*, 2002, **41**, 748-756.
11. C. C. Perry and T. Keeling-Tucker, *Jbic*, 2000, **5**, 537-550.
12. C. C. Perry, Belton, D.., Shafran, K., *Studies of biosilicas; structural aspects, chemical principles, model studies and the future*, Springer 2003.
13. T. Kendall, *Industrial materials*, 2000, 49-59.
14. C. J. Brinker and G. W. Scherrer, *Sol-Gel science - The physics and chemistry of Sol-Gel Processing.*, Acedemic Press, London, 1990.
15. L. L. Hench and J. K. West, *Chem. Rev.*, 1990, **90**, 33-72.
16. H. Jones, *SiFnews*, 2000, 15-17.
17. K. Schwarz and D. B. Milne, *Nature*, 1972, **239**, 333-.
18. E. M. Carlisle, *Journal of Nutrition*, 1980, **110**, 352-359.
19. J. D. Birchall, *Chem. Soc. Rev.*, 1995, **24**, 351-&.
20. Simpson T. and V. B., eds., *Silicon and siliceous structures in biological systems*, Springer Verlag, Wien, 1981.
21. M. Sumper and N. Kröger, *J. Mater. Chem.*, 2004, **14**, 2059-2065.
22. M. Hildebrand, K. Dahlin and B. E. Volcani, *Mol Gen Genet*, 1998, **260**, 480-486.
23. D. W. Lewin, *J. Gen Physiol.*, 1955, **39**, 1-10.
24. D. W. Lewin, *Can. J. Microbiol.*, 1957, **3**, 427-433.
25. Y. Del Amo and M. A. Brzezinski, *J. Phycol.*, 1999, **35**, 1162-1170.
26. G. F. Riedel and D. M. Nelson, *J. Phycol.*, 1985, **21**, 168-171.
27. P. Bhattacharyya and B. E. Volcani, *P. Natl. Acad. Sci-Biol.*, 1980, **77**, 6386-6390.
28. F. Azam, *Planta*, 1974, **121**, 205-212.
29. V. Martin-Jezequel, M. Hildebrand and M. A. Brzezinski, *J. Phycol.*, 2000, **36**, 821-840.
30. C. W. Sullivan, *J. Phycol.*, 1977, **13**, 86-91.
31. M. Hildebrand, B. E. Volcani, W. Gassmann and J. I. Schroeder, *Nature*, 1997, **385**, 688-689.

32. M. Hildebrand, *Silicic acid transport and its control during cell wall silicification in diatoms*, Wiley-VCH, Weinheim, 2000.
33. S. W. Chisholm, F. Azam and R. W. Eppley, *Limnol. Oceanogr.*, 1978, **23**, 518-529.
34. H. L. Conway and P. J. Harrison, *Mar. Biol.*, 1977, **43**, 33-43.
35. M. Hildebrand and R. Wetherbee, *Components and control of silicification in Diatoms*, Springer, New York, 2003.
36. M. Hildebrand, *Prog. Org. Coat.*, 2003, **47**, 256-266.
37. E. G. Vrieling, W. W. C. Gieskes and T. P. M. Beelen, *J. Phycol.*, 1999, **35**, 548-559.
38. S. Mann, *Biomineralization Principles and Concepts in Bioinorganic Materials Chemistry* Oxford University Press, Oxford, 2001.
39. J. V. Coombs, B. E. Volcani, *Planta*, 1968, **82**, 280-292.
40. R. E. Hecky, K. Mopper, P. Kilham and E. T. Degens, *Mar. Biol.*, 1973, **19**, 323-331.
41. D. M. Swift and A. P. Wheeler, *J. Phycol.*, 1992, **28**, 202-209.
42. N. Kröger, C. Bergsdorf and M. Sumper, *EMBO Journal*, 1994, **13**, 4676-4683.
43. N. Kröger, C. Bergsdorf and M. Sumper, *Eur. J. Biochem.*, 1996, **239**, 259-264.
44. N. Kröger, G. Lehmann, R. Rachel and M. Sumper, *Eur. J. Biochem.*, 1997, **250**, 99-105.
45. N. Kröger, R. Deutzmann, C. Bergsdorf. and M. Sumper, *Proc. Natl. Acad. Sci. USA*, 2000, **97**, 14133-14138.
46. N. Kröger, R. Deutzmann and M. Sumper, *Science*, 1999, **286**, 1129-1132.
47. N. Kröger, R. Deutzmann and M. Sumper, *J. Biol. Chem.*, 2001, **276**, 26066–26070.
48. N. Poulsen and N. Kröger, *J. Biol. Chem.*, 2004, **279**, 42993-42999.
49. N. Poulsen, M. Sumper and N. Kröger, *Proc. Natl. Acad. Sci. USA*, 2003, **100**, 12075-12080.
50. N. Poulsen and N. Kröger, *J. Biol. Chem.*, 2004, **279**, 42993-42999.
51. S. Wenzl, R. Deutzmann, R. Hett, E. Hochmuth and M. Sumper, *Angewandte Chemie*, 2004, **43**, 5933-5936.
52. N. Kröger, R. Deutzmann, C. Bergsdorf and Sumper. M., *Proc. Natl. Acad. Sci. USA*, 2000, **97**, 14133-14138.
53. M. Sumper and G. Lehmann, *Chembiochem*, 2006, **7**, 1419-1427.
54. M. Sumper, E. Brunner and G. Lehmanna, *Febs Lett.*, 2005, **579**, 3765-3769.
55. N. Kröger, S. Lorenz, E. Brunner and M. Sumper, *Science*, 2002, **298**, 584-586.
56. M. Sumper, *Science*, 2002, **295**, 2430-2433.
57. M. J. Uriz, X. Turon and M. A. Becerro, *Silica Deposition in Demosponges*, Springer, New York, 2003.
58. M. J. Uriz, X. Turon, M. A. Becerro and G. Agell, *Microsc. Res. Tech.*, 2003, **62**, 279-299.
59. T. L. Simpson, *Effects of Germania on silica deposition in sponges*, Springer, Berlin, 1981.
60. C. Levi, J. L. Barton, C. Guillemet, E. Lebras and P. Lehuede, *J. Mater. Sci. Lett.*, 1989, **8**, 337-339.

61. W. E. G. Müller, O. V. Kaluzhnaya, S. I. Belikov, M. Rothenberger, H. C. Schroeder, A. Reiber, J. A. Kaandorp, B. Manz, d. Mietchen and F. Volke, *J. Struct. Biol.*, 2006.
62. R. Garrone, T. L. Simpson and Pottu-Boumendil., *Ultra structure and deposition of silica in sponges*, Springer, Berlin, 1981.
63. K. Shimizu, J. Cha, G. D. Stucky and D. E. Morse, *Proc. Natl. Acad. Sci. USA*, 1998, **95**, 6234-6238.
64. J. N. Cha, K. Shimizu, Y. Zhou, S. C. Christiansen, B. F. Chmelka, G. D. Stucky and D. E. Morse, *Proc. Natl. Acad. Sci. USA*, 1999, **96**, 361-365.
65. A. Krasko, B. Lorenz, R. Batel, H. C. Schroder, I. M. Muller and W. E. G. Muller, *Eur. J. Biochem.*, 2000, **267**, 4878-4887.
66. Y. Zhou, Shimizu, K., Cha, J.N., Stucky, G. D.; Morse, D. E., *Angew. Chem. Int. Ed.*, 1999, **38**, 780-782.
67. A. Krasko, V. Gamulin, J. Seack, R. Steffen, H. C. Schroeder and W. E. G. Muller, *Mol. Mar. Biol. Biotech.*, 1997, **6**, 296-307.
68. A. Pisera, *Microsc. Res. Tech.*, 2003, **62**, 312-326.
69. E. Epstein, *Proc. Natl. Acad. Sci. USA*, 1994, **91**, 11-17.
70. E. Epstein, *Annu. Rev. Plan. Phys.*, 1999, **50**, 641-664.
71. J. F. Ma and N. Yamaji, *Trends Plant. Sci.*, 2006, **11**, 392-397.
72. J. F. Ma, *Functions of silicon in Higher Plants*, Springer, New York, 2003.
73. C. C. Perry and T. Keeling-Tucker, *Colloid Polym. Sci.*, 2003, **281**, 652-664.
74. H. Kauss, K. Seehaus, R. Franke, S. Gilbert, R. A. Dietrich and N. Kröger, *Plant J.*, 2003, **33**, 87-96.
75. C. C. Harrison, *Phytochemistry*, 1996, **41**, 37-42.
76. C. C. Harrison and N. Loton, *J. Chem. Soc. Faraday Trans.*, 1995, **91**, 4287-4297.
77. C. C. Perry and T. Keeling-Tucker, *Chem. Commun.*, 1998, 2587-2588.
78. S. Mann and G. A. Ozin, *Nature*, 1996, **382**, 313-318.
79. D. E. Morse, *TIBTECH.*, 1999, **June**, 230-232.
80. C. W. Foo, S. V. Patwardhan, D. J. Belton, B. Kitchel, D. Anastasiades, J. Huang, R. R. Naik, C. C. Perry, D. L. Kaplan, *Proc. Natl. Acad. Sci. USA*, 2006, **103**, 9428-9433.
81. S. V. Patwardhan, S. J. Clarson and C. C. Perry, *Chem. Commun.*, 2005, 1113-1121.
82. P. J. Lopez, C. Gautier, J. Livage and T. Coradin, *Curr. Nanosci.*, 2005, **1**, 73-83.
83. H. Yang, N. Coombs and G. A. Ozin, *Nature*, 1997, 692-695.
84. C. T. Kresge, M. E. Leonowicz, W. J. Roth, J. C. Vartuli and J. S. Beck, *Nature*, 1992, **359**, 710-712.
85. K. J. C. van Bommel, A. Friggeri and S. Shinkai, *Angew. Chem. Int. Ed.*, 2003, **42**, 980-999.
86. T. Mizutani, H. Nagase, N. Fujiwara and H. Ogoshi, *Bull. Chem. Soc. Jpn.*, 1998, **71**, 2017-2022.
87. T. Mizutani, H. Nagase and H. Ogoshi, *Chem. Lett.*, 1998, 133-134.
88. D. Belton, S. V. Patwardhan and C. C. Perry, *Chem. Commun.*,2005, 3475-3477.
89. D. J. Belton, S. V. Patwardhan.; C. C. Perry, *J. Mater. Chem.*, 2005, **15**, 4629-4638.
90. H. Menzel, S. Horstmann, P. Behrens, P. Barnreuther, I. Krueger and M. Jahns, *Chem. Commun.*, 2003, 2994-2995.

91. N. Kröger, M. Sumper., *The Biochemistry of Silica Formation in diatoms*, Wiley-VCH, Chichester, 2000.
92. V. V. Annenkov, S. V. Patwardhan, D. Belton, E. N. Danilovtseva and C. C. Perry, *Chem. Commun.*, 2006, 1521-1523.
93. T. Coradin and J. Livage, *Coll. Surf. B Biointerfaces*, 2001, **21**, 329 - 336.
94. D. Belton, G. Paine, S. V. Patwardhan and C. C. Perry, *J. Mater. Chem.*, 2004, **14**, 2231-2241.
95. M. R. Knecht and D. W. Wright, *Langmuir*, 2004, **20**, 4728-4732.
96. M. R. Knecht, S. L. Sewell and D. W. Wright, *Langmuir*, 2005, **21**, 2058-2061.
97. M. R. Knecht and D. W. Wright, *Chem. Mater.*, 2004, **16**, 4890-4895.
98. S. A. Miller, E. D. Hong and D. Wright, *Macromol. Biosci.*, 2006, **6**, 839-845.
99. K. M. Roth, Y. Zhou, W. Yang and D. E. Morse, *J. Am. Chem. Soc.*, 2005, **127**, 325-330.
100. R. R. Naik, L. L. Brott, S. J. Clarson and M. O. Stone, *Journal of Nanoscience and Nanotechnology*, 2002, **2**, 95-100.
101. K. I. Sano and K. Shiba, *J. Am. Chem. Soc.*, 2003, **125**, 14234-14235.
102. K. I. Sano, H. Sasaki and K. Shiba, *Langmuir*, 2005, **21**, 3090-3095.
103. S. V. Patwardhan, N. Mukherjee and S. J. Clarson, *J. Inorg. Organomet. Polym.*, 2001, **11**, 193-198.
104. S. V. Patwardhan and S. J. Clarson, *J. Inorg. Organomet. Polym.*, 2003, **13**, 193-203.
105. S. V. Patwardhan and S. J. Clarson, *J. Inorg. Organomet. Polym.*, 2003, **13**, 49-53.
106. S. V. Patwardhan and S. J. Clarson, *Polym. Bull.*, 2002, **48**, 367-372.
107. S. V. Patwardhan and S. J. Clarson, *Silicon Chem.*, 2002, **1**, 207-214.
108. V. V. Annenkov, E. N. Danilovtseva, E. A. Filina and Y. V. Likhoshway, *J. Polym. Sci., Part A: Polym. Chem.*, 2006, **44**, 820-827.
109. S. V. Patwardhan, N. Mukherjee and S. J. Clarson, *J. Inorg. Organomet. Polym.*, 2001, **11**, 117-121.
110. S. V. Patwardhan, N. Mukherjee and S. J. Clarson, *Silicon Chem.*, 2002, **1**, 47-54.
111. S. V. Patwardhan, N. Mukherjee, M. Steinitz-Kannan and S. J. Clarson, *Chem. Commun.*, 2003, 1122-1123.
112. M. M. Tomczak, D. D. Glawe, L. F. Drummy, C. G. Lawrence, M. O. Stone, C. C. Perry, D. J. Pochan, T. J. Deming and R. R. Naik, *J. Am. Chem. Soc.*, 2005, **127**, 12577-12582.
113. H. G. Cui, V. Krikorian, J. Thompson, A. P. Nowak, T. J. Deming and D. J. Pochan, *Macromolecules*, 2005, **38**, 7371-7377.
114. K. M. Hawkins, S. S. S. Wang, D. M. Ford and D. F. Shantz, *J. Am. Chem. Soc.*, 2004, **126**, 9112-9119.
115. V C. Sundar, A. D.Yablon, J. L.Grazul, M. Ilan, J. Aizenberg, *Nature*, 2003, **424**, 899-900.
116. T. M. Davis, M. A. Snyder, J. E. Krohn and M. Tsapatsis, *Chem. Mater.*, 2006, **18**, 5814-5816.
117. S. V. Patwardhan, R. Maheshwari, N. Mukherjee, K. L. Kiick and S. J. Clarson, *Biomacromolecules*, 2006, **7**, 491-497.
118. J. N. Cha, G. D. Stucky, D. E. Morse and T. J. Deming, *Nature*, 2000, 289-291.

119. W. L. K. Schwoyer, *Polyelectrolytes for water and wastewater treatment* CRC Press, 1981.
120. S. V. Patwardhan and S. J. Clarson, *Mater. Sci. Eng*, 2003, **23**, 495-499.
121. S. V. Patwardhan, M. F. Durstock and S. J. Clarson, Silicones and silicone-modified materials; Synthesis and properties of silicones and silicone-modified materials, San Diego, CA, 2001.
122. S. V. Patwardhan and S. J. Clarson, *J. Inorg. Organomet. Polym.*, 2002, **12**, 109-116.
123. M. Sumper, S. Lorenz and E. Brunner, *Angew. Chem. Int. Ed.*, 2003, **42**, 5192-5195.
124. E. Brunner, K. Lutz and M. Sumper, *PCCP*, 2004, **6**, 854-857.
125. K. Lutz, C. Groger, M. Sumper and E. Brunner, *PCCP*, 2005, **7**, 2812-2815.
126. M. Sumper, *Angew. Chem. Int. Ed.*, 2004, **43**, 2251-2254.
127. M. Sumper and E. Brunner, *Adv. Funct. Mater.*, 2006, **16**, 17-26.
128. C. C. Perry and Y. Lu, *J. Chem. Soc. Faraday Trans.*, 1992, **88**, 2915-2921.
129. C. S. Zollfrank, H. Griel, P., *Adv. Mater.*, 2007, **19**, 984-987.
130. R. H. Jin and J. J. Yuan, *Chem. Commun.*,2005, 1399-1401.
131. R. H. Jin and J. J. Yuan, *Macromol. Chem. Phys.*, 2005, **206**, 2160-2170.
132. J. J. Yuan and R. H. Jin, *Adv. Mater*, 2005, **17**, 885-+.
133. R. H. Jin and J. J. Yuan, *Chem. Mater.*, 2006, **18**, 3390-3396.
134. J. J. Yuan, P. X. Zhu, N. Fukazawa and R. H. Jin, *Adv. Funct. Mater.*, 2006, **16**, 2205-2212.
135. P. X. Zhu, N. Fukazawa and R. H. Jin, *Small*, 2007, **3**, 394-398.
136. Y. Y. Wu, G. S. Cheng, K. Katsov, S. W. Sides, J. F. Wang, J. Tang, G. H. Fredrickson, M. Moskovits and G. D. Stucky, *Nat. Mater.*, 2004, **3**, 816-822.
137. H. El Rassy, E. Belamie, J. Livage and T. Coradin, *Langmuir*, 2005, **21**, 8584-8587.
138. C. Gautier, P. J. Lopez, M. Hemadi, J. Livage and T. Coradin, *Langmuir*, 2006, **22**, 9092-9095.
139. F. Rodriguez, D. D. Glawe, R. R. Naik, K. P. Hallinan and M. O. Stone, *Biomacromolecules*, 2004, **5**, 261-265.
140. R. R. Naik, P. W. Whitlock, F. Rodriguez, L. L. Brott, D. D. Glawe, S. J. Clarson and M. O. Stone, *Chem.Commun.*, 2003, 238-239.
141. L. L. Brott, R. R. Naik, D. J. Pikas, S. M. Kirkpatrick, D. W. Tomlin, P. W. Whitlock, S. J. Clarson and M. O. Stone, *Nature*, 2001, 291-292.
142. M. R. Knecht and D. W. Wright, *Chem. Commun.*, 2003, 3038-3039.
143. S. L. Sewell and D. W. Wright, *Chem. Mater.*, 2006, **18**, 3108-3113.
144. K. E. Cole, A. N. Ortiz, M. A. Schoonen and A. M. Valentine, *Chem. Mater.*, 2006, **18**, 4592-4599.
145. N. Kröger, M. B. Dickerson, G. Ahmad, Y. Cai, M. S. Haluska, K. H. Sandhage, N. Poulsen and V. C. Sheppard, *Angew. Chem. Int. Ed.*, 2006, **45**, 7239-7243.
146. S. V. Patwardhan and S. J. Clarson, *Polymer*, 2005, **46**, 4474-4479.
147. M. N. Tahir, P. Theato, W. E. G. Muller, H. C. Schroeder, A. Janshoff, J. Zhang, J. Huth and W. Tremel, *Chem.Commun.*, 2004, 2848-2849.
148. J. L. Sumerel, W. J. Yang, D. Kisailus, J. C. Weaver, J. H. Choi and D. E. Morse, *Chem. Mater.*, 2003, **15**, 4804-4809.

149. M. N. Tahir, P. Theato, W. E. G. Muller, H. C. Schroder, A. Borejko, S. Faiss, A. Janshoff, J. Huth and W. Tremel, *Chem. Commun.*, 2005, 5533-5535.
150. M. N. Tahir, M. Eberhardt, H. A. Therese, U. Kolb, P. Theato, W. E. G. Muller, H. C. Schroeder and W. Tremel, *Angew. Chem. Int. Ed.*, 2006, **45**, 4803-4809.

Chapter 2 – Experimental Methods

Part I: Instrumentation and Operating Procedure

2.1 The measurement of silicic acid concentration using a spectrophotometric assay: The molybdenum blue method.

There are many ways to determine the amount of silicon in a sample ranging from inductively coupled plasma spectroscopy (ICP) to a colorimetric assay. This thesis is concerned with the formation of silica from silicic acid and the dissolution of silica to form silicic acid in an aqueous environment. The molybdenum blue assay is ideal for determining low concentrations (ppm) of orthosilicic acid in aqueous solution. The formation of silica is inversely proportional to the concentration of silicic acid in solution at time t. The primary concern when undertaking a kinetic assay is to employ an effective quenching technique. The assay must also have a sufficiently low detection limit such that detailed investigations can be made. The condensation of orthosilicic acid to form silica generates a mixture of species in solution as discussed in section 1.2. Effective quenching of the reaction system is achieved by employing acidic conditions (pH 1) where condensation reactions are minimised and degradation of oligomeric silicon species is negligible. It should be noted here that acidic quenching is not 100 % efficient as small oligomers such as dimers are known to dissociate to form orthosilicic acid.[1]

Recognition of orthosilicic acid over other silicon species comes about through coordination of a hexacoordinated coordinated silicon atom with molybdic acid to form yellow silicomolybic acid (Equation 1).[2]

$$Si(OH)_4 + 2H_2O \rightarrow H_8SiO_6 \qquad (1)$$

$$H_8SiO_6 + 12MoO_4^{2-} + 24H^+ \rightarrow H_8[Si(Mo_2O_7)_6] + 12H_2O \qquad (2)$$

The silicomolybdic acid complex is formed by the reaction of molybdic acid with the hexacoordinated silicon has a cage structure, formed by twelve MoO_6 octahedra made up of four groups of three, where each of the three octahedra share an oxygen atom which forms one corner of a central tetrahedron to which the central silicon atom co-ordinates. The geometry of the cage structure is specific in recognition to orthosilicic acid, however, one important limitation of the method is that although orthosilicic acid is the only species coordinated by the MoO_6 cage, the origin of orthosilicic acid cannot be control and hence oligomers that rapidly dissociate to orthosilicic acid are also quantified.[1] Unpublished work by Belton *et al.* has shown that the monomer is complexed in 75 s at 293 K, furthermore it was shown that dimeric silicic acid takes 600 s to fully dissociate and polysilicic acid depolymerises slow enough to allow a distinction to be made.[3]

Reduction of the silicomolybic (yellow) acid to silicomolybdous acid (blue), which has a higher extinction co-efficient and enables orthosilicic acid concentrations as low as 0.1 ppm to be measured. The reducing reagent used must not reduce the residual molybdic acid and must also reduce the silicomolybdic acid fast enough to prevent any interference from silicate oligomer dissociation. The best reported reducing agent is a mixture of 4-methylaminophenol (METOL), sulfite and oxalic acid which achieves reduction in *ca.* 90 min and is colour stable for at least 48 h.[1, 3]

Treatment of the data is simple but effective and allows the investigation of the formation of trimers and the preferential reaction of silicic acid with larger oligomers. The reaction of silicic acid to form tirmers is termed the 3rd order region and is the earliest measurable decrease in silicic acid concentration using the molybdenum blue assay. This is because the molybdenum blue assay is unable to distinguish between monomeric and dimeric silicic acid as the dimers quickly dissociated to form silicic acid. The time period over which the 3rd order region dominates is determined by a plot of $1/[Si(OH)_4]^2$ against time where deviation away from a linear relationship signals the end of the 3rd order region. The preferential reaction of silicic acid with oliogomers is a reversible reaction and as such the rate constant is split into a forward and a reverse reaction k_+ and k_- and is determined by a plot of $\ln[Si(OH)_4]$ against time which gives a linear relationship. Deviation away from the linear relationship signals the end of the region. The full derivation for this kinectic approach has been

published by Harrison *et al.*[4] and the full derivation is presented in D. J. Belton's PhD thesis.[3]

2.2 Fourier transform tnfrared spectroscopy (FTIR)

FTIR has been used to identify entrained material within silica. The characteristic stretches for silica are listed in Table 2.3.1.[5, 6]

Wavenumber /cm^{-1}	Transition
3745-3750	Isolated silanol group O-H stretch showing no hydrogen bonding
3650-3660	Isolated silanol group showing long range hydrogen bonding O-H stretch
3540-3550	Adjacent silanol pairs showing mutual hydrogen bonding O-H stretch
3400-3500	Adsorbed water molecule O-H stretch
1100-1250	Asymmetrical stretch of Si-O-Si in silica matrix
850-950	Si-OH vibration
800	Symmetrical stretch of Si-O-Si in silica matrix
460-520	Si-O-Si rocking and bending transitions

Table 2.2.2 – Characteristic FTIR stretches of silica.[1]

The samples were analysed using a Magna IR-750 infrared spectrometer (Thermo Nicolet) by transmission. In this method potassium bromide (KBr) is used as an IR inactive dilutant and support for the sample. The sample (1 mg) and KBr (200 mg) were ground together until a homogeneous powder was achieved. The sample was then fused using a stainless steel die at 10 tonnes and reduced pressure.

2.3 Photon correlation spectroscopy (PCS)

Photon correlation spectroscopy or dynamic light scattering (DLS) is used to determine particle sizes typically between 2 nm and 10 μm using visible light as a source of radiation. The principle of the technique is to measure the diffusion of particles through a media, it does this by effectively measuring the Brownian motion of a particle by illuminating it with a laser and analysing the intensity fluctuations in

the scattered light. Samples were prepared almost identically to those when kinetic measurements were undertaken, except the solution were prepared using dd water filtered through a 0.2 μm syringe filter to minimise dust contamination. Exactly the same criteria were applied for the sample to be considered valid as outlined in section 2.1.1. Two instruments were used during this project; a Coulter N4 plus particle sizer and a Malvern zetasizer NanoS. The Coulter N4 plus particle sizer was fitted with a He-Ne 632.8 nm, 30 mW laser and particle measurements were made at 90 ° to the sample. The Malvern zetasizer NanoS was fitted with a He-Ne 532 nm, 30 mW laser and particle measurements were made at 173 °. Calibration of the instruments was carried out using a 60 nm latex standard. Particle measurements were made from the condensing system at regular intervals depending the rate of aggregation at 25°C unless otherwise stated. Where fast aggregation was observed readings were taken frequently (every 30 s) and when aggregation was slow measurements were taken less frequently (every 5-60 min).

2.4 Thermal gravimetric analysis

Samples were analysed using a Perkin Elmer Pyris 6 thermal gravimetric analyzer. The measurements were made with respect to the mass loss at a given temperature. Samples were run in air to allow complete combustion of organic material. The crucible was first tarred on the balance, the sample (*ca.* 3 mg) was then placed in the crucible and held at 303 K in the furnace for 10 min prior to analysis to allow the weight to stabilise. The furnace temperature was then increased at a 10 K min^{-1} under air to a temperature of 1173 K where the final temperature was then held for 60 min.

2.5 Nitrogen gas adsorption/desorption analysis

Samples were analysed using a Nova Quantachrome 3200e. A known weight of sample was placed in an analysis tube and degassed for 7 h at 403 K under vacuum. Samples were analysed using nitrogen as the adsorbent at 77 K with an equilibration time of 10 min. The specific surface area was obtained *via* the BET method where nitrogen is assumed to have a cross sectional area of 0.16 nm^2. Pore size distributions were calculated by the application of BJH theory to the desorption branch of the isotherms.

2.6 Electron microscopy

Scanning electron microscopy was used to visualise the morphology of silica precipitated from both the unbuffered TMOS system and the KSiCat system. Samples for SEM/EDS analysis were mounted onto aluminium stubs with a carbon conductive pad as an interface between the aluminium stub and the sample. All loose aggregates were removed by tapping the stub before the silica samples were gold coated with argon plasma at 1.2 kV, 4 mbar, for 2 min using an Edwards S150B sputter coater. Images were acquired using a JEOL JSM-840A scanning electron microscope with an accelerating voltage of 20 kV. EDS was carried on samples at 20 kV, at a working distance of 20 mm, using an Oxford instruments INCA x-sight EDS.

Samples for TEM were mounted on stainless steal 200 mess grids from a solid state and analysed on a Jeol 2010 TEM at 200 kV.

2.7 X-ray powder diffraction

Powder XRD measurements were conducted using a Hiltonbrooks modified Philips PW1050 Powder Diffractometer operated at 42.5 kV/18 mA with a copper source Cu K_{α}, 1.540562 Å

2.8 Elemental analysis

Samples were run at London Metropolitan University using a CE-440 Elemental Analyser.

References

1. R. K. Iler, *The Chemistry of Silica* John Wiley & Sons, New York, 1979.
2. J. D. H. Strickland, *J. Am. Chem. Soc.*, 1952, **74**, 872-876.
3. D. Belton, The influence of small molecules on the precipitation of silica, Nottingham Trent University, 2005.
4. C. C. Harrison and N. Loton, *J. Chem. Soc. Faraday Trans.*, 1995, **91**, 4287-4297.
5. C. N. M. Banwell, E. M. McCash, *Fundamentals of Molecular Spectroscopy* 4th edn., McGraw-Hill Publishing Company, london, 1994.
6. D. A. Skoog, *Principle of Instrumental Analysis*, 4th edn., Saunders College Publishing, Fort Worth, 1992.

Part II: The effect of counter ions on the formation of silica: A comparative study between dipotassium tris(1,2-benzenediolato-*O,O'*)silicate and tetramethoxysilane.

2.9 Introduction

Investigation into the formation of silica in biology and for industrial applications, centres around solutions of orthosilicic either in a super-saturated or as in nature unsaturated solutions. Orthosilicic acid is known to occur universally throughout aqueous media at unsaturated levels.[1] Organisms such as diatoms, sponges and higher plants selectively uptake orthosilicic acid and through a variety of processes that are not fully understood, genetically control the selective deposition of silica. As mentioned previously in section 1.3 silica is produced in a variety of ways. Current solution techniques tend to utilise highly basic sodium silicate solutions which are neutralised using sulphuric acid to form a slurry.[2, 3] Sodium silicate is used as a precursor for industrial silica because it is relatively inexpensive, whilst dipotassium tris(1,2-benzenediolato-*O,O'*)silicate is extremely expensive and TMOS has numerous safety concerns. Supersaturated solutions of orthosilicic acid can be prepared by the hydrolysis of halides, esters and acyl derivatives.[1] TMOS is a well established precursor for the formation of silica *in vitro* and has been used in many bioinspired and biomimetic studies.[4-6] In principle there are a wide range of silica precursors that can be used to study the formation of silica in the presence of additives ranging from alkoxysilanes, sodium silicate often termed "water glass", ethylene glycol modified silane (tetra(2-hydroxyethyl)orthosilicate) and dipotassium tris(1,2-benzenediolato-*O,O'*)silicate (KSiCat). To date four precursors have been primarily used to study the formation of silica with a biological "twist" *in vitro*; dipotassium tris(1,2-benzenediolato-*O,O'*)silicate, TMOS, TEOS and sodium

silicate. The choice of which silica precursor to be used in the study should not be underestimated as almost every feature of the precursor will affect the silica produced. Silica formation is usually investigated using supersaturated solutions of orthosilicic acid which are unstable. To generate a supersaturated solution containing silicic acid a stabilised precursor solution must be employed. For instance, dipotassium tris(1,2-benzenediolato-*O,O'*)silicate is stable in aqueous solution. The addition of a known amount of acid (*e.g.* HCl) hydrolyses the octahedral complex to form a supersaturated solution of pure orthosilicic acid and three molar equivalent of catechol known to aid silica dissolution and two molar equivalents of potassium chloride.[9] Alkoxysilanes can also be used to prepare supersaturated silicon solutions containing orthosilicic acid. The solutions should not be described as pure as they contain oligomeric silicon species other than orthosilicic acid. The conversion of an alkoxysilane to a supersaturated solution containing orthosilicic acid requires a hydrolysis period to convert the alkoxy groups ($^-OCH_3$) to hydroxyl groups (^-OH). This is typically achieved using acidic conditions and is accomplished in 15 mins when a 1 M solution of TMOS is hydrolysed using 1 mM HCl. The disadvantage of this system is the formation of methanol which, if one assumes complete hydrolysis, is four times the concentration of the solution containing the orthosilicic acid to be studied. Furthermore, upon removal of a single alkoxy group from the precursor molecule, a hydroxyl group is produced and at supersaturated silicon levels this is free to react with a similar molecule through a condensation reaction. These reactions are minimised by using acidic reaction conditions. Condensation of the supersaturated solution containing orthosilicic acid is accelerated by neutralisation using a buffer, typically between 50 and 500 mM. Tris-HCl, phosphate, phosphate-citrate, acetate and borate buffers have all been used to as a medium to; [7]

- Dilute the hydrolysing solution of TMOS,
- To control the pH of the condensing system,
- As a media to add the additive to the condensing system.

The use of a buffer introduces additional ionic compounds at significant concentration. Since cations are known to interact with negatively charged silicon species generated during the condensation of orthosilicic acid these are obviously undesirable and can often mask the true role of an additive.[8]

Whichever precursor is chosen to study the formation of silica *in vitro*, one must also consider the role of the counter ions generated from the silica precursor and the buffer if used. In this study, for the first time, TMOS has been used to as the precursor to silica in the absence of a buffer. This approach has not been studied previously because hard acid, hard base neutralisations are notoriously difficult to control. Despite this, in this study the molybdenum blue assay has been conducted on 30 mM solutions containing orthosilicic generated from TMOS. The role of counter ions and molecules in the condensation of silicic acid generated from two different silica precursors, dipotassium tris(1,2-benzenediolato-*O,O'*)silicate (KSiCat) and tetramethoxysilane (TMOS) have been examined.

2.10 Methodology

2.10.1 Establishing a procedure for the formation of silica using TMOS.

Hydrolysis of TMOS

TMOS (173 µl) was hydrolysed at a concentration of 1 M in 1 ml of 1 mM HCl for 15 mins. The hydrolysis was monitored using the molybdenum blue method, the concentration of hydrolysing TMOS was reduced by *ca.* 30 times to obtain an absorbance value within the linear region of the molybdenum blue assay. The sampling volume for a 30 mM solution of orthosilicic acid is 10 µl. Pipetting 0.3 µl is not feasible bearing in mind the accuracy that is required to observe any condensation during the hydrolysis period. A combination of dilutions and reduced sampling volume was employed to achieve the desired final silicon concentration.

A Jeol ECX-400 (400 MHz) NMR spectrometer was used to quantify the amount of methanol produced during the hydrolysis of TMOS. Methanol standards were prepared by placing 20-80 µl of methanol and making the total volume to 10 ml of dd water and running ^{1}H NMR. An insert that contained D_2O and 1 % 2,2-Dimethyk-2-silapentane-5-sulfonic acid (DSS) was used as a lock signal. The CH_3 peaks and DSS peak were integrated for each sample, the DSS:CH_3 ratio was calculated and plotted against methanol volume to create a standard curve. The 30 mM TMOS sample was then run under the same conditions and the amount of methanol quantified using the standard curve.

The silica species in solution after the hydrolysis period were investigated using the same NMR spectrometer. 1 M solutions of TMOS in 1 mM HCl (with insert as previously described) were investigated using ^{29}Si (79.7 MHz) NMR during the hydrolysis period to monitor condensation.

2.10.2 The molybdenum blue assay

Reagents

Molybdenum reagent – Quenching reagent

Ammonium molybdate tetrahydrate (20 g, 16.2 mM) was dissolved in dd water (500 ml). Concentrated hydrochloric acid (37 %, 60 ml) was added to the ammonium molybdate solution and made was up to 1000 ml with dd water after cooling. This solution was then diluted at a ratio of 1:10 with dd water and 16.5 ml of solution was used to quench the condensing silica system being studied.

Reducing reagent

Oxalic acid (20 g, 0.22 moles), 4-methylaminophenolsulfate (6.67 g, 0.019 moles) and sodium sulphite (4 g, 31.7 mM) were dissolved in deionised water (500 ml).

Concentrated sulfuric acid (100 ml, 98 %) was added and the solution and diluted to 1000 ml with deionised water after cooling.

Silica synthesis and kinetic assay

There were two silica precursors used throughout this study, TMOS and dipotassium tris(1,2-benzenediolato-*O,O'*)silicate. TMOS was hydrolysed at a concentration of 1 M in 1 ml of 1 mM HCl. 0.3 ml of the TMOS solution was pipetted into the neutralising solution which contained KOH (4.5 ml of 1 mM) and diluted with 5.2 ml of deionised and distilled water (dd water). Upon injection of the TMOS solution into the neutralising solution the timer was started.

The dipotassium tris(1,2-benzenediolato-*O,O'*)silicate (97 %, 0.14 g, 30 mM $K_2[Si(C_6H_4O_2)_3].2H_2O$ referred to as KSiCat,) was dissolved in H_2O (9.76 ml). To that solution, 240 ±10 µl of 2 M HCl, (this varied from batch to batch of KSiCat total volume = 10 ml) was added. The addition of the 2M HCl to the solution of KSiCat starts the dissociation of KSiCat to form silicic acid, this process is complete in *ca.* 20 s.[9]

For both systems (upon neutralisation or dissociation), 10 µl aliquots of the condensing systems were taken and pipetted into one of the plastic containers containing 16.5 ml of molybdenum reagent. This process was repeated continuously with decreasing frequency as the condensation reaction proceeds. The pH of the condensing system was measured after 10 mins where it must be pH 6.8± 0.2. A typical assay has 20 readings over the first 15 mins. The reducing reagent (8 ml) is added to the molybdenum reagent solutions 15 mins after the addition of the 10 µl aliquot of the condensing system has been added. After 60 mins the rate of change of molybdenum blue active species is negligible and only one further equilibrium reading was taken after 24 h. The absorbance of the molybdenum blue solutions were measured *ca.* 16 h after preparation, at 810 nm using a Unicam UV-Vis UV1 spectrophotometer. The silica produced can be isolated *ca.* 16 h (this time varies if

an additive is being studied) to yield a silica gel, which was washed thoroughly with dd water to remove any catechol and potassium chloride entrapped within the silica. The yield of silica is approximately 10 mg but we can not be sure of the exact molecular weight. If we assume the silica produced is SiO_2, the yield is 56 %, although it should be noted that only 10 % of the starting silicon concentration remains in solution. The yield will also depend on the isolation method. Typically, centrifugation at 3000 R.P.M. using a Sovall RT7 plus is used which can leave some silica suspended in solution.

The investigation of an additives effect on the condensation process was carried out by redistributing the dd water used to dissolve the KSiCat or in the case of TMOS the 5.2 ml of dd water used in the neutralising solution. Typically 2 ml of dd water is used to dissolve the additive and this is then added immediately after dissociation or neutralisation, unless otherwise stated.

The counter ions (K^+ and Cl^-) from the KSiCat and HCl respectively, were studied in the TMOS system; this was accomplished by dissolving the counter ions in 2ml dd water and titrating to pH 6.8 using 2 µl of 1 M KOH for catechol and 5 µl of 1 mM HCl, (denoted additive solution). The total volume of the system was kept constant at 10 ml by reducing the amount of dd water used to dilute the 1 mM KOH to form the neutralising solution in the TMOS system and the amount of water used to dissolve the KSiCat.

The rate of aggregation was measured using dynamic light scattering using a Malvern zetasizer nanoS. Nitrogen gas adsorption measurements were conducted using a Quantachrome Nova 3200e surface area and pore size analyzer on the materials isolated after 24 h. Surface areas were then determined using the BET method where nitrogen is assumed to have a cross-sectional area of 0.16 nm^2, [10] over the range of relative pressures 0.05 – 0.3 (with respect to a measured atmospheric pressure) at which point the monolayer is assumed to assemble. Pore radii were determined by the BJH method using the desorption branch of the isotherm.[11]

2.11 Results and Discussion

2.11.1 The hydrolysis of TMOS

Initially it was important to establish the reactions occurring during the hydrolysis period. The molybdenum blue assay was used to determine the amount of condensation occurring during the 15 min hydrolysis period. To investigate the condensation occurring during the hydrolysis period, the concentration of molybdenum blue active species was measured over a 15 min period. Surprisingly, over the 15 min hydrolysis period no condensation was detected. It should be noted that the molybdenum blue assay can only detect monomer and dimmers. When larger dilutions were employed to increase the pipetting volume this introduced a mixing variable which also reduced the accuracy. Since dimers have been shown to rapidly dissociate to the monomer under acid conditions, condensation may be occurring but it is undetectable using the molybdenum blue assay. Physical evidence suggests that condensation is definitely occurring since after 24 h the 1 M TMOS solution gels. ^{29}Si was used to investigate the condensation reaction. Figure 2.11.1.1a shows the ^{29}Si NMR of a 1 M solution of TMOS in 99.5 % ethanol. The solution is stable, no condensation occurs. The single peak at -78.3 ppm is that of $Si(OCH_3)_4$ and was collected over a 20 min period. The instrumental settings were then optimised to maximise the intensity of the ^{29}Si peaks. Figure 2.11.1.1b shows the spectra collected from 7.5 to 15 mins where it can be seen that the peak at -72.3 ppm can be attributed to Q^0 species and the peak at -81.6 ppm can be attributed to Q^1 species. Reported values were -73 to 73.5 ppm and *ca.* -82 ppm respectively for monomer and dimer and linear trimer respectively.

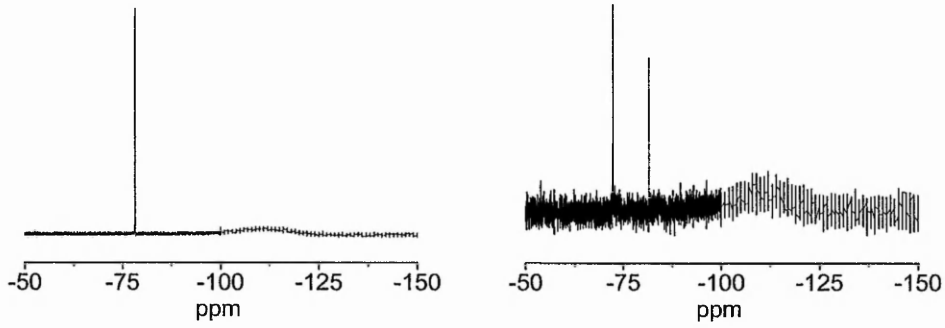

Figure 2.11.1.1a) – ^{29}Si NMR spectra of TMOS in ethanol, b) – spectra collected between 7.5 and 15 mins showing Q^0 and Q^1 species.

The presence of Q^1 species in the ^{29}Si NMR spectra clearly illustrates that condensation is occurring during the hydrolysis period and shows the hydrolysis period generates a mixture of silicon species. Unfortunately it has not been possible to perform the same experiment using KSiCat due to solubility issues, however, Belton has studied the dissociation of KSiCat using ^{1}H NMR.[9]

The complete hydrolysis of TMOS was investigated using proton NMR Figure 2.11.1.2 shows the calibration curve obtained from the methanol standards. The TMOS solution (30 mM immediately after neutralisation) was analysed after the methanol standards. Results indicated that the TMOS was completely hydrolysed by comparison of the amount of methanol in solution with the theoretical value.

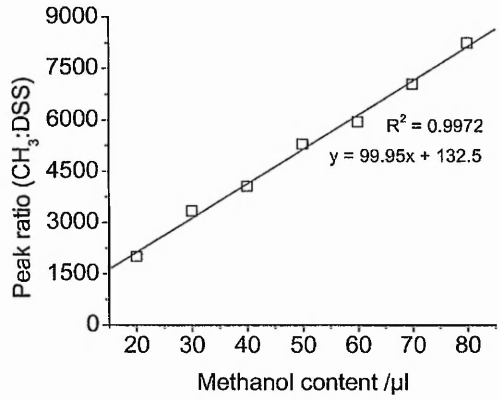

Figure 2.11.1.2 – Calibration curve for the methanol content for determining the release of methanol from the hydrolysis of TMOS.

2.12 The kinetics of silica formation

The kinetics of the 30 mM KSiCat and TMOS condensing systems in aqueous solutions were investigated using the molybdenum blue method over a 15 min period. The kinetics of the TMOS system were analysed in a similar way to the KSiCat system.[8] Figure 2.12.1 shows the average 3rd order and reversible 1st order rate constants established over 5 assays. The 3rd order rate constants were established over the first 190 s. The linear region over which the 3rd order rate constant is calculated extends from 30 s longer than in the KSiCat system, probably because of the mixture of species generated by the hydrolysis period in the TMOS system.

a)

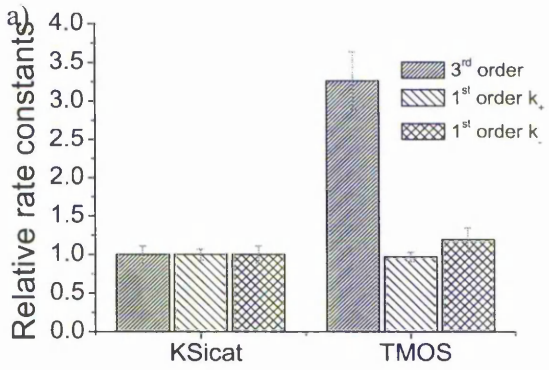

b)

Precursor	TMOS			KSiCat		
Rate constant	3rd order	1st order k_+	1st order k_-	3rd order	1st order k_+	1st order k_-
Average	$4.23 \cdot 10^{-06}$	$1.29 \cdot 10^{-03}$	$1.32 \cdot 10^{-04}$	$1.03 \cdot 10^{-06}$	$9.39 \cdot 10^{-04}$	$9.71 \cdot 10^{-05}$
Standard deviation	$4.88 \cdot 10^{-07}$	$7.99 \cdot 10^{-05}$	$1.72 \cdot 10^{-05}$	$1.13 \cdot 10^{-07}$	$6.57 \cdot 10^{-05}$	$1.03 \cdot 10^{-05}$
% error	11.53 %	6.21 %	13.02 %	11.00 %	7.00 %	10.60 %

Figure 2.12.1 a) – Comparison of the kinetics of the 30 mM KSiCat system with 30 mM TMOS system. b) The rate constants for the 30 mM KSiCat and TMOS systems.

The 3rd order rate constant was found to be 3.26 times faster in the TMOS system, which will be discussed later. The reversible first order kinetics remained statistically unchanged. The reversible 1st order rate was determined over a common time period (240-540 s) although the linear region extended for a longer period of time in the KSiCat system. The 1st order rate constant describes the formation (k_+) and dissolution (k_-) of oligomers and higher species. Although the rate constants for both systems are similar in magnitude it should be noted in the TMOS system there is approximately 25 % less silicic acid after 240 s when the first order kinetics begins in the TMOS system. One might hypothesise that the significant differences in the rates of reaction are due to the counter ions and molecules present in the respective systems. Catechol is known to aid the dissolution of silica and as such it would not seem unreasonable to hypothesis that the presence of 90 mM of catechol

in the KSiCat system could significantly reduce the 3rd order rate constant.[12]

2.13 The role of counter ions and by products in the formation of silica.

The role of counter ions, catechol and methanol were investigated by adding 90 mM of catechol and 60 mM of KCl to the TMOS system. The effect of methanol was also was also investigated by adding 120 mM of methanol to the KSiCat system, the results are shown in Figure 2.13.1.

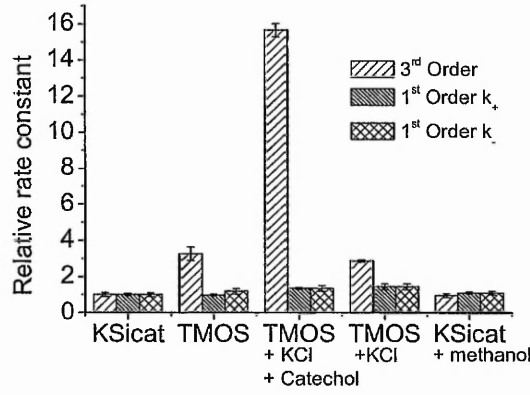

Figure 2.13.1 – The effect of counter ions and molecules on the kinetics of silica formation, relative rates are shown with respect to the 30 mM KSiCat system.

Methanol has no statistically significant effect in the KSiCat system. The role of KCl and catechol in the TMOS system increases the kinetics of the TMOS system by 15 times, when compared to the KSiCat and 3.26 times when compared to the TMOS system. Interestingly, the presence of KCl alone has no statistical effect on the 3rd order rate constant when compared to blank TMOS system. The influence of KCl and catechol on the kinetics of silica formation in the TMOS system is to increase the rate constants; therefore we can conclude it is not the presence of the KCl and catechol in the KSiCat system that reduces the rate of silica formation. Instead the change in pH with respect to time in the respective model systems has been investigated.

2.14 Investigating the neutralisation, dilution and formation of the 30 mM aqueous solutions containing orthosilicic acid.

The pH or the concentration of H^+ ions in solution is known to have a significant effect on the rate of condensation in a supersaturated solution of silicic acid.[1] Therefore, since the two systems start at opposite ends of the pH scale immediately after neutralisation (KSiCat is basic but immediately after neutralisation it becomes acidic and TMOS is hydrolysed in acid conditions but immediately after neutralisation remain basic), this might be responsible for highly significant differences in the 3rd order rate constants. Figure 2.14.1 shows the pH profiles of the respective model systems upon neutralisation. The KSiCat system is initially basic, upon the addition of a known amount of HCl to the system the dipotassium tris(1,2-benzenediolato-*O,O'*)silicate complex dissociates within approximately 20 s.[9] However the pH of the system does not reach 6.6 (the lowest pH defined as acceptable for kinetic analysis) until *ca.* 120 s. The TMOS system by comparison is acidic and is injected into the neutralising system (which is basic) the system reaches pH 7 (the highest pH defined as acceptable for kinetic analysis) in approximately 48 s. The additional time period for KSiCat to reach pH 6.8 ±0.2 (quality control limits) is therefore likely to be responsible for the observed difference in 3rd order kinetic rates between the two systems and is indicative of the buffering effect caused by catechol. Secondly it is also important to note that KSiCat approaches an equilibrium pH from low a pH value and the TMOS system approaches equilibrium from high pH. The rates of silicic acid condensation are known to increase initially from circumneutral pH to higher pH values and reduce at higher pH values and reduce from circumneutral pH to acidic conditions.[1] It is therefore hypothesised that this is an essential factor when trying to explain the differences observed in the 3rd order rate constants.

a)

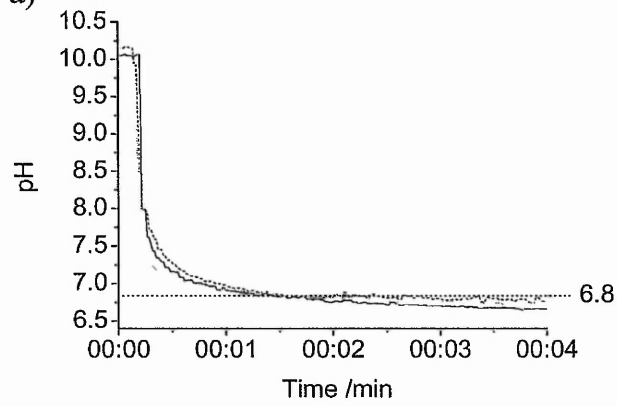

Precursor	TMOS			Average	Std. deviation
Time to 6.8 ±0.2 /s	47	56	40	48	8.02

b)

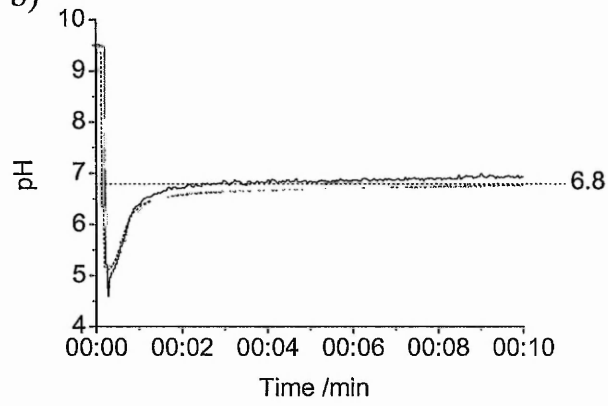

Precursor	KSiCat			Average	Std. deviation
Time to 6.8 ±0.2 /s	76	127	121	108	27.87

Figure 2.14.1 – Comparison of the time taken for TMOS to reach pH 7 the earliest and KSiCat to reach pH 6.6, both systems would therefore satisfy the criterion set for the kinetic results to be accepted. Both systems tend to 6.8 in the time period shown and fluctuate inline with the tolerance of the pH meter used after this time, where the pH remains within tolerance of 6.8 ±0.2.

2.15 Investigating the rates of particle aggregation and the effect of counter ions and methanol.

The aggregation characteristics of the two model systems were investigated using DLS. The TMOS system did not exhibit any measurable particle size by DLS, however, when the TMOS system was investigated in the presence of KCl (60 mM), aggregation was observed and the rate was found to be similar to that of the KSiCat system as shown in Figure 2.15.1. The presence of 90 mM catechol was also investigated where aggregation was also observed but at a significantly slower rate than KCl in the TMOS system. The inclusion of KCl and catechol in the TMOS system at the same concentration as in the KSiCat system showed aggregation as expected. However, the rate was slightly faster in the KSiCat system, this might be indicative of the presence Q^1 species present in the ^{29}Si NMR as shown earlier in Figure 2.11.1.1. When the role of methanol was investigated in the KSiCat system at a concentration of 120 mM rate, aggregation was found to reduce suggesting that the difference in rates of aggregation between KSiCat and TMOS with KCl and catechol might be more prominent if one could remove the methanol from the TMOS system. The role of a 100 mM phosphate buffer in the TMOS system as used in several biomimetic and bioinspired studies was also investigated. It was found that a sodium phosphate buffer also aided aggregation in the TMOS system. It can conclude from this section of work that the unbuffered TMOS system developed in this study does not exhibit aggregation probably due to the low concentration of counter ions. The addition of salts to the system probably causes surface charge neutralisation and thus aggregation can occur as reviewed by Iler.[1]

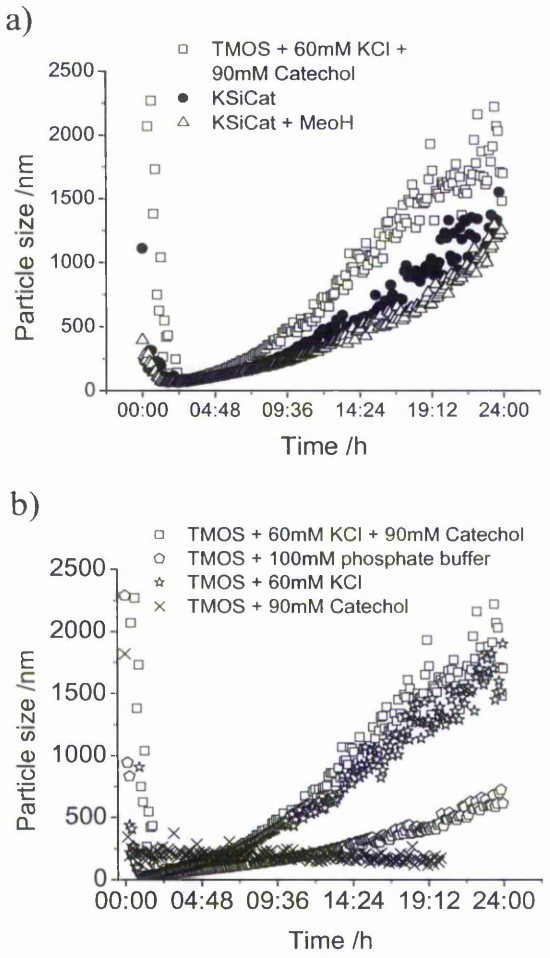

Figure 2.15.1 – a) DLS of TMOS in the presence of salts and KSiCat in the presence of methanol and without. b) Investigation into the effect of KCl and catechol on the TMOS system.

2.16 Materials Characterisation

The materials produced from the aggregation studies above were isolated by centrifugation and washed with water 3 times to ensure the removal of any counter ions not entrained within the material and then freeze dried. This was not possible for the TMOS system in the absence of salts, instead the TMOS solution was freeze dried. The material produced after freeze drying was then washed 3 times with dd water for a comparison to the materials where aggregation has been observed. The gas adsorption results are shown in Figure 2.16.1) where interestingly it can be seen

that the washed TMOS material shows a significantly higher surface area than that of the unwashed material, possibly indicating the removal of KCl from the material. The material produced in the presence of KCl and catechol using TMOS shows very similar properties to the KSiCat blank system which it was designed to mimic, providing indirect evidence that the presence of methanol in the TMOS system has no significant effect on the formation of silica. The same conclusion was drawn from the results when KSiCat was studied in the presence of methanol; no significant change in the material produced was observed when comparing it to the KSiCat blank.

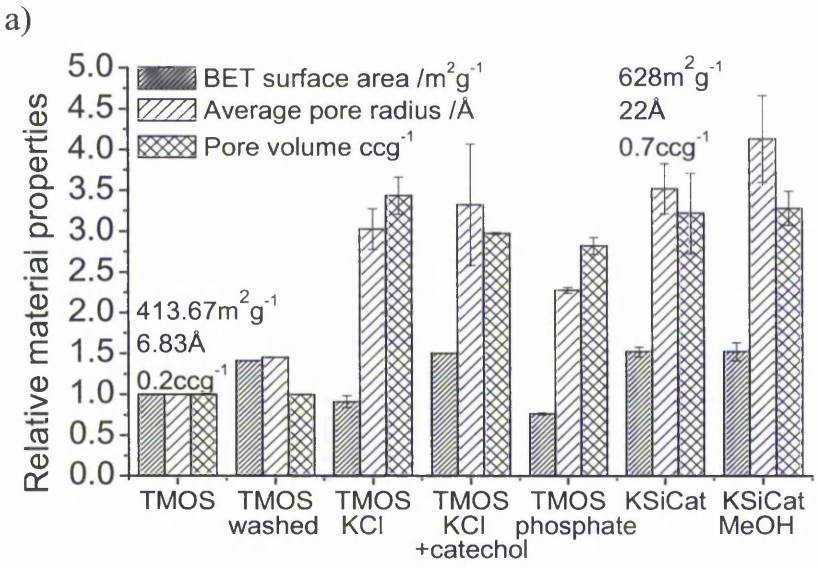

Figure 2.16.1a) Material characterisation by nitrogen gas adsorption.

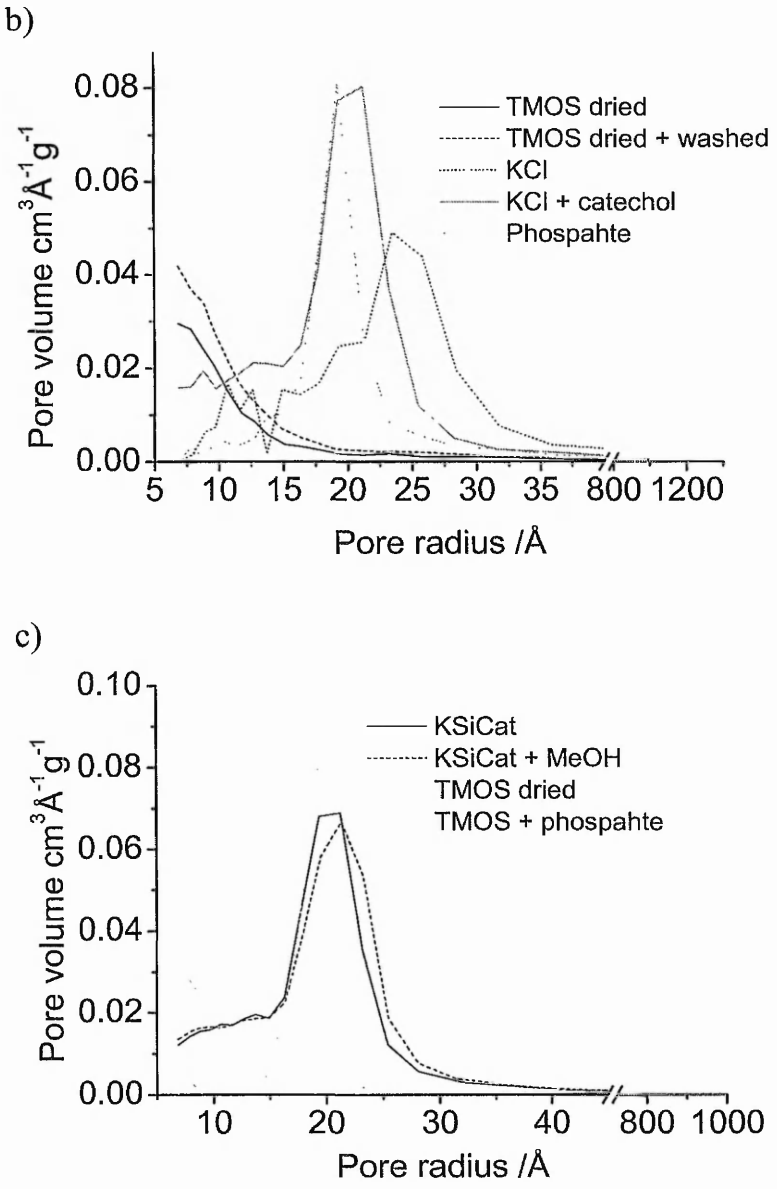

Figure 2.16.1 cont. b) Pores size distribution plot of the TMOS system and inclusion of counter ions. c) Pore size distribution ploy showing the inclusion of methanol in the KSiCat system and the TMOS system in the absence and inclusion of phosphate buffer.

Figure 2.16.1b shows the porosity distribution of the materials produced when studying the effect of counter ions in the KSiCat system. The data shows an increase in the porosity when comparing the freeze dried TMOS system to washed TMOS system. This indicates that by washing the material more of the pores have

become available increasing the surface area of the material, this suggests that these pores were full of KCl previously crystallised in the drying process and formed from the HCl present when hydrolysing the TMOS and the KOH used to neutralise the acidic hydrolysing system. The inclusion of KCl in this system drastically changes the porosity of the system such that a wide pore size distribution centring about at *ca.* 23.5 Å is produced. The change in porosity can perhaps be attributed to interactions between negatively charged silicon species and positively charged potassium ions. Interestingly, when KCl and catechol are studied in the TMOS system the pore size becomes more uniform, shown as a reduction in peak width in Figure 2.16.1b and centres at about *ca.* 21.2 Å. Introduction of a mono basic sodium phosphate buffer (100 mM) to the condensing TMOS system tightens the porosity distribution of the material still further which centres at about 19.3 Å. Interestingly, the change in porosity can be compared for sodium phosphate system, KCl and the KCl and catechol system. The porosity change could be attributed to the change in counter ion from K^+ in the KCl systems to Na^+ in the buffered system. The results seem to suggest that there could be a relationship between the type of counter ion, the concentration of the counter ion and the porosity exhibited by the silica produced. This effect has previously been reported by Harrison *et al.* where cations were shown to control the porosity of silica using different counter ions in tris(1,2-benzenediolato-*O,O'*)silicates.[25] However, pore sizes were substantially larger in the tris(1,2-benzenediolato-*O,O'*)silicate systems than those exhibited in this study and furthermore the concentration of the counter ion is dependent on the tris(1,2-benzenediolato-*O,O'*)silicate used. Moreover, in the TMOS system we can examine the effect of catechol by comparing the TMOs system to the KSiCat system. It was concluded that the introduction of catechol to the system reduces the pore size of the silica when compared to the TMOS with just KCl.

The presence of methanol in the KSiCat system has no significant effect on the porosity of the material produced when compared to the KSiCat blank as shown in Figure 2.16.1c. Comparison of the KSiCat blank system and the TMOS system in the presence of KCl and catechol shows remarkably similar porosity centring about;

21.39 and 21.25Å respectively.

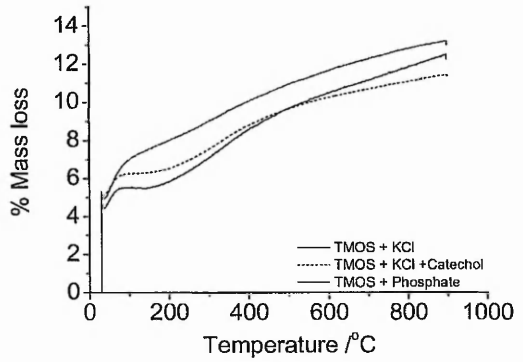

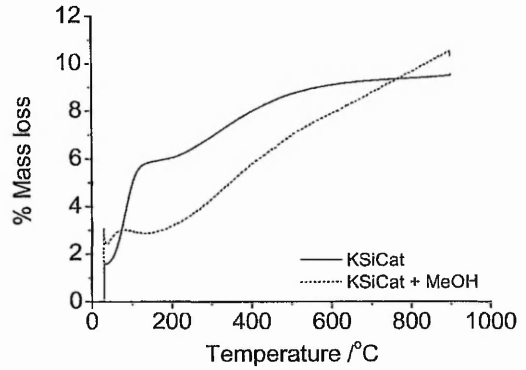

Precursor	TMOS				
Additive	Dried	Washed + dried	KCl	KCl + Catechol	Phosphate
% Mass loss between 400 and 850 °C	2.84	1.58	3.61	2.47	2.98

	% Mass loss between 400 and 850 °C
KSiCat	1.38
KSiCat + MeOH	4.35

Figure 2.16.2 – Thermal gravimetric analysis (TGA) of materials produced using the KSiCat and TMOS precursors with different counter ions and by products from the respective systems.

Thermal gravimetric analysis was performed on the samples; the results are presented in Figure 2.16.2. Unsurprisingly, the samples contained very little organic material. The silica prepared using the TMOS system was a brilliant white compared to the silica prepared using KSiCat which has a brown tinge to it thought to be because of catechol that has hydrolysed and become entrapped within the material. The organic material entrapped within a matrix is usually seen as mass loss above 400 °C mass loss prior to 400 °C being designated as physisorbed and chemisorbed water. The organic mass loss has been tabulated in Figure 2.16.2 for the materials produced during this study. The TMOS materials contain similar amounts of entrained organic material as the materials produced using the KSiCat system; this is unexpected as the KSiCat quite clearly has a catechol derived species entrained within it from its colour prior to thermal analysis. The TMOS derived silica one assumes would have very little or no organic material entrained within its structure as hydrolysis removed the methoxy group, producing methanol. The only explanation for the entrained organic material in TMOS would appear to be methoxy groups that have not been hydrolysed from TMOS structure. Organic material that is chemically bound to the silica is expected to be removed between 450 and 650 °C.

2.17 Conclusions

This section establishes a new method for analysing the kinetics of silica formation using an unbuffered TMOS system. This comprehensive study on the formation of silica using this system and compared the kinetics, aggregation and characterised those materials using a number of key techniques involved in studying the formation of silica *in vitro*. The key characteristics of the two systems are characterised in Figure 2.17.1.

Kinetics

Precursor	TMOS			KSiCat		
Rate constant	3^{rd} order	1st order k_+	1^{st} order k_-	3^{rd} order	1st order k_+	1^{st} order k_-
Average	$4.23 \cdot 10^{-06}$	$1.29 \cdot 10^{-03}$	$1.32 \cdot 10^{-04}$	$1.03 \cdot 10^{-06}$	$9.39 \cdot 10^{-04}$	$9.71 \cdot 10^{-05}$
Relative rate constants	3.26	0.97	1.19	1	1	1

Aggregation

Final particle size	NONE	1500 nm
Time to reach nm_f	NONE	24 h

Materials characterisation

BET surface area /m^2g^{-1}	413	628
BJH Average pore radius /Å	6.83	22
BJH Average pore volume /cm^3g^{-1}	0.2	0.7
% Entrained Organics	2.84	1.38
Primary species	Mixture Q^0 and Q^1 species	$Si(OH)_4$ Q^0

Figure 2.17.1- Summary of the chemical and physical properties of TMOS and KSiCat model systems.

The characterisations of the model systems used throughout this study has enabled detailed comparisons to be made between additives studied *in vitro* throughout this thesis. Furthermore by exploiting the properties of the respective model systems it has been possible to gain a significant insight into the role of the counter ions and by products formed from each of the silica precursors. The role of KCl in the KSiCat system is to aggregate negatively on the silica particles making aggregation energetically favourable. The sodium and potassium cations netraise the surface charge neutralisation mechanism has been established. Detailed investigations were not carried out, but potentially the data suggests relationship between the type of cation used and the porosity of the material produced. Furthermore, there may also

be a relationship between the ionic strength and the pore size distribution of the material produced; this will be investigated further where necessary.

The work presented in this chapter will serve as a foundation for the work that follows where the role of small molecules in silica formation will be dealt with as well as the underlying molecular interactions that dictate the physical and chemical properties of the silica produced. The work is not especially novel however it does highlight the importance of understanding the model system employed and the molecular interactions that can occur especially when using a buffer to control the pH in the TMOS system. Establishing a method for studying the effect of counter ions in silica formation will allow subsequent investigations on the role of additives in silica formation to be carried out in a more comprehensive manner and aid in our studies of the molecular interactions between additives and silicon species during silica formation.

References

1. R. K. Iler, *The Chemistry of Silica* John Wiley & Sons, New York, 1979.
2. L. L. Hench and J. K. West, *Chem.l Rev.*, 1990, **90**, 33-72.
3. G. W. Scherrer and C. J. Brinker., *Sol-Gel science - The physics and chemistry of Sol-Gel Processing.*, Acedemic Press, London, 1990.
4. S. V. Patwardhan, S. J. Clarson and C. C. Perry, *Chemical Commun.*, 2005, 1113-1121.
5. M. Sumper and N. Kröger, *J. Mater. Chem.*, 2004, **14**, 2059-2065.
6. R. Tacke, *Angew. Chem. Int. Ed.*, 1999, **38**, 3015-3018.
7. S. V. Patwardhan, C. Raab, N. Hüsing and S. J. Clarson, *Silicon Chem.*, 2003, 279-285.
8. C. C. Harrison and N. Loton, *J. Chem. Soc. Faraday Trans.*, 1995, **91**, 4287-4297.
9. D. Belton, The influence of small molecules on the precipitation of silica, Nottingham Trent University, 2005.
10. S. Brunauer, P. H. Emmett and E. Teller, *J. Am. Chem. Soc.*, 1938, **60**, 309.
11. E. P. Barrett, L. G. Joyner and P. P. Halenda, *J. Am. Chem. Soc.*, 1951, **73**, 373.
12. P. Bennett and D. I. Siegel, *Nature*, 1987, **326**, 684-686.

Chapter 3 - The Role of Organic Molecules in the Stability of Silicon Species in Unsaturated Systems: *Implications for biological and bioinspired silicification*

3.1. Introduction

The aqueous chemistry of silica and silicic acids, dissolution and precipitation in particular, is of interest to a wide scientific community due to its impact on the biological, geological and chemical cycle of minerals. Hence it is important to understand the stability of various silicon species under a range of conditions of silicon concentration, pH and the presence of inorganic and organic ions. For example, biosilicification, where precipitation of silica to form remarkable nano-patterned materials occurs under ambient conditions and is genetically controlled, has been an inspirational source in the development of new silica based materials and the mechanisms involved in the uptake, stabilisation and precipitation of silicon (in some form) has attracted attention recently.[1, 2]

The biosilica cell wall (frustule) found in diatoms is synthesised from silicic acid found universally in water at unsaturated levels.[3] The formation of the frustule occurs in intracellular compartments called the silica deposition vesicle (SDV), where it has been shown that silicon is accumulated from the surrounding unsaturated environment (in an as yet unknown form) at supersaturated concentrations between 19 and 104 mM.[4] Biosilicas are inorganic-organic hybrid materials and the organic phase has been isolated from several higher plants, sponges and diatoms. Several classes of biomolecules have been isolated from silicified diatom cell walls including silaffins[5] and long chain polyamines (LCPA).[6] Silicatein, a central protein filament has been extracted from sponge spicules (*Tethya aurantia*)[7] and glycoproteins have been extracted from *Phalaris canariensis*, *Phragmites* and *Equisetum telmateia*.[8, 9] The molecules extracted from silica accumulating organisms have been investigated for their effects on silica formation *in vitro*. Structural control has been observed where

spheres of specific diameters can be formed when, silaffins and LCPA extracted from diatoms are added to pre-hydrolysed solutions of tetramethoxysilane (TMOS).[1] Silicatein protein filaments have been shown to catalyse the hydrolysis of tetraethoxysilane (TEOS) *in vitro*, where silica is deposited on the filament surface.[10, 11] Biomolecules extracted from the siliceous phase in *Equisetum telmateia* were studied *in vitro* using a silicic acid precursor; dipotassium tris(1,2-benzenediolato-*O,O'*)silicate, where crystalline silica was formed under ambient conditions and circumneutral pH.[12] The identification of specific molecular and structural features observed in biomolecules extracted from silica accumulating organism has enabled the development of bioinspired additives to be studied *in vitro*.

The role of additives in silica formation has been comprehensively reviewed recently where bioinspired and biomimetic additives control *in vitro* silica formation by one or more key processes. It was hypothesised that additives can (i) catalyse condensation reactions, (ii) influence aggregation and/or (iii) act as scaffolds for silica formation[13]. Common amine functionality exists between most of the additives that have exhibited a significant effect on the formation of silica. Amino acids,[14-17] small amine containing molecules (less than 1 kDa)[14, 15, 18-22] and polyelectrolytes[23, 24] have been specifically studied as model systems to gain an understanding of each moiety exhibited by the biomolecules thought to control silicification *in vivo*. Many of the additives studied, small molecules in particular, exhibit drastic effects on silica formation *in vitro*. In order to explain such behaviour, several mechanisms have been suggested. For example, Sumper *et al.*[25] proposed a mechanism for the condensation of silicic acid molecules in the presence of propylamines, where the formation of hydrogen bonds between an unprotonated amine group and silicic acid catalyse silicic acid condensation. On the other hand, Belton *et al.* proposed the condensation of a silicic acid molecule on silica particles mediated by an amine adsorbed on the particle.[21] The fundamental difference between the two mechanisms being the silica species involved, *i.e.* condensation between two silicic acid molecules proposed by Sumper *et al.* and Belton *et al.* proposed that condensation occurring between a surface silanol group and a molecule of silicic acid.[21, 25]

Silicic acid, the soluble form of silica and silicates, has been reported to occur at unsaturated levels (*i.e.* <2 mM or 100 ppm) between 5-15 ppm (5.2-15.6 μM) in sea

water and 5-35 ppm (5.2-36.4 μM) in fresh water.[3, 26, 27] The stability of silica is dependent on the molecular and physical characteristics of the material, including crystallinity, surface chemistry, surface area and particle size. The dissolution of amorphous silica and quartz has been studied extensively to investigate the transport of silica from mineral to aqueous reservoirs in the silicon biogeochemical cycle.[28] The dissolution of silica in aqueous solution is a depolymerisation reaction that is typically catalysed by hydroxide ions. Numerous examples exist in the literature where organic compounds such as acids and catechol (1,2-dihydroxybenzene) and related compounds have been shown to increase the amount of monosilicic acid present and the rate of dissolution of quartz,[26, 29, 30] although no direct evidence of organo-silicon interactions have been specifically identified in natural waters.[31] Organic rich environments such as soils, sediments and oil field formation waters, often contain higher amounts of monosilicic acid.[31]

The involvement of organic molecules in the dissolution and deposition of silica alters the stability of silica species thereby shifting the equilibrium between silicates and their soluble form (silicic acid). This forms a rationale for the first part of this study. Firstly, the role of organic molecules, derived from biosilicifying organisms, in an unsaturated environment with respect to silicic acid. From the literature on bioinspired silicification as summarised above, it can be noted that all the studies were performed using silicic acid at supersaturated concentrations (typically 30 mM or 100 mM). However, no attempts have been made to study the roles of additives in unsaturated silicic acid solutions, even though the silicon concentration in natural waters is unsaturated.

This aim of the present study is to investigate the stability of silica species at unsaturated silicic acid levels with and without the presence of additives and to identify the silica species towards which the additives are active (*i.e.* "active" silica species). The ultimate goal is to investigate if we can alter the stability of silica species in solution in a controlled fashion. The silica precursors used for *in vitro* studies vary greatly from an ethyleneglycol modified silane (tetra(2-hydroxyethyl)orthosilicate), alkoxysilanes (TEOS and TMOS), sodium silicate and dipotassium tris(1,2-benzenediolato-*O,O'*)silicate, each having their own advantages and disadvantages. The principal difference between the precursors is the generation

of different precursor mixtures of silica species. For instance, tetramethoxysilane (TMOS) requires a hydrolysis period under acid conditions for silicic acid to be produced. Here lies the principal problem, upon the hydrolysis of several methoxy groups, condensation reactions can occur. Furthermore it is also possible that a molecule of TMOS may not undergo complete hydrolysis, creating a mixture of species that are all capable of condensation reactions. It therefore becomes important to know the population of silica species in a given sample and more importantly, behaviours and interactions with of these organic additives.

In order to investigate aforementioned aspects, three distinct approaches have designed and are explained below. In the first approach, only one silica species – orthosilicic acid was studied. At supersaturated concentrations, rapid silica formation occurs in the presence of bioinspired additives. In the experiments discribed below, the effects of additives at unsaturated silicic acid concentrations are studied. In the s approach, a supersaturated solution of silicic acid was allowed to condense for a given time in the absence of any additives. This generates a mixture of silica species; the population balance depends on the pre-condensation time. This solution was then diluted to 1 mM (*i.e.* unsaturated concentration of silicon) containing a mixture of silica species and the stability with and without the presence of additives was studied. In the third approach, the stability of silica particles was studied in the presence of additives. It is believed that the results obtained will help better understand the stability of silica species and the molecular interactions between silica species and organic additives.

3.2. Experimental

3.2.1. Materials

Dipotassium tris(1,2-benzenediolato-*O,O'*)silicate (97 %, Aldrich) and commercial silica, Gasil 23D (Ineos) were used as the sources of silica. The former was purified by dissolving in methanol followed by separation by filtration to remove an insoluble fraction with removal of methanol by rotary evaporation. The purity of the silicon catecholate complex was confirmed with ^{1}H NMR using a Jeol ECX-400 spectrometer and the molybdosilicate assay to >99 %. The additives used were poly-

(L-lysine) (PLL, MW 22100 g mol^{-1}), poly(allylamine hydrochloride) (PAH, MW 15000 g mol^{-1}), poly(ethylenimine) (PEI, MW 25000 g mol^{-1}), diaminoethane, 97 % (DAE), diethylenetriamine, 99 % (DETA), triethylenetetramine, 97% (TETA), tetraethylenepentamine, 98 % (TEPA), pentaethylenehexamine, (PEHA) and 1,10-diaminodecane, 97 % (1,10 DA), (all of which were purchased from Aldrich). In addition, dipropylenetriamine, (N3) and tetrapropylenepentamine, (N5) were also used as additives. These molecules were synthesised in house; the purity was confirmed to be 99 % by NMR studies.[22] Experiments to study the stability (dissolution and precipitation) of silicic acid, polysilicic acids and silica species (together termed as "silica species") were undertaken using the three methods as detailed below.

3.2.2. Unsaturated Solution Studies: Method I.

Solutions of silicic acid (1 mM) were made by dissolving 0.466 g, 1 mM of dipotassium tris(1,2-benzenediolato-*O,O'*)silicate in of dd water (950 ml). A predetermined amount of 2 M HCl (800 µl) was then placed into a separate plastic *vial* and made up to 50 ml with dd water. Addition of the acid solution to the dipotassium tris(1,2-benzenediolato-*O,O'*)silicate dissociates the complex to yield one litre of a solution of silicic acid (1 mM) at pH 6.8 ±0.2.

The organic amines were dissolved in the acid containing solution and added as the hydrochloride to the 1 mM KSiCat solution. The total starting volume of the system was kept constant at 1 litre ±1 cm^3. The additives were studied using a Si:N ratio of 1:1 or 1:6 and the free silicic acid was monitored over a period of 30 h using a modification to the molybdenum blue method, as previously reported.[32]

At predetermined times, aliquots (200 µl) were taken and placed into a solution of molybdic acid solution (16.5 ml). The molybdic acid solution was left for 15 mins to allow any dimers to dissociate to monomers and react with the molybdic acid to form a silicomolybdic acid complex. The silicomolybdic acid complex was reduced to silicomolybdous acid and left to stand at room temperature. After approximately 24 h, an aliquot was transferred to a polymethacrylate cell and the absorbance measured at

810 nm using a Unicam UV/Vis UV2 spectrometer. These results were compared to typical calibration data to obtain an accurate measurement of the concentration

3.2.3. A study of pre-condensed silica solutions followed by dilution to 1mM silica (termed "*pre-condensed unsaturated*" solutions): Method II.

Dipotassium tris(1,2-benzenediolato-*O*,*O'*)silicate (0.56 g) was dissolved in of dd water (40 ml) and 2 M HCl (990 µl) was added to create a solution of silicic acid at pH 6.8 ±0.2 were prepared using as described previously.[32] The solutions were allowed to condense for a predetermined amount of time (depending on what pre-condensation time was to be studied) and then diluted to 1 mM using dd water.

The additives studied are listed in section 3.2.1 above. The Si:N ratio studied was 1:6 unless otherwise stated. The additives were dissolved in water (50 ml) and titrated to pH 6.8 using 1 M HCl or 1 M KOH depending on the additive (PAH, TETA, TEPA was purchased as the hydrochloride and required base to adjust the pH to 6.8). This solution was then diluted to 500 ml. The precondensed silica was then intially diluted to 2 mM by taking 33.33 ml (1 mM) of precondensed silica solution and diluting with dd water to 500 ml using a volumetric flask. This solution was then immediately poured into the additive contain solution (previously diluted to 500 ml) to make the complete dilution to 1 mM. Complete dilution from 30 mM to 1 mM took 40 s, to ensure homogeneity the sample was stirred for the first five mins. The molybdenum blue method was used to monitor the dissolution of the silica species in solution as previously described in section 3.2.2. Silica precipitates were isolated by centrifugation at 3000 R.P.M. using a Sorvall RT7 plus centrifuge and washed 3 times with dd water and lyophilized prior to further analysis.

The effect of PEHA at a ratio of 1:6 Si:N on pre-condensed silica systems was studied in greater detail. Pre-condensation times between 3 and 160 mins prior to dilution were investigated. The concentration of silicic acid was monitored immediately after dilution and thereafter using the molybdenum blue method described previously.

The precipitation of silica could not be monitored by photon correlation spectroscopy due to an insufficient number of scattering species in solution. Instead an alternative semi-quantitative approach was undertaken, whereby the total amount of silicon remaining in solution was measured. Upon mixing an additive solution and a pre-condensed silica solution, 2 ml portions of the resulting solution were pipetted into 2.5 ml eppendorf tubes and left to stand. At pre-determined reaction times, samples were centrifuged for 1 min at 15000 R.P.M. in a Sanyo micro centaur. This approach meant that particles aggregated by additives were compacted at the bottom of the tube. A 1 ml portion of the supernatant was then taken and mixed with 2M NaOH (1 ml) immediately after centrifugation and the sample were then heated to 80 °C for 60 mins to ensure complete digestion to molybdenum blue active species. The NaOH (200 µl) digested supernatant was taken and the concentration of silicic acid measured using the molybdenum blue assay.

3.2.4. The dissolution of commercial silica: Method III

A suspension of commercial silica (1 mM) was prepared in the presence of the additive to be studied (the molecular weight of the silica as SiO_2 was estimated to be 60, as the silica had been prepared by pyrolysis). Solutions of the bioinspired additives (Si:N ratio 1:6) were prepared and the pH adjusted to 6.8 ±0.1 using 2 M HCl, the final volume was 1 litre ±1 cm^3. The solutions were sealed and allowed to equilibrate overnight whilst stirring at 675 ±5 R.P.M. using a 15 place stirrer in a water bath at 25°C ±2 °C, and the concentration of silicic acid monitored with respect to time over a period of 5 *ca.* 15 days.

3.3. Materials characterisations

Electron microscopy was carried out on lyophilized samples using a Jeol JSM-840A Scanning Electron Microscope. Nitrogen gas adsorption/desorption analysis was carried out on lyophilized samples using a Quantachrome Nova 3200e surface area and pore size analyzer. Prior to analysis, samples were degassed overnight at 130 °C under vacuum. Surface areas were then determined *via* the BET method where nitrogen is assumed to have a cross-sectional area of 0.16 nm^2,[33] over the range of relative pressures 0.05 – 0.3 at which point the monolayer is assumed to assemble.

Pore radii were determined by the BJH method using the desorption branch of the isotherm.[34] Thermal gravimetric analysis was carried out on selected samples using a Perkin Elmer Pyris 6 TGA. The samples were heated at 10 °C min^{-1} from 30 to 900 °C in air to ensure complete combustion of all organic material retained within the material. FTIR analysis was conducted using a Magna IR-750 infrared spectrometer (Thermo Nicolet) on KBr pellets that contained 1 mg of sample and 200 mg of spectroscopic grade potassium bromide (KBr) that had previously been dried. The PEHA doped silica was prepared by dissolving PEHA into ethanol and mixing it with a known amount of Gasil silica (Ineos, calculated as SiO_2). The ethanol was left to evaporate at room temperature and KBr discs were made as described previously.

3.4. Results

3.4.1. Unsaturated silicic acid solution studies

The additives chosen for this study are all known for their ability to facilitate silica formation in supersaturated aqueous solutions of silica precursors.[19, 21, 35-37] In this study, the additives were studied in a unsaturated solution of silicic acid (1 mM). The silicic acid concentration was then monitored for *ca.* 24 h using the molybdenum blue method. The concentration of silicic acid remained constant irrespective of the additive used and the ratio of Si:N studied, Figure 3.4.1.1.

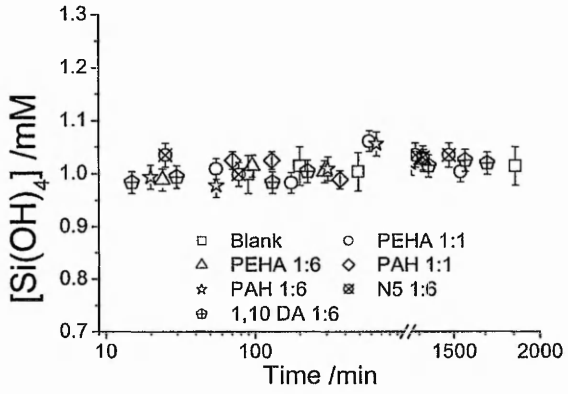

Figure 3.4.1.1 - Concentration of silicic acid with and without the presence of organic additives. Representative points for complete data series shown. Error bars show one standard deviation.

The additives chosen for study comprised; a) small amine functionalised molecules and b) amine functionalised polyelectrolytes that are known to be highly active in supersaturated condensing silica systems. Throughout the 24 h time period the additives at a Si:N ratio of 1:1 or 1:6 did not induce condensation in an unsaturated silicic acid environment. It is perhaps surprising to find that the organic additives known to promote silica formation at supersaturated silicic acid concentrations become inactive at unsaturated levels of the 1 mM silicic acid. This may suggests that the additives studied are not active towards the silicic acid monomer, but rather require the presence of higher mers and particles to act on. In order to investigate this hypothesis an experiment was undertaken where silicic acid was allowed to condense at a supersaturated concentration (30 mM) for a pre-determined time period in the absence of any additives. It was then diluted to a global unsaturated concentration of 1 mM with respect to total concentration of silicon. The effect of additives on the precipitation and dissolution of silica species with time was then studied on this diluted solution.

3.4.2. A study of pre-condensed solutions diluted to 1 mM without additives.

A pre-condensed solution of silicic acid (30 mM) was allowed to condense for different periods of time from 3 to 160 mins followed by immediate dilution to 1 mM to investigate the stability of silica species. The pre-condensation times were 3, 5, 7, 15, 60 and 160 mins and were chosen in order to represent a distinct collection of silica species based on our knowledge of the model condensing system. The information about these samples obtained from our previous studies is summarised below.[32, 38-40] At precondensation times <4 mins the trimerisation reaction dominates, thus 3 mins was selected to study trimers. After 5 mins it has been found by Liquid Chromatography Mass Spectroscopy (LCMS) that small particles and silicic acid dominates the spectrum up to 15 mins.[40] Thus, 5, 7 and 15 mins were chosen to study small particles and their stabilities. 1 nm particles are first observed by DLS after 60 mins and this determined the selection of the 60 min condensing time.[32] The 160 mins pre-condensation time was selected to investigate the stability of larger particles and the maturation process.

The concentration of silicic acid in solution was monitored after dilution to 1 mM initially for a 60 min pre-condensed silica systems in the absence of additives ("*blank*"). Surprisingly we found that the concentration of silicic acid increased with time, indicating that silica particles of *ca.* 1 nm as determined by DLS data[32] are not stable upon dilution to a silicon concentration of 1 mM (Figure 3.5.2.1, see below for detailed discussion). Thus, instead of dealing with a stable silica system, the stability of silica particles in an unsaturated system was investigated, and therefore the effect of organic additives on the dissolution of silica species was investigated. This is not considered as an equilibrium because under theses conditions the silica species react fully with water to form orthosilicic acid and since the concentration remains below the saturation point of silica there is no evidence to suggest a reverse reaction where silica could reform. Before studying the effects of additives we therefore sought to establish a baseline for which our investigation into the effect of additives on 1 mM pre-condensed silica system could be compared to. This was accomplished by extensive investigations of the "blank" system and the inclusion of 18 time points for analysis from 3 to 160 mins of pre-condensing time.

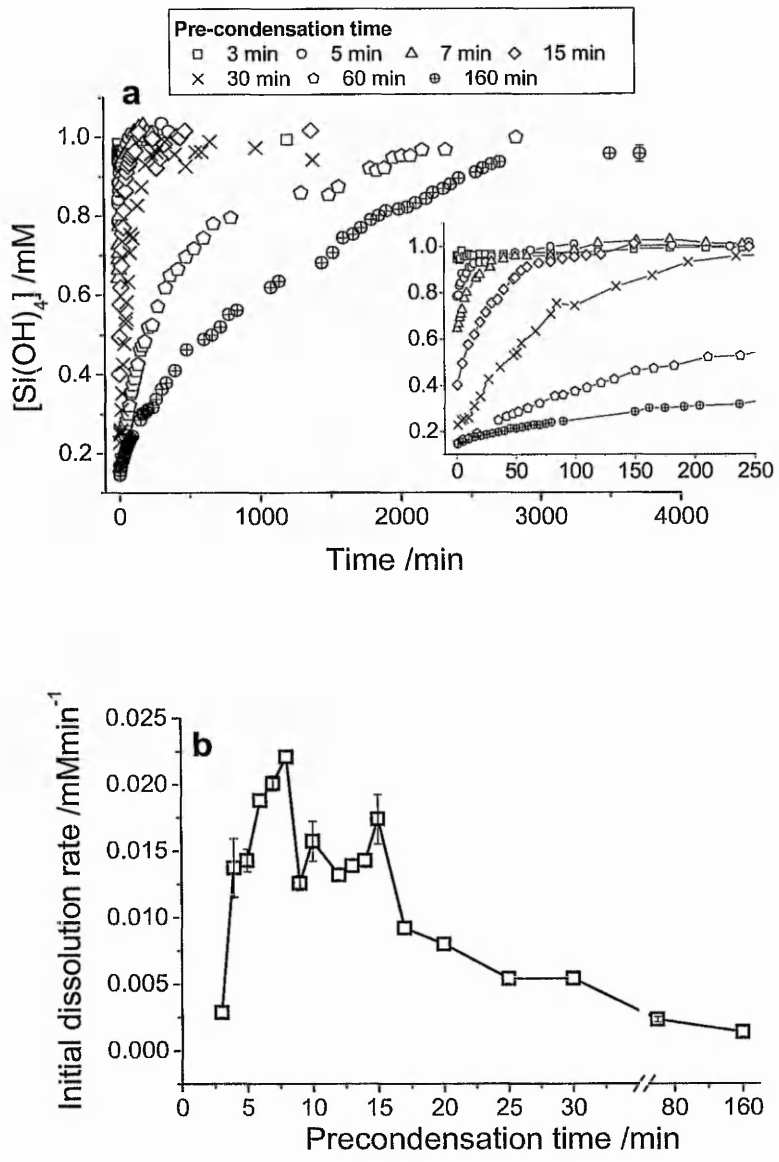

Figure 3.4.2.1a) – The dissolution of a 30 mM condensed silica system after dilution to 1 mM, b) The initial rate of dissolution of silica species when a pre-condensed system was diluted to 1 mM.

Figure 3.4.2.1a shows the dissolution curves for the different pre-condensation time which indicates that the stability of the silica species in solution rapidly changes even over a small time increment. The calculation of the initial rates of dissolution of the samples was performed in order to obtain information about the stability of the samples and is presented in Figure 3.4.2.1b. The data show that the initial rate of dissolution varies with precondensation time in a non-systematic manner. The initial rate of dissolution is representative of the stability and population of species present

in solution. The data suggest that the stability of the silica species reaches a minimum after 8 mins where the initial rate of dissolution is the fastest. Figure 3.5.2.1b shows an initial decrease in particle stability (an increase in initial rate of dissolution), suggesting trimers are more stable than other silica species created by condensation. This observation seems peculiar until one considers the equilibrium position at a pre-condensation time of 3 mins when a more feasible explanation can be proposed. The concentration of silicic acid at 3 mins condensation time is 0.94 mM. When one considers the reverse reaction: a silicon species dissociating to silicic acid, the initial concentration of free silicic acid at 3 mins will shift the equilibrium towards the formation of silica particles. Since the concentration of "silicon" is less than the solubility of "silicon" in water, this reaction is unfavourable. Instead the effect of the high silicic acid concentration will be to increase the time taken for equilibrium to be established. Thus as the condensation time increases, initially we see that the concentration of silicic acid in solution becomes less significant with increasing time. This explains the apparent initial decrease in stability when one would have expected an increase in stability to be observed.

As the condensation time is increased still further, other stability minima were observed at 9 and 15 mins, these could represent points where the silica species gain charge, generating a less stable higher charge density silica species. Further increases in condensation time result in a decrease in initial rate of dissolution suggesting an increase of particle size and stability. It is proposed that the absence of any further stability minima after 15 mins is because the particles have grown sufficiently in size such that the any additional charge does not significantly change the charge density of the particle, hence a stability minima is not observed.

For all time points investigated the molybdate detectable levels of silicic acid increase with time until they reach an equilibrium concentration of *ca.* 1 mM, Figure 3.4.2.1a. The data indicates that on dilution, the position of equilibrium between silicic acid and silica species is shifted to the left, and the reverse reaction of silica species dissolving to form silicic acid is the favoured reaction.

When considering the initial rate of dissolution of a sample it is important to realise that a pre-condensed silica solution will contain a mixture of silica species. This was

highlighted when comparing the expected initial silicic acid concentration to the experimental values obtained after dilution; It was found that the observed concentration is always higher than the expected concentration of silicic acid. This suggests that there is a highly unstable population of silica species that dissociate in the time required to prepare and measure the first sample (<40 s). The longer the condensation time the less significant this difference becomes. For 3 mins pre-condensed samples the % difference between observed and expected initial concentration is *ca.* 16 % and tends to 1 % for samples of a pre-condensation time of 60 mins.

3.4.3. A study of pre-condensed silica solutions following dilution to 1 mM silica in the presence of a range of bioinspired additives.

The study of small molecules in unsaturated silicic acid systems (Figure 3.4.1.1) has demonstrated that the role of the amine group in silica formation is not to promote the condensation of orthosilicic acid. Instead, as shown below bioinspired amine functionalised molecules influence thermodynamically favourable processes, *i.e.* the condensation of silicic acid at supersaturated levels,[13, 19, 21, 35-37] but are unable to change the equilibrium constant sufficiently (if at all) to allow the condensation of two silicic acid molecules at unsaturated concentrations. Belton *et al.* have observed increases in the rate of formation of trimers in supersaturated silicic acid systems in the presence of bioinspired additives, implying catalysis of the reaction between a monomeric and dimeric species to form a trimer.[26]

In the following, we studied the effects of organic additives on the stability of pre-condensed unsaturated silica systems. Initially the activity of a range of bioinspired additives was screened. Solutions of silica particles (1 mM) were prepared by allowing a solution of silicic acid (30 mM) to condense for 60 mins followed by diluting this system to a final silicon concentration of 1 mM, the amines were then added to these solutions. By diluting the system to 1 mM, condensation and aggregation are effectively halted, thus any further aggregation or condensation observed will be solely due to the presence of the additive. Based on the literature it was hypothesised that the additives would promote aggregation and possibly exert

some structural control on a pre-condensed silica system (1 mM), since negatively charged silica particles and positively charged amine groups are present.[2]

The effect of our chosen bioinspired additives on the dissolution kinetics is presented in Figure 3.4.3.1, where the additives have been separated into polyelectrolytes and small molecules. The separation on the basis of size clearly distinguishes the effect of the additives on dissolution with small molecules showing small increases (*ca.* 2-3 times) in the initial rate of dissolution when compared to the blank, where as polyelectrolytes show large increases (*ca.* 6 times) in the relative initial rates of dissolution (Figure 3.4.3.1c, d). The time to reach equilibrium (t_{eq} - i.e. to dissolve silica species to 1 mM silicic acid) was also recorded for all the samples. The reciprocal of t_{eq} is plotted in Figure 3.4.3.1c, d from which it can be seen, as expected, that with higher dissolution rates, t_{eq} is large. When small molecules were used as additives an important distinction between the behaviour of the silica system in the presence of the long chain polyelectrolytes and the small molecules was noticed. In the presence of small molecules a precipitate was formed as shown in Figure 3.4.3.1.

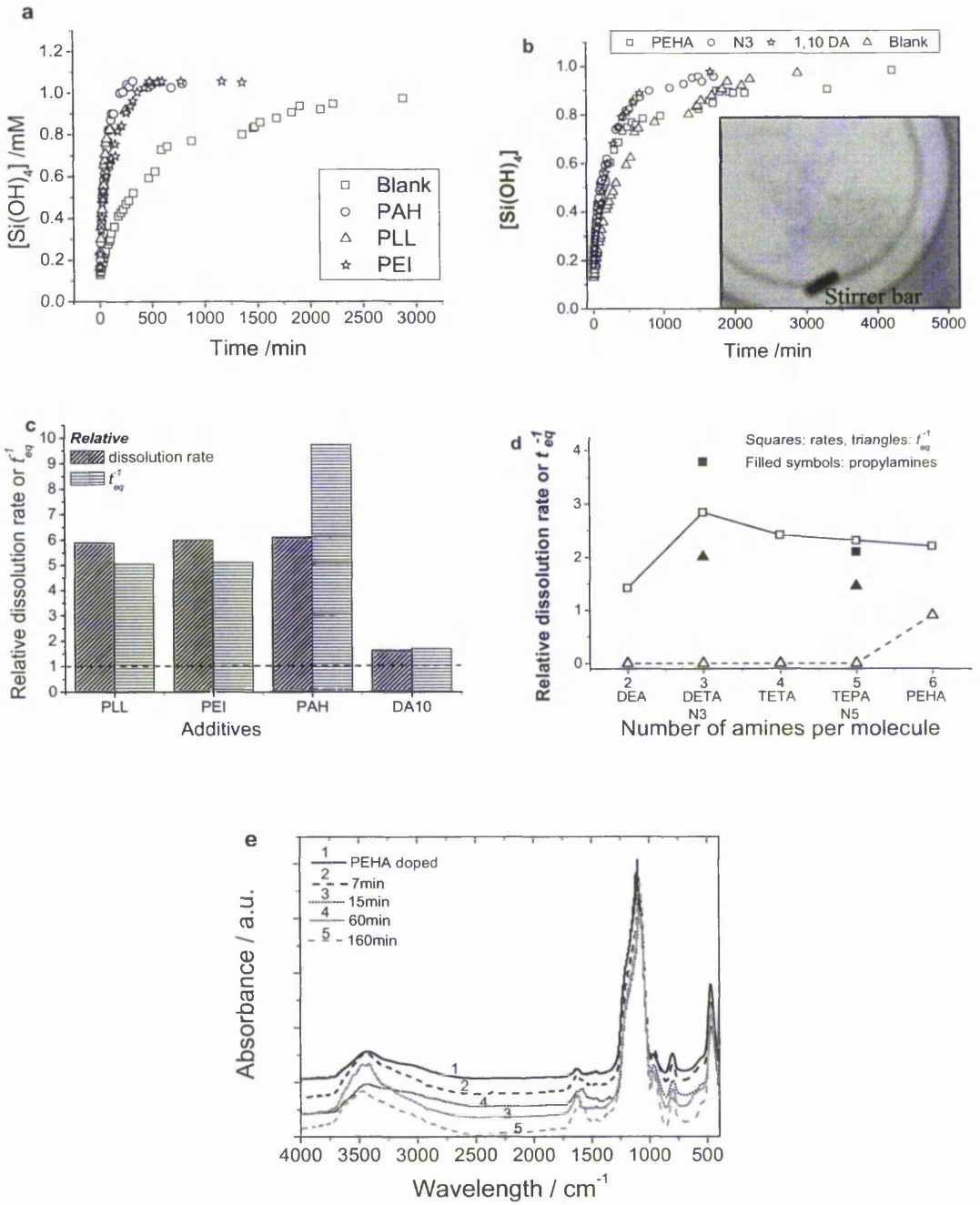

Figure 3.4.3.1. - The dissolution of 60 min pre-condensed silica diluted to 1 mM in the presence of a) polyelectrolytes and b) small molecules respectively. Insert in b) shows precipitate after 1 h. Initial rates of dissolution and inverse equilibrium times in the presence of c) polyelectrolytes and d) small molecules. e) FTIR spectra of silica samples isolated after 1 h from different pre-condensed silica systems in the presence of PEHA, compared to silica doped with PEHA.

A precipitate was observed to form in the presence of TEPA, PEHA, N3 and N5 and not when shorter chain ethyleneamines or polyelectrolytes were used, this shows that

silica particles can be aggregated from an unsaturated silica environment. It is possible that the precipitate is formed due to the ability of the small amines to bridge the silica particles through electrostatic interactions. However, it is puzzling to note that precipitation is not observed in the presence of polyelectrolytes and currently this not understood. Note if these materials are not isolated from the liquid phase dissolution continues when a 1 mM silicic acid equilibrium concentration is eventually reached. The dissolution rate is observed to increase with the number of nitrogen atoms per molecule and then remains approximately constant for samples which form a precipitate can form (TEPA and PEHA), Figure 3.4.3.1d. Interestingly, addition of TETA shows an initial rate of dissolution similar to TEPA and PEHA, however no precipitate could be isolated by centrifugation. The precipitates isolated after 1 h were identified as silica by FTIR (Figure 3.4.3.1e) and contained *ca.* 5 % entrapped organic material irrespective of the precondensation time (by TGA analysis, as calculated from the mass loss between 400 and 600 °C), compared to a blank silica which contained 1 % organic material (blank sample is silica isolated from a 30 mM system at 24 h because the unsaturated blank sample did not precipitate), Appendix 1 Figure 2. To confirm the entrapment of organic material, the material isolated from the unsaturated pre-condensed silica system was analysed by FTIR and compared with commercial silica samples doped with PEHA. The presence of peaks between 1500-1600 cm^{-1}, Figure 3.4.3.1e confirms the occlusion of amines in the silica samples. Analysis of the precipitates formed by TEPA, N5 and PEHA from a 60 min pre-condensed silica after a dissolution time of 60 mins showed that the surface area of the silica formed in the presence of the additives increased from N5 (241 ±51 m^2g^{-1}) to PEHA (352 ±24 m^2g^{-1}) and TEPA (384 ±19 m^2g^{-1}), indicating that the additives, not only aggregated the silica particles, but also modified condensation reactions, as more highly condensed silica is known to exhibit a lower surface area.[26] Figure 3.4.3.2 shows SEM images of the materials isolated after 60 mins from a 60 min pre-condensed solution of silica in the presence of TEPA, PEHA and N5. Belton *et al.* suggest silica particles aggregated rapidly tend to show more open silica structures[41], this would also appear to be the case in this system where PEHA and TEPA exhibit silica where large cavities can quite clearly be seen and the primary aggregate size is quite large. The appearance of the N5 silica is somewhat different where smaller primary aggregates are observed and the cavities can no longer be seen. The smaller primary aggregates could be caused by the additives ability to catalyse condensation

and hence the silica has reached a more mature state when compared to TEPA and PEHA.

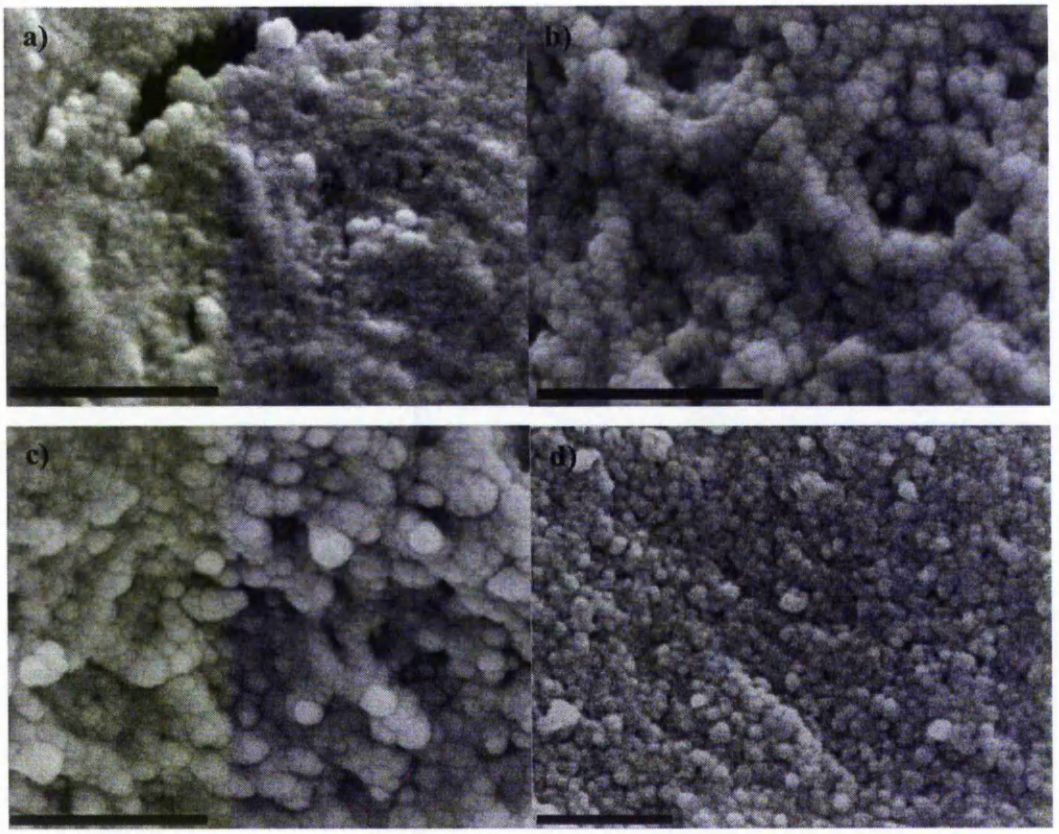

Figure 3.4.3.2 - SEM images and particle sizes of (a) N5, 137 ±23 nm, (b) TEPA, 131 ±15 nm and (c) PEHA, 222 ±39 nm respectively, using 60 min pre-condensation time and isolating the precipitate after 60 mins of dissolution time. (d) Blank silica isolated from 30 mM condensing system after 24 h, 105±15.21 nm. Bars = 2 μm for (a)-(c) and 1 μm for (d).

3.4.4. Investigating the effect of bioinspired additives on the dissolution of commercial silica.

The observation that polyelectrolytes dissolve silica at unsaturated levels was investigated further using highly condensed commercial silica samples. (supplied by Ineos Gasil 23D; 267 ± 9 m^2g^{-1}). A representative series of additives were investigated at the same Si:N ratio as previously used for the pre-condensed silica investigations (Si content of solution was 1 mM, Si:N 1:6). Figure 3.5.4.1a shows the dissolution of silica with respect to time, where a trend similar to that found when using pre-condensed silica systems was observed. Small molecules such as DETA

that are unable to bridge the particle double layer and polyelectrolytes such as PEI significantly increased the rate of dissolution of silica. However, small molecules that are able to bridge the particle double layer had the opposite effect; the silica suspended in solution was in fact stabilised by the presence of the additive. For comparison we also investigated the effect of NaCl. Previously it was found that the rate of dissolution of quartz in NaCl solutions was 21 times faster than the that in water (see below for discussion).[42] We found in our system that 50 mM NaCl increased the initial rate of dissolution of commercial silica by 7 times compared to that in water (Figure 3.4.4.1b).

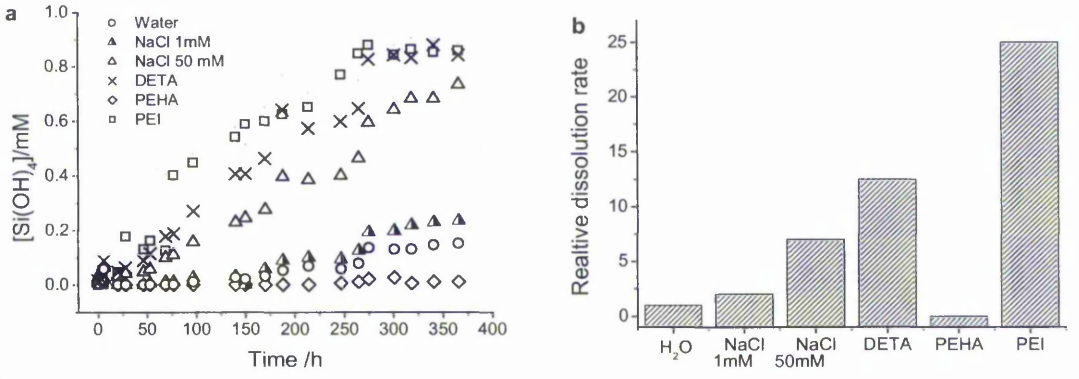

Figure 3.4.4.1 - a) Dissolution of Gasil 23D in the presence of bioinspired additives and NaCl. b) The initial rates of dissolution of commercial silica in the presence of additives relative to the blank. Silica in the presence of PEHA showed no dissolution over a 200 h period.

From the experimental data above it can quite clearly be seen that the stability of silica in solution varies in the presence of positive charged species in solution. The ability of a polyelectrolyte to enhance silica dissolution in all the silica systems studied indicates that the interaction between the polyelectrolyte molecules and negatively charged silica particles is different to that of small molecules. Evidence has been provided to suggest that small molecules bridge the particle double layer, which promotes aggregation. The inability of polyelectrolyes to exhibit the same phenomena leads one to speculate that the orientation of the polyelectrolyte at the silica surface is coiled in such a way that a positively charged nitrogen atoms does extend past the particle double layer. However, polyelectrolyte molecules are often likened to rod like molecules and hence adopting such an orientation would be intriguing prospect.

3.4.5. Identifying the "active" silica species

From the foregoing, it can be deduced that depending on the initial silica speciation and the organic additive present, the stability of silica samples varies largely. It is therefore important to determine a species (or a collection of species) of silica that can be aggregated by a given additive; the "active" silica species. PEHA, which increased the dissolution rate as well as induced precipitation in pre-condensed unsaturated silica solutions, was selected for this study. A range of pre-condensation times were investigated to allow for the behaviour of a range of different silica species to be probed.

The effect of PEHA on the initial rate of dissolution on 1mM pre-condensed silica species is shown in Figure 3.4.5.1 alongside data collected for the blank samples. The addition of PEHA increased the rate of dissolution for samples pre-condensed for 3 and 5 mins. For pre-condensing times ≥7 mins, precipitation was observed, which coincided with a sharp drop in the initial rate of dissolution; notably this also coincides with the least stable silica species in the blank system (7-8 mins).

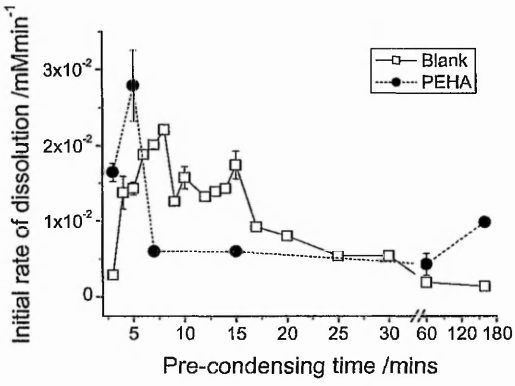

Figure 3.4.5.1 - The initial rate of dissolution of pre-condensed silica systems in the presence of and absence of PEHA.

It has been shown by LCMS that after 5 mins condensing time, only silicic acid and particulate silica exist.[40] Thus, we hypothesise that it is the introduction of surface charge to silica particles that allows the presence of PEHA to induce precipitation *via* aggregation. Thus, the mechanism for aggregation is likely to be one involving surface charge neutralisation and particle bridging. Further increases in the pre-

condensation time were found to have little effect on the initial dissolution rate in the presence of PEHA. The formation of a precipitate distinctly changes the system, from a high surface area silica sol to a comparatively low surface area, phase separated system.

The formation of a silica precipitate in a globally unsaturated environment is novel. The precipitation process was followed by monitoring the amount of silica remaining in solution with respect to time, using a centrifugation method (see section 3.2.3). The effect of PEHA on a 15 mins pre-condensed unsaturated sample is shown in Figure 3.4.5.2, where the total silicon concentration arising from all of the species present in the supernatant is presented as well as the amount of silica remaining in solution (by digestion of the supernatant to molybdenum blue active species). The initial decline in total silicon content in the supernatant is indicative of the formation of a precipitate with 37 % of the total silica in solution being precipitated within 25 mins. A further increase in the total silicon content in the supernatant was observed and is presumably due to the slow dissolution of the precipitate. When the free silicic acid concentration in the system (without sodium hydroxide digestion) is assessed, a continuous increase is observed until an equilibrium concentration of 1 mM is reached. This result again suggests that PEHA is acting on the larger mers and causing precipitation, while not having any effect on orthosilicic acid. The amount of precipitated silica was found to increase to 89 and 93 % at *ca.* 10 mins when the precondensation time was 60 and 160 mins (Appendix 1 Figure 1), further supporting our hypothesis that PEHA is only active towards higher silica species.

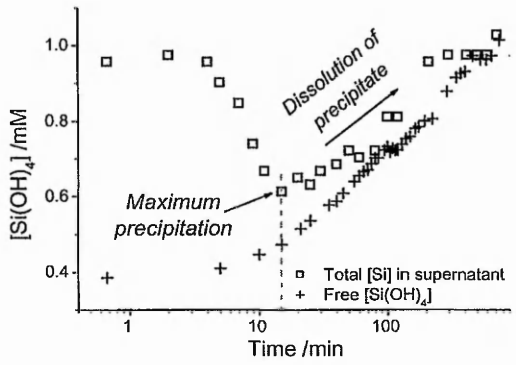

Figure 3.4.5.2 - The precipitation of silica from a 1 mM, 15 min pre-condensed silica solution.

3.5. Discussion and Conclusions.

We have investigated the roles of a series of amine containing organic molecules in controlling the stability of a range of silica species. For the range of bioinspired additives explored to date, we have found no evidence to support the hypothesis that additives directly influence the condensation of orthosilicic acid as the initial step in the process to form silica.

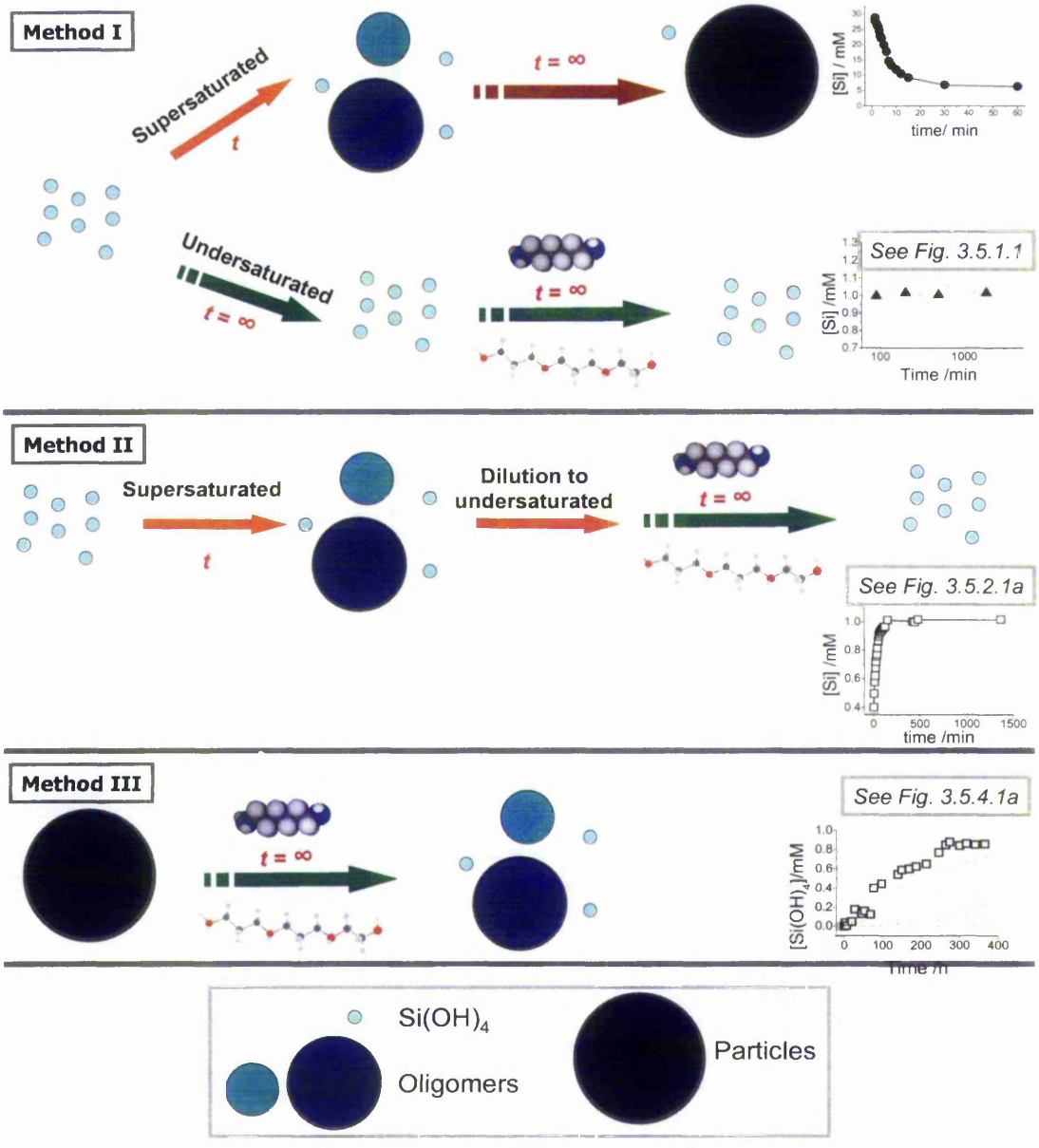

Scheme 3.5.1 - Schematic representation of the summary of the three approaches employed to study the interactions of organic additives with silica species present at unsaturated concentrations.

From the experimental data reported here it has been concluded that the bioinspired additives used in this study can be classified according to their behaviour in a globally unsaturated silica environment. It has been found that by using a pre-condensed solution of silica species (1 mM) that bioinspired polyelectrolytes dramatically increase the rate of dissolution of silica particles. Bioinspired small molecules by comparison also aid dissolution, but importantly can also precipitate silica in this environment when the length of the bioinspired additive extends past the particle double layer (reported to be >11.1 Å and <14.72 Å)[43]. Interestingly the precipitate formed also undergoes dissolution with the solution reaching equilibrium (silicic acid concentration *ca.* 1 mM as detected by the molybdenum blue method). The siliceous materials formed during these studies where found to vary with the small molecules used to form the precipitate; indicating that small molecules not only aggregate silica species but also modify condensation reactions as shown by the variation in surface area of the materials isolated.

The study of pre-condensed silica species in unsaturated environments has shown very interesting results. The initial rates of dissolution of different silica species generated by varying precondensation times were compared. It has been found that by increasing the precondensation time in a systematic fashion, the stability of the silica species generated did not increase linearly as perhaps one might have expected. Instead, distinct periods of instability were found which we hypothesise are due to species of high charge density. The addition of PEHA to these reactive solutions allowed us to determine the earliest precipitatable species which in turn coincided with the least stable silica species as measured from the comparison of initial dissolution rates from the blank system.

The mechanism by which small molecules precipitate silica particles at supersaturated and pre-condensed unsaturated silica systems, involves the aggregation of charged silica particles. The mechanism by which polyelectrolytes aid the dissolution of charged silica species in an unsaturated environment requires further investigation. However, one conclusion can be drawn: it is unlikely that polyelectrolyte molecules extend past the particle

double layer otherwise precipitation of silica particle *via* particles bridging could have occurred.

The dissolution of both amorphous and crystalline silica has been studied for many decades,[26, 29, 44] and it is generally accepted that amorphous silica is more reactive than its crystalline counter parts. The rationale for study usually involves understanding the geochemical silica cycle in accordance with changes in environmental chemistry due to human activities. Interest in silicate mineral dissolution has been vast, and studies have focused on understanding how the compositions of surrounding solutes affect the dissolution kinetics of silicate minerals. The conclusion that has been reached is that the dissolution of silica is controlled by interactions between cations (such as K^+) and the negatively charged silica surface at circumneutral pH with the rate of dissolution being governed by the strength of the Si-O bond. Dove and *et al.*[42, 45, 46] investigated the effect of dissolved cations on amorphous silica and quartz dissolution, where for quartz the enhancing effect increases from "pure water" < Mg^{2+} < Ca^{2+} ≈ Li^+, Na^+ and K^+ < Ba^{2+}.[45] The effect of concentration was also investigated where it was found that concentrations greater than 0.05 molal showed little difference when compared to dissolution in pure water.[47] However, at concentration less than 0.05 molar the rate was found to increase by 21 times. The interaction of positively charged ions with a negatively charged silica surface is likely to be the reason for the observed increase in dissolution, however, the precise role of this interaction is unclear. Interestingly the activation energy for dissolution was unchanged in the presence of Na^+ suggesting that the presence of cations increases the probability of a dissolution reaction occurring. It has thus been hypothesised that the presence of cations in the dissolving medium alters the nucleophilic properties of water, where the attracted solvated cation resides in the interfacial region and imposes its own solvation characteristics on the silica surface which aids in dissolution, implying that the activity of water has been increased by the presence of the cations.[42] It is tempting to conclude that the bioinspired molecules studied in unsaturated silica environments aid dissolution by a similar mechanism. However, several observations require more in depth analysis. Our hypothesis that a charged species must extend past the particle

double layer in order for aggregation to be observed, suggests that polyelectrolyte molecules are able to wrap themselves around small charged particles. Monte Carlo simulations by Stoll *et al.*[48] suggest that this conformation may be possible although there is, at present, no experimental data to support this mode. Furthermore, it is intriguing to find that PEHA reduced the rate of dissolution of commercial silica, when compared to the blank suggesting a stabilisation of silica particles, which is the opposite effect to that observed in the pre-condensed silica system. It is believed that these results will be of interest to researchers studying precipitation and dissolution of silica and silicates, for example in the fields of biological, geological and chemical cycle of silicon and scaling of silicates.

References:

1. M. Sumper and N. Kröger, *J. Mater. Chem.*, 2004, **14**, 2059-2065.
2. S. V. Patwardhan, S. J. Clarson and C. C. Perry, *Chem. Commun.*, 2005, 1113-1121.
3. P. Treguer, D. M. Nelson, A. J. Vanbennekom, D. J. Demaster, A. Leynaert and B. Queguiner, *Science*, 1995, **268**, 375-379.
4. V. Martin-Jezequel, M. Hildebrand and M. A. Brzezinski, *J. Phycol.*, 2000, **36**, 821-840.
5. N. Kröger, S. Lorenz, E. Brunner and M. Sumper, *Science*, 2002, **298**, 584-586.
6. M. Sumper and N. Kröger, *J. Mater. Chem.*, 2004, **14**, 2059 - 2065.
7. J. N. Cha, K. Shimizu, Y. Zhou, S. C. Christiansen, B. F. Chmelka, G. D. Stucky and D. E. Morse, *Proc. Natl. Acad. Sci. USA*, 1999, **96**, 361-365.
8. C. C. Harrison, *Phytochemistry*, 1996, **41**, 37-42.
9. C. C. Perry and T. Keeling-Tucker, *J. Biol. Inorg. Chem*, 2000, **5**, 537-550.
10. J. N. Cha, K. Shimizu, Y. Zhou, S. C. Christiansen, B. F. Chmelka, G. D. Stucky and D. E. Morse, *Proc. Natl. Acad. Sci. USA*, 1999, **96**, 361-365.
11. Y. S. Zhou, Katsuhiko; Cha, Jennifer N.; Stucky, Galen D.; Morse, Daniel E, *Angew. Chem. Int. Ed.*, 1999, **38**, 780-782.
12. C. C. Perry and T. Keeling-Tucker, *Chem. Commun.*, 1998, 2587-2588.
13. S. V. Patwardhan, S. J. Clarson and C. C. Perry, *Chem. Commun.*, 2005, **9**, 1113-1121.
14. T. Mizutani, H. Nagase, N. Fujiwara and H. Ogoshi, *Bull. Chem. Soc. Jpn.*, 1998, **71**, 2017-2022.
15. L. Sudheendra and A. R. Raju, *Mater. Res. Bull.*, 2002, **37**, 151.
16. T. Coradin and J. Livage, *Colloids Surf. B*, 2001, **21**, 329-336.
17. D. Belton, G. Paine, S. V. Patwardhan and C. C. Perry, *J. Mater. Chem.*, 2004, **14**, 2231-2241.
18. L. L. Brott, D. J. Pikas, R. R. Naik, S. M. Kirkpatrick, D. W. Tomlin, P. W. Whitlock, S. J. Clarson and M. O. Stone, *Nature*, 2001, **413**, 291.
19. D. Belton, S. V. Patwardhan and C. C. Perry, *Chem. Commun.*, 2005, 3475-3477.
20. K. M. Roth, Y. Zhou, W. Yang and D. E. Morse, *J. Am. Chem. Soc.*, 2005, **127**, 325-330.
21. D. Belton, S. V. Patwardhan and C. C. Perry, *J. Mater. Chem.*, 2005, **15**, 4629-4638.
22. V. V. Annenkov, S. V. Patwardhan, D. Belton, E. N. Danilovtseva and C. C. Perry, *Chem. Commun.*, 2006, 1521-1523.
23. T. Coradin, O. Durupthy and J. Livage, *Langmuir*, 2002, **18**, 2331-2336.
24. S. V. Patwardhan and S. J. Clarson, *Silicon Chem.*, 2002, **1**, 207-214.
25. N. Kröger and M. Sumper, in *Biomineralization: from biology to biotechnology and medical application*, ed. E. Baeuerlein, Wiley-VCH, Editon edn., 2000.
26. R. K. Iler, *The Chemistry of Silica* John Wiley & Sons, New York, 1979.
27. H. Strandh, L. G. M. Petersson, L. Sjöberg and U. Wahlgren, *Geochimica Et Cosmochimica Acta*, 1997, **61**, 2577-2587.
28. S. Sjöberg, *J. Non-cryst. Solids*, 1996, **196**, 51-57.
29. P. C. Bennett, M. E. Melcer, D. I. Siegel and J. P. Hassett, *Geochim. Cosmochim. Acta*, 1988, **52**, 1521-1530.

30. P. C. Bennett, *Geochim. Cosmochim. Acta*, 1991, **55**, 1781-1797.
31. P. Bennett and D. I. Siegel, *Nature*, 1987, **326**, 684-686.
32. D. Belton, G. Paine, S. V. Patwardhan and C. C. Perry, *J. Mater. Chem.*, 2004, **14**, 2231-2241.
33. S. Brunauer, P. H. Emmett and E. Teller, *J. Am. Chem. Soc.*, 1938, **60**, 309.
34. E. P. Barrett, L. G. Joyner and P. P. Halenda, *J. Am. Chem. Soc.*, 1951, **73**, 373.
35. V. V. Annenkov, S. V. Patwardhan, D. Belton, E. N. Danilovtseva and C. C. Perry, *Chem. Commun.*, 2006, **published online**, DOI:10.1039/B515967A.
36. S. V. Patwardhan, N. Mukherjee and S. J. Clarson, *Silicon Chem.*, 2002, **1**, 47.
37. S. V. Patwardhan, N. Mukherjee, M. Steinitz-Kannan and S. J. Clarson, *Chem. Commun.*, 2003, **10**, 1122-1123.
38. C. C. Harrison and N. Loton, *J. Chem. Soc. Faraday Trans.*, 1995, **91**, 4287-4297.
39. D. J. Belton and C. C. Perry, unpublished data.
40. D. Belton, The influence of small molecules on the precipitation of silica, Nottingham Trent University, 2005.
41. D. Belton, S. V. Patwardhan and C. C. Perry, *Chem. Commun.*, 2005, 3475-3477.
42. J. P. Icenhower and P. M. Dove, *Geochim. Cosmochim. Acta*, 2000, **64**, 4193-4203.
43. D. J. P. Belton, Siddharth V.; Perry, Carole C., *J. Mater. Chem.*, 2005, **15**, 4629-4638.
44. J. W. Tester, W. G. Worley, B. A. Robinson, C. O. Grigsby and J. L. Feerer, *Geochim. Cosmochim. Acta*, 1994, **58**, 2407-2420.
45. P. M. Dove and C. J. Nix, *Geochim. Cosmochim. Acta*, 1997, **61**, 3329-3340.
46. P. M. Dove, *Geochim. Cosmochim. Acta*, 1999, **63**, 3715-3727.
47. G. S. Wirth and J. M. Gieskes, *J. Colloid Interface Sci.*, 1979, **68**, 492-500.
48. S. Stoll and P. Chodanowski, *Macromolecules*, 2002, **35**, 9556-9562.

Chapter 4 - Are hydroxyl containing biomolecules important in (bio)silicification? A model study

4.1 Introduction

The cell wall of diatoms (the frustule) is one of nature's most remarkable nanopatterned siliceous materials. The nanopatterning is under genetic control since high reproducibility is observed from generation to generation. The frustule is encased by an organic coating that protects it from dissolution[1] and it is widely thought that organic molecules contained within or associated with biosilica have an important role to play in biosilicification. As early as 1973, Hecky *et al.*[2] suggested that investigation of the composition of the organic coating could lead to an understanding of biosilicification. Subsequent analysis of diatom frustule bioextracts identified the presence of glycoproteins enriched in glycine and hydroxyl-containing amino acids (serine and threonine).[2] The authors proposed that the hydroxyl-containing amino acids might react with orthosilicic acid monomers (leading to the formation of Si-O-C bonds), thus serving as templates for orientation and growth of the sili*ca.* Other researchers working on diatoms also found entrained organic material containing high amounts of serine that was hypothesized to be indirectly involved in biosilicification.[3] Studies of silicified sponge spicules from *Tethya aurantia* have identified a protein, silicatein α – that contains serine both at the active site and in clusters on the protein surface. This protein is able to catalyze, *in vitro*, the hydrolysis of alkoxide groups present in tetraethoxysilane (TEOS, a silica precursor).[4-6] Hydrogen bonding between the serine-26 hydroxyl group and the imidazole nitrogen of the histidine-165 residue has been suggested to aid nucleophilic attack on the silicon centre generating a C-O-Si covalently bonded intermediate, with addition of water completing the hydrolysis of TEOS.[4-6]

Mixtures of biopolymers containing high levels of serine have also been extracted from silicified higher plants including hairs on the lemma of *Phalaris canariensis*, from *Equisetum telmateia* and *Equisetum arvense*.[7] Although the extracts were found to modify the forms of silica generated *in vitro*, their interaction with silicon containing species at the molecular level was not thought to arise from direct Si-O-C covalently bonds. Other hydroxyl containing carbohydrate biopolymers extracted from the same species were found to modify growth and aggregation rather than act as catalysts for the direct formation of silica.[8] At present, there is no experimental evidence available for the presence of Si-O-C covalent bonds in such plant silicas,[9] although computational models show the energetic feasibility of such bonds being formed.

For example, a study by *Lobel et al* using AM1 molecular orbital calculations to simulate the polycondensation of four orthosilicic acid molecules onto a polyserine β-sheet template showed this process to be energetically *via*ble.[10, 11] In addition, if Si-O-C bonds are to be formed in the presence of hydroxyl groups then they are likely to occur *via* 5 or even 6 coordinated intermediates. These have been identified experimentally using ^{29}Si NMR of 'Si-polyol' mixtures at basic pH, but not at biologically relevant pH.[12, 13] *Ab initio* Hartree-Fock (HF) molecular orbital calculations also support the formation of six- and penta-coordinated silicon species[14, 15], but only from $H_3SiO_4^-$ (orthosilicic acid has a pKa of 9.816) at high pH. These conditions are not compatible with the conditions found in most bodies of water (sea water is pH 8.5) and for one of the well studied silicified diatom species where the silica deposition vesicle is proposed to be slightly acidic).[17] Thus it is unlikely that silicon complexes with polyalcohols such as sugars and serine are likely to play an important role in silicon bioaccumulation and biosilicification.

Attempts to understand the roles that hydroxyl-containing (bio)macromolecules might play in biosilicification have been undertaken by *in vitro* studies of silica formation in the presence of a range of hydroxyl containing model compounds such as small carbohydrates, polyserine and polyethyleneglycol.[8,18-22] The concentration and molecular weight of polyethylene glycol was added to a silica precipitating solution. It was found that PEG affected the porsoitiy of the silica and its morphologies.[22] For example, PEG

with MW = 600 produced mesoporous silica, whereas PEG with molecular weight of 2000 produced smooth microporous silica spheres. Increasing the number of glucose units within a molecule affected the ability of the additive to regulate the growth of particles with a minimum of four glucose groups chemically bonded being necessary for control of growth.[18] It is also known that the addition of serine or threonine to model silica formation reactions produces silica with different surface characteristics.[23]

It is quite clear however, that the roles of hydroxyl functionalized biomolecules in silica formation are not fully understood, although the literature suggests that interactions could be either through covalent or non-bonded interactions.[24] In order to address this problem, a systematic study was preformed as follows. The role of two proteins rich in hydroxyl containing amino acids - native sericin protein extracted from *Bombyx mori* and a recombinant sericin precursor peptide in the formation of silica *in vitro* was investigated. These proteins were chosen for the following reasons: (i) their high content of hydroxyl-containing residues (*ca.* 60 %) and (ii) sericin proteins are not associated with silica, hence are not expected to have specific interactions with "silicon". Furthermore, we investigated the role of hydroxyl containing "small" model molecules - alkanediols ("diols") - in silica formation to study the interactions between silicon species and hydroxyl functionalized species, if any. The results and their implications are discussed below in the context of biosilicification and biomineralization.

4.2 Experimental

4.2.1 Materials

Silica synthesis was performed using dipotassium tris (1,2-benzenediolato-*O,O'*)silicate as the precursor as described previously.[23] The alkanediols used in the model system kinetics; 1,2-ethanediol 99% (BDH), 1,3-propanediol 98% (ACROS), 1,4-butanediol 99 %, 1,5-pentanediol 96 %, 1,6-hexanediol 99 % and 1,7-heptanediol 95 % (Aldrich). Polyserine (MW = 3000-10000) was obtained from ICN Biomedicals. Catechol (99 %, Aldrich) and potassium chloride (AnalaR BDH) were used in the photon correlation

spectroscopy study. Native sericin proteins were extracted from cocoons of the silkworm Bombyx mori using previously described protocols.[25] The protein was purified using Slide-A-Lyzer dialysis cassettes (molecular weight cut-off = 3,500) against deionized distilled water. The sericin peptides were prepared from cloned repeats of the consensus sequence of the native proteins as previously described.[26] The recombinant sericin peptide, 32.1 kDa, was purified by affinity chromatography, followed by the same dialysis method for native sericin.

4.2.2 Materials synthesis and characterization

Native sericin and sericin precursor were obtained as described above and were inserted into the aqueous precipitating model system at 1, 5 and 10 % by weight of the expected precipitated silica from a blank sample. The sericin precursor used has a molecular weight of 3612.4 $gmol^{-1}$ of which 23 of the 38 amino acids (*ca.* 60 %) of the synthesized repeating unit contain a hydroxyl group. The alkanediols were typically added into the model at 15 mM (Si:OH 1:1 *i.e.* 100 %), 30 mM (Si:OH 1:2 *i.e.* 200 %), 60 mM (Si:OH 1:4 *i.e.* 400 %) and 150 mM (Si:OH 1:10 *i.e.* 1000 %).

Kinetic studies were carried out using a colorimetric method and the particle formation, growth and aggregation behavior of the condensing system was measured using PCS as described elsewhere.[23] Silica was isolated from the condensing system after 24 and 168 h reaction by centrifugation, washing three times with deionized water and lyophilized for further analysis. Microscopy was carried out on lyophilized samples using a Jeol JSM-840A Scanning Electron Microscope. Nitrogen gas adsorption/desorption analysis was carried out on lyophilized samples using a Quantachrome Nova 3200e surface area and pore size analyzer. Prior to analysis, samples were degassed overnight at 120 °C under vacuum. Surface areas were then determined *via* the BET method where nitrogen is assumed to have a cross-sectional area of 0.16 nm^2,[27] over the range of relative pressures 0.05 – 0.3 at which point the monolayer is assumed to assemble. Pore radii were determined by the BJH method using the desorption branch of the isotherm.[28] Statistical analysis was undertaken on gas adsorption data similar to that described above for

kinetics experiments. All infrared spectroscopy measurements were conduced using a Magna IR 750 infrared spectrometer (Thermo Nicolet) fitted with a single-bounce diamond ATR (Grazeby Specac). The instrument was continuously purged with dry air for a minimum of 12 h prior to sample analysis. Spectrum collection parameters were set as follows: resolution set at 4 cm^{-1}, interferometer speed 0.4747 cms^{-1}, averaging 512 or 1024 scans.[29] Thermal gravimetric analysis was carried out on selected samples using a Perkin Elmer Pyris 6 TGA. The samples were heated at 10 °C min^{-1} from 30 to 900 °C in air to ensure complete combustion of all organic material retained within the material.

4.2.3 Statistical analysis

Statistical significance for the data was analyzed using student t-test. A confidence limit of 95 % corresponding to $\alpha = 0.05$ was typically used, unless otherwise specified. Any data lying inside this envelop has a 95 % probability of being statistically significant. The confidence interval (C. I.) for a small dataset (<30 samples) was calculated by: C.I. $= \bar{x} \pm t_x \hat{\sigma}_x$ where $\sigma_x = s \setminus \sqrt{n}$ which is the standard error of the mean, $\bar{x}$ = mean of the sample database, t_x = t value obtained for a given degrees of freedom and α and s = standard de*via*tion. For the data presented as relative values, the ratio of the second term in the equation for C.I. and the mean was used. For data presented in Figure 2b, correlation analysis was performed in order to test the statistically significant changes in trends. The Spearman correlation coefficient (which does not require normally distributed data) was used.

4.3 Results and Discussion

Sericin extracted from *Bombyx mori* spider web and a recombinant sericin precursor at three different concentrations: 1, 5 and 10 % by weight of precipitated silica from our model aqueous precipitating system at pH 6.8 was studied.[30] This allowed a comparison of activity, if any, with proteins studied in our laboratory including those extracted from *E. arvense*.[31, 32] In the kinetic experiments, the loss of orthosilicic acid was measured over a period of 24 h which yielded information on various stages of silica

polymerization (*e.g.* trimerisation and oligomerisation).[16, 33] The kinetic transformation identified by the rate constant k_{3rd} arises from the formation of trimers from monomeric and dimeric species. The addition and dissolution of orthosilicic acid to trimers and larger oligomeric species is best described as a reversible first order reaction with rate constants k_+ and k_- respectively. The rate constant k_- is also a measure of equilibrium solubility of orthosilicic acid. The experimental data on silica polymerization in the presence of sericin proteins showed that the sericin proteins exhibited no major statistically significant catalytic effects on the formation of trimers (k_{3rd}) at any of the concentrations studied (Figure 4.3.1a, b, Appendix 1 Table 1). Similarly, only small effects were observed on the oligomerisation process (k_+ and k_-), Figure 4.3.1a, b. There was no evidence for the stabilisation of orthosilicic acid at equilibrium for any of the concentrations of sericin proteins studied (reflected from the values of k_- in Figure 4.3.1a, b.

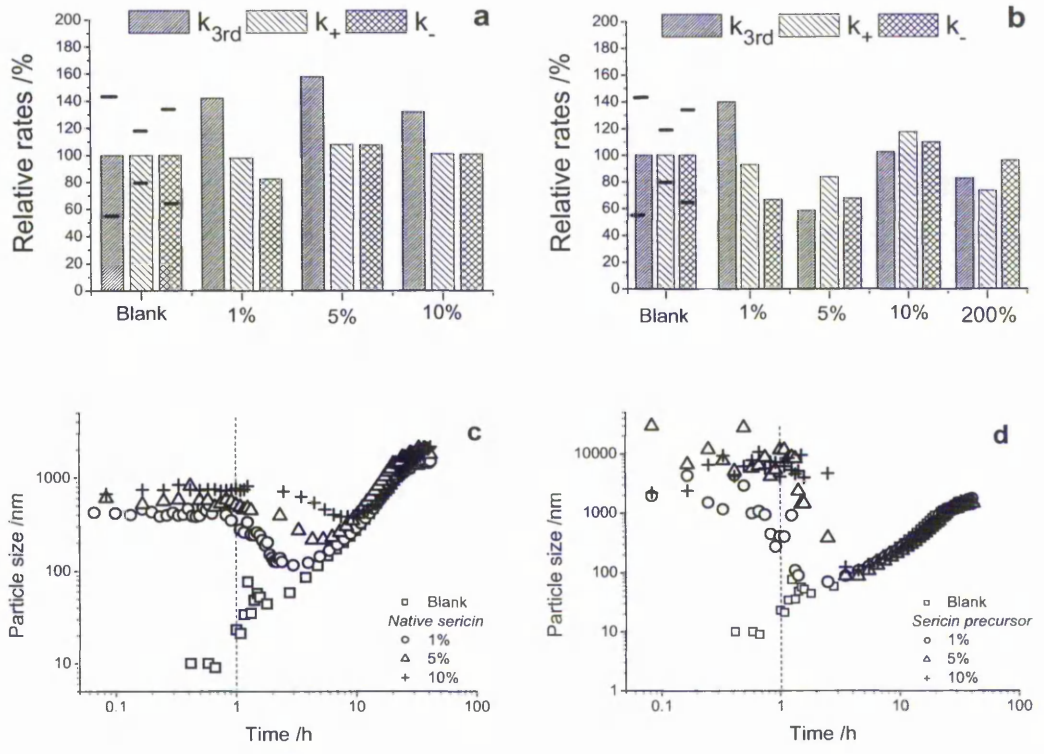

Figure 4.3.1. - The effect of sericin proteins on a, b) silica polymerization kinetics and c, d) silica particle growth. a, c) native sericin and b, d) sericin precursor. Horizontal bars on blank data in a) represent 95%

confidence limit. Dotted line in b, d) indicates the time at which particle formation is measurable in the blank system.

The effect of sericin proteins on the formation, growth and aggregation of silica oligomers and particles was investigated by Photon Correlation Spectroscopy (PCS). When present in a condensing silicic acid system, the sericin proteins were found to aggregate in solution, even before any silica particle were formed as evidenced from PCS data shown in Figure 4.3.1c, d. For the blank sample, particle formation is apparent after *ca.* one h of reaction. For the samples with protein added to the reaction medium, the initial protein structures observed were found to dissociate once silica particles started to form (*i.e.* after 1 h reaction time), Figure 4.3.1c, d. Perhaps the formation of silica disrupts the protein structures or forming silica particles become the more dominant scattering species in solution. Thereafter the rate of particle growth and aggregation was found to be similar to the blank system. It should be noted that no precipitation was observed even after 20 h of reaction. The dissociation of the sericin protein aggregates over 1-3 h period of reaction suggests only weak intramolecular interactions between protein molecules and silicate species, and therefore, it seems unlikely that sericin is acting as a template for silica formation.

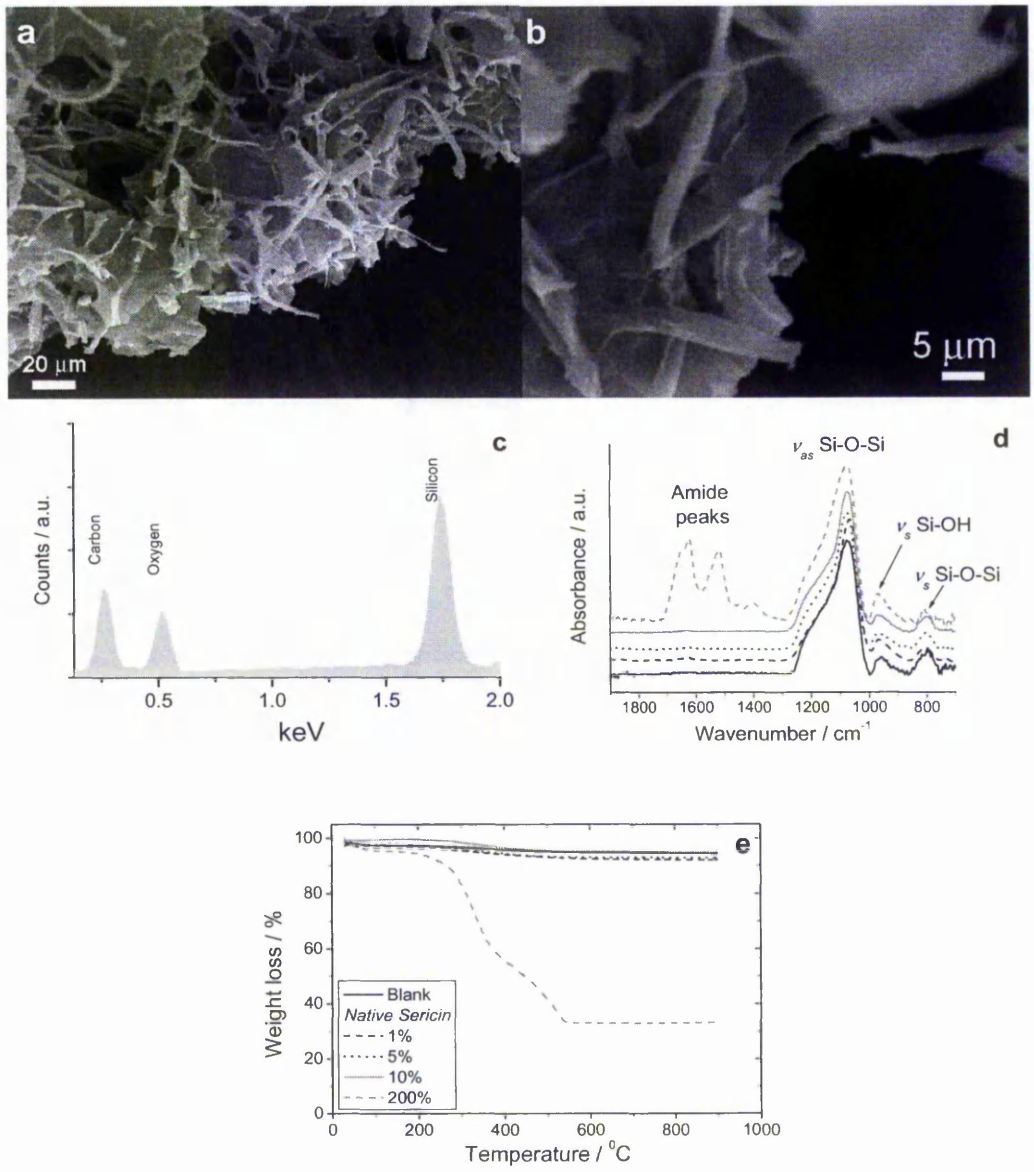

Figure 4.3.2.a, b) SEM image of silica morphology and c) EDS analysis for native sericin-silica composite, Si:OH = 1. d) ATR-FTIR and e) TGA data obtained from silica samples prepared in the presence of a range of native sericin concentrations. Curves in d) bottom to top, represent initial concentration of native sericin proteins 0, 1, 5, 10 and 200 %.

After seven days of reaction time, silica samples were precipitated by centrifugation, washed with water and lyophilized. Scanning Electron Microscopy (SEM), nitrogen adsorption analysis, Attenuated Total Reflection Fourier Transform Infrared Spectroscopy (ATR-FTIR) and TGA were performed on the materials isolated in order to

determine whether (i) the presence of sericin proteins have any effects on the materials properties and (ii) proteins are associated with sili*ca*. Silica samples prepared in the presence of sericin proteins at 1-10 wt % did not show any significant de*via*tion in morphology from the blank sample suggesting only small, if any, effects (data not shown). However, when proteins were present at higher ratios (Si:OH = 1:1 *i.e.* 200 %), morphological changes were observed (Figure 4.3.2a, b). The SEM images suggest the formation of an organic-inorganic "mixture". Elemental analysis performed by Energy Dispersive Spectroscopy (EDS) suggested the formation of silica and the presence of organic component (Figure 4.3.2c). In order to investigate the occlusion of sericin proteins in silica, ATR-FTIR and TGA analyses were performed on the lyophilized samples. The formation of silica was confirmed from peaks from ATR-FTIR data in the region 800-1300 cm^{-1} (Figure 4.3.2d). Peaks between 1400-1800 cm^{-1}, which represent the characteristic protein amide bands, were detected only for the silica samples with the highest protein concentration and were absent for the other samples (Figure 4.3.2d).[29] The data obtained from TGA for the low (1-10 wt %) protein content samples exhibited <5 % weight loss over the temperature range 30-900 °C which is insignificant compared to the weight loss observed for the blank sample (*ca.* 3 %). On the other hand, about 70 % weight loss was recorded for the samples prepared in the presence of native sericin protein at a concentration of 200 %, of which *ca.* 35 % of the loss occurred between 400-600 °C representing a loss due to organic content (Figure 4.3.2e). Taken together, the SEM, TGA and ATR-FTIR data infer that for materials isolated after seven days, native sericin protein molecules when present at lower concentrations (1-10 wt %) did not show any effect on the silica morphologies and also were not occluded in the samples. When present at higher concentration (200 %), its presence affected silica morphology and was found to co-precipitate with sili*ca*. The presence of sericin proteins did not show any statistically significant effects on the surface area of silicas generated (Appendix 1 Figure 1 and Table 2) with the largest effect being seen for 5 % native sericin where the surface area of silica was reduced by 25 % when compared with the blank system.

The results obtained from sericin-silica polymerization experiments are in striking contrast to the effects of other biomolecules studied in the past, *e.g.* R5, silaffins, cationic

recombinant proteins, polylysines, polyarginine, polyhistidine, lysozyme, *etc.*[34-38] Although, these biomolecules and sericin proteins are capable of hydrogen bonding, the main difference is that the former are highly cationically charged under experimental conditions (*i.e.* pH 7). Hydroxyl functionalized side chains are not protonated at *ca.* pH 7 and will not interact electrostatically with silica molecules, instead, hydrogen bonding can occur. These interactions are often weak (5-65 kJ mol^{-1}) and labile. BSA, which has a low pI, did not show an effect on silica formation *in vitro* at circumneutral pH,[6, 34] consistent with the data presented here. In order to verify this hypothesis, the effect of polyserine in silica formation was studied. Indeed, the presence of polyserine neither significantly affected the early stages of silicic acid condensation (see Appendix 1 Table 1) nor altered the particle growth when compared with a blank system (data not shown). The results obtained from the use of polyserine in silicification are in agreement with those presented above for sericin proteins. Our results suggest that the formation and growth of silica particles disrupts sericin aggregates and that sericin proteins do not act as catalysts, templates or aggregation promoting agents.

Protein, wt%	1	5	10	200
Si:OH	200	40	30	1

Table 4.3.1 - Ratio of silicon to hydroxyl from the sericin precursor used in the model silica precipitating system.

For the results reported above the approximate ratios of Si to hydroxyl groups from the sericin precursor were estimated (Table 4.3.1). At the ratios investigated, these levels would be unlikely to significantly affect silica formation. One would intuitively expect hydrogen bonding interactions between (poly)silicic acid and a largely hydroxyl containing protein. However, the ratio of silicon to hydroxyl groups from such a protein would be in excess even under all the reaction conditions currently explored such that any effect of hydrogen bonding by the protein to silicon species would be expected to be small, unless that protein exhibited an exceptional silicon specific catalytic or inhibitory effect. Experiments were conducted at higher concentrations of the sericin precursor (Si:OH = 1) and it was found that even at this concentration there was no statistically

significant effect on the rate constants of early stages of silica polymerization (Figure 4.3.1b). The work presented on Sericin was not carried out by the author of this thesis and is included for completeness.[39]

In order to further probe molecular interactions between orthosilicic acid and hydroxyl functionalized molecules, model studies were undertaken where the behavior of 'simple' molecules – alkanediols – in silica formation was investigated. A series of alkanediols with increasing carbon chain length from 2-7 was used (even longer carbon chain additives were no longer soluble in the aqueous model system). Alkanediols were added to the model silica system at silicon to hydroxyl ratios of 1:1 (100 %) to 1:10 (1000 %) and the effects on various stages of silica polymerization studied. Figure 4.3.1a shows the kinetic results obtained for the alkanediols at a silicon to hydroxyl ratio of one.

The variation in the rate of formation of trimers from orthosilicic acid remained statistically unchanged for all alkanediols when the silicon to hydroxyl ratio was one, suggesting no significant interactions between the alkanediol and monomeric and dimeric orthosilicic acid species at this concentration. The forward oligomerisation reaction also showed a statistically negligible change in rate constant. However, the reverse oligomerisation reaction (dissolution) showed a small but statistically significant increase in rate constant, which is related to the concentration of orthosilicic acid at equilibrium (Figure 4.3.3a). The average equilibrium concentration of orthosilicic acid was observed to increase by *ca.* 16 % with respect to blank system. Thermal gravimetric analysis on lyophilized samples showed <3 % weight loss between 400 and 600 °C even when alkanediols were present at 1:10 Si:OH ratios (data not shown), suggesting that no organic material was retained inside the sili*ca.* Results from the TGA analysis imply that the alkanediols remain in the solution phase of the condensing system and that the ratio of alkanediol to orthosilicic acid will increase as silica polymerization progresses such that a much higher OH:Si ratio could be reached at equilibrium resulting in the observed higher dissolution rate constant (Figure 4.3.3a).

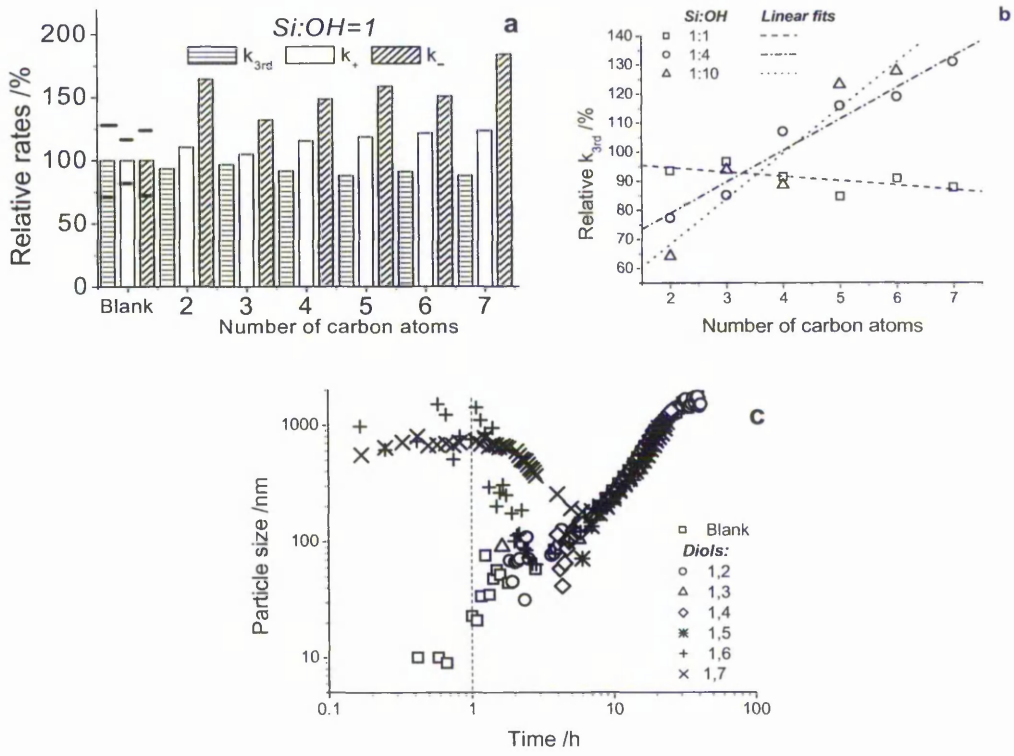

Figure 4.3.3a) The effect of alkanediols on the kinetics of silica formation at a Si : OH ratio of 1:1. Horizontal bars on blank data in a) represent 95% confidence limit. b) For Si : OH = 1:1, 1:4 and 1:10, the effect of increasing carbon chain length on k_{3rd}. NB: for Si:OH=1:10, data from 1,7 diol is omitted due to its poor solubility at that concentration. c) Particle formation in the presence alkanediols in the model system at Si:OH = 1:1. Dotted line in c) indicates the time at which particle formation is measurable in blank system.

The possible interactions of (poly)silicic acid molecules with alkanediols was investigated by increasing the diol concentration (silicon to OH ratio = 1:2, 1:4 and 1:10). For Si:OH = 1:2, there was no significant change observed in the trimerisation rate constant (Appendix Table 1). However, for higher alkanediol concentrations studied, for example at an Si : OH ratio 1:4, the trimerisation rate constant k_{3rd} increased with increasing carbon chain length as shown in Figure 3b, but no significant change in k_+ was observed (Appendix 1 Table 1). A similar effect was observed for Si:OH=1:10 (Figure 4.3.3b). Correlation analysis performed using the Spearman correlation coefficient on the trends shown in Figure 4.3.2b revealed that there is no statistical similarity between the

trend observed for Si:OH = 1:1 and Si:OH = 1:4 or Si:OH = 1:10. In other words, the trends observed for k_{3rd} with respect to carbon chain length for Si:OH = 1:4 and Si:OH=1:10 are statistically distinct compared with the trend observed for Si:OH=1:1. This effect can be explained by the hydrophobic effect as has previously been observed for the addition of diaminoalkanes to a model silicifying system.[40] The increase in the rate of formation of trimers is possibly due to the formation of alkanediol rich domains in solution. 1,2-ethanediol is miscible in water and hence the hydrophobic effect is not observed. Instead 1,2-ethanediol is incorporated into the bulk water structure. Increasing the hydrophobicity of the alkanediol at this concentration may create micelles which could be favorable due to the reduced solubility of the longer carbon chain alkanediols.

The possible formation of alkanediol micelles using PCS in the model system (i) in the absence of silicon, but containing KCl and catechol (both being by-products of the dissociation of the silicon-catecholate complex used as the silicic acid precursor) and (ii) in water (absence of silicon, KCl and catechol)was investigated. The results show that KCl and catechol form particles of size *ca.* 1000 nm which are observed in the presence of diols of carbon chain length 2-5C, suggesting no or little micellisation for these alkanediols (structures have a large error bar suggesting a highly unstable system). However, the formation of micelles in 1,6-hexanediol and 1,7-heptanediol of sizes *ca.* 600 nm and *ca.* 300 nm respectively were clearly observed (Appendix 1 Figure 2). When present in water (in the absence of silicon, KCl or catechol), no particle formation was observed for 1,2-ethanediol and 1,3-propanediol. However, particles (*ca.* 200-400 nm) were formed for chain lengths above three suggesting the formation of micelles (Appendix 1 Figure 4.3.2). This observation could explain the non-linearity in the k_{3rd} data shown in Figure 4.3.3b for Si:OH – 1:4 and 1:10. The presence of higher alkanediols containing hydrophobic regions could effectively make orthosilicic acid more reactive due to the hydrophobic effect,[41] observed as an increase in the rate of formation of trimers. A further increase in alkanediol concentration to 1000 % (Si:OH = 1:10) did not increase the changes in k_{3rd} (Figure 4.3.3b). Perhaps, once the critical micelle concentration is reached any further increase in alkanediol concentration does not have any effect on the trimerisation rate constants. It is difficult to interpret the reduction in

k_{3rd} observed for 1,2-ethanediol and 1,3-propanediol at Si:OH=1:4. For 1, 2-ethanediol and 1,3-propanediol where they remain soluble in water, they could hydrogen bond with orthosilicic acid making it less reactive and causing a reduction in k_{3rd} (Figure 4.3.3b). This was also confirmed in the case of 1,2 ethanediol where it was found that an increase in diol concentration (Si:OH ratio from 1:4 to 1:10) showed further reduction in relative k_{3rd} rate constant from 0.77 to 0.64 (Figure 4.3.3b).

Particle growth monitored using PCS in the presence of alkanediols at different Si:OH ratios revealed no significant effect, however, in the alkanediols where micelles are formed (1,6-hexanediol and 1,7-heptanediol), an initial aggregate size is observed similar to the structures observed in the micelle study (Figure 4.3.3c). These aggregates were found to dissociate at times from 100 to 375 mins after the start of the reaction as silica particles form and thereafter the aggregation rate was found to be similar to the blank. Similar behavior was observed for sericin (Figure 4.3.1c, d), providing further evidence that hydrogen bonding alone is not strong enough to act as a template for silica formation.

The materials produced from the use of alkanediols were characterized by SEM, TGA and gas adsorption. The particle sizes as observed by SEM were found to increase slightly in the presence of alkanediols (Figure 4.3.4, Appendix 1 Figure 3). The addition of 1,2-ethanediol at an Si:OH ratio of 1:10 produced particles with a bimodal size distribution *ca.* 150 and *ca.* 225 nm; the latter being statistically significant (Figure 4.3.4). This is in direct contrast to the significant reduction in silica particle size observed in the presence of glycerol.[42] However, it should be noted that firstly, the precursor used in that study was tetramethoxysilane (TMOS). Secondly, glycerol was used as a "co-additive" along with the *R5* peptide or poly-(L-lysine) at high concentrations (up to 60 % / volume) thus introducing effects due to the *R5* peptide or poly-(L-lysine)-glycerol interactions that affect solution properties. The occlusion of alkanediols was studied by TGA; the data obtained showed that the alkanediols were not retained within the silica even at an Si:OH ratio of 1:10 (data not shown). Gas adsorption measurements on samples prepared at Si:OH = 1 revealed that there was no statistically significant change in surface areas or porosities of silicas. While, at Si:OH = 1:4, a

statistically significant reduction in surface area from ~600 m^2g^{-1} for the blank system to ~450 m^2g^{-1} for silica prepared in the presence of alkanediols was observed with no apparent trend with respect to carbon chain length (Appendix 1 Table 2).

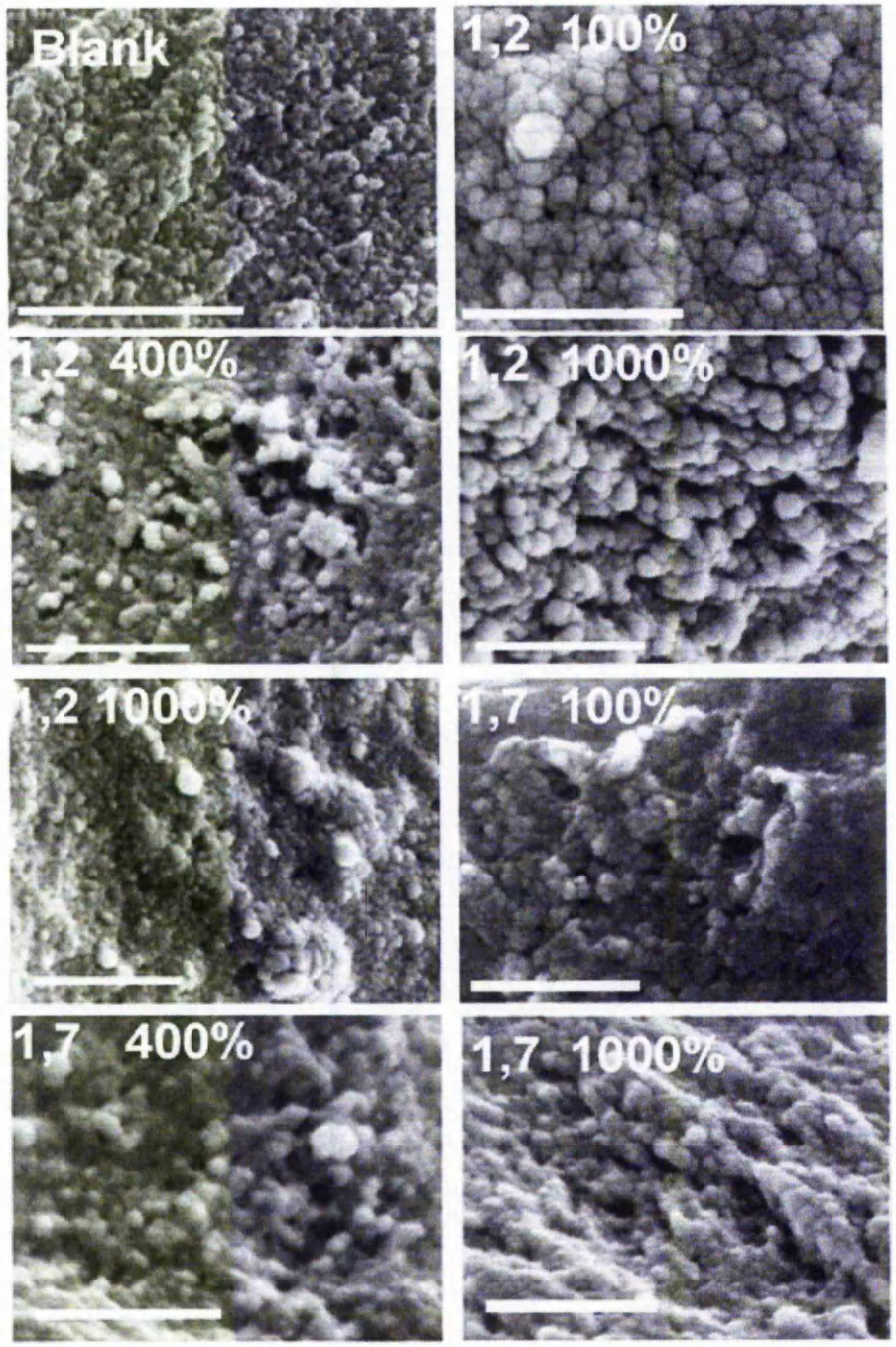

Figure 4.3.4 - Representative SEM of silica samples prepared with or without the presence of diols. Two data sets for 1,2-ethanediol 1000% are shown due to bimodal particle sizes. Scale bars = 2 μm.

In order to gain further insights into the roles of hydroxyl-containing organic species in silica formation, the amounts of hydroxyls from bioextracts isolated from biosilicas of plants, sponges and diatoms was estimated(Table 4.3.2). The estimated values suggest a large excess of "Si" over hydroxyl-containing species from bioextracts. Experimental data presented in this paper show that even when present at higher amounts (up to 1000 %), alkanediols neither drastically affect the silica formation process nor do they show any dramatic effects on product properties.

	% Protein [a]	%OH AA [b]	Si:OH
Plants[1]	0.1[c]	[d]	54800
Sponges[2]	1	22	225000
Diatoms	0.7-28 [3]	17-35	40-880
	0.8 [4]	23	1110
	5 5[3]	38	6500

Table 4.3.2 - Estimates of ratios of silicon from biosilica to hydroxyls from bioextracts.

[a] With respect to dry biosilica, [b] % amino acids with hydroxyl side groups, [c] total organic content, [d] 250 pmole of hydroxyl containing residues/μg organic content.

Although additional information needs to be obtained through further investigations, the data obtained in the present detailed study points to the following hypotheses for the role of hydroxyl containing biomolecules in silicification that could perhaps be of relevance to biosilicifying systems. In the first case, hydroxyl-containing organic molecules are not at all involved 'chemically' in the formation of sili*ca.* Instead, they may be only assisting in rendering stability and solubility to the organic molecules found occluded in sili*ca.* For example, the hydroxyl-rich domains found in silicateins could possibly have indirect roles to play in biosilicification such as protection of active sites or assisting the assembly of biomolecules.[45] The second possibility is that assuming the hydroxyl-containing organic molecules affect silica formation, then the environments of silicic acid polymerization could be highly deficient in water (*e.g.* compartmentalization) in order to increase the effects of hydroxyl functional groups of proteins in silica formation. The interaction occurring between orthosilicic acid and the hydroxyl groups are likely to be

hydrogen bonds. It should be noted that most of the model systems studied to date are aqueous based. Thus, species that could potentially bond to orthosilicic acid include: other orthosilicic acid molecules, water and the organic additives. However, as it is present in a large excess, water will override any hydrogen bonding effects exerted by organic additives. It is believed that the results presented herein may assist us in gaining a better understanding of biosilicification and perhaps other biomineralization processes. Only further chemical and biological experimentation will identify which of these possibilities or combination thereof actually occur.

4.4 Conclusions

In summary, the role of both hydroxyl functionalized biomolecules and alkanediols on silica formation have been systematically investigated *in vitro*. The results demonstrate that in aqueous systems the effect of hydroxyl-containing additives is negligible although as the molar ratio of Si:OH groups decrease the effect of these molecules become more apparent. It is worth noting that hydroxyl functionalized molecules have been found to regulate *in vitro* mineralization of calcium carbonate for example.[45-47] The evidence presented above leads us to believe that Si-O-C bonds are unlikely to form but further work, including NMR analysis and theoretical modeling, is required to support this hypothesis. If covalent bonds between silicon and hydroxyl functionalized additives were to form, one would expect to observe significant changes in the rate of condensation of orthosilicic acid together with entrapment of the additives in the silica formed.

References

1. T. L. Simpson, B. E.Volcani, *Silicon and Siliceous Structures in Biological Systems*. Springer-Verlag: New York, 1981.
2. R. E. Hecky, K. Mopper, P. Kilham, E. T. Degens, *Mar. Biol.* 1973, **19**, 323-331.
3. D. M. Swift, A. P. Wheeler, *J. Phycol.* 1992, **28**, (2), 202-209.
4. J. N. Cha, K. Shimizu, Y. Zhou, S. C. Christiansen, B. F. Chmelka, G. D. Stucky, D. E. Morse, *Proc. Natl. Acad. Sci. USA* 1999, **96**, (2), 361-365.
5. K. Shimizu, J. N. Cha, G. D. Stucky, D. E. Morse, *Proc. Natl. Acad. Sci. USA* 1998, **95**, (11), 6234-6238.
6. Y. Zhou, K. Shimizu, J. N. Cha, G. D. Stucky, D. E. Morse, *Angew. Chem. Int. Ed.* 1999, **38**, (6), 780-782.
7. C. C. Harrison, *Phytochemistry* 1996, **41**, 37-42.
8. C. C. Harrison, Y. Lu, In *Biomineralization 93*, Allemand, D., Cuif, J.-P., Eds. Musee oceanographique: Monaco, 1994.
9. C. C. Perry, S. Mann, Aspects of biological silicification. In *Origin, Evolution and modern aspects of biomineralisation in plants and animals*, Cricks, R. E., Ed. Plenum Press: New York 1989 p419.
10. K. D. Lobel, J. K. West, L. L. Hench, *Mar. Biol.* 1996, **126**, (3), 353-360.
11. K. D. Lobel, J. K. West, L. L. Hench, *J. Mater. Sci. Lett.* 1996, **15**, (8), 648-650.
12. J. B. Lambert, G. Lu, S. R. Singer, V. M. Kolb, *J. Am. Ceram. Soc.* 2004, **126**, (31), 9611-9625.
13. S. D. Kinrade, J. W. Del Nin, A. S. Schach, T. A. Sloan, K. L. Wilson, C. T. G. Knight, *Science* 1999, **285**, (5433), 1542-1545.
14. N. Sahai, *Geochim. Cosmochim. Acta* 2004, **68**, (2), 227-237.
15. N. Sahai, J. A. Tossell, *Geochim. Cosmochim. Acta* 2001, **65**, (13), 2043-2053.
16. P. B. Kaufman, P. Dayanandan, Y. Takeoka, W. C. Bigelow, J. D. Jones, R. K. Iler, Silicon in shoots of higher plants. In *Silicon and siliceous structures in biological systems*, Simpson, T. L., Volcani, B. E., Eds. Springer-Verlag: New York, 1981.
17. E. G. Vrieling, W. W. C. Gieskes, T. P. M. Beelen, *J. Phycol.* 1999, **35**, 548.
18. C. C. Perry, Y. Lu, *J. Chem. Soc. Faraday. Trans.* 1992, **88**, (19), 2915-2921.
19. S. V. Patwardhan, *Silicification and Biosilicification: Role of Macromolecules in Bioinspired Silica Synthesis*. Ph.D. Dissertation, University of Cincinnati: 2003.
20. T. Coradin, J. Livage, *Colloids Surf. B* 2001, **21**, (4), 329-336.
21. L. Sudheendra, A. R. Raju, *Mater. Res. Bull.* 2002, **37**, 151.
22. Q. Y. Sun, T. P. M. Beelen, R. A. van Santen, S. Hazelaar, E. G. Vrieling, W. W. C. Gieskes, *J. Phys. Chem. B* 2002, **106**, (44), 11539-11548.
23. D. Belton, G. Paine, S. V. Patwardhan, C. C. Perry, *J. Mater. Chem.* 2004, **14**, (14), 2231-2241.
24. S. V. Patwardhan, D. Belton, G. Tilburey, C. C. Perry, In *ACS Symp. Ser. xxx*, in press, 2006.
25. S. Sofia, M. B. McCarthy, G. Gronowicz, D. L. Kaplan, *J. Biomed. Mater. Res.* 2001, **54**, (1), 139-148.
26. J. Huang, R. Valluzzi, E. Bini, B. Vernaglia, D. L. Kaplan, *J. Biol. Chem.* 2003, **278**, (46), 46117-46123.
27. S. Brunauer, P. H. Emmett, E. Teller, *J. Am. Chem. Soc.* 1938, **60**, (2), 309-319.
28. E. P. Barrett, L. G. Joyner, P. P. Halenda, *J. Am. Chem. Soc.* 1951, **73**, (1), 373-380.

29. S. V. Patwardhan, R. Maheshwari, N. Mukherjee, K. L. Kiick, S. J. Clarson, *Biomacromolecules* 2006, **7**, (2), 491-7.
30. Our aqueous model silicifying system utilizes dipotassium tris(1,2-benzenediolato-*O,O'*)silicate, an aqueous soluble silicon precursor, which upon the addition of a predetermined amount of hydrochloric acid liberates orthosilicic acid at *ca.* 6.8. Note that no buffer is required in this system as the catechol generated from the dissociation of the complex is sufficient to buffer the system. The concentration of orthosilicic acid used throughout all experiments was *ca.* 30mM and the levels of undissociated complex were found to be negligible from ^{1}H-NMR of catechol as described previously (ref. 23). The model system allows kinetic studies to be performed on the transformation from monomer to oligomeric species through to useful materials. It should be noted that the precursor for orthosilicic acid, (dipotassium tris(1,2-benzenediolato-*O,O'*)silicate) generates three molar equivalents of catechol which is itself a diol (Si:OH ratio 1:6). The effect of catechol on the condensation of orthosilicic acid has been normalised throughout all the experiments by comparison of data against a blank condensing system where no additive has been added.
31. C. C. Perry, T. Keeling-Tucker, *J. Biol. Inorg. Chem* 2000, **5**, (5), 537-550.
32. C. C. Perry, T. Keeling-Tucker, T., Model studies of colloidal silica precipitation using biosilica extracts from Equisetum telmateia. *Colloid Polym. Sci.* 2003, **281**, (7), 652-664.
33. C. C. Harrison, N. Loton, *J. C. Soc. Faraday Trans.* 1995, **91**, (23), 4287-4297.
34. T. Coradin, A. Coupe, J. Livage, In *Biological Biomimetic Materials-Properties to Function*, Aizenberg, J., McKittrick, J. M., Orme, C. A., Eds. MRS Symp. Proc. 724: 2002, pp 147-152.
35. S. V. Patwardhan, S. J. Clarson, C. C. Perry, *Chem. Commun.* 2005, **9**, 1113-1121.
36. S. V. Patwardhan, K. Shiba, C. Raab, N. Husing, S. J. Clarson, In *Polymer Biocatalysis and Biomaterials*, Cheng, H. N., Gross, R. A., Eds. Oxford University Press: 2005.
37. P. J. Lopez, C. Gautier, J. Livage, T. Coradin, *Current Nanoscience* 2005, **1**, (1), 73-83.
38. S. V. Patwardhan, K. Shiba, H. C. Schroeder, W. E. G. Muller, S. J. Clarson, C. C. Perry, The Role of Bioinspired Peptide and Recombinant Proteins in Silica Polymerisation. In *The Science and Technology of Silicones*, in press, 2006.
39. G. E. Tilburey, S. V. Patwardhan, J. Huang, D. L. Kaplan, C. C. Perry, *J. Phys. Chem. B* 2007, **111**, (17), 4630-4638. The work carried out on Sericin was not conducted by the thesis author and is included for completeness.
40. D. Belton, S. V. Patwardhan, C. C. Perry, *Chem. Commun.* 2005, (27), 3475-7.
41. F. Rodriguez, D. D. Glawe, R. R. Naik, K. P. Hallinan, M. O. Stone, *Biomacromolecules* 2004, **5**, (2), 261-265.
42. Belton, D. J., Perry, C. C., unpublished data.
43. N. Kröger, R. Deutzmann, M. Sumper, *Science* 1999, **286**, (5442), 1129-1132.
44. M. M. Murr, D. E. Morse, *Proc. Natl. Acad. Sci. USA* 2005, **102**, (33), 11657-11662.
45. J. Aizenberg, A. J. Black, G. H. Whitesides, *J. Am. Chem. Soc.* 1999, **121**, (18), 4500-4509.

46. J. Aizenberg, A. J. Black, G. M. Whitesides, *Nature* 1999, **398**, (6727), 495-498.
47. I. W. Kim, R. E. Robertson, Zand, R., *Crystal Growth & Design* 2005, **5**, (2), 513-522.

Chapter 5 – Using Azamacrocyclic molecules to control the formation of silica.

Part I: The Formation of Inorganic-Organic Hybrid Needle-like Tetragonal Prisms.

5.1 Introduction

In nature processes such as the transport of oxygen round mammalian bodies and photosynthesis in plants have been shown to be controlled by either ions, small cyclic molecules or in some cases light.[1,2] The importance of these processes in nature prompted scientists to investigate the metal ion chemistry and the ability to stabilise metal cations in unusual oxidation states, where often materials exhibiting unusual or enhanced properties are formed.[1, 3] In haemoglobin and chlorophyll the metal ion was found to be coordinated to nitrogen containing macrocyclic molecules known as phyphorins. Macrocyclic molecules usually contain between 3 and 6 donor atoms, where a metal ion is coordinated in the macrocyclic cavity. As with simple polydenate ligands the coordination of a metal ion through two donor atom usually forms 5, 6 or occasionally 7 membered chelate rings. The size of the macrocyclic cavity often dictates the properties of the resulting metal complex and is usually dependent on the number and type of atoms in the macrocyclic ring. The nature of macrocyclic molecules introduces stereochemical constraints and despite a certain degree of flexibility within the ring, selective binding of one metal cation or anion over another is a regular occurrence in macrocyclic chemistry.[1, 2, 4, 5] If a metal ion is too large to fit in a cavity and provided the ring is not sterically hindered by sp^2 hybridised atoms, folding can occur. For instance, 4 of the 6 coordination sites of an octahedral structure can be occupied by a macrocyclic ligand or the metal ion can be displaced from the donor plane of the ring. The introduction of sp^2 hybridised atoms and delocalisation into the macrocyclic ring enables the ring to act as an "electron sink", where metal ions in unusual oxidation states can be stabilised.[1]

Azamacrocyclic molecules are known to specifically bind to transition metal and lanthanides ions forming thermodynamically stable complexes.[2, 4, 6] This has led to the development of a new generation of abiotic host molecules that contain a signalling or responsive functional group enabling the development of molecular sensors.[2, 4] The chelation of Gd III by azamacrocyclic molecules gives molecular species that can be used as contrast agents in magnetic resonance imaging (MRI), where strong binding of the metal and occupation of most of the available coordination sites is vital.[7] Azamacrocyclic molecules such as 1,4,8,11-tetraazacyclotetradecane (cyclam) and related compounds have been used in the preparation of new inorganic-organic hybrid materials such as gallium phosphates,[8, 9] novel microporous aluminophosphates[10] and magnesioaluminophosphates.[11]

Interestingly, the azamacrocyclic molecules have been found to interact with the crystallising inorganic framework in two different ways; the first is found in gallium phosphate hybrid materials. The azamacrocyclic molecule, cyclam was found to be covalently bonded to the zeolite-like gallium phosphate framework. This structure permits metal cation exchange with other ions forming stronger complexes with the macrocycle, such as Cu^{2+}.[12] The type of interaction was found in metalloaluminophosphates where the azamacrocyclic molecule, 1,4,8,11 tetramethyl 1,4,8,11-tetraazacyclodecane (4MC) was found to act as a structure directing agent around which the inorganic framework crystallises forming STA-6, 7 and 8 structures depending on the metal cation present.[11, 13, 14] One further example exists; where the azamacrocyclic molecule is present in the crystal structure of the material, but does not coordinate a metal ion because the metal ions are insufficient in size. Gallium in the presence of 1, 4, 7, 10, 13, 16-hexaazacyclooctadecane is one such example where the gallium ion is too small to be effectively coordinated to the azamacrocyclic molecule resulting in the azamacrocyclic molecule not being bound to the framework.[15]

Molecular self assembly has become one of the fastest growing areas of research in materials chemistry over the past decade, leading to the production of biologically inspired nanomaterials.[16] One such area of research is the formation of bioinspired nano-patterned silica materials where inspiration has been taken from silica accumulating organisms such as diatoms,[17] sponges and higher plants.[18] Several

classes of biomolecules have been extracted from diatoms, of which two have been shown to be intimately associated with diatom biosilica, namely silaffins and long chain polyamines (LCPA). Silaffins are highly post-translationally modified peptides derived from the sil1 protein in *C.fusiformis*, where a number of lysine residues have been shown to have N-methylated polypropyleneimine side chains consisting of between 4 and 9 repeating units.[19, 20] Knecht and Wright preformed site-directed mutagenesis on an integral peptide sequence found in silaffins known as *R5* where it was shown the arginine-arginine-isoleucine-leucine (RRIL) motif found at the C-terminus of *R5* was found to act as an organising element.[21] Organisation of the *R5* peptide in this manner was shown to create a locally high concentration of amine containing amino acid side chains and was shown to promote the precipitation of silica *in vitro*. This work provided the first evidence that molecular self-assembly was important in biosilicification and since that time a number of new bioinspired and biomimetic silica morphologies have been produced through molecular self-assembly.[21]

LCPA in centric diatoms are species specific with between 14 and 20 nitrogen atoms routinely making up the structure.[17] The polypropyleneimine units are attached to a putrescine molecule where the nitrogen atoms exhibit varying degrees and patterns of methylation.[22] Since the extraction and characterisation of biomolecules from silica accumulating organisms, a common theme has developed in the area of bioinspired and biomimetic silica formation *in vitro*. Molecular additives ranging from polyelectrolytes to small molecules (mw >1000) having a significant effect on silica formation *in vitro* either catalytically or through molecular templating usually contain some degree of amine functionality.[23, 24]

Small molecules, including amino acids[25] with varying degrees of complexity have been investigated by Perry *et al.* It has been shown that the molecular architecture has a significant effect on the catalytic ability and morphological control exerted on the formation of silica *in vitro*.[26-28] These studies focus on understanding the molecular interactions between silicon species and amine functionalised small molecules. These studies also showed with regularity that it is the ability of the additives being studied to self-assemble into a macroscopic structure that template and catalyses the formation of silica *in vitro*. Furthermore, mechanisms based on the hydrophobic

effect and the electrostatic effect have been proposed for the catalytic effects exhibited when diaminoalkanes with increasing chain length were studied *in vitro*.[26] In another case work based on understanding the function of the molecular spacing between nitrogen atoms has resulted in a mechanism being proposed for the formation of highly condensed silica spheres when using pentaethylenehexamine.[27]

Patwardhan *et al.* have studied the effect of a number of polyelectrolytes on the formation of silica *in vitro* which inspired many other researchers to work on the same molecules.[29] Work on poly(allylamine) hydrochloride (PAH) *in vitro* first reported by Patwardhan *et al.*[30] has been continued by Sumper *et al.* where the self assembly of PAH into a spherical moiety has been shown to catalyse and template the formation of silica spheres *in vitro* through a phase separation mechanism.[31, 32] Patwardhan *et al.* also studied the effect of poly-(L-lysine) on silica formation where quite remarkable silica structures were formed.[33] Further studies by the same group have showed that the formation of hexagonal silica plates is dependent on the self assembly of poly-(L-lysine) in an alpha helical conformation into a hexagonal template, which is independent of chirality.[34] A number of other silica morphologies have been produced by Jin *et al.* where the morphology of the PEI-directed silica can be changed by altering the reaction conditions such as polymer architecture, concentration and the reaction medium.[35] The most interesting of the morphologies from this group has been the formation of hollow nano-fibres where a high molecular weight (500000) linear PEI was used to template the formation of silica using TMOS or TEOS.[35] Silica tubes were prepared by Coradin *et al.* by the condensation of sodium silicate in a confined media name a polycarbonate membrane that was dissolved away after several impregnation steps and the silica isolated.[36] Finally, organic inorganic hybrid silica tubes have also been prepared by Moreau *et al.* using a bridged silsesquioxanes in which a chiral silylated diureidocyclohexyl derivative was hydroylsed and self-templated the formation of amorphous hybrid silicas.[37]

The investigations into the effect of amine molecular architecture on the formation of novel silica morphologies were continued in this chapter. The unique ability of azamacrocyclic molecules to interact with crystallising solids lead to the hypothesis that they might also interact with a forming amorphous inorganic material such as silica. Combined with the knowledge that amine functionalised molecules have been

shown to interact and control the morphology of silica formed *in vitro* it was hypothesised that azamacrocyclic molecules would have a pronounced effect on the formation of silica *in vitro*. The molecular interactions identified during silica formation using other small molecules, such as the hydrophobic and electrostatic effect have been shown to control the formation of silica *in vitro*. The study of cyclic molecules introduces two further possible molecular interactions. Firstly one must consider the interactions between cyclic species. Cyclic molecules might be able to self-assemble into alternately charged layers separated by anionically charged counter ions at circumneutral pH, due to their planar conformation. Furthermore, cyclic species by their very nature have a cavity in which an anionic species could be coordinated giving the possibility of host guest chemistry. Alternatively, neither of these interactions may occur but we felt sure that because cationically charged molecules have been shown to interact with silicon species, we would form novel silica structures with interesting properties.

In Part I the role of 1,4,8,11-tetraazacyclotetradecane (cyclam) and molecules derived from its structure are investigated in the formation of organic-inorganic hybrid materials using dipotassium tris(1,2-benzenediolato-*O,O'*) precursors. This led to the synthesis of crystalline organic-inorganic hybrid tetragonal prisms and other morphologies using molecules related to the structure of cyclam. In Part II we report a more conventional approach to studying azamacrocyclic molecules on the formation of silica where azamacrocyclic molecules with a ring size greater than ≥14 atoms show an exceptional ability of catalyse the formation of silicas at remarkably low concentrations using the unbuffered TMOS system developed in Chapter 2 Part II. Furthermore we characterise the silicas produced and examine the role of phosphate in the formation of silica with remarkably well defined pore structures and comment of the role of molecular speciation in silica formation. Finally, we report the rapid formation of monodispersed silica spheres where the size can be controlled by the additive used and the pH of the condensing system.

5.2 Materials and Methods

5.2.1 The synthesis of crystalline inorganic-organic hybrid materials.

Dipotassium tris(1,2-benzenediolato-*O,O'*)silicate (KSiCat) (Aldrich) and purified further using methanol as a solvent for recrystallisation, any insoluble impurities were filtered off and the methanol removed by rotary evaporation. The remaining solid was dried further in a vacuum oven at 40 °C for approximately 24 h. The purity was confirmed to be > 99 % by ^{1}H NMR using a Jeol ECX-400 spectrometer. Dipotassium tris(1,2-benzenediolato-*O,O'*)germanate 97 % (KGeCat), cyclam 98 %, *N,N,N',N'*-tetramethylethylenediamine 99.5 % (4MEDAE), *N,N,N',N'*-tetramethyl-1,4-butanediamine 98 % (4MEDAB) and *N,N,N',N'*-tetramethyl-1,6-hexanediamine 99 % (4MEDAH) (all purchased from Aldrich) and used without further purification.

Initially preparation of the needle like tetragonal prisms was carried by weighing out 0.14 g (30 mM) of KSiCat and dissolving it in 7.76 ml of distilled and deionised water (dd water). A solution of cyclam was prepared at a Si:N ratio of 10:1 (0.0015 g, 7.5 µM) and dissolved in dd water (2 ml). 2 M HCl (240 µl) required to dissociate the dipotassium tris(1,2-benzenediolato-*O,O'*)silicate complex was added to the cyclam solution. The two solutions were mixed, the pH was taken after 15 mins and the precipitate isolated by centrifugation after 60 mins, unless otherwise stated. The precipitate was washed with dd water (40 ml) followed by centrifugation, this process was repeated 3 times and the material was frozen and freeze dried.

Large crystals were prepared for single crystal silicon diffraction. This was achieved by chilling the titrated cyclam solution and the KSiCat solution in an ice bath for 20 mins prior to the solution being mixed. The precipitating system was then put back into the ice bath where the temperature remained at approximately 5 °C for 60 mins prior to isolation of the tetragonal prisms as described previously.

The pH study involved a slight modification to this procedure to avoid the competition for protons in solution. The pH was varied by adding different amount 2 M HCl to the KSiCat solution to achieve a desired pH, followed by the addition of the cyclam solution that had been titrated to the same pH as the KSiCat would achieve

after 15 mins. The titration curves used to determine the amount of 0.1 M HCl added to the cyclam and 2 M HCl added to KSiCat solution is shown in Figure 5.3.5.2. The same procedure was used to make the dipotassium tris(1,2-benzenediolato-*O,O'*)germanate (KGeCat titration curve shown in Figure 5.3.7.1.) This insured that the speciation of the cyclam was maintained as much as possible at the final pH of the solution. The same procedure was adopted for the materials prepared with 4MEDAE, 4MEDAB and 4MEDAH (titration curves are shown in Figure 5.4.1).

5.2.2 The synthesis of silica spheres using azamacrocyclic molecules.

The silica precursors used throughout this study were tetramethoxysilane (TMOS) and dipotassium tris(1,2-benzenediolato-*O,O'*)silicate (KSiCat). The precursors were purchased from Sigma Aldrich. KSiCat was purified by dissolving in methanol followed by separation by filtration to remove the insoluble fraction with removal of methanol by rotary evaporation. The purity of the KSiCat was confirmed with ^{1}H NMR and molybdosilicate assay to >99 %. The starting concentration of silica precursors was 30 mM throughout the silicate and silica studies unless otherwise stated.

The azamacrocyclic molecules used for this study were purchased from Sigma Aldrich. The structures of these molecules investigated are shown in Scheme 5.2.2.1, the speciation diagrams[38] where appropriate are shown in Appendix 3 Figure 1.

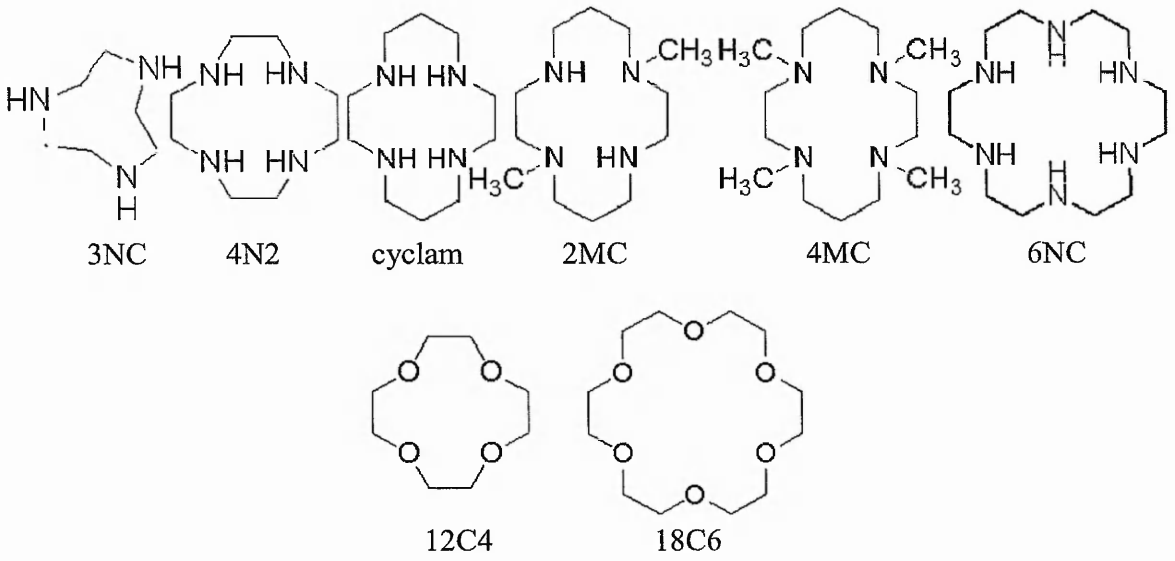

Scheme 5.2.2.1 – From left to right, top to bottom 1,4,7-triazacyclononane (3NC), 1,4,7,10-tetraazacyclododecane (4N2), 1,4,8,11-tetraazacyclodecane (cyclam), 1,8 dimethyl 1,4,8,11-tetraazacyclodecane (2MC), 1,4,8,11-tetra methyl 1,4,8,11 tetraazacyclodecane (4MC), 1,4,7,10,13,16-hexaazacyclooctadecane (6NC). 12-crown-4 (12C4) and 18-crown-6 (18C6).

The azamacrocyclic molecules were studied using a 30 mM condensing system the silicon:nitrogen (Si:N) ratio was changed from 1:1 (7.5 mM), 10:5 (3.75 mM) and 10:1 (0.75 mM) using KSiCat and 10:1 when using TMOS. The amount of acid required to achieve pH 6.8 was derived from the 10:1 titration curves shown in Figure 5.3.5.2, for instance if the Si:N ratio was increased from 10:1 to 10:5 the amount of acid was mutilplied by 5.

Kinetic studies using TMOS required a hydrolysis period to convert the precursor to a solution containing orthosilicic acid prior to the start of the analysis, (it should be noted that the hydrolysis of TMOS creates a mixture of species where orthosilicic acid is the predominant species in solution (see ^{29}Si NMR in section 2.12.2). TMOS was hydrolysed at a concentration of 1 M (173 µl) in 1 ml of 1 mM HCl solution for 15 mins. The TMOS solution was then diluted and neutralised to pH 6.8 ±0.2 in one step. 1 mM KOH (4.5 ml) (diluted from a 1 M KOH standard purchased from Fisher Scientific) was diluted with of deionised and distilled water (5.2 ml) (neutralising solution). The hydrolysed TMOS solution (0.3 ml) was pipetted into the neutralising solution. Where additives were studied in the TMOS condensing system, the additives were dissolved in dd water (2 ml) and the solutions pH was adjusted to pH

6.8 ±0.1 with 0.1 M HCl as per the titration curves in Appendix 3 Figure 2. When the titrated additives solutions were simply added to the neutralising solution, the final pH was not pH 6.8 ±0.2. An additional 4.5 µl of 2 M KOH was required to achieve the desired pH and was added to the TMOS neutralising solution. The addition of the additive solution was made immediately after the TMOS had been pipetted into the neutralising solution.

The kinetics of the TMOS system were measured by taking 10 µl portions of the condensing solution at predetermined time intervals into a solution of 16.5 ml of molybdic acid solution forming silicomolybdic acid, which after 15 mins was reduced to silicomolybdous acid. After 24 h the absorbance of the solution was measured at 810 nm. The materials produced were typically isolated after 24 h unless otherwise stated. The particle formation and aggregation behaviour of the condensing system was measured using a Malvern Zetasizer NanoS a 25 °C. Microscopy was carried out on lyophilized samples using a Jeol JSM-840A scanning electron microscope unless otherwise stated. Nitrogen gas adsorption/desorption analysis was carried out on lyophilized samples using a Quantachrome Nova 3200e surface area and pore size analyzer. Prior to analysis, samples were degassed overnight at 130 °C under vacuum. Surface areas were then determined *via* the BET method where nitrogen is assumed to have a cross-sectional area of 0.16 nm^2,[39] over the range of relative pressures 0.05 – 0.3 at which point the monolayer is assumed to assemble. Pore radii were determined by the BJH method using the desorption branch of the isotherm.[40] Thermal gravimetric analysis was carried out on selected samples using a Perkin Elmer Pyris 6 TGA. The samples were heated at 10 °C min^{-1} from 30 to 900 °C in air to insure complete combustion of all organic material retained within the material.

5.2.3 Species specific addition of the azamacrocyclic molecules in the formation of silica using KSiCat.

The experimental procedure initially used to study the azamacrocyclic molecules in 30 mM silicic acid solutions generated from KSiCat was to dissolve the azamacrocyclic molecule in dd water (2 ml) and then add a predetermined amount of 2 M HCl (see titration curve Figure 5.3.5.2a) required to dissociate the KSiCat

(dissolved in the remaining volume of dd water) and generate 10 ml of 30 mM condensing solution of silicic acid at pH 6.8 ±0.2 in the presence of an additive.

Advances in the project and the work carried out with cyclam revealed the need for method development, where it was found that the speciation of the azamacrocyclic molecules was extremely important. Method 1 involved the addition of the acid required to dissociate the KSiCat to the additive solution. When the speciation of the azamacrocyclic molecule is considered, method 1 involved the addition of the azamacrocyclic molecule in a fully protonated state. Instead, the procedure was modified so that the 2 M HCl required to dissociate the complex was added to the KSiCat solution after 30 s the additive containing solution was added, which had previously been titrated to pH 6.8, as depicted in Scheme 5.2.3.1 – method 2. Finally a third method was developed where the azamacrocyclic molecule was added under basic conditions. The procedure is identical to method 2 except the azamacrocyclic solution was not titrated to pH 6.8 and instead was added as the base (approximately pH 11) – method 3. The method development was introduced in recognition that the different protonation states of the azamacrocyclic molecules could have different effects on the formation of silica.

	Solution 1	Solution 2	Solution 3
Method 1 - Protonated addition	30mM KSiCat	Azamacrocyclic + 2M HCl	
Method 2 - Species specific addition	30mM KSiCat	Azamacrocyclic, pH 6.8	2M HCl
Method 3 - Basic addition	30mM KSiCat	Azamacrocyclic, pH 11	2M HCl

Table 5.2.3.1 – Method 1 - Protonated addition of the azamacrocycles when using KSiCat initially used to study azamacrocyclic molecules in KSiCat. Method 2 – Species specific addition of azamacrocyclic molecules to KSiCat and TMOS. Method 3 – The azamacrocyclic molecule is added in an unprotonated form, basic addition.

5.3 Results and discussion

5.3.1 The synthesis of inorganic-organic hybrid needle-like tetragonal prisms

The formation of needle like tetragonal prism were observed when a solution of cyclam with a silicon:nitrogen (Si:N) ratio of 10:1 was added to a 30 mM solution of KSiCat with a pH of 6.8 ±0.2. A precipitate formed almost immediately and was

isolated after 24 h by centrifugation, washed with dd water and lyophilised. Figure 5.3.1.1f shows an SEM micrograph of the precipitate isolated after 24 h where it can be seen that a mixture of structures are present; needle-like hollow tetragonal prisms (referred to as tetragonal prisms) and pieces of material with no specific morphology. Initially the formation of these structures was investigated using a time dependent study . Figure 5.3.1.1 shows that the morphology of the material is time dependent, where initially it can be seen that the formation of a sheet like material after 25 s and tetragonal prisms after 5 mins. The tetragonal prisms form after 5 mins and mature with increasing time. The tetragonal prisms appear relatively homogenous in size and shape after 60 mins. Thereafter, the homogeneity of isolated material is lost and the material with a non-specific structure starts to dominate the isolated material after 346 mins. Comparison of the material isolated after 346 mins and 24 h shows little change in the structures and composition of the sample. The formation of two materials; tetragonal prisms followed by a material with a non-specific structure can be attributed to competing processes, where perhaps a critical concentration of cyclam is needed to form the tetragonal prisms. Once the concentration of cyclam is lower than this threshold a second material forms in the presence of the residual cyclam. The formation of the material showing no morphological control can be attributed to be the condensation of silicic acid forming silica in the presence of residual cyclam. If this hypothesis is correct the formation of silica after 132 mins indicates that cyclam is involved in the formation since the earliest time silica can be isolated by centrifugation from a 30 mM blank condensing system of silicic acid is *ca.* 16 h.

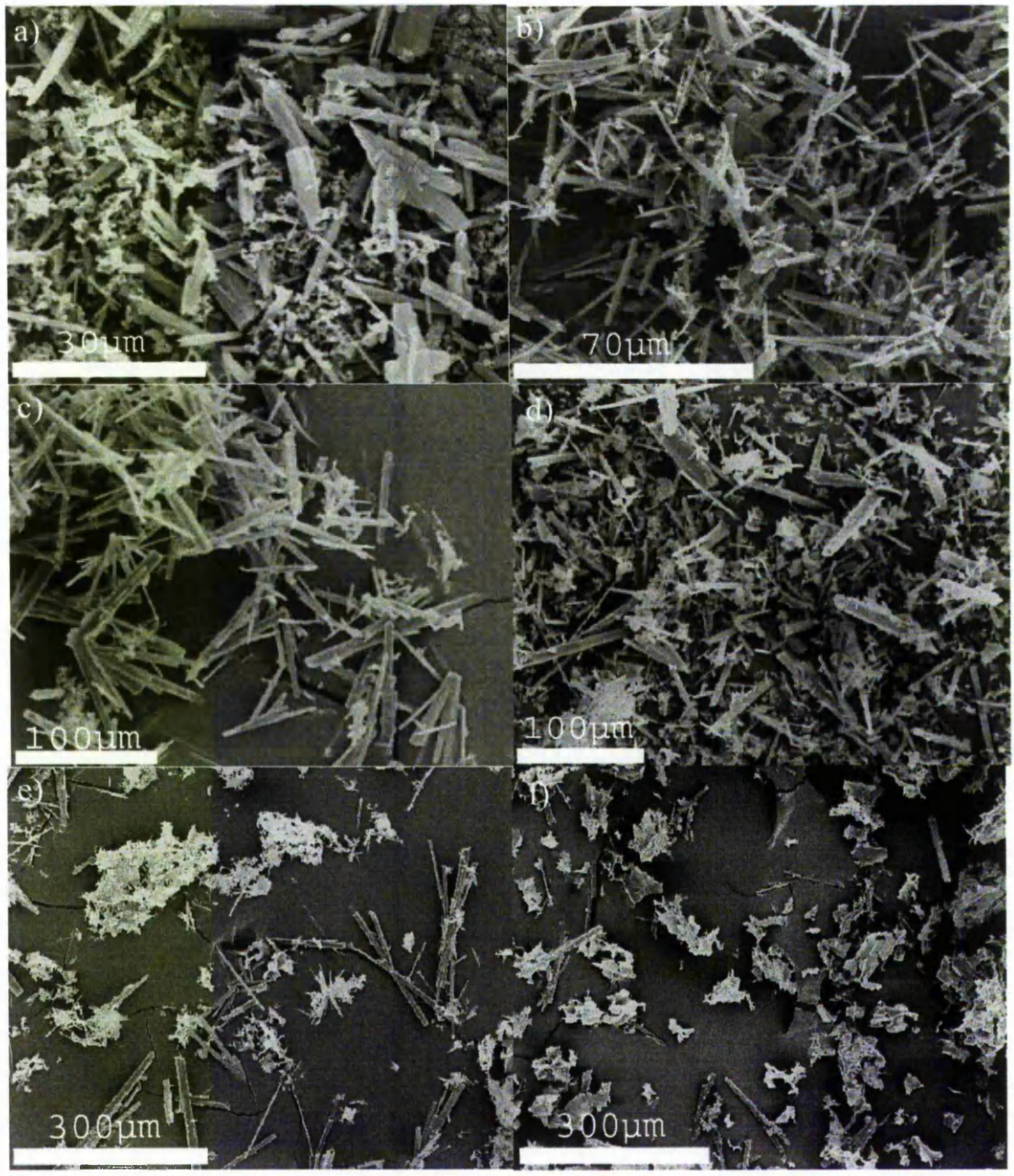

Figure 5.3.1.1 – SEM micrographs of material isolated after; a) 25 s, b) 5 mins, c) 60 mins, d) 132 mins, e) 346 mins and f) 24 h.

It can be seen from Figure 5.3.1.1c that after 60 mins the tetragonal prisms dominated the structures generated in solution. With regard to the type of material produced the sample could now be considered "pure" although tight morphological control *i.e.* size and shape had not been achieved.

5.3.2 Structural characterisation of the tetragonal prisms

Closer inspection of the tetragonal prism structure shows a remarkably well defined structure where an opening can be seen (Figure 5.3.2.1a). The tetragonal prism can be seen to comprise two concentric tubes with a more granular material filling the gap between concentric tubes as depicted by Figure 5.3.2.1c. However, the "broken" tetragonal prism shown in Figure 5.3.2.1b seems to contradict this observation where it would appear that the tetragonal prism has formed from a central nucleation point and comprise of three pieces; a central filament which connects two external planar sheets, this hypothesis is supported by Figure 5.3.2.1a where a distinct grain boundary can be seen on the left external surface. Figure 5.3.2.1d and e shows the tetragonal prisms contain some silicon and oxygen in their structure from EDXA mapping, however, surprisingly the oxygen mapping does not show such a clear correlation as shown in Figure 5.3.2.1e. Finally, a map for potassium was performed to confirm the tetragonal prisms were not causing KCl to precipitate.

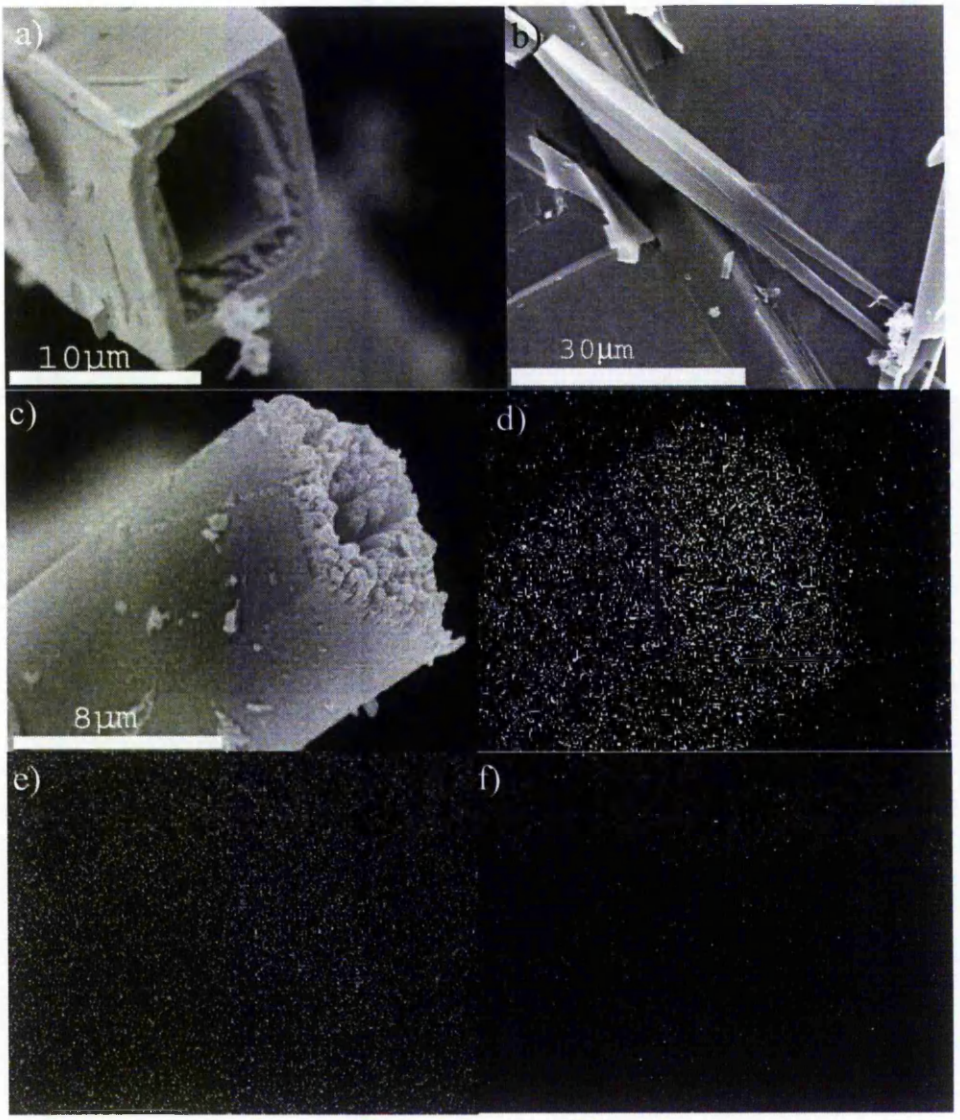

Figure 5.3.2.1a) - showing the tetragonal prism have a hole, b) showing a "broken" tetragonal prism c) shows a tetragonal prism with granular material extruding from the entrance, d) shows EDXA mapping for silicon, e) oxygen and f) potassium.

To investigate the structure of the tetragonal prisms in greater detail we used TEM. The micrographs shown in Figure 5.3.2.2 are of some of the smallest tetragonal prisms, it can be seen that the tetragonal prisms are indeed hollow for the most part, although it remains unclear what size the primary particles of the tetragonal prisms are. In Figure 5.3.2.2a it can be seen a web like structure, where potentially a primary particle size could be determined; however Figure 5.3.2.2b shows no visible primary particle size. Grinding the needles prior to TEM also showed the web like structure as shown in Figure 5.3.2.2c however, pieces of tetragonal prism still remained where no visible primary particle size can be seen as depicted by the insert in Figure

5.3.2.2c. The TEM also provided evidence to suggest the tetragonal prisms were in fact crystalline (data not shown).

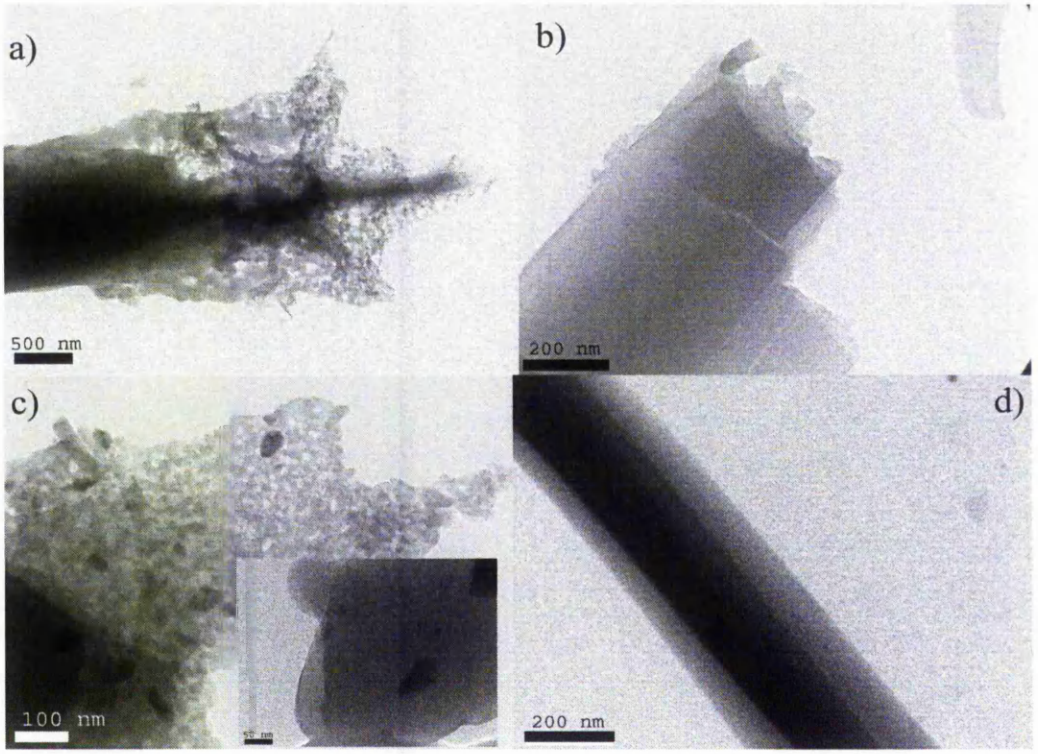

Figure 5.3.2.2 – TEM micrographs of tetragonal prisms formed at pH 6.8 at a Si:N ratio of 10:1 after 60 mins.

5.3.3 Material characterisation and structure determination of the tetragonal prisms

FTIR and powder X-ray diffraction were performed on the tetragonal prisms to determine the composition of the tetragonal prisms and the extent of the crystallinity in the tetragonal prisms.

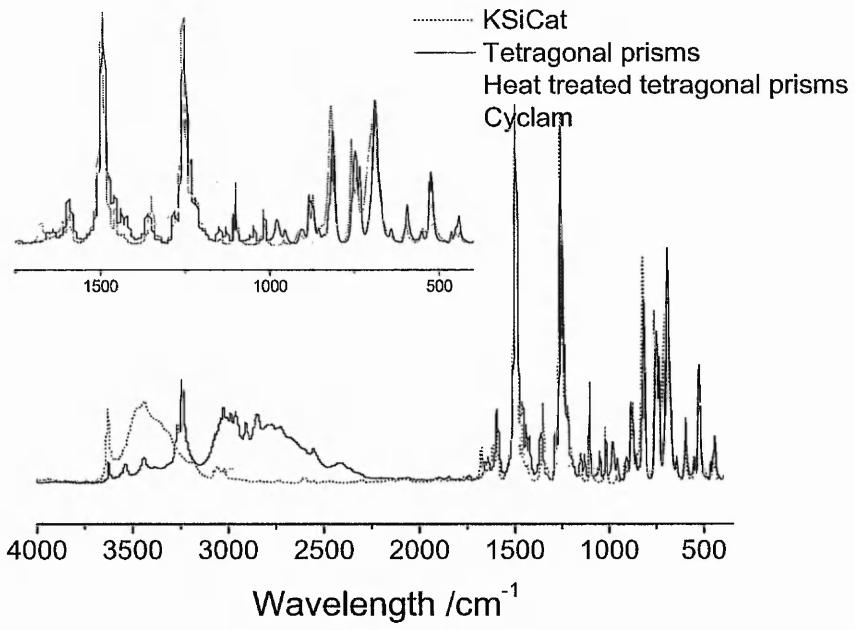

Figure 5.3.3.1 – FTIR spectra of tetragonal prism, KSiCat and cyclam, insert shows close up of 1750-450 cm^{-1} where the Si-O peak at 1100 cm^{-1} is retained from KSiCat in the tetragonal prisms. Upon heat treatment the Si-O stretch is broad showing the presence of amorphous silica.

The FTIR spectra shown in Figure 5.3.3.1 contains two distinct regions; region 1 from 4000-2250 cm^{-1} and region 2; 1750-400 cm^{-1} which includes the region commonly known as the finger print region. Interestingly, a striking differences in region 1 highlighted by the secondary N-H band centred at *ca.* 3200 cm^{-1} can be seen, which clearly showing the presence of cyclam in the structure. Moreover, the loss of the an O-H stretch at *ca.* 3500 cm^{-1} thought to be water contained in the KSiCat structure which appears to be replaced by the presence of cyclam. Interestingly, when one compares the region 2 (see insert Figure 5.3.3.1) is compared for the samples there are only slight differences where the peaks are shifted to slightly higher wavenumbers in the tetragonal prisms. The characteristic peaks at *ca.* 1500, 1250 and 1100 cm^{-1} attributed to substituted aromatic molecules, the aryl =C-O and the Si-O stretch respectively, all appear in both spectra indicating the presence of tris(1,2-benzenediolato-*O,O'*)silicate (SiCat) in the structure where it is assumed that at least one of the potassium ions has been replaced by charge associated with the cyclam ring. The Si-O band appears narrow in both the tetragonal prisms and in KSiCat indicating that the Si-O bond are all in similar environments and since the peak has

not shifted in the tetragonal prisms when compared to KSiCat we hypothesised that the silicon atoms remain octahedrally coordinated. After heat treatment (Figure 5.3.3.1 insert) the Si-O band at 1100 cm^{-1} appears broad, characteristic of amorphous silica; Si-O-Si antisymmetric stretching vibrations and the peak at 805 cm^{-1} of symmetric Si-O-Si stretching.

Having isolated "pure" samples of tetragonal prism the material was characterised using powder XRD and thermal gravimetric analysis as shown in Figure 5.3.3.2a and b. It can be seen that the material lost 85 % of its mass over the full temperature range and 41 % (which corresponds quite well to the calculated value for the CHN see Figure 5.3.3.3 between 400 and 800 °C which can be attributed to the loss of organic material. Interestingly, the material isolated after 5 mins in comparison to 60 mins showed a very similar thermal decomposition profile indicating that once precipitated the tetragonal prisms do not interact with condensing silicic acid as the % organic material did not decrease significantly.

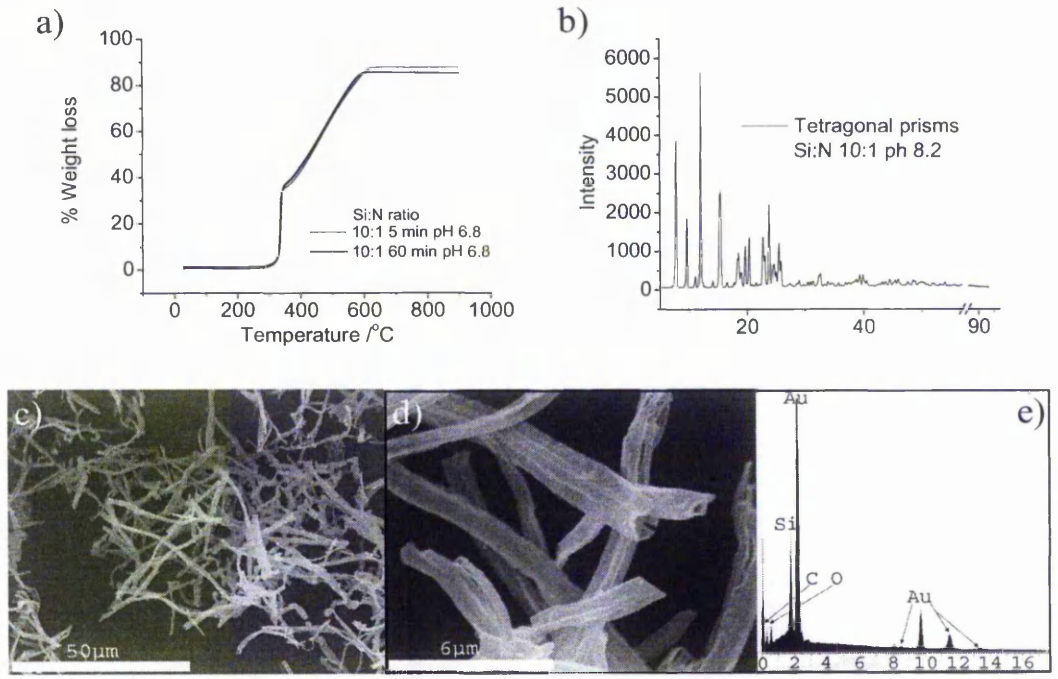

Figure 5.3.3.2a) – Thermal gravimetric analysis of tetragonal prisms prepared at an Si:N ratio of 1:10 isolated after 5 and 60 mins, b) Powder XRD of tetragonal prisms formed at pH 8.2 with an Si:N ratio of 10:1, c and d) SEM micrographs show the heat treated material and the partial retention of tetragonal prism structure, e) EDX spectra of heat treated tetragonal prisms.

To characterise the material further solid state NMR and CHN analysis was performed on the tetragonal prisms as shown in Figure 5.3.3.3. Solid state ^{29}Si NMR shows a characteristic peak of silicon octahedrally coordinated at -142 ppm. The ^{13}C NMR showed characteristic peaks of aromatic carbon atoms in the same positions as the starting precursor dipotassium tris(1,2-benzenediolato-*O,O'*) silicate at 111, 150 and 180 ppm, moreover the peaks at 24, 42 and 46 ppm can be assigned to cyclam which have been shifted to slightly lower ppm values probably because of the hydrogen bonding in the tetragonal prisms (see section 5.3.5). The other bands can be assigned as low spinning side bands as shown in Figure 5.3.3.3b. The low spinning side bands have been associated with the primary peaks assigned to cyclam and SiCat according to the J coupling values and peak shapes Figure 5.3.3.3b. CHN analysis on the purest 60 min sample was used to calculate the ratio of cyclam to KSiCat based on the assumption that the % nitrogen found in the tetragonal prisms could be attributed solely to the proportion of cyclam in the tetragonal prisms. This was then used to calculate the amount of carbon and hydrogen associated with the nitrogen according to the molecular ratios in the cyclam structure. The remaining carbon could then be attributed to the SiCat complex and the respective percentages of hydrogen, silicon and oxygen can be calculated. Finally, knowing the percentage of cyclam and KSiCat respectively, the structual molar ratio of 0.98:1 was calculated for the ratio of SiCat to cyclam as shown in Figure 5.3.3.3c. This data allowed established that the complexed species must be cyclam^{2+}, as no evidence of potassium remaining in the tetragonal prisms to balance the complex charge was found.

The data presented from the FTIR, ^{29}Si NMR and TGA has provided conclusive evidence that the tetragonal prism are in fact a complex formed between undissociated SiCat and cyclam, where the tetragonal prism morphology is assumed to form by molecular self assembly. The hypothesis that the tetragonal prism were made from SiCat was confirmed indirectly by two simple assays, the first involved investigating the formation of the tetragonal prisms in the absence of KSiCat complex. This can be achieved by allowing the KSiCat to dissociate completely to orthosilicic acid prior to the addition of the cyclam solution. This was achieved by the addition of the predetermined amount of acid directly to the KSiCat solution, followed by addition of the cyclam solution after 30 s. The 30 s time delay is sufficient to allow the KSiCat to dissociate fully.[41] The absence of KSiCat in the system removes the key ingredient

for tetragonal prism formation and no prisms are formed. The second assay involved investigating the solubility of the tetragonal prisms in an acidic solution. Assuming the hypothesis was correct one would expect the SiCat to dissociate in acid conditions thus the prism would dissolve immediately upon contact with an acidic solution. This was achieved by suspending the tetragonal prisms in dd water, with the addition of 2 M HCl (50 µl). Both tests proved positive for SiCat. The evidence provided by these tests is indirect but in light of the other characterisations carried out this provided sufficient evidence to confirm the composition of the tetragonal prisms. This confirmed the presence of SiCat, which shows similar properties to KSiCat. The presence of the amine was confirmed by solid state NMR and the absence of potassium by EDX.

a)

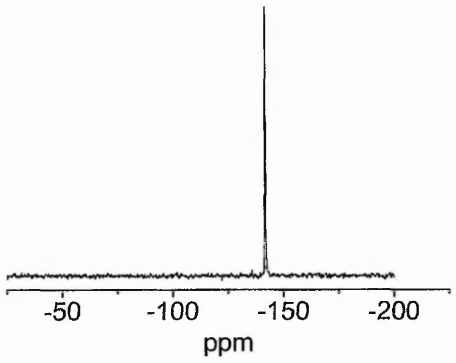

b)

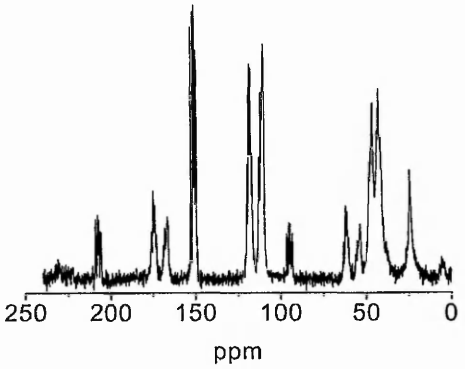

cyclam: 24 42 46 /ppm

SiCat: 110 117 150 173 /ppm

53 166 4 231 95 207 61 =>

c)

	% Total	% carbon	% nitrogen	% hydrogen	% silicon	% oxygen
Tetragonal prisms		**43.1**	**6.7**	**4.5**		
% cyclam	47.8	14.3	6.7	2.9		
% Remaining		28.8	0.0	1.6		
% KSiCat	46.9	3.5	0.0	1.0	3.7	12.8
% Ratio KSiCat:cyclam	0.98:1					
Molar Ratio KSiCat:cyclam	1:1.72					

Figure 5.3.3.3a) ^{29}Si and b) ^{13}C solid state NMR of tetragonal prisms, c) CHN analysis, and calculations used to predict the molecular ratio of cyclam to KSiCat in the tetragonal prisms. Where => signifies the second side band could be shifted further down field out of the ppm range scanned. Solid state NMR was carried out at Durham University by David Apperley.

5.3.4 Single crystal silicon diffraction

Preliminary data from single crystal silicon diffraction (because the r value is high) was obtained suggesting our hypothesis is correct, that cyclam^{2+} species is present in tetragonal prisms shown in Figure 5.3.4.1 at a ratio of 1:1 KSiCat:cyclam. However, this does not explain why the smallest crystals are observed at pH 10 (see section 5.3.5.3). The formation of small crystals is indicative of the fastest rate of tetragonal prism formation which was observed at pH 10. From the cyclam speciation diagram pH 10 corresponds to the maximum concentration of the cyclam^{+} species. This suggests that in fact the mechanism for tetragonal prism formation is based upon a two step mechanism. Initially it is hypothesised that the cyclam^{+} species forms a hydrogen bond to the SiCat molecule, this must therefore make protonation of the

nitrogen atom diagonally opposite favourable which then hydrogen bonds to a second SiCat molecule. This would then account for the cyclam^{2+} species in the structure, but the fastest rate of formation being observed in the presence of the highest concentration of the cyclam^{+} species.

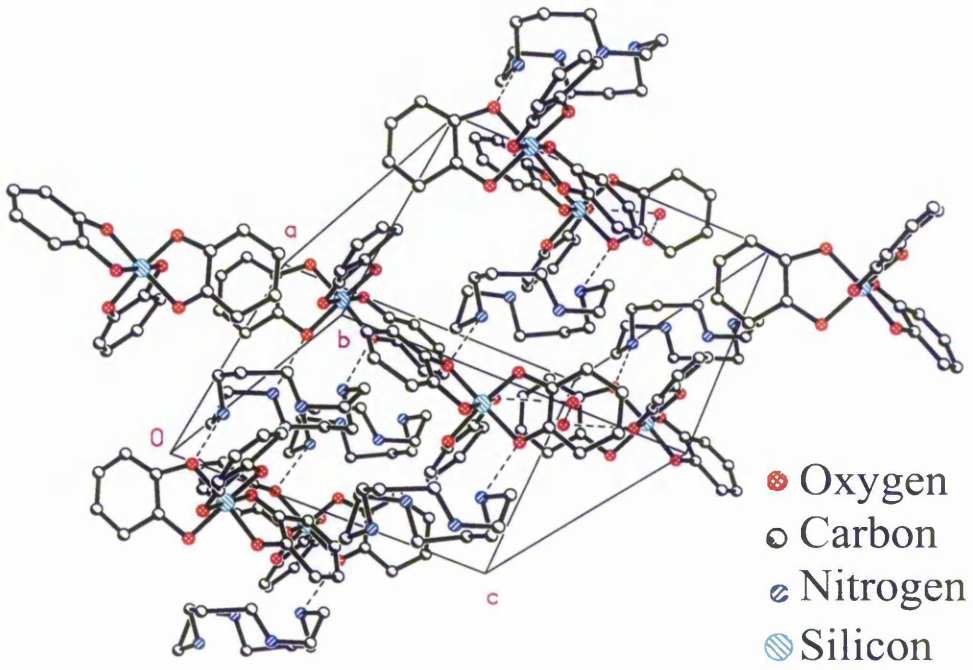

Figure 5.3.4.1 – Preliminary structural analysis of the tetragonal prism by single crystal silicon diffraction carried out by Prof. Alex Slawin, St Andrew's University.

It can be seen that a hydrogen bond exists between the lone pair of electrons on the SiCat oxygen atom and it is assumed the charged amine group on the cyclam molecules. But there is evidence to suggest from the distance between the protonated cyclam nitrogen and the lone pair of electrons on the SiCat molecule and some X-ray diffraction density to suggest that a water molecule bridges between the cyclam and SiCat molecule as shown in Figure 5.3.4.2. No evidence was found for the hydrogen atoms on the water molecule. The asymmetric unit cell is shown from two angles in Figure 5.3.4.2.

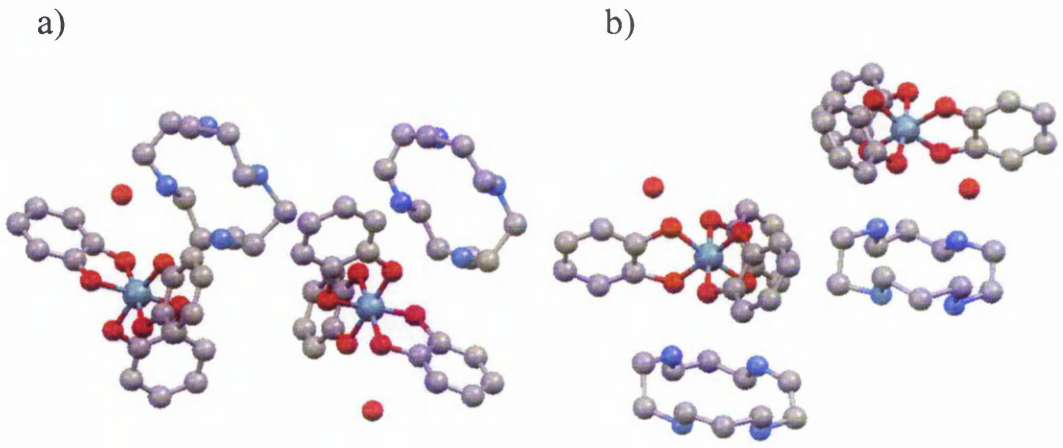

Figure 5.3.4.2 – Asymmetric unit cell of the tetragonal prisms showing possible position of two water molecules.

Each cyclam molecules is bound to two different SiCat molecules forming. A layer like structure exists of cyclam and SiCat molecules where the cyclam and SiCat molecules are situated in alternate layers when viewed along the a-axis as shown in Figure 5.3.4.3.

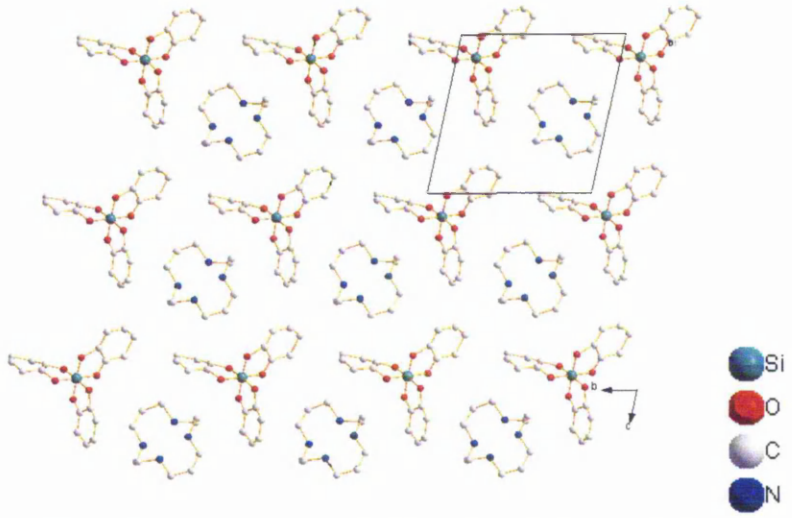

Figure 5.3.4.3 – layer network exhibited by SiCat and cyclam in the tetragonal prisms.

Finally with regard to the single crystal data obtained, a powder XRD pattern from the data was generated which can be compared to the XRD pattern recorded experimentally. Figure 5.3.4.4a shows the observed powder pattern for tetragonal prisms formed at pH 9.6, which was found correlate best to the generated powder pattern shown in Figure 5.3.4.4b.

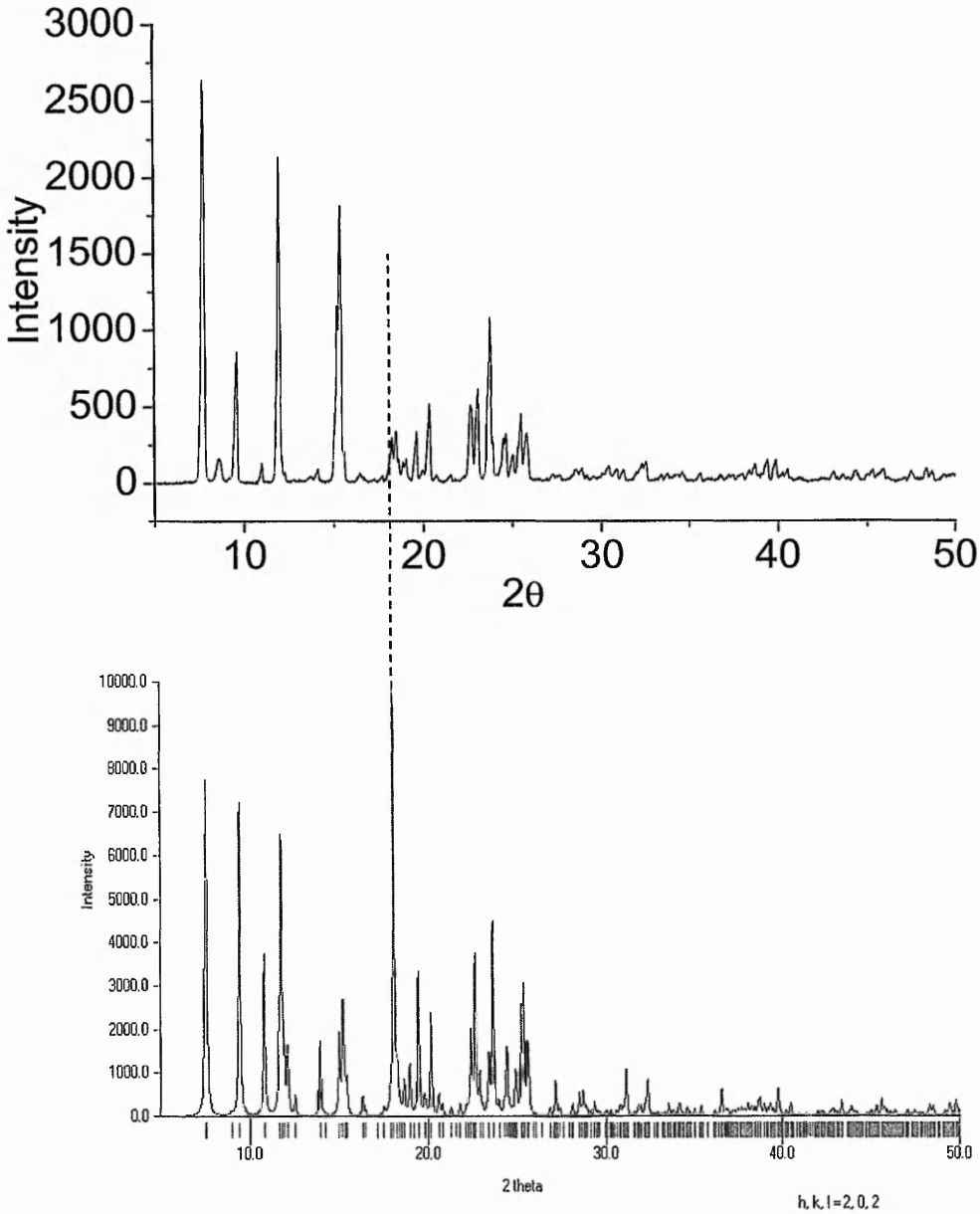

Figure 5.3.4.4a) – Observed powder pattern for tetragonal prisms precipitated at pH 9.6. b) Generated powder pattern from single crystal silicon diffraction.

The observed and generated powder pattern were found to agree reasonable well, however one distinct difference between the spectra can be seen as highlighted by the dotted line at in Figure 5.3.4.4 and we are currently investigating why such an intense peak could be missing from the observed spectra. Two suggestions have been made by our collaborator (Dr Gary Hix) on this matter; one was the presence of a crystalline contaminant possibly quartz and the other was due to preferred orientation which can

artificially enhance or reduce the presence of a peak in a measured powder pattern. With further refinement of the procedure used to form the tetragonal prisms we hope to achieve crystals more suitable for single crystal XRD which will enable us to fully solve the crystal structure. The refinement details, bond angle and bond lengths are given in Appendix 3 Table 1-5. The authors wish to acknowledge Professor Alex Slawin of the University of St Andrews for preliminary single crystal data and Dr Gary Hix of Nottingham Trent University for help interpreting the data.

5.3.5 The effect of pH, concentration and reduced temperature on the formation of tetragonal prisms.

The formation of the tetragonal prisms with respect to pH, concentration and reduced temperature was investigated. The interactions of cationically charged species has been reported to be highly influential in both templating and the catalysis of silica formation.[23] The molecular structure of the cyclam allows up to four positive charges to be present simultaneously on the ring structure. To model the accumulation of charge on cyclam from basic to acidic conditions we used SPARC[38] to estimate the speciation diagram. This would allow us to probe the molecular interactions between cyclam and KSiCat. The speciation diagram for cyclam calculated using SPARC is shown in Figure 5.3.5.1.

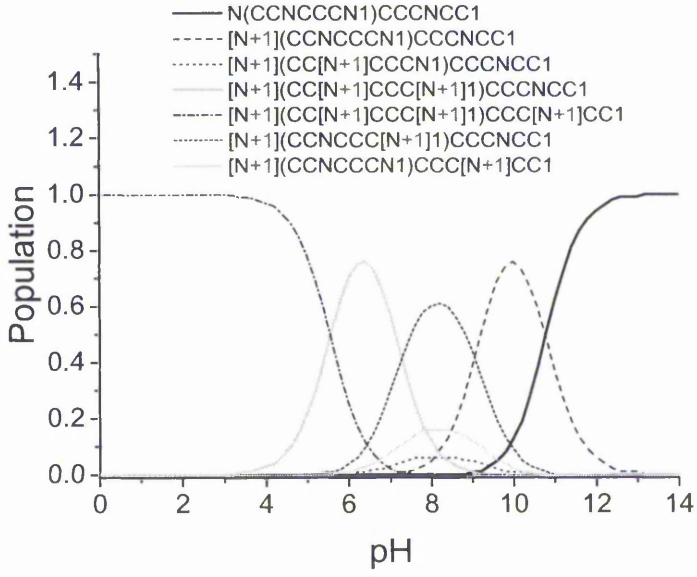

Figure 5.3.5.1 – cyclam speciation calculated using SPARC.

It is known that cyclam exhibits an unusual speciation where protonation of the forth amine requires less energy than the third[42] and as such it should be stressed that we have used the calculated speciation diagram from SPARC only as a guide for our pH studies. With the identification that cyclam^{2+} was probably present in the tetragonal prism structure, the homogeneity of the tetragonal prisms was improved by titrating the cyclam solution to the pH to be studied prior to mixing with the KSiCat solution. Addition of acid directly to the KSiCat followed immediately by the cyclam solution should minimise the competition for protons in solution and reduce the changes in cyclam speciation Figure 5.3.5.2 shows the titration curves for cyclam and KSiCat used to calculate the volume of acid required to investigate the effect of pH on the formation of the tetragonal prisms. Figure 5.3.5.3c shows the effect of the addition of cyclam titrated to pH 6.8 and can be compared to Figure 5.3.1.1c to see the improved homogeneity of the tetragonal prisms.

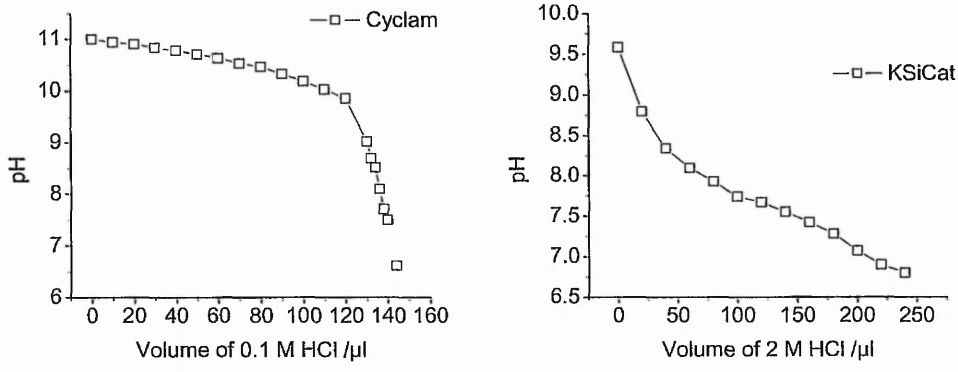

Figure 5.3.5.2 – Titration curves used to calculate the amount of acid required to investigate the effect of pH on the formation of the tetragonal prisms.

Figure 5.3.5.3 shows the effect of pH on the dimensions of the tetragonal prisms formed at a Si:N ratio of 10:1, it should be noted that the pH range shown reflects the range over which tetragonal prism formation occurs. The tetragonal prisms formed at pH 12 are not included because the prisms are heterogeneous. addition of acid to achieve pH values lower than 6.54 equates to a stoichiometric excess of acid being added and results in extremely rapid dissociation of the KSiCat complex and a pH value of <4. The rapid dissociation effectively means that KSiCat does not exist in solution and hence neither do the tetragonal prisms.

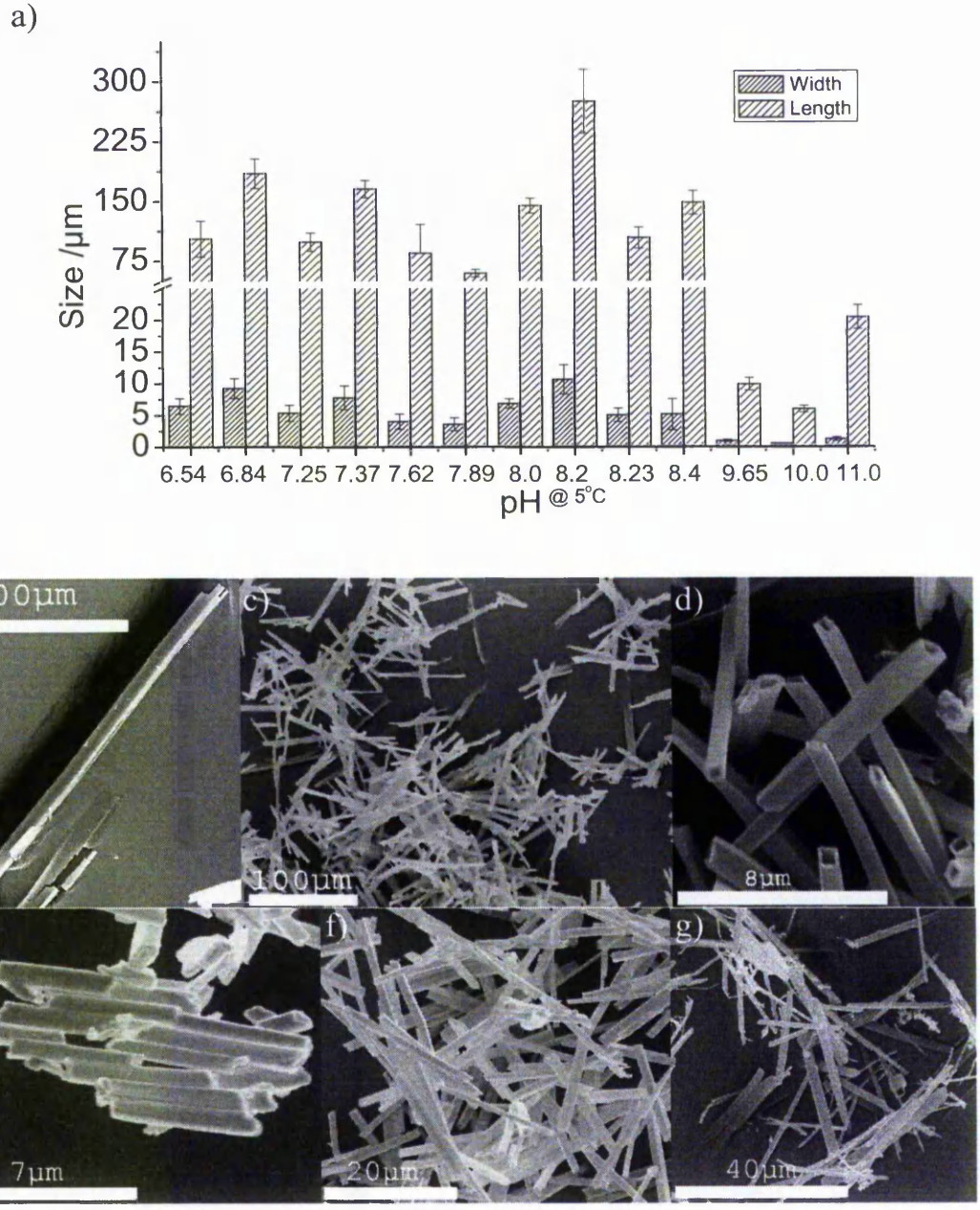

Figure 5.3.5.3a) – The effect of pH and reduced temperature on the dimensions of the tetragonal prism. Note; two dimensions have been shown, length and depth, width has not been characterised primarily because in most cases this is within 1 standard deviation of the mean depth. b) tetragonal prism precipitated at pH 8.23 after 1 h @ 5°C, (species specific addition). c) tetragonal prism precipitated at 6.8 after 1 h. d) tetragonal prisms precipitated at pH 9.6 isolated after 1 h. e) Tetragonal prisms precipitated at pH 10. (smallest). f-g) precipitated at pH 11 and 12.

The yields of the tetragonal prisms have been calculated over the pH range of 6.950 to 9.65. Table 5.3.5.1 shows the yields obtained with respect to pH and cocnetration assuming the crystal structure observed in Figure 5.3.4.1 is correct.

Molecular formula $C_{28}N_4O_8H_{48}Si$

Molecular weight of new complex = 588.33
No μmoles of cyclam = 7.4

a)

pH	Mass of complex /mg	No. moles of complex /μM	Yield /%
6.95	3.9	6.63	89.6
7.182	3.7	6.29	85.0
7.374	3.5	5.95	80.4
7.506	3.2	5.44	73.5
7.64	3.3	5.61	75.8
7.768	4	6.80	91.9
7.922	2.7	4.59	62.0
8.094	4.2	7.14	96.5
8.356	3.3	5.61	75.8
8.715	4.3	7.31	98.8
9.650	4.3	7.31	98.8

b)

Concentration	Mass of complex /mg	No. moles cyclam /μM	No. moles of complex /μM	Yield /%
10:3	10.6	22.5	18.01709925	80.1
10:5	19.8	37.4	33.65458161	90.0
10:7	27.1	52.4	46.06258392	87.9
10:10	32.2	74.9	54.73118828	73.1

Table – 5.3.5.1 – Calculation of the yields for the cyclam complex with respect to a) pH, b) concentration

Interestingly, the size of the tetragonal prisms seems to be independent of pH probably due to le Chatelier's principle where as the concentration of the cyclam$^+$ species is used up through tetragonal prism formation, more is created in order to maintain a constant molecular species ratio for a given pH. Interestingly, a significant drop in the size of the tetragonal prisms was observed in the absence of acid addition at pH 9.650. This can be explained when one considers the hydrolysis reaction that occurs when acid is added to KSiCat. KSiCat dissociates on the addition of acid thus reducing the concentration of the available for complexation. This slows the complexation of cyclam with SiCat and allows larger crystals to form. In the absence of acid a stable system exists where the concentration of KSiCat is not changing and secondly is the highest concentration studied as dissociation does not occur. The increased concentration and availability of KSiCat results in an increase in the rate of tetragonal prism formation and smaller crystals. Surprisingly, at pH 10 a further reduction in needle size was observed. To reach pH 10, 1 M KOH (10 μl) was added

to KSiCat, which initiates basic hydrolysis of KSiCat, therefore the previous explanation for the decrease in crystal size can not be applied here. Since temperature was kept constant the rate of crystal formation could only have been increased by an increase in the concentration of the cyclam species involved in tetragonal prism formation. At pH 10, the dominant species in solution is the $cyclam^{+}$ species (76 % from SPARC speciation). Therefore, these results lead us to hypothesise that the increase in the concentration of $cyclam^{1+}$ is the reason why the crystal size reduces when increasing the pH from 9.65 to 10.

5.3.6 The effect of concentration on the formation of tetragonal prisms

The effect of Si:N ratio on the formation of the tetragonal prisms was investigated where it was anticipated that the yield of the tetragonal prisms would increase. However, increasing the cyclam concentration could also cause the tetragonal prisms to form faster which might compromise the homogeneity of the sample and effect the size of the tetragonal prisms. The effect of cyclam concentration on tetragonal prism formation was investigated, the SEM micrographs shown in Figure 5.3.6.1 show that increasing the concentration of the cyclam in solution has two effects; firstly, multiple nucleation sites are created resulting in stars and larger structures shown in Figure 5.3.6.1b where the Si:N ratio is 10:5 and secondly at Si:N ratios of 10:10 the tetragonal prisms become deformed as shown in Figure 5.3.6.1e. The yields of the complex associated with increasing the concentration of cyclam are given in Table 5.3.5.1.

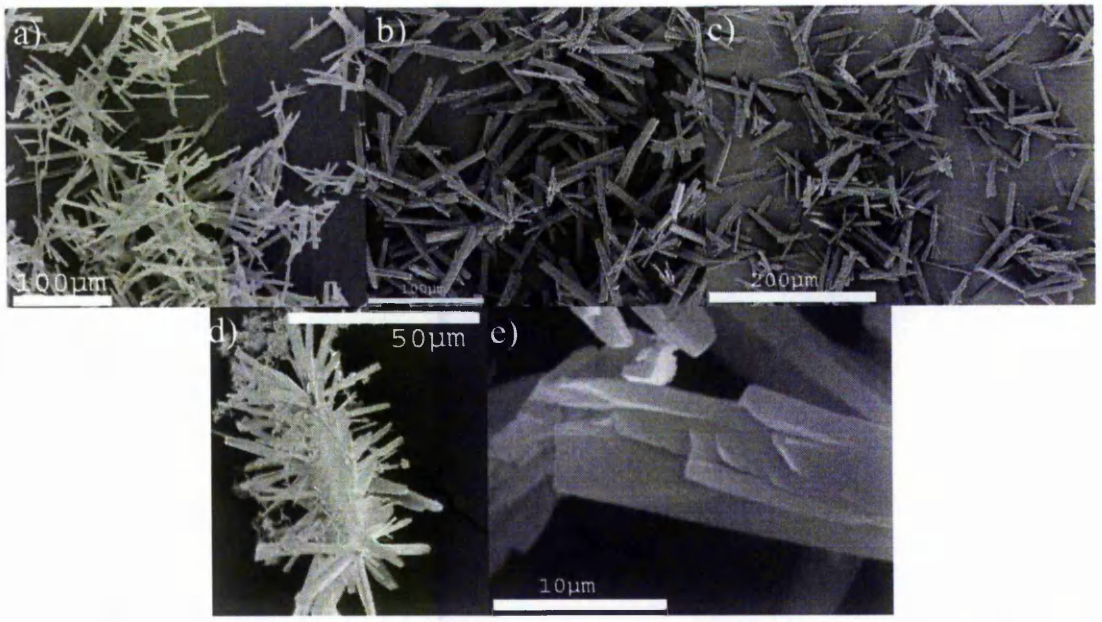

Figure 5.3.6.1 – The effect of Si:N concentration on the formation tetragonal prisms at pH 8.2 and a) 10:1, b) 10:3, c) 10:5, d)10:5, e) 10:10 isolated after 60 mins. Multiple nucleation sites are created producing stars and larger structures shown in Figures b) and d) at Si:N ratios 10:3 and 10:5 and tetragonal prism deformation at 10:10.

5.3.7 The formation and characterisation of tetragonal prisms using dipotassium tris(1,2-benzenediolato-*O,O'*)germanate

Intrigued by the ease by which the tetragonal prisms form and whether the formation was specific to silicon, the effect of cyclam on the KGeCat was investigated. The properties of germanium are very similar to silicon; the atomic radii are similar (122.3 pm and 117.6 pm respectively) which suggests a similar complex might be formed if we used dipotassium tris(1,2-benzenediolato-*O,O'*)germanate (KGeCat) instead of KSiCat. However, unpublished data by Patwardhan *et al.* has shown that KGeCat and KSiCat behave quite differently upon the addition of acid. KGeCat does not form a basic solution when dissolved in dd water and the addition of acid to KGeCat does not generate a 100 % solution of $Ge(OH)_4$ until a pH of *ca.* 2 has been reached. Furthermore, this reaction appears to be reversible upon the addition of alkali. Figure 5.3.7.1 shows the titration curve used to study the effect of pH using KGeCat.

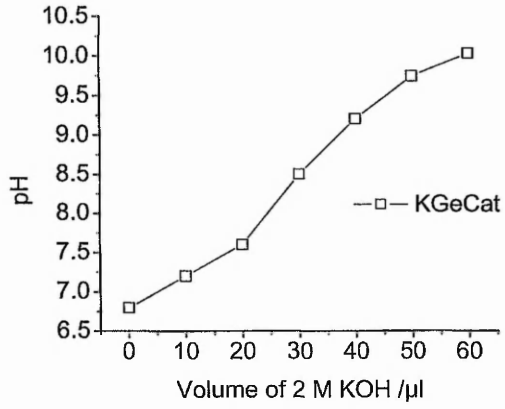

Figure 5.3.7.1 – Titration curve used to study the effect of pH on the formation of GeCat tetragonal prisms.

Initially the formation oftetragonal prism using KGeCat at pH 6.7 was studied, the pH achieved by dissolving KGeCat in dd water. Our hypothesis was correct and tetragonal prisms were formed at a Ge:N ratio of 10:1. Figure 5.3.7.2 summaries the formation and studies carried out using KGeCat including the effect of pH and concentration.

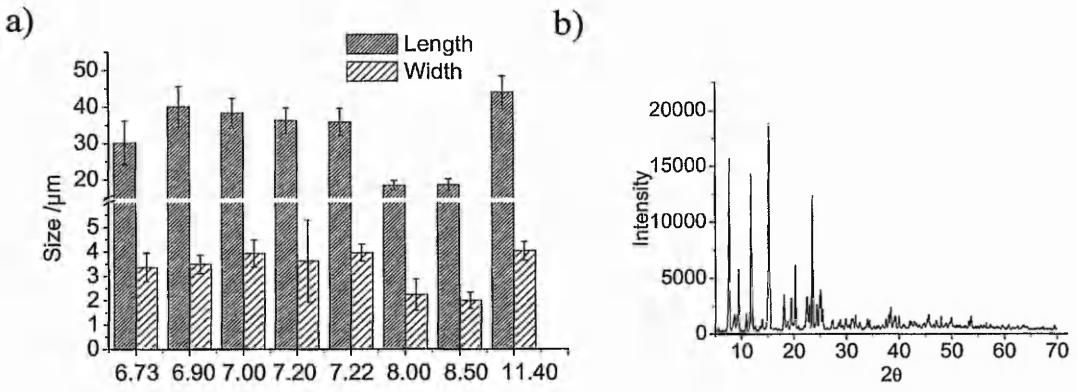

Figure 5.3.7.2 – Summary of results obtained when using KGeCat and cyclam at a Ge:N ratio of 10:1 to form tetragonal prisms. a) Effect of pH on Ge tetragonal prism formation b) Powder XRD of the tetragonal prisms formed from KGeCat at pH 10.3.

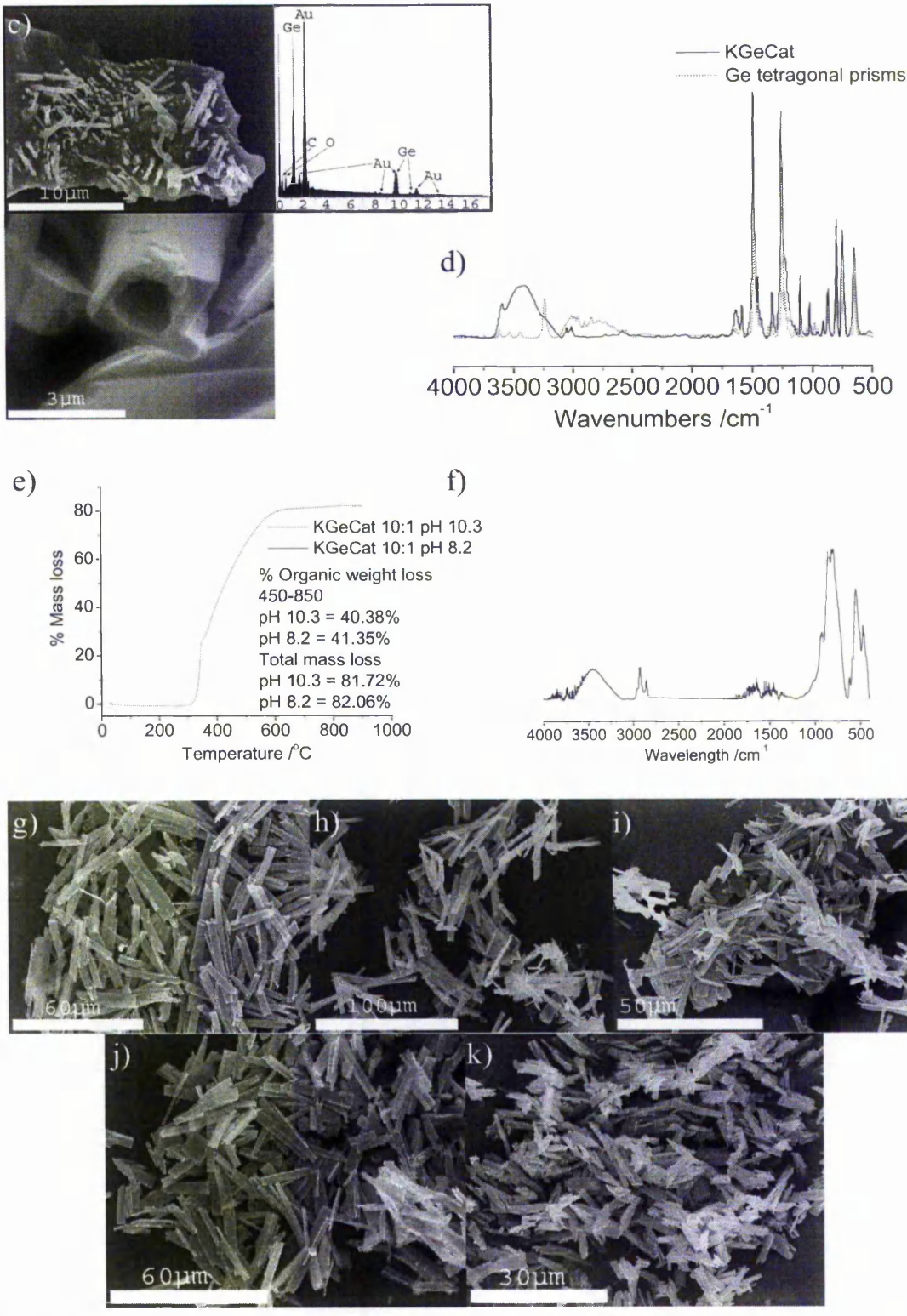

Figure 5.3.7.2 cont. - c) SEM micrographs; Top left: thermally treated KGeCat tetragonal prisms, top right; EDXA spectra confirming the material is germanium based. Bottom: germanium tetragonal prism. d) FTIR of Ge tetragonal prism and KGeCat e) TGA at pH 8.2 and 10.3. f) FTIR of thermally treated Ge tetragonal prisms g-k) effect of concentration on Ge tetragonal prism formation; 10:1, 10:3, 10:5, 10:7, 10:10 respectively.

The effect of pH was investigated on the formation of the Ge tetragonal prisms, similarly to the prisms formed using KSiCat the dimensions of the prisms did not change significantly, although it should be noted that the Ge tetragonal prisms were significantly smaller than the silicon prisms. This can be attributed to the acid base properties of KGeCat and KSiCat, where KGeCat has a pH of 6.67 in H_2O and KSiCat has pH of 9.6. The yield of the germanium complex varies between 3.5 mg and 4.2 mg over the complete pH range studied with no general trend (% yields have not been quoted because the crystal structure is unknown at this time). In order to obtain comparable pH ranges one must add KOH to KGeCat, which does not cause dissociation, however, the addition of acid to the KSiCat system causes dissociation thus reducing the rate of formation of the tetragonal prism allowing larger structures to form. The appearance of the thermally treated germanium tetragonal prism shown in (Figure 5.3.7.2c) shows that the tetragonal prism morphology is not retained. We are currently investigating if we can retain the structure of the Ge tetragonal prisms by heating to lower temperatures. Interestingly, the powder obtained from the thermally treatment of the Ge tetragonal prisms retains some colour, appearing cream in colour to the eye. The FTIR shown in Figure 5.3.7.2f shows two peaks at 2922 and 2854 cm^{-1} respectively, which can be assigned to CH_2 stretches indicating that not all the organic material has been removed even after heating to 900 °C for 2 h in air. This is very surprising and might be indicative of the way the germania is formed although this is merely speculation. The large multiplet of peaks at *ca.* 850 cm^{-1} can be assigned to Ge-O-Ge and O-Ge-O stretching and deformation modes characteristic of germania. The effect of cyclam concentration was investigated similar to that when KSiCat was used; increasing the concentration of cyclam produced smaller tetragonal prism and also exhibited a less well defined structure as can be seen quite clearly in Figure 5.3.7.2k. The single crystal pattern of the germanium tetragonal prisms has not been investigated to date, although it is hypothesised that it wil be very similar to the structure of the silicon containing tetragonal prisms.

5.3.8 Investigating the effect of other azamacrocyclic compounds on the precipitation of dipotassium tris(1,2-benzenediolato-*O,O'*)silicate

To further understand the function of azamacrocyclic ring in the formation of tetragonal prisms we investigated a range of cyclic molecules. The azamacrocyclic

molecules and derivatives of cyclam chosen for study were 1,4,7-triazacyclononane (3NC), 1,4,7,10-tetraazacyclododecane (4N2), 1,8-dimethyl-1,4,8,11-tetraazacyclodecane (2MC), 1,4,8,11-tetramethyl-1,4,8,11-tetraazacyclodecane (4MC), 1,4,7,10,13,16-hexaazacyclooctadecane (6NC), 12-crown-4 (12C4) and 18-crown-6 (18C6). Investigations of the azamacrocyclic molecules listed above allowed us to study the effect of ring size and ring fuctionalisation. Surprisingly, it was found that none of the azamacrocyclic molecules apart from cyclam were able to complex KSiCat in a similar manner to cyclam. This provided evidence that complexation is highly dependent on ring size. Furthermore, the investigation of 2MC and 4MC in KSiCat solutions also showed no evidence of complexation, indicating that complexation might also be dependent on steric constraints caused by the functionalisation of the azamacrocyclic ring. The methylation of the cyclam ring does not effect the molecule's ability to accumulate charge as shown by the SPARC species diagrams presented in Appendix 3 Figure 1 and therefore this can be ruled out as the reason for the absence of complexation. Figure 5.3.5.1 shows the expected crystal structure for the tetragonal prisms formed using SiCat and cyclam, where it can be seen that nitrogen atoms in positions 4 and 11 are hydrogen bonded through a water molecule to the lone pair of electrons on the oxygen atoms in two different SiCat molecules. This is because the nitrogen atoms in the cyclam molecule will more readily accept a proton than the oxygen atoms in SiCat. The methylation observed in 2MC and 4MC does not effect the molecules ability to hydrogen bond, however methylation will dictate the conformation the cyclam ring adopts and makes some conformations more energetically unfavourable than others.[1] Since complexation is not observed we can conclude that the configuration adopted by 2MC and 4MC rings are not the same as cyclam in the tetragonal prisms and thus complexation is not observed. Alternatively, the inclusion of the methyl group in the cyclam structure might effect the molecular packing of the cyclam molecules, where steric hindrance between the methyl groups and the tris(1,2-benzenediolato-*O,O'*) groups on the SiCat molecule may be sufficient to make complexation unfavourable.

5.3.9 Summary

The formation of crystalline tetragonal prisms has been achieved using dipotassium tris(1,2-benzenediolato- *O,O'*)silicate and cyclam; an azamacrocyclic molecule. The reaction occurs through the displacement of the potassium ions in the inorganic complex probably by a two step mechanism where the $[cyclam]^+$ species hydrogen bonds to the SiCat at position 4 in the molecule which activates the nitrogen atom in position 11 which is then able to form a second hydrogen bond linking two SiCat molecules, as depicted in Figure 5.3.5.1 showing the unit cell obtained through single crystal silicon diffraction, although this is only preliminary data. The tetragonal prisms can be formed over a large pH range extending from pH 6.5 to pH 12 which corresponds to the region where dissociation of KSiCat dissociates slow enough to allow complexation and where charged $[cyclam]^+$ species occurs in solution. The homogeneity of the tetragonal prisms is improved by titrating an aqueous solution of the azamacrocyclic molecule to a desired pH prior to addition to the KSiCat solution. This minimises the competition for protons in solution between the dissociating KSiCat and $[cyclam]^+$. However, in the absence of a hydrolysing KSiCat complex, (*i.e.* no acid or alkali added) the size of the tetragonal prism appears smaller which can be attributed to the increased KSiCat concentration as the system is no longer hydrolysing upon addition of the cyclam solution. Increasing the concentration of the $cyclam^{1+}$ species also seems to reduce the size (pH 10) of the tetragonal prisms which provided an indication of the two step mechanism proposed for tetragonal prism formation. The effects of cyclam concentration and reduced temperature have also been studied were it was found that the structure of the tetragonal prism was compromised at higher concentrations. Reducing the temperature to 5 °C allowed larger crystals to be formed (250 μm in length) at 10:1 Si:N ratio. The tetragonal prisms are predominantly composed of organic material, however, upon removal of the organic component by heating to 900 °C the *ca.* 15 % inorganic material remarkably retains the general tetragonal morphology, although it does reduce in size. Interestingly, investigations into other azamacrocyclic molecules which might also precipitate SiCat from solution were not successful, thus it can be concluded that both the ring size and ring conformation are critical to the formation of the tetragonal prisms. The precipitation of SiCat from an aqueous solution at 25 °C is the first time cyclam has been used to precipitate and control the morphology of a novel crystalline

silicon and germanium hybrid material. The tetragonal prisms provide a useful route to controlling the structure of amorphous silica which is produced once the organic component of the tetragonal prisms has been thermally removed. Furthermore this displacement reaction is not limited to KSiCat, similar structure can be prepared using dipotassium tris(1,2-benzenediolato-*O,O'*)germanate, however, to date it has not been possible to retain the structure of the germania. The inorganic component of the tris(1,2-benzenediolato-*O,O'*) compound does not seems to play a role in the formation of the tetragonal prisms shown by cyclams ability to precipitate tetragonal prisms from solutions of dipotassium tris(1,2-benzenediolato-*O,O'*)germanate which leads to the hypothesise that the reaction will occur for any inorganic compound where a dipotassium tris(1,2-benzenediolato-*O,O'*) complex can be prepared. If this hypothesis proves to be correct there appears no why this procedure should not facilitate the production and morphological control of many inorganic materials. Furthermore, the macrocyclic cavity in cyclam may allow metal ions to be incorporated into the tetragonal prism morphology, allowing materials with electrical properties to be produced. Moreover, it might also be possible to align and pattern the tetragonal prisms on surfaces either through direct growth or through arrangement onto a surface, both possibilities seem feasible, and once achieved could lead to both optical and electrical applications.

5.4 The precipitation of tris(1,2-benzenediolato-*O,O'*)silicate complexes using tertiary amines.

After investigating an array of azamacrocyclic molecules for their ability to complex KSiCat which proved unsuccessful, selectively a range of amines containing primary, secondary and tertiary amines functionality at a Si:N ratio of 1:1 at pH 6.8 ±0.2 was screened as shown in Table 5.4.1.

Name	Amine architecture
N,N'-Bis(3-aminopropyl)-1,3-propanediamine	1/2
Bis(3-aminopropyl)amine	1/2
N,N'-Dimethyl-1,6-hexanediamine	2
Tris(dimethylamino)methane	3
1,1,4,7,10,10-Hexamethyltriethylenetetramine	3
3,3'-Iminobis(N,N-dimethylpropylamine)	3
1,3-Diamino-2-hydroxypropane-N,N,N',N'-tetraacetic acid	3
3-(Dimethylamino)-1-propylamine	3
N,N,N',N'-Tetramethyldiaminomethane	3
N,N,N',N'-Tetramethylethylenediamine	3
N,N,N',N'-Tetramethyl-1,4-butanediamine	3
N,N,N',N'-Tetramethyl-1,6-hexanediamine	3
N,N,N',N'',N''-Pentamethyldiethylenetriamine	3/1
N,N,N'-Trimethyl-1,3-propanediamine	3/1
N,N,N'-Trimethylethylenediamine	3/2

Table 5.4.1 – Amine molecules studied for activity in complexing KSiCat, 1 = primary, 2 = secondary, 3 = tertiary.

It was found that several other amines were able to forms a complex with SiCat. From the selection of amines that were investigated it was found that secondary amines do not form complexes with SiCat. Tertiary amines were also investigated where complexation did occur in a similar fashion to cyclam. The role of tertiary diaminoalkanes with 2 ,4 and 6 carbon atoms between the amine groups namely; *N,N,N',N'*-tetramethylethylenediamine (4MEDAE), *N,N,N',N'*-tetramethyl-1,4-butanediamine (4MEDAB) and *N,N,N',N'*-tetramethyl-1,6-hexanediamine (4MEDAH) was investigated. SPARC was used to aid our studies of the effect of molecular speciation on the structure of the material produced. The speciation diagrams for 4MEDAE, 4MEDAB and 4MEDAH are shown in Figure 5.4.1. Interestingly for a given pH, the population of the single protonated species decreases as the number of carbon atoms increases between the nitrogen atoms, presumably due to the inductive effect, making the nitrogen atom more susceptible to protonation. Furthermore, the singularly charged species reduces in concentration as the number of carbon atoms increases between the nitrogen atoms. The titration profiles of the tertiary amines were investigated in order to conduct a full pH study. The titration curves are shown in Figure 5.4.1 d-f where 15 mM (Si:N = 1:1) solutions of each amine were titrated with 0.1 M HCl.

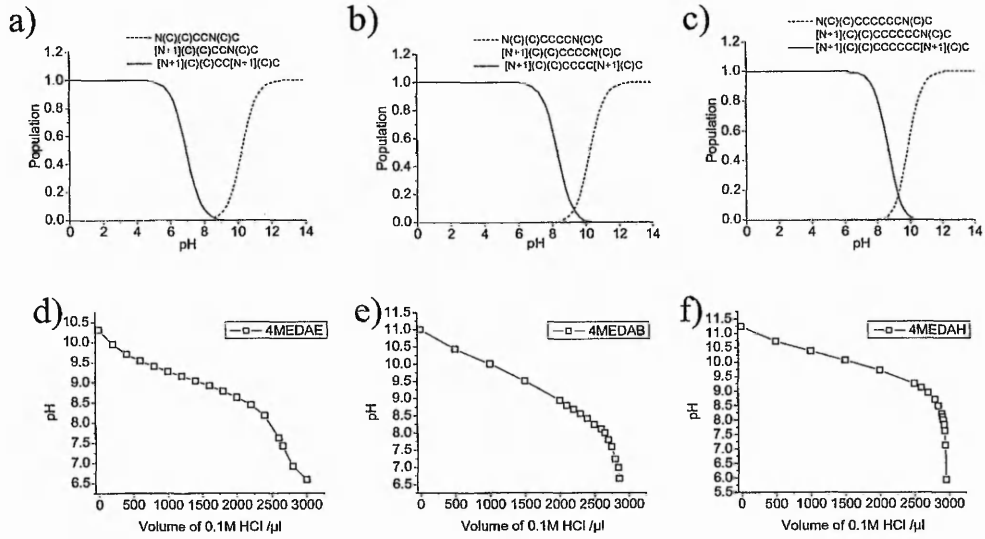

Figure 5.4.1 – Speciation diagrams for a) 4MEDAE, b) 4MEDAB and c) 4MEDAH generated using SPARC pK_a calculator[38] and d-f) respective titration curves used to investigate effective of pH.

5.4.1 The precipitation and characterisation of silica and SiCat precipitated using *N*,*N*,*N*',*N*'-tetramethylethylenediamine (4MEDAE).

The structures formed in the presence of 4MEDAE showed a high dependency on the pH of the solution. Needle-like hexagonal prism (hexagonal prisms), hexagonal rods and spherical silica were precipitated from solution of SiCat at different pH values.

Figure 5.4.1.1 shows the effect of pH on the morphology of the material precipitated from solution. Initially it can be seen from the SEM micrographs in Figure 5.4.1.1a that the precipitated material can be described as randomly generated fibres at pH 6, which changes the morphology to spheres at pH 6.22, Figure 5.4.1.1b. Both of which were confirmed to be amorphous silica by FTIR.

Hollow hexagonal prisms are first observed at pH 6.85 in the presence of what appears to be amorphous silica as shown in Figure 5.4.1.1c, this was confirmed by adding acid to isolated material which caused the hexagonal prisms to dissociate but had no effect on the amorphous silica which was washed, lypholised and confirm to be silica by FTIR (Figure 5.4.1.2b). Increasing the pH from 7.00 changes the morphology of the hollow hexagonal prisms to hexagonal rods at pH 8.51 Figure 5.4.1.1h, whilst it can be seen at pH 8.21 the end of the hexagonal rod starts to

become capped, Figure 5.4.1.1f, this could be due to the increasing concentration of KSiCat that is available in solution. At higher pH values the hexagonal rods increase in size until pH 8.9 where the size appears to stabilise before reducing in size at pH 9.35 as shown in Figure 5.4.1.1i).

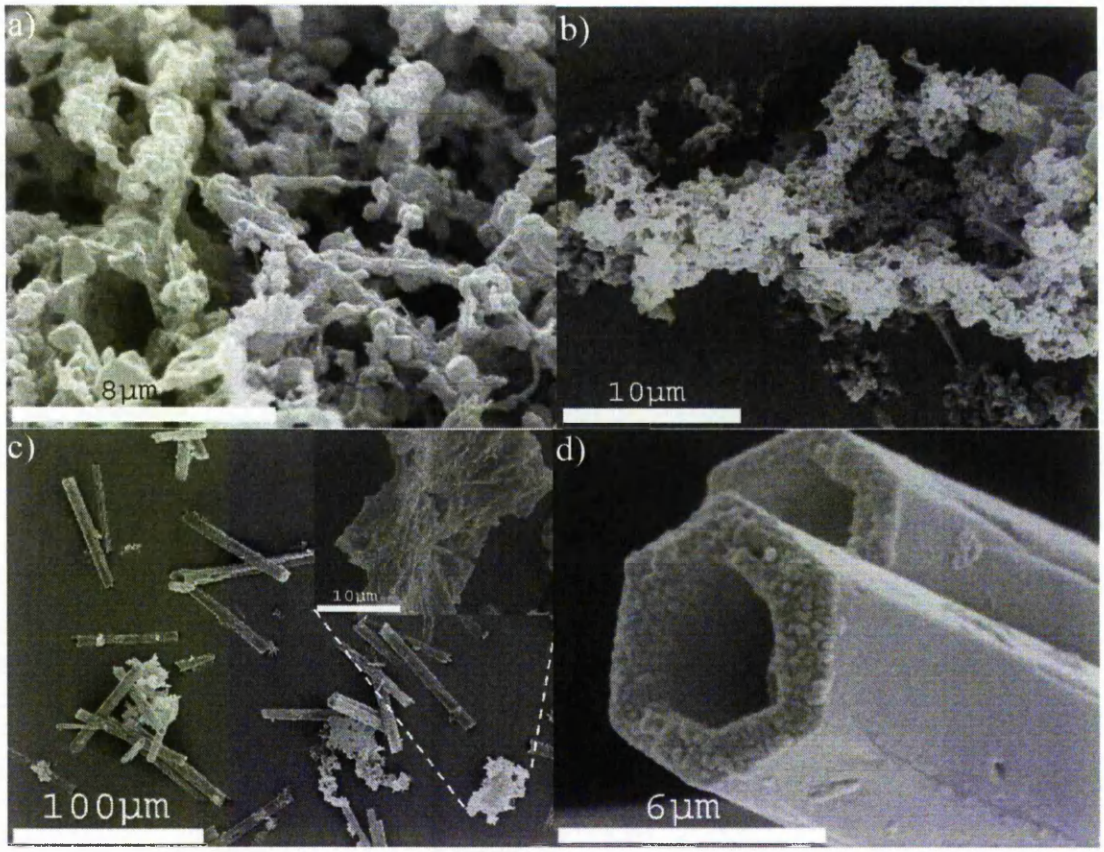

Figure 5.4.1.1) - SEM micrographs show the structures precipitated from solution at; a) pH 6.00, b) pH 6.22, c) and d) pH 6.85

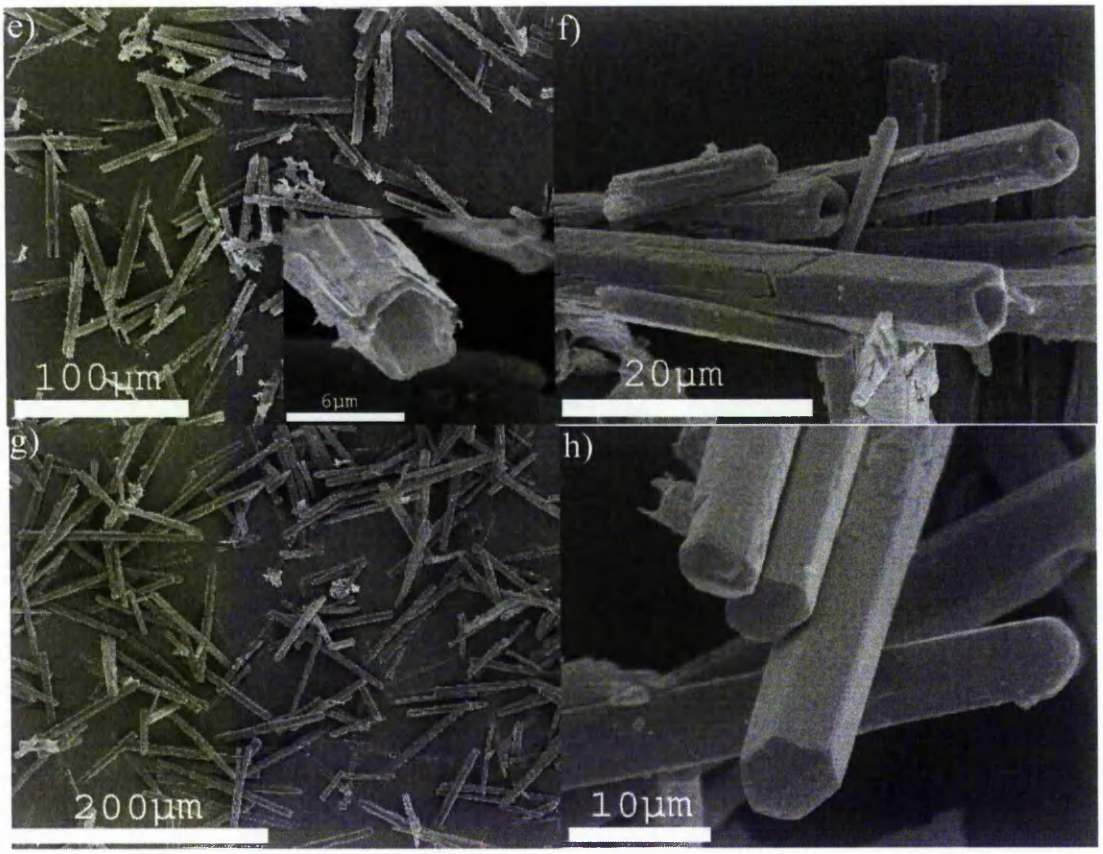

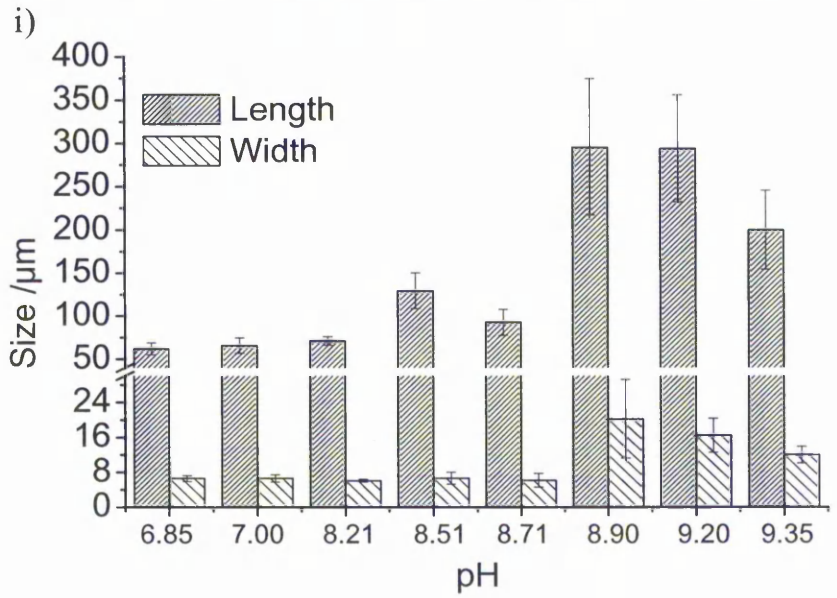

Figure 5.4.1.1 cont. – e) pH 7 f) pH 8.21. g) and h) pH 8.51. i) The formation of hexagonal prism and rods prepared at a Si:N ratio of 1:1 whilst varying the pH, error bars are 1 standard deviation from the mean.

It should be noted that the pH range shown is representative of the pHs where a precipitate could be isolated after 60 mins, pHs outside this range did not show any precipitation over this time period. The materials shown were isolated from the liquid phase. Material that crystallised on the container walls has not been analysed to date but did not appear (by naked eye) to exhibit the same morphology and as such yield have not been quoted. The exact mechanism of complex formation requires significantly more analysis than has been performed thus far. However, surprisingly when 4MEDAE was added to the KSiCat in which no acid had been added (*ca.* pH 9.65) no precipitate was formed. This suggests that complexation between 4MEDAE and SiCat has either; a higher activation energy than complexation using cyclam or complex formation is *via* a different mechanism when using 4MEDAE. Assuming complex formation is similar to the mechanism exhibited by cyclam it would seem likely that the $[4MEDAE]^{2+}$ species is complexed and in order for complexation to occur there must be a critical concentration of the 2+ species which is supported by the evidence that complexation does not occur at KSiCat's native pH of 9.65 where the concentration of the $[4MEDAE]^{2+}$ species is low. The change in material morphology can be attributed to 2 factors: the first is the molecular speciation of 4MEDAE which changes with pH and the second is the concentration of SiCat in solution. One would predict the formation of hexagonal prisms is due to the high concentration of 2+ species. The largest species are observed at pH 8.9 where 95 % of the species are singularly charged, but the concentration of KSiCat remaining in solution is significantly higher than at pH 8.6 and the concentration of singularly charged species remains approximately the same. One would assume the 4MEDAE is in the 2+ state when complexed, but the largest structures are observed at pH 8.9, where the 1+ species dominates. In contrast the greatest structural control is observed at pH 6.85 where hollow hexagonal prisms are observed and a greater proportion of the 2+ species are present and complexation is observed. Perhaps the greater structural control is due to the higher portion of 2+ species forming hollow hexagonal prisms and the hexagonal rods are formed by a two step mechanism where one nitrogen hydrogen bonds first and the second nitrogen atom hydrogens bonds after. This appears to the only obvious way a bifunctional molecule could link 2 SiCat molecules if indeed the mode of complexation is similar to that observed with cyclam. These hypothesises need to be confirmed by single crystal XRD.

5.4.2 Material characterisation

The hexagonal rods were characterised by SEM, EDXA, powder XRD, TGA and FTIR. Figure 5.4.2.1 shows the TGA of the hexagonal rods formed at pH 8.51 where it can bee seen that in total 88 % of the materials mass is lost upon heating to 900 °C of which 37 % can be attributed to organic material lost between 400 and 650 °C.

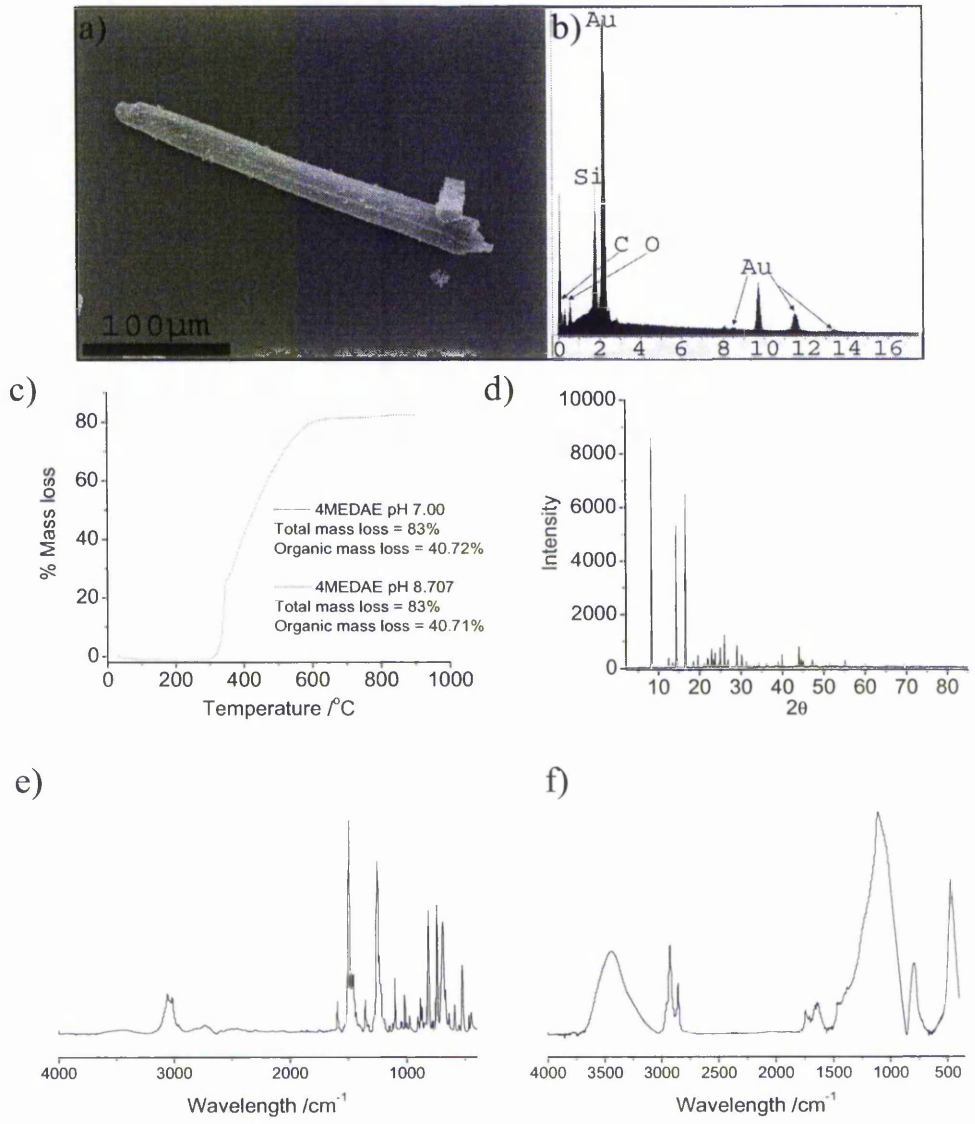

Figure 5.4.2.1a) SEM micrograph of the material remaining after TGA showing retention of the rod morphology accompanied by b) the EDXA spectra showing the material is silicon based. c) TGA of hexagonal prisms formed at pH 8.51 Si:N ratio1:1. d) Powder XRD of hexagonal rods prior to TGA. e) and f) FTIR spectra before and after thermal treatment.

Figure 5.4.2.1a shows remarkable retention of the rod-like morphology despite being just 13 % silica, however the material seems to lose its hexagonal appearance. The material precipitated at pH 8.51 was investigated using FTIR before and after thermal gravimetric analysis. Figure 5.4.2.1e shows the FTIR spectra of the material produced at pH 8.51 prior to thermal analysis indicating the presence of the SiCat, where characteristic peaks at *ca.* 3060 and 3015 cm^{-1} and a sharp peak at 1100 cm^{-1} indicate aromatic C-H bonds and Si-O in an octahedral conformation respectively. Interestingly, as seen with the KGeCat tetragonal prisms Figure 5.4.2.1f shows some organic material remains in the thermally treated tetragonal prisms indicated firstly by the CH_3 peaks at 2924 and 2854 cm^{-1} and secondly the peaks at 1743 and 1637cm^{-1} which one would hypothesise to be an N-H band but the exact nature of which will require further analysis as its position seems to indicate an amide bond, which seems highly unlikely to occur. Figure 5.4.2.2 shows the FTIR spectra of the hollow hexagonal prisms formed at pH 6.85 before and after washing with acid. Initially we see the characteristic aromatic C-H bands at 3020 and 3060 cm^{-1} from the tris(1,2-benzenediolato-*O,O'*) in the SiCat molecules and the peak at 1100 cm^{-1} shows a bimodal system exhibiting a wide base attributable to amorphous silica and a sharp peak attributable to the SiCat complex in the hexagonal prisms. Upon washing with acid the hexagonal prism dissociated releasing silicic acid and 4MEDAE whilst having no effect on the material without any specific morphology. The remaining material was washed with dd water three times and analysed by FTIR, which confirmed the material with no specific morphology was in fact amorphous silica as shown in Figure 5.4.2.2b. Interestingly, the FTIR spectrum shows a peak at 1630 cm^{-1} an N-H stretch attributed to be amine entrapped in the amorphous silica.

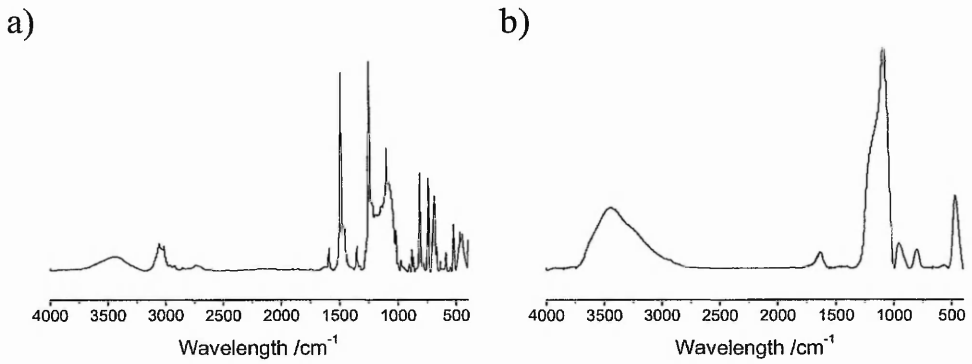

Figure 5.4.2.2a) FTIR spectra of material produced using 4MEDAE at pH 6.85 prior to thermal treatment and b) after thermal treatment.

The ability of a smaller molecule to complex SiCat in a similar morphology to cyclam it seemed logical to investigate derivatives of 4MEDAE whilst maintaining the tertiary amine functionality.

5.4.3 The effect of carbon chain length on the morphology of the precipitate by tertiary diaminoalkanes.

4MEDAB was investigated, where B (butane) relates to the number of carbon atoms separating the tertiary amine groups, increased from 2 to 4. Unsurprisingly this molecule also forms a complex with KSiCat. Figure 5.4.3.1 shows the morphology of the material precipitated from solution after 60 mins, where a hexagonal plate morphology can be prepared at pH 8.25 at a Si:N ratio of 1:1. It was found while trying to study a complete pH range the precipitates formed at pH 8.25-8.9 could not be isolated as it dissolved when the material was washed with dd water to insure the precipitate was free of KCl. This indicated that either the precipitate was composed of KCl or the complex formed between KSiCat and 4MEDAB was now highly unstable to even mildly acid conditions exhibited by dd water *ca.* pH 5.

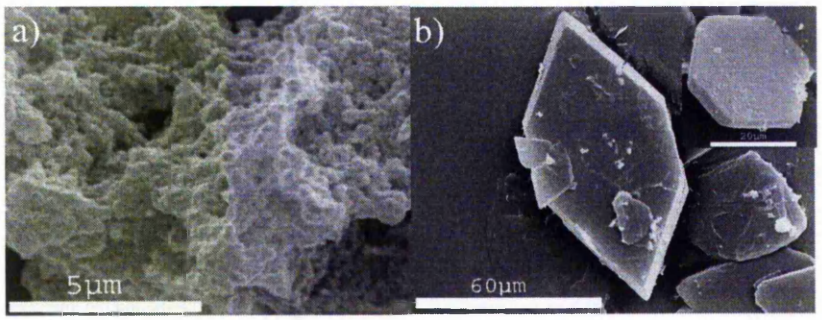

Figure 5.4.3.1 – Morphology of precipitate made using 4MEDAB at a Si:N ratio of 1:1 isolated after 1 h. a) pH 6.8, b) pH 8.25, insert shows other hexagonal structures observed.

In order to confirm our hypothesis that the hexagonal plates precipitated at pH 8.25 were in fact SiCat complexed by 4MEDAB and not simply precipitated KCl we preformed FTIR on the isolated samples. Figure 5.4.3.2 clearly shows our hypothesis was correct.

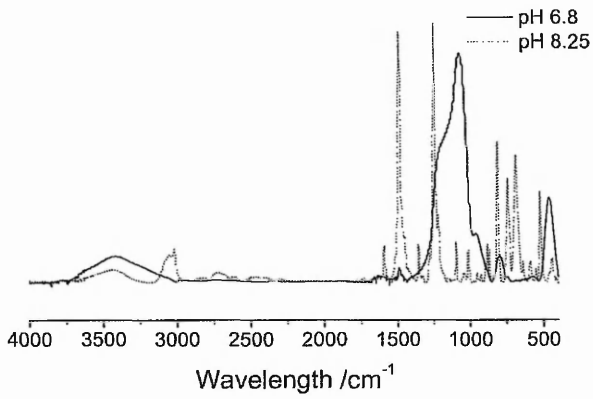

Figure 5.4.3.2 – FTIR spectra of precipitated material using 4MEDAB at Si:N 1:1 at pH 6.8 silica is precipitated. At pH 8.25 SiCat is precipitated.

It was found by increasing the carbon chain length of the tertiary diaminoalkane that significantly less structural control is observed. It does not seem coincidental that two molecules with structural similarities precipitate hexagonal rods and hexagonal plates. Instead it would seem more than likely that a change in molecular orientation causes a direction change in crystal growth. Indirect evidence for this hypothesis came from the specific nature of the interactions between cyclam and SiCat where we found that ring size is crucial in order for complexation to occur. Hence, in the case of 4MEDAE and 4MEDAB the molecular orientation of the 4MEDAB will change due to steric hindrance with the phenyl groups on the SiCat thus changing the preferred direction of crystal growth. This hypothesis will of course have to be confirmed by single crystal silicon diffraction.

Finally, the effect of increasing the carbon from 4 to 6 carbon atoms was investigated, using 4MEDAH (Hexane). Complexation was not immediately obvious even at high pH values >8 (samples prepared using 4MEDAE and 4MEDAB precipitated in mins), Figure 5.4.5.3 shows the morphology of the material precipitated after and 60 mins with the exception of Figure 5.4.5.3e which was isolated after 24 h. Figure 5.4.5.3f shows the silica isolated after 24 h at pH 6.8 where it can be seen silica with silica particles with a spherical morphology have assembled into sheets clearly visible to the naked eye. The material precipitated using 4MEDAH can be categorised into two groups: 1) silica precipitated at low pH where the proportion of undissociated KSiCat is low and the tertiary amine catalyses the formation and precipitation of silica and 2)

where the proportion of undissociated KSiCat is high and complexation is observed. FTIR spectra of the precipitated material shown in Figure 5.4.5.3g and h clearly shows the difference between the two types of material where characteristic peaks of silica can be seen at pH 7.030, 7.359 and 7.963 and characteristic peaks of KSiCat can be seen at pH 8.459 and pH 8.804. It can be seen that the morphology of the precipitated SiCat changes when the carbon chain length was increased from 2 to 4 and from 4 to 6, complexation still occurs however, no specific morphology can be seen in the later case. This suggests an increase in the disorder, which we hypothesise to be because of steric hindrance between the carbon chain and the phenyl groups on SiCat.

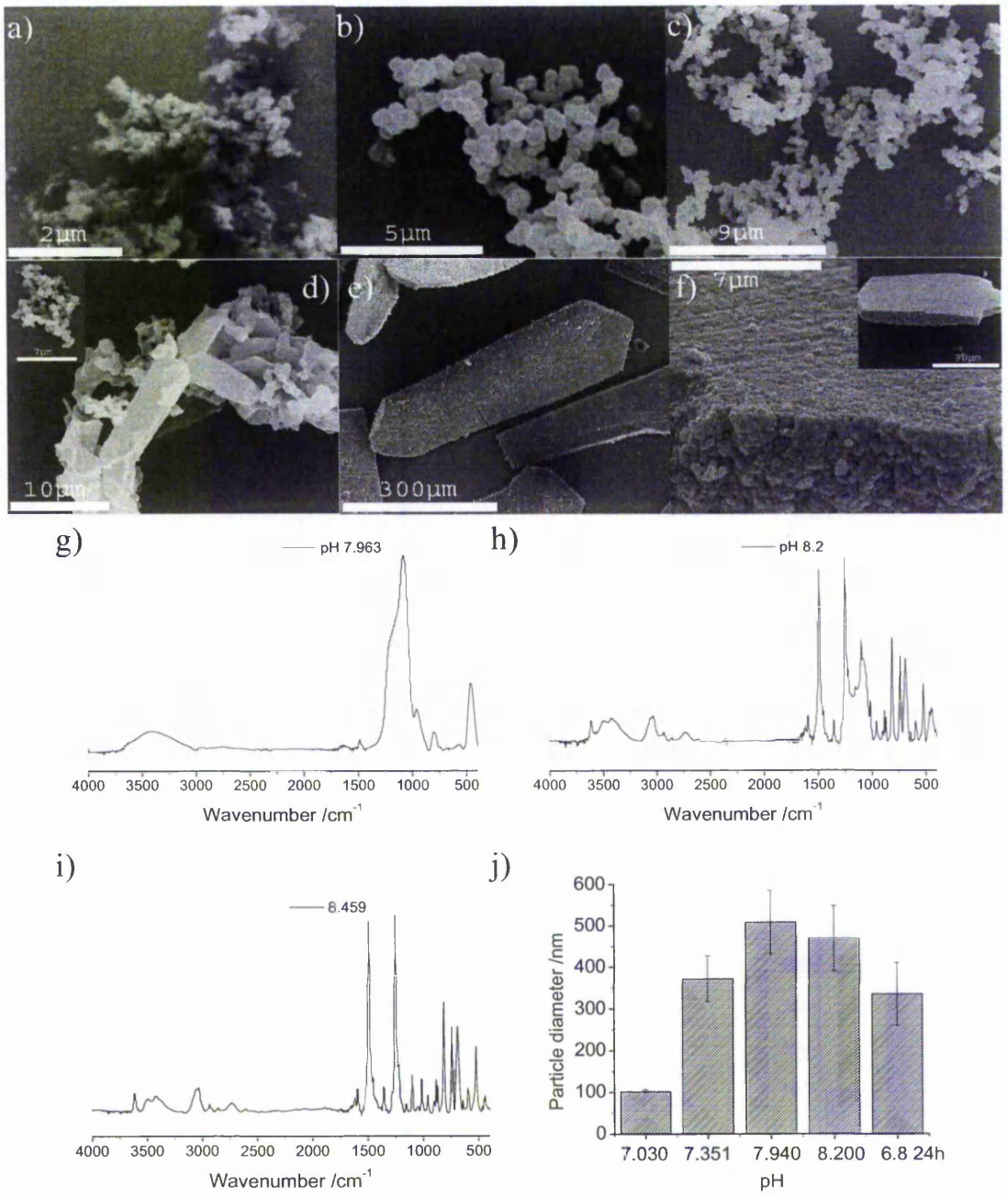

Figure 5.4.3.3 – Morphology of the precipitate isolated after 60 mins using 4MEDAH at an Si:N ratio of 1:1 after 1 h at pH a) 7.030 b) 7.351 insert shows this system is bimodal containing amorphous silica with a spherical morphology and larger plate-like structures c) 7.963 d) 8.2 and e) 8.459 and f) 6.8 after 24 h, insert shows macroscopic structure of the spherical particles assembled into a macroscopic sheet. g-i) FTIR spectra of material isolated at pH 7.963, 8.2 and 8.459. j) characterisation of the silica spheres precipitated at pH 7-8.2 after 60 mins and at pH 6.8 after 24 h.

The FTIR spectra shown in Figure 5.4.3.3g-i show the transition of the precipitated material from silica characterised by the Si-O-Si peak at 1100 cm^{-1}. The material

isolated at pH 8.2 as depicted by the SEM micrograph shows a bimodal system thought to comprise silica spheres and larger plate-like structures though to be complexed SiCat. The FTIR shown in Figure 5.4.5.3h seems to confirm this hypothesis as it shows characteristic peaks of SiCat at 1495 and 1248 cm^{-1} attributable to a substituted aromatic ring and the aryl =C-0 respectively. Importantly the confirmation that this is a bimodal system comes from the broad band centring at 1100 cm^{-1} which is sharp at the top of the peak but broad at the base. This indicates some complexed SiCat where the Si-O is probably in a single octahedrally coordinated environment and the broadening at the base is cause by the presence of amorphous silica. The FTIR spectra shown in Figure 5.4.3.3i is characteristic of complexed SiCat and when compared to the material isolated at pH 8.2 a sharp peak at 1100 cm^{-1} and no broadening at the base indicating that the conditions now favour SiCat complexation and not silica formation.

5.5 Summary

The role of tertiary amine of varying carbon chain length in the complexation KSiCat and formation of silica has been shown above. The molecular speciation of the tertiary amine and the concentration of undissociated KSiCat governs the morphology and type of material produced. 4MEDAE complexes SiCat at pH 6.85-7 to form hexagonal hollow prisms, varying the pH further results in a change of material morphology. The material precipitated changes from being hexagonal hollow prisms to hexagonal rods, through what seems to be a capping of the prisms. The formation of the hexagonal prism at pH 6.8 shows that 4MEDAE has an extremely high affinity for KSiCat. In order for a final pH of 6.8 to be reached enough HCl to fully dissociate KSiCat to $Si(OH)_4$ is required. However, this process takes approximate 20 s and addition of the tertiary amine prior to this indicates that formation of the hexagonal prism is more favourable than dissociation of KSiCat to $Si(OH)_4$. The SEM micrograph in Figure 5.4.1.1c shows that amorphous silica is also generated at pH 6.85 which we assume is because some KSiCat dissociates to form $Si(OH)_4$ which condenses in the presence of 4MEDAE to from silica as discussed previously. The crystal structure of the hexagonal prisms will be investigated in due course to fully elucidate the molecular selfassembly of the tertiary amine, currently the crystals available for single crystal X-ray diffraction do provide sufficient data for structural

analysis. One interesting point to note is that unlike cyclam the tertiary amines were unable to precipitate material at pH 9.65. At pH 9.65 KSiCat has no acid added to it, thus is a stable undissociating system. This suggests formation of the hexagonal prisms is dependent not only on the availability of KSiCat but also the availability of either free protons or KSiCat beginning to dissociate. Interestingly, as the carbon chain length between the tertiary amine groups increases the affinity of the tertiary amine for KSiCat seems to diminish as silica is formed in preference to complexation at pH 6.8 when 4MEDAB was investigated. However, at pH 8.5, where there is a sufficient undissociated KSiCat in solution and the concentration of the tertiary amine in the singularly charged state is sufficient, complexation occurs and hexagonal plates are precipitated from solution. Moreover, when 4MEDAH is used a similar effect seems to occur where silica with a spherical morphology is precipitated between pH 6.8 and 7.9 which increases in size with increasing pH until complexation is favoured although no structural control is observed.

5.6 The effect of azamacrocyclic molecules on the formation of silica

The work present here investigates the role of azamacrocycles in silica formation using two different precursors to silica. The findings from the study of azamacrocycles have produced some very interesting crystalline inorganic-organic hybrid materials (silicon and germanium) which have needle-like tetragonal prisms morphology. The tetragonal prisms are a dipotassium tris(1,2-benzenediolate-*O,O'*)silicate (KSiCat), cyclam 1:1 complex, where cyclam acts as a template for the formation of the tetragonal prism as previously described in section 5.3.1.

Following the discovery that tetragonal prisms are formed using cyclam, a series of azamacrocyclic molecules were investigated in the KSiCat silica precipitating system. Interestingly, it was found that cyclam is unique in its ability to precipitate the tetragonal prisms, however, the other azamacrocyclic molecules have a profound effect on the formation of silica. A systematic investigation was conducted to determine the effect of size of the azamacrocyclic ring, the hydrophobicity of the cyclam ring on silica formation. Two quite different silica precursors were used, TMOS and KSiCat. The silica formed exhibits both controlled morphology and material characteristics. For the first time the catalytic ability of the azamacrocyclic

molecules on the formation of silica has been investigated using unbuffered TMOS solutions, which has allowed an exceptional understanding to be gained on the role of additives and counter ions on the formation of silica (Chapter 2 Part II).

5.7 The kinetics of silica formation in the presence of azamacrocyclic molecules.

The effect of azamacrocyclic molecules on the formation of silica was investigated initially using three different Si:N concentrations. In previous studies have investigated the effect of concentration with respect to an Si:N ratio, which has allowed an understanding of the molecular interactions between silicon and nitrogen atoms. Previously the Si:N ratio investiagted varied from 1:1 to 1:4 Si:N ratio.[25-27] In this study the exceptional ability of the azamacrocycles to catalyse silica formation made it almost impossible to study the reaction kinetics at a 1:1 Si:N ratio. The kinetic measurements were carried out using 30 mM solutions containing orthosilicic acid produced using TMOS, instead of KSiCat, at a Si:N ratio of 10:1. The formation of the tetragonal prisms prevents KSiCat dissociating to form orthosilicic acid and thus the effect of cyclam on the formation of silica could not be studied. To overcome this problem, TMOS was used as a silica precursor in an unbuffered system to avoid unwanted interactions between additives, buffer and silica species. TMOS has been used in many bioinspired and biomimetic silica studies, however the use of alkoxysilanes as a precursor pose several interesting questions. Alkoxysilanes require a hydrolysis period under acid conditions where it is reported that silicic acid is generated. Typically this is achieved in 15 mins, during this time we have shown in Chapter 2 Part II that during the hydrolyisis period TMOS undergoes condensation reaction to form Q^1 species and furthermore it is unlikely that on a molecular scale complete hydroysis can occur. The hydrolysis reaction generates methanol in solution, which is known not to be present in biological organisms. Traditionally TMOS systems utilise a buffer to neutralise the acid hydrolysis conditions, however the introduction a buffer increases the potential for interactions between the buffer, silica species and possible the additive thus masking the true role of the additive in silica formation difficult to identify. Recently a procedure was established for measuring the condensation of TMOS at circumneutral pH using KOH to neutralise the system.

Figure 5.7.1a shows examples of the raw data collected from the molybdenum blue assay, where a TMOS system in the absence of an additive (Blk) and with 3NC and cyclam is shown. It is immediately obvious that cyclam is having a dramatic effect on the rate of silica formation from the first measurement, where 21 % of the initial concentration of silicic acid has been converted to species undetectable by the molybdenum blue assay (species larger than dimers). The results are shown in Figure 5.7.1b, where it can be seen that the ring size plays a critical role in the ability of the azamacrocyclic molecule to catalyse the formation of silica. Interestingly when the ring contains 9 atoms (3NC), the rate of trimerisation is approximately halved (relative 3rd order rate 0.55), but the ring size increases to 12 atoms (4N2) the kinetics increases to a rate comparable to the TMOS system in the absence of an additive. Increasing the ring size from 12 to 14 atoms (cyclam, 2MC and 4MC) has a huge effect on the formation of trimers (3rd order rate constant), increasing the ring size to 18 atoms (6NC) reduces the rate compared to the 14 atom ring azamacrocyclic molecules.

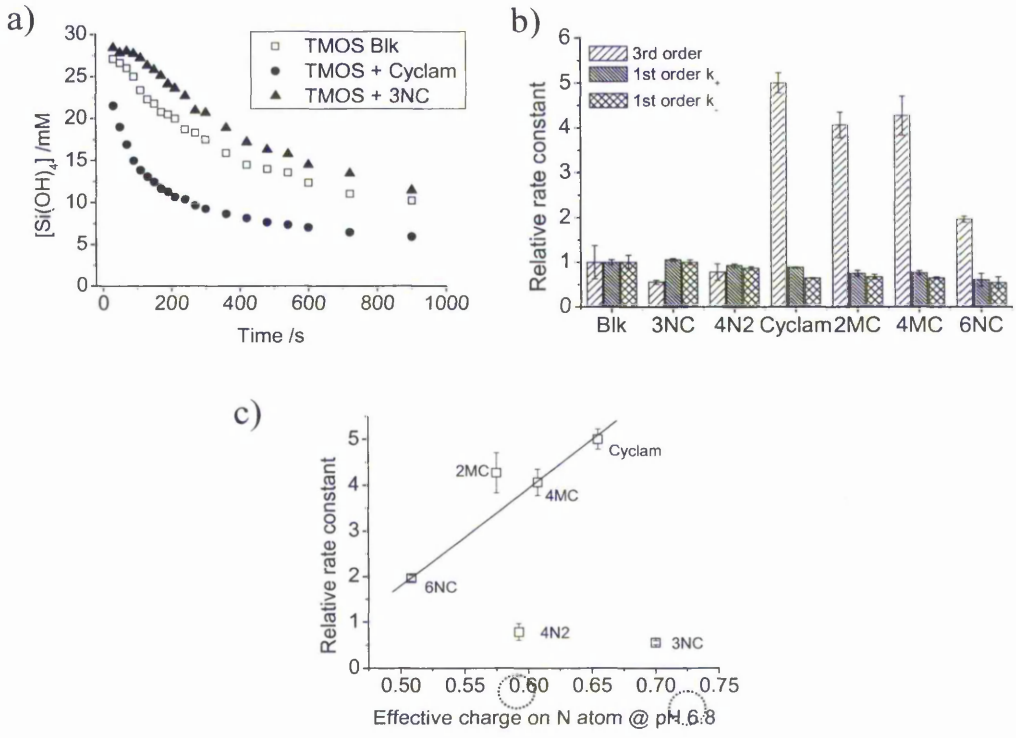

Figure 5.7.1a) Raw data from molybdenum blue assay, b) The kinetics of silica formation in the presence of azamacrocyclic molecules at a Si:N ratio of 10:1, c) The relative 3rd order rate constant for the formation of trimers is plotted against effective charge on each nitrogen atom at pH 6.8.

Initially one might hypothesise that the more nitrogen atoms in the ring, the faster the kinetics of silica formation and initial results would suggest this hypothesis appears to be correct when one considers 3NC to cyclam. However, quite clearly when one considers the kinetics of silica formation for larger molecules such as 2MC, 4MC and 6NC the initial hypothesis is incorrect. Instead one must consider both the ring size and the charge on the ring. Figure 5.7.1.1c shows a plot of the effective charge on a nitrogen atom in the ring. This has been calculated from the speciation diagrams for each of the azamacrocyclic molecules (Appendix 3 Figure 1). The charge on the ring was calculated using Equation 5.7.1.

$$I = \frac{\sum(S_1 \times I_1 + S_n + I_n)}{N} \qquad (5.7.1)$$

*Where: **I** is Effective charge per nitrogen atom, **S** is the Fraction of species and **N** is the number of nitrogen atoms in molecule*

When the effective charge on a nitrogen atom in the ring is plotted against the relative third order rate constant it become quite clear that the ring must contain ≥ 12 atoms to have a significant effect on the kinetics of silica formation and secondly where this is true: the greater the effective charge per nitrogen molecule the faster the 3rd order rate constant. The empirical relationship identified above describes the relationship between charge and the kinetics of silica formation for azamacrocyclic molecules. However, if one tries to incorporate the kinetics of silica formation for 3NC and 4N2 by compensating for the number of atoms in the ring it would appear that there are more factors governing the relationship between a molecules structure than its charge and the kinetics of silica formation. The number of carbon atoms between nitrogen atoms should be considered. As with the ethyleneamines[27] and propyleneamines, a link has not been found between the molecular structure and the kinetics of silica formation, although generally the propyleneamines can be considered to have a greater effect on the formation of silica).[28] It therefore seems likely the results obtained for 3NC and 4N2 cannot be incorporated into the "effective charge model" because the molecules only contain C2 spacings between nitrogen atoms, but this does not explain why 6NC fits the relationship. Furthermore, these calculations are

based on SPARC which does not take into account that the fourth nitrogen requires less energy to be protonated than the third in cyclam.[42] Investigations will continue into the role of propylamine functionality and why the third carbon in the spacing has such a profound effect on silica formation. So far, despite a number of investigations into the role of the propylamine functionality the answer remains elusive.

The forward constant of the reversible 1st order rate constant describes the condensation of silicic acid with larger silica species, where the reverse reaction is the dissolution of silicic acid from large silica species. These rate constants do not significantly change in the case of 3NC and 4N2, however, when one considers cyclam and larger species it is important to remember that the first order rate constants are a function of the amount of silicic acid remaining in solution (Equation 5.7.2), which has been reduced by approximately 40% when compared to the blank TMOS system.

$$A - A_{\infty} = e^{-kt} \qquad (5.7.2)$$

Where: ***A*** *is the [Si(OH)$_4$] at time t,* A_{∞} *is the [Si(OH)$_4$] at equilibrium,* ***k*** *is the Overall first order rate constant (from which* k_+ *and* k_- *are derived) and* ***t*** *is time.*

Hence as the concentration of silicic acid is 40 % lower at the start of the first order region A-A_{∞} goes down as will k.

5.8 The effect of azamacrocyclic molecules on the rate of aggregation

Dynamic light scattering was used to investigate the rates of aggregation of silica species generated from 30 mM solutions of orthosilicic acid from KSiCat and TMOS. As mentioned in the materials and methods section, these materials were produced using method 1, protonated addition. Figure 5.8.1 shows the DLS of the azamacrocyclic molecules (excluding cyclam because of complexation using KSiCat) at a Si:N ratio of 10:1. Appendix 3 Figure 4 shows the results obtained for azamacrocyclic molecules for three concentrations studied 1:1, 10:5 and 10:1 using KSiCat, notably several of the systems immediately precipitate at higher concentrations.

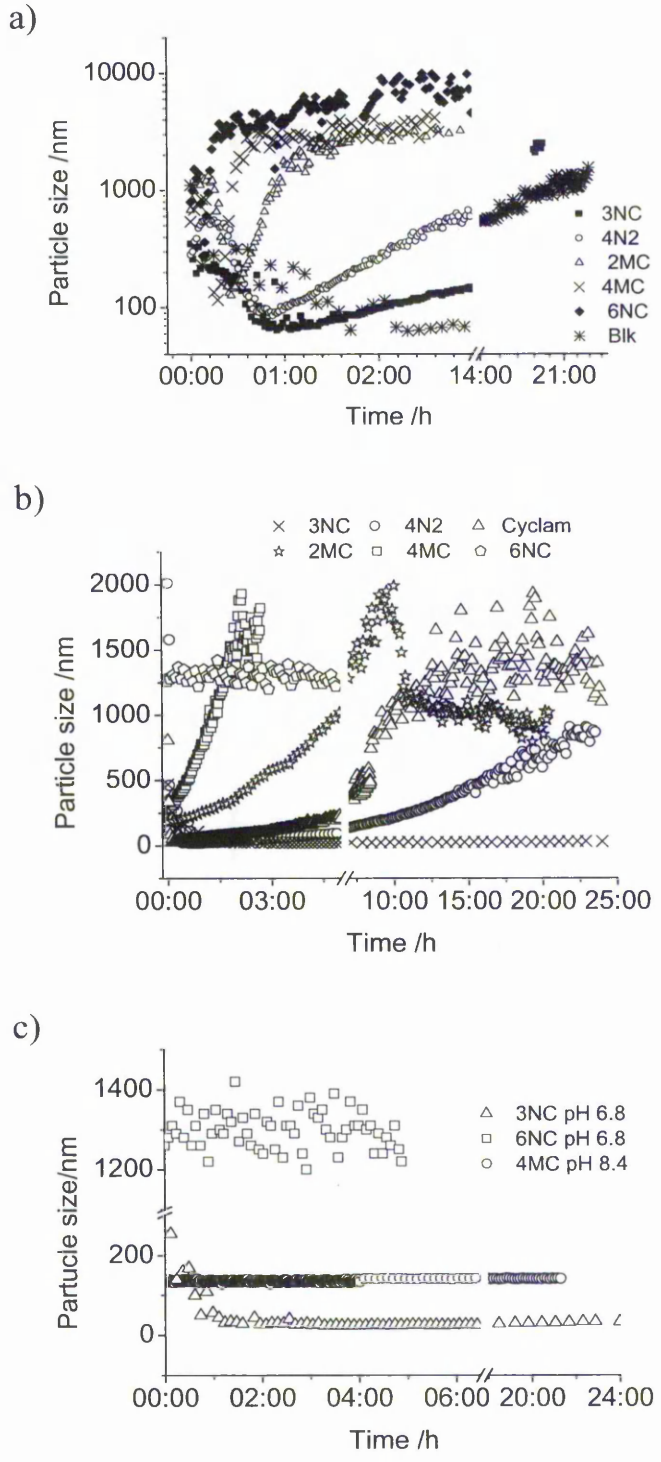

Figure 5.8.1 – Dynamic light scattering of azamacrocyclic molecules when a) KSiCat using the protonated method. b) TMOS used as silica precursors and the Si:N ratio was 10:1. c) The stabilisation of silica particles using TMOS in the presence of 4MC allows a stabilised silica sol to be produced.

From the KSiCat data, a trend can be seen whereby increasing the number of nitrogen atoms in the azamacrocyclic molecule increases the rate of aggregation. Interestingly, the aggregation profiles using TMOS as the silica precursor show quite different profiles observed when compared to KSiCat. Initially a comparison should be made between the blank systems (Chapter 2 Part II), where the TMOS system in the presence of KCl with or without catechol at similar levels to the KSiCat system induces aggregation. In the KSiCat system linear growth is observed until a maximum stable particle size, once particles start to form in the system. The aggregation profiles of the azamacrocyclic molecules in the two model systems are quite different. In the KSiCat system growth tends appears towards linearity, where as in the TMOS system a mixture of growth patterns can be seen. In general it can be seen that aggregation is faster in the KSiCat system, probably due to the presence of KCl and in particular K^+ ions, previously shown to promote aggregation (Chapter 2 Part II). In the case of cyclam in TMOS, particle growth is slow initially, followed by a rapid growth period which then levels off at a final maximum particle size. Interestingly 2MC shows rapid growth initially, followed by a rapid drop in particle growth, possibly due to larger particles precipitating out of solution leaving *ca.* 1000 nm particles suspended in solution. In the case of 3NC, a stable particle size of approximately 30 nm was observed after 2 h, which gradually increases over time and after a 96 h period a gel was isolated. This result seems to suggest the formation of a pseudo stable sol of 30 nm particles from the z-average data obtained. A similar result is obtained for 6NC except the particles are much bigger and the particle size distribution does not seem to be as stable. By changing the pH of the 4MC TMOS system to 8.4 this allows a stable sol of *ca.* 140 nm particles to form (Figure 5.8.1c and will be discussed later).

5.9 Materials characterisation.

The materials were isolated after 24 h, with the exception of 3NC which was isolated after 96 h in the unbuffered TMOS system due to the slow rate of aggregation as mentioned previously. The materials were characterised by SEM, TGA and nitrogen gas adsorption/desorption.

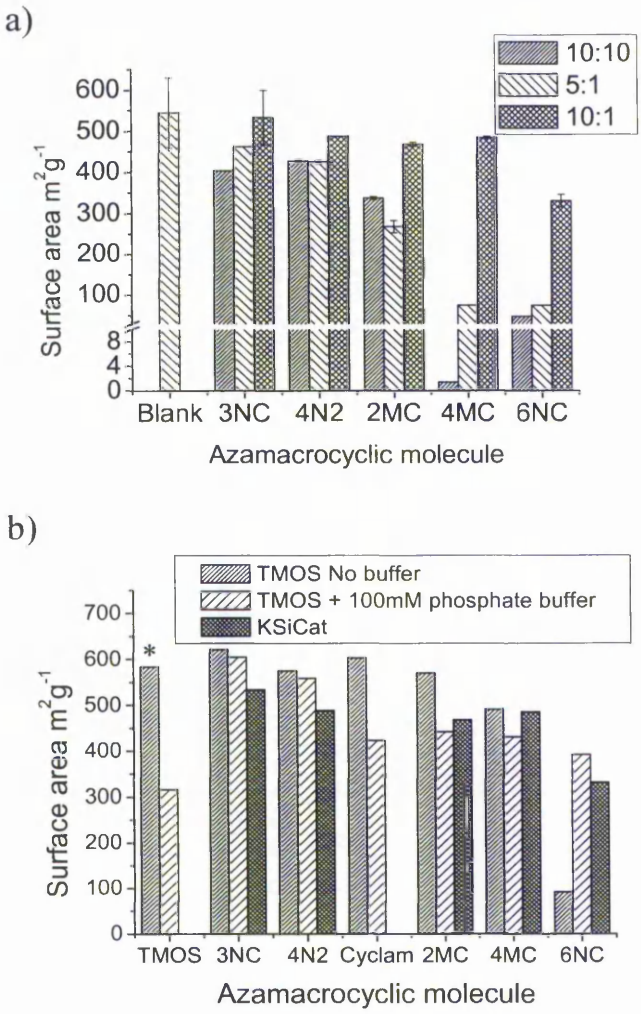

Figure 5.9.1a) – The change in material surface area produced using KSiCat with decreasing Si:N ratio from 1:1 to 10:1. b) Comparison of materials produced using the azamacrocyclic molecules in KSiCat, TMOS and TMOS and 100 mM phosphate buffer at a Si:N ratio 10:1, *TMOS system usually shows no aggregation in the absence of cations or a buffer, this sample was freeze dried and then washed and dried again.

The results shown in Figure 5.9.1a indicate that in most cases, by increasing the concentration of the azamacrocyclic compound in solution the BET surface area decreases. Figure 5.9.1b shows the materials are comparable for KSiCat and TMOS, although in general the materials produced with KSiCat have a higher surface area. The inclusion of a buffer into the TMOS system generaly decreases the surface area when compared to the unbuffered TMOS materials. The buffered TMOS system with 3NC induced gelation and the material was isolated after 24 h instead of 96 h in the unbuffered system almost certainly due to the presence of cations (Na^+). One can see

that the buffered TMOS blank system has a surface area of *ca.* 316 m^2g^{-1} in the presence of a buffer, but inclusion of 3NC and 4N2 into the buffered TMOS system increases the surface area dramatically to *ca.* 600 m^2g^{-1}, suggesting an interaction between the buffer and the azamacrocyclic molecule in order to reduce the effect on the buffer on the exhibited surface area. It does not seem unreasonable to hypothesis that the interaction between the buffer and 3NC could be due to coordination of phosphate in the 3NC cavity, especially when one considers the similarity in size of phosphate and orthosilicic acid and the measured 3rd order rate constant was half that of the blank in the presence of 3NC. This also suggests that orthosilicic acid could also be coordinated in the 3NC cavity. Furthermore, one might suggest the increased time to isolate a precipitate (96 h instead of 24 h) also suggests orthosilicic acid coordination. This is also not surprising if one considers the ^{29}Si data presented in Chapter 2 that showed that after hydrolysis TMOS is a mixture of Q^0 and Q^1 species, which if this hypothesis is correct the precipitated material after 96 h using 3NC would therefore represent the condensation of residual orthosilicic acid that had not been coordinated by 3NC due to the Si:N being 10:1 and Q^1 species. The precipitated material after 96 h would therefore be expected to have a surface area similar to the unbuffered TMOS system which was isolated by drying, washing and then drying again (DWD), this is indeed the case. Unfortunately we were unable to verify our hypothesis that orthosilicic acid can be stabilised using 3NC due to time restriction although further investigation will be mentioned in Chapter 6 section 2 - Further work.

When compared to the blank TMOS (DWD) again a surface area of 583.13 m^2g^{-1} was observed, which suggest the presence of a phosphate buffer has a significant effect on the surface area exhibited by the material. Unfortunately, the kinetics in the phosphate buffered TMOS system could not studied due to complexation of phosphate with the molybdenum reagent. This essentially means a new protocol must be established to insure the kinetics of silica formation are not masked by the complexation of phosphate to the molybdenum reagent and highlights the fact that phosphate buffers interact strongly in silica formation and have a role to play in biosilicification.[19]

The materials made using KSiCat have been produced using method 1 – protonated addition. Having established that the $[cyclam]^{2+}$ species ([N+1](CCNCCC[N+1]1)CCCNCC1) is required for the formation of the tetragonal prisms, the role of the speciation in the formation of silica was investigated. As mentioned in the materials and method section, two further methods were developed; the rationale for such an approach is given below.

The homogeneity of the tetragonal prisms produced using KSiCat and cyclam was improved by adjusting the additive solution to the pH to be studied. The azamacrocyclic molecules were studied in a similar way (method 2 – species specific addition, see materials and methods section) to minimise the competition for protons in solution. Method 1 was used to prepare all of the materials reported up to this point, which involves the addition of a predetermined amount (see titration curves Figure 5.4.1 + 240 µl 2 M HCl for KSiCat) of HCl to the azamacrocyclic solution, thus adding the azamacrocyclic molecule in a fully protonated state. Upon addition of the azamacrocyclic solution to the solution of KSiCat, the speciation of the azamacrocyclic molecule will progressively change as the solution approaches the equilibrium pH 6.8. This can be described as a "competition for protons". When one considers the procedure used to create a blank 30 mM of silicic acid derived from KSiCat it involves the addition of acid to a pure solution of KSiCat. A stoichiometric amount of acid is required to fully dissociate the KSiCat complex and achieve pH 6.8, the protons are "fully available" for this process to occur. The approach adopted in method 1, where the protons are associated with the azamacrocyclic molecule are not "fully available" to dissociate the KSiCat complex. Therefore the azamacrocyclic molecule must first be partially deprotonated to allow the KSiCat to fully dissociate. Furthermore, as highlighted in Chapter 2 Part II, the pH changes prior to the KSiCat system stabilising at pH 6.8 and will also contribute to the continually changing speciation of the azamacrocyclic molecule being studied. Method 2 – species specific addition minimises the azamacrocyclic speciation changes, although it does not eliminate them. The azamacrocyclic molecule is added as the pH is recovering in the KSiCat system at *ca.* pH 5.2 whilst still ensuring only orthosilicic acid is in solution. Method 3 – basic addition was developed to study the azamacrocyclic molecule in an initially unprotonated state. One important point should be mentioned here, the final pH for all three methods was kept constant at pH 6.8 which was reached after 15

mins. Thus despite adding the azamacrocyclic molecules as different molecular species this would not be maintained for any period of time and the azamacrocyclic species will immediately tend toward the pH of the solution and the molecular species present at that pH. Thus any effects in the materials produced will be due to interaction of the azamacrocyclic molecules during the very early stages of silica formation and these effects are expected to be small.

The porosity and its relationship with the pore volume of the materials produced proved to be very interesting; Figure 5.9.2 shows the porosity of the materials produced using the three methods for KSiCat and TMOS in the presence of phosphate buffer (100 mM, PB) and without a buffer (NB). In the KSiCat system the influence of adding the azamacrocyclic molecules in different states of protonation generated materials with different porosities. In all cases the pore size distribution was narrower when the TMOS system was used unless microporous silica was produced. This seems to suggest that the presence of KCl and catechol in the KSiCat system plays a role in templating the porosity of the material. In the case of 3NC the narrowest pore size distribution was obtained when a fully protonated species was added and in the case of 4N2, species specific addition gave the narrowest pore size distribution. The materials produced using 4MC in the KSiCat system had an extremely tight porosity and also exhibited a distinct porosity change when the materials were prepared by the three different methods. The porosity changes from 16.3 Å when 4MC was added in a fully protonated state (method 1), to 9.7 Å when 4MC was added in a partially protonated state (method 2 - species specific addition) and addition of the 4MC as a base produces a material with no mesoporousity.

The introduction of phosphate buffer to the TMOS system templates the silica formed which has a narrow pore size distribution centred at 19.5 Å. There is no effect of 3NC and 4N2 on the pore size distribution in the buffered TMOS system. The material produced using 4MC in TMOS system does not show any mesoporousity and the surface area remains unchanged from the KSiCat system. Appendix 3 Figure 4 shows similar plots for the other materials produced using the cyclam, 2MC and 6NC. The materials produced using the azamacrocyclic molecules tend from having large pores to small pore as the azamacrocyclic ring increases in size. The effect of azamacrocyclic concentration on the porosity of the materials in the KSiCat system

was to widen the pore size distribution such that specific pore size peaks were not visible, this is might be because the materials form so quickly that a regular pore size in unable to form.

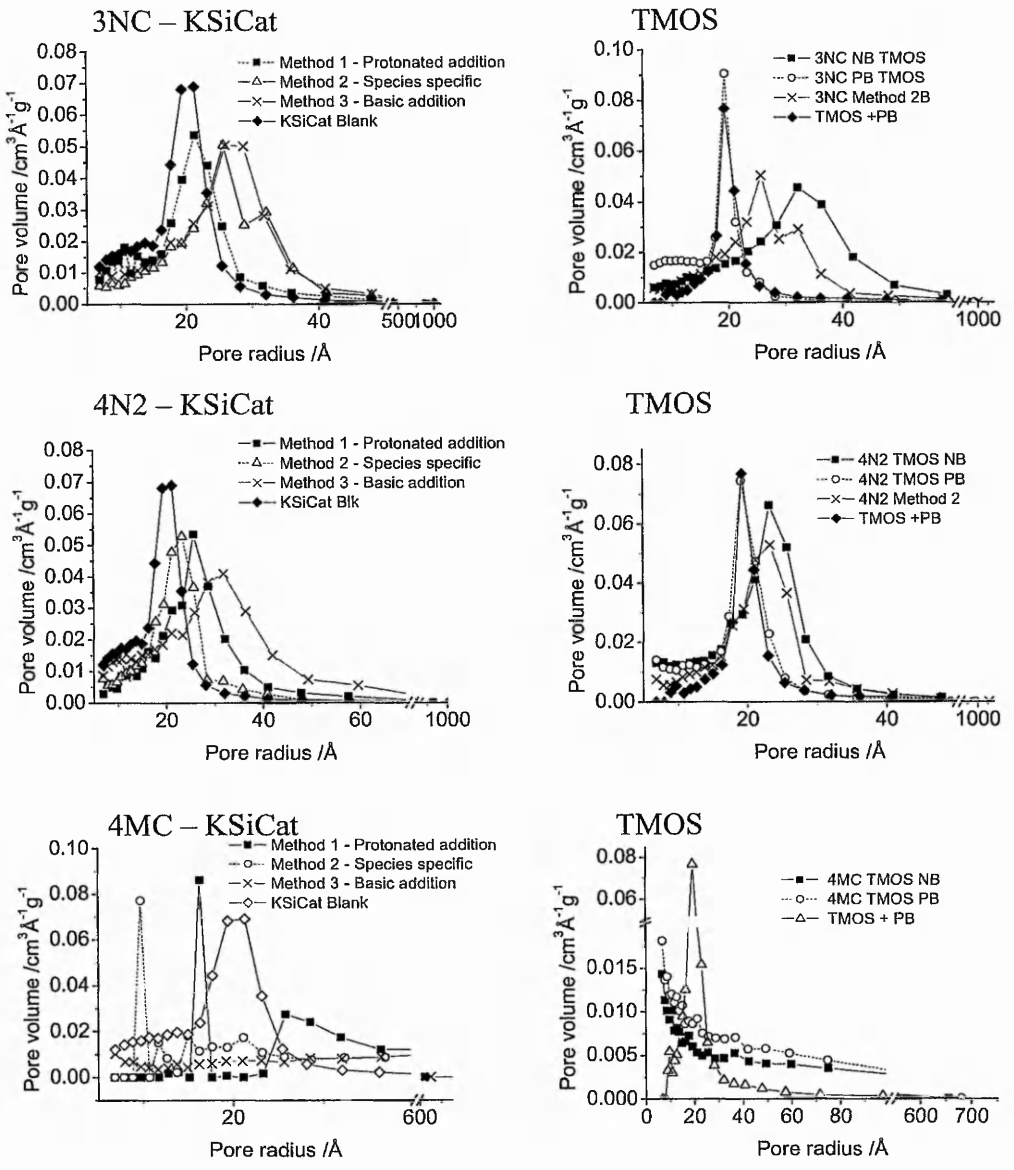

Figure 5.9.2 – The porosity/volume distribution graphs of materials prepared using 3NC and 4N2 using KSiCat, where the azamacrocyclic molecule was added using three different species; protonated, species specific and basic. Materials were also prepared using TMOS in a 100 mM phosphate buffered and unbuffered system.

The materials were analysed for their organic content using thermal gravimetric analysis. The organic material in the materials was calculated by the mass loss between 400 and 800 °C. Figure 5.9.3 shows the TGA profiles for the materials

produced using KSiCat and TMOS at pH 6.8 ±0.2. The TGA analysis shows that a significant amount of the amine is retained inside the silica and in the case of 6NC a large proportion of the 6NC is retained with in the silica. The use of a phosphate buffer in the TMOS system reduced the amount of organic material retained within the silica and in the case of 6NC the reduction was by *ca.* 61 %.

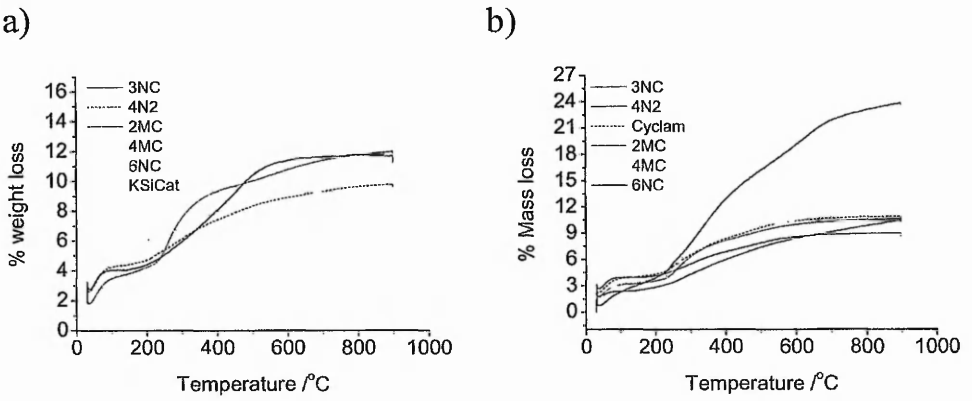

Precursor	KSiCat						
Additive	Blk	3NC	4N2	cyclam	2MC	4MC	6NC
% Mass loss 400 – 800 °C	1.42	3.66	2.31		2.58	1.98	5.47086
	TMOS NB						
		4.18	2.10	2.53	2.40	2.27	10.58

Precursor	TMOS PB						
Additive	Blk	3NC	4N2	cyclam	2MC	4MC	6NC
% Mass loss 400-800 °C	2.98	3.3	3.5	3.128	3.87	3.8	4.04

Figure 5.9.3 – Thermal gravimetric analysis of materials produced at pH 6.8 using a) KSiCat, b) TMOS no buffer.

The morphology of the silica produced was examined by SEM as shown in Figure 5.9.4, where it can be seen that the materials become more granular when the size of the azamacrocyclic ring was increased and the materials structure becomes more open probably because rate of aggregation is fast.

KSiCat

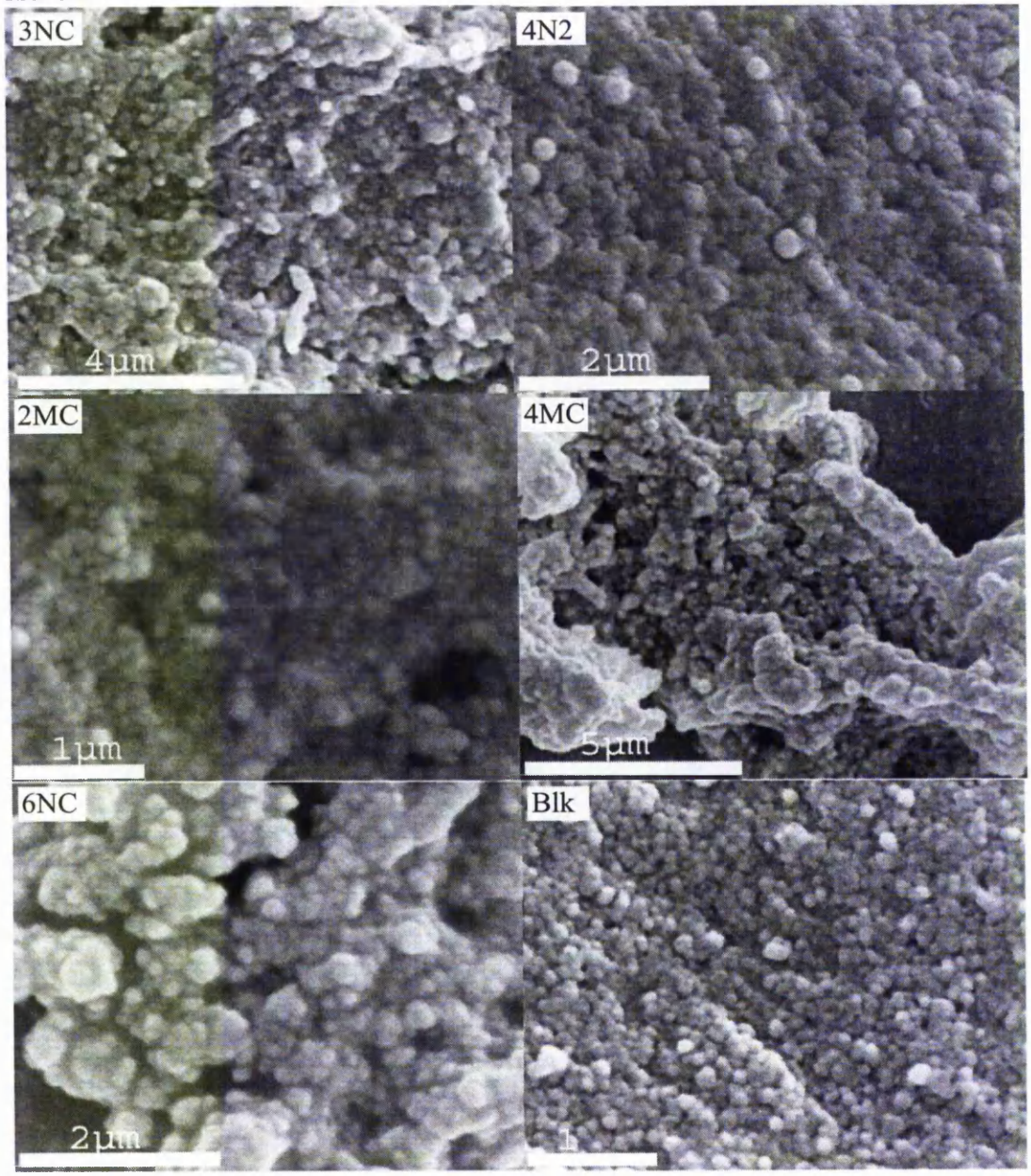

TMOS NB

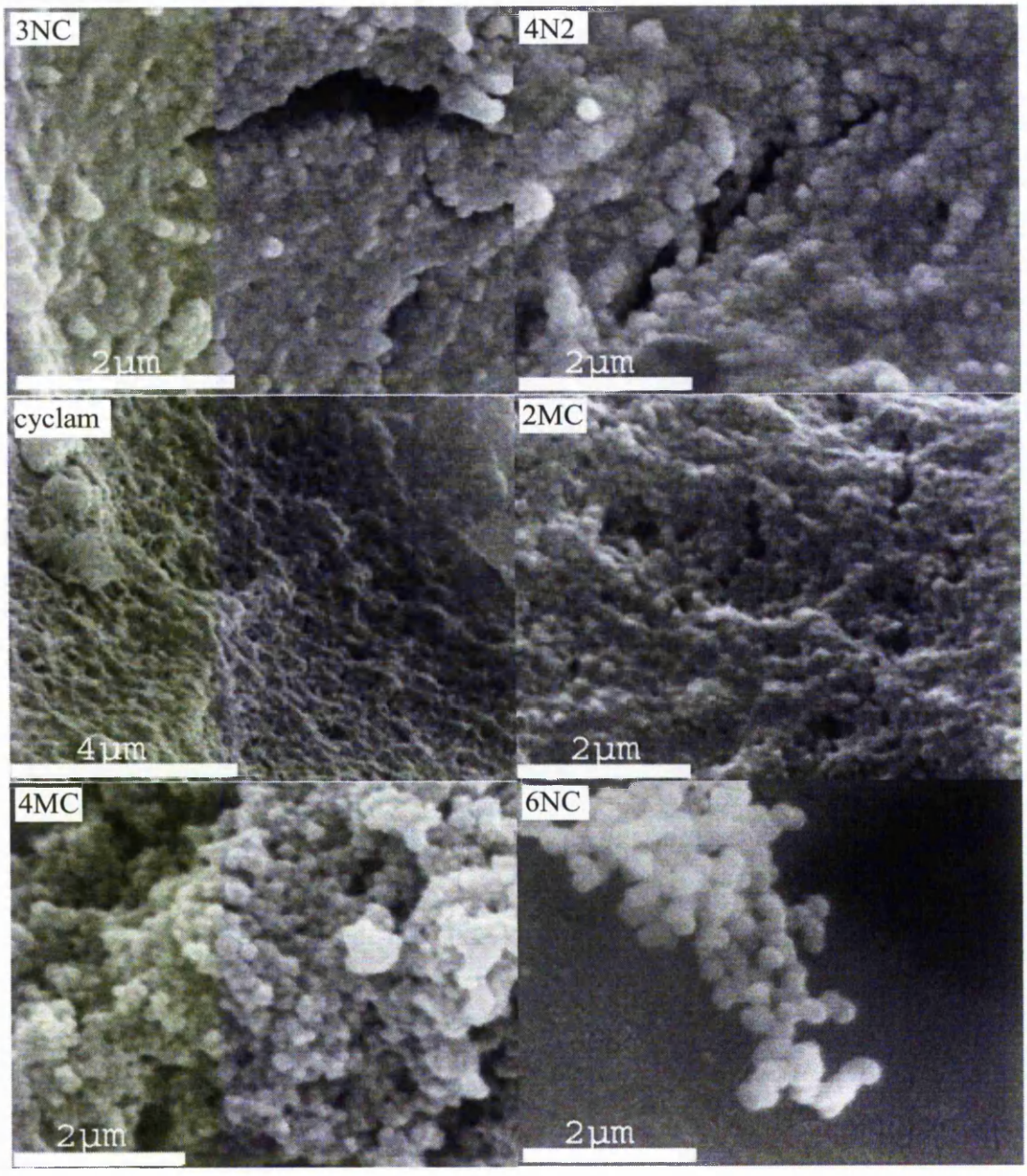

Figure 5.9.4 – SEM images of materials produced using the azamacrocyclic molecules at 10:1 Si:N ratio in KSiCat and TMOS NB system at pH 6.8 ±0.2.

Figure 5.9.5 shows the primary aggregate size measure using the SEM images. It can be seen that the primary aggregate remains relatively constant for the materials produced using KSiCat. The aggregate size for the materials produced using the unbuffered TMOS system initial reduced when increasing the ring size to 14 atoms. The primary aggregate size then remains statistically unchanged when cyclam, 2MC

and 4MC were investigated. The particle size observed using 6NC was *ca.* 307 nm which is contradictory to the results obtained by dynamic light scattering, where the particle size measure was *ca.* 1200 nm. This suggests that of species measured by dynamic light scattering were aggregates of spheres and could account for the large variation in particle sizes measured.

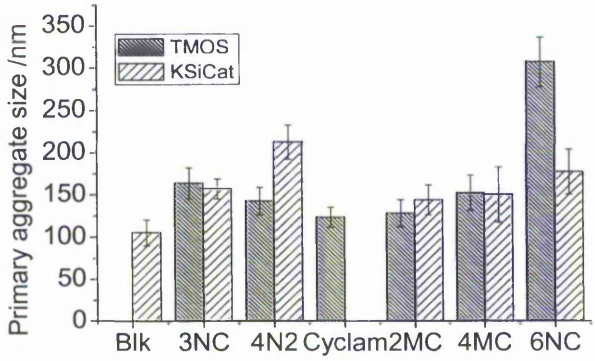

Figure 5.9.5 – Primary aggregate size of the materials produced using KSiCat and TMOS NB measured from SEM images.

5.10 The synthesis of momodispersed silica spheres using azamacrocyclic molecules.

The effect of pH on the morphology of the silica produced using the azamacrocyclic molecules was investigated using the unbuffered TMOS system to see if the stabilisation of silica particles was unique to 3NC, 4MC and 6NC. The results are shown in Figure 5.10.1 where it can be seen the stabilised particle size is dependent on the pH of the solution and the azamacrocyclic molecules used.

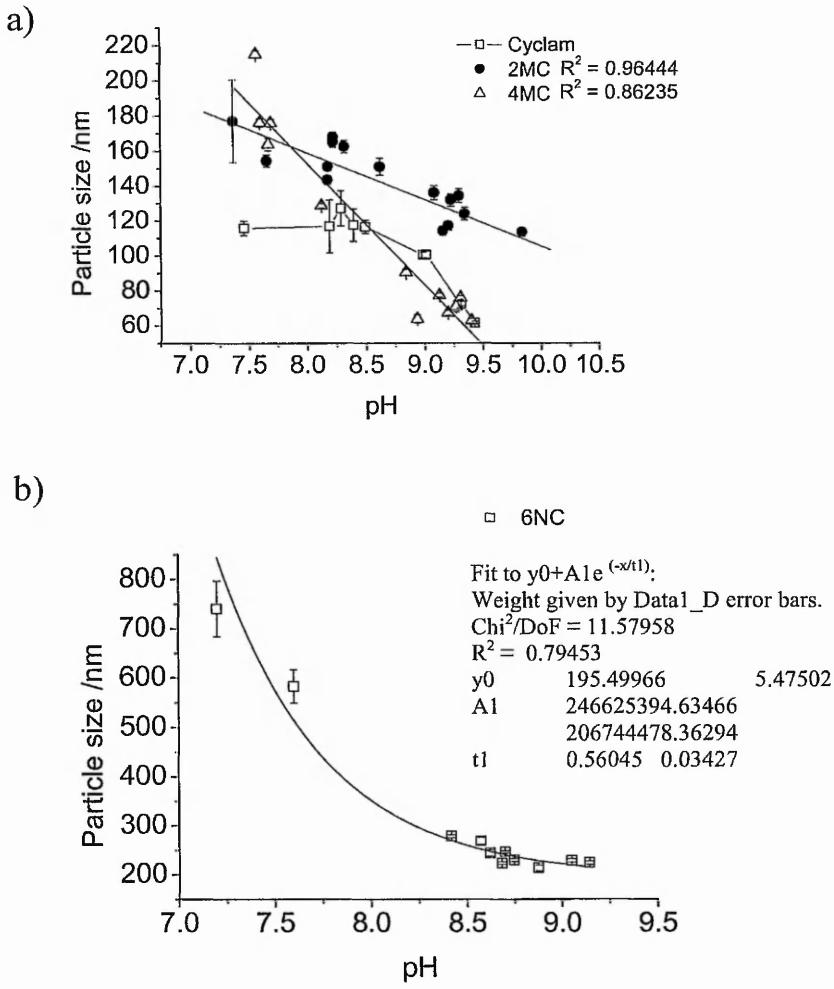

Figure 5.10.1 – The effect of pH on the formation of particles using the azamacrocyclic molecules in the unbuffered TMOS system, a) using cyclam, 2MC and 4MC and b) using 6NC. Error bars show one standard deviation from the mean particle size.

The particle sizes plotted are calculated using the z-average in contrast to that exhibited in Figure 5.9.1c) and only systems showing a single peak size distribution have been plotted. The z-average is indicates an average particle size, when a multi modal algorithm was fitted to the data a more detailed analysis of the particulate species in solution. This showed that the particles observed for 3NC and 4N2 were actually bimodal systems. The formation of the spheres in solution is thought to be templated through droplet formation. To date droplet formation has not been observed using the dynamic light scattering, it is hoped that freeze fracturing will allow droplet formation to be observed. Theoretically, the largest droplets are formed at low pH where the charge on the azamacrocyclic ring is high, intermolecular

repulsions are high; increasing the pH of the solution reduces the charge on the azamacrocyclic ring and therefore allows the molecules to pack more tightly in the droplet, which causing the droplet size to decrease, thus templating smaller spheres. Zeta potential measurements using 4MC in a 30 mM solution of TMOS where aggregation has been shown to occur at pH 6.8 shows the aggregating particle have a zeta potential of *ca.* -0.1. This was contrasted to the same solution at pH 8.453 where the particles have a zeta potential of *ca.* -1.5. The higher zeta potential at pH 8.453 suggests that when 2 particles collide the repulsive forces are significant enough in size to prevent aggregation and instead of a silica gel or network being formed a silica sol is favoured.

5.11 The effect of crown ethers on the formation of silica

Two crown ethers; 12-crown-4 (12C4) and 18-crown-6 (18C6) were investigated to compare the results obtained using nitrogen atoms to oxygen atoms in a macrocyclic ring. The kinetics of silica formation were studied using 30 mM unbuffered solutions of TMOS, the KSiCat system could have been used as the crown ethers did not form a complex to the KSiCat. The results are shown in Figure 5.11.1, where it can be seen that the increasing the crown ether ring size from 12 to 18 atoms decreases the 3rd order rate constant. The reduced 3rd order rate constant signifies a reduced rate of formation of trimers. Perry *et al.* suggest that hydroxyl groups do not have a role to play in the formation of silica.[43] Here, the presence of ether groups in a macrocyclic molecule clearly shows a significant reduction in the 3rd order rate constant, suggesting either stabilisation of orthosilicic acid or of the dimer (the molybdenum blue cannot distinguish between monomer and dimer). It can be hypothesise this to be due to the coordination of the silicon species in the cavity of the crown ether which reduces the availability of orthosilicic acid and reduces the 3rd order rate constant.

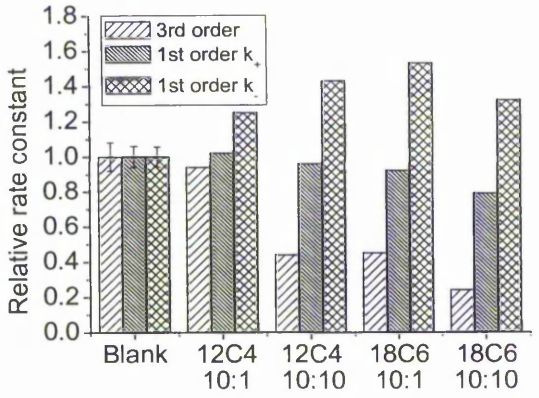

Figure 5.11.1 – Kinetics of silica formation for crown ethers 12C4 and 18C6 using an unbuffered TMOS system at two different Si:O concentration 10:1 and 10:10. Error bars are one % standard deviation from mean.

Dynamic light scattering of the crown ethers in an unbuffered TMOS system showed unsurprisingly no stable particle size at 24 h as with the unbuffered blank TMOS system possibly because the concentration of cationic species in solution is low. Dynamic light scattering results using KSiCat as a precursor to silica formation are shown in Figure 5.11.2.

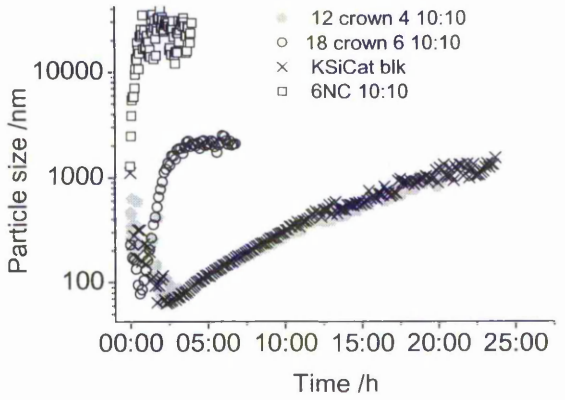

Figure 5.11.2 – Dynamic light scattering of 12C4 and 18C6 compared to 6NC.

Interestingly 12C6 does not deviate from the aggregation profile of the blank KSiCat system. Surprisingly 18C6 does effect the rate of aggregation significantly. The exact reason for this is unclear at this time, although it would seem likely that since no stable particle size is observed in the TMOS system that an interaction is occurring between one of the counter ions and the crown ethers, possibly K^+. The materials

were characterised by nitrogen gas adsorption/desorption, TGA and SEM. The results are summarised in Figure 5.11.3 which serve as an excellent comparison between the highly influential azamacrocyclic molecules and the benign crown ethers. Replacement of the nitrogen atoms with oxygen atoms in the crown ethers has been shown to drastically change the ability of the molecule to catalyse silica formation. It remains puzzling how 18C6 reduces the rate of trimer formation using an unbuffered solution of TMOS, but increases the rate of aggregation in the KSiCat system unless there is an unwanted interaction between a counter ion and 18C6, possibly through a host guest interaction.

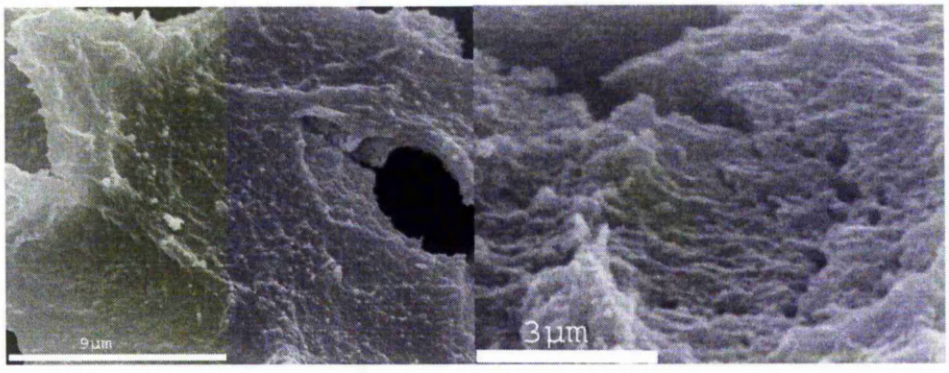

Figure 5.11.3 – SEM micrographs of the material produced using a) 12C4 and b) 18C6.

5.12 Summary

In this work we have investigated the role of azamacrocyclic molecules using two different precursors to a solution of orthosilicic acid. The first was from KSiCat known to form a solution of "pure" orthosilicic acid in the presence of catechol and KCl (90 mM and 60 mM respectively). The second precursor was TMOS, an alkoxysilane that requires a hydrolysis period of 15 mins prior to dilution for use in model silica studies. The dilution of TMOS to the desired concentration usually utilises a buffer (phosphate, acetate, citrate and Tris-HCl have been used in (biosilicification studies).[44] We have shown using ^{29}Si NMR that condensation occurs during the hydrolysis period and as such it is unlikely that TMOS is a precursor to a "pure" solution of silicic acid see Chapter 2.

We have shown through a systematic study of azamacrocyclic molecules where we have selectively used the different precursors to investigate, compare and understand

the interaction of azamacrocyclic molecule in the formation of silica. Furthermore, the interactions of a phosphate buffer in the TMOS system have been identified and through comparisons between KSiCat and TMOS the role of cationic counter ions in KSiCat has been identified. It has been shown that azamacrocyclic molecules having a ring size ≥ 14 of which four of the atoms are nitrogen atoms have a pronounced catalytic effect on the condensation of silicon species generated from a hydrolysed solution of TMOS. There appears to be an empirical relationship between the effective charge on a nitrogen atom in the ring and the rate of catalysis. When the number of atoms in the ring was incorporate into the calculation to include molecules with less than 14 atoms the relationship was no longer found to be true. This indicates that there is not a simple relationship between a molecules charge and catalytic activity observed experimentally. Instead it can be hypothesise that the number of carbons separating each nitrogen atom is also important when trying to establish a mathematical relationship between a molecules structure and the catalytic activity it possesses. The materials produced using the respective precursors were characterised, it was found that the properties of the materials can be changed by varying the speciation of the azamacrocyclic molecule. Three different speciation states were investigated; protonated, partially protonated and unprotonated. It was found that the porosity and pore size distribution of the materials changed. Interestingly, when TMOS was used in the presence of a 100 mM phosphate buffer the materials were found to be templated by the buffer in the case of 3NC and 4N2, and the surface area was found to significantly increase when compared to the blank material produced in the presence of phosphate buffer, possible indicating an interaction between the buffer and the azamacrocyclic molecule. Finally, the effect of the pH on the condensing TMOS system was investigated where it was found that monodispersed solutions of spherical particles could be stabilised. It has been suggested that the mechanism for sphere formation was related to the formation of amine droplets in solution which template sphere formation. It has been shown that the spherical particles where stabilised due to surface charge neutralisation where it was found that particles that aggregated at pH 6.8 have a zeta potential of -0.1 ±0.2 and particles that showed no aggregation at pH 8.45 have a zeta potential of -1.5.

5.13 Conclusion

In this section of work it has been shown that the complexation of SiCat by cyclam 4MEDAE is a powerful tool for forming crystalline inorganic-organic hybrid materials with a specific morphology, which once heated to 900 °C form amorphous silica with limited preservation of the original materials structure. It has been shown that the homogeneity of the precipitated tetragonal prism using cyclam is dependent on the method utilised to prepare the tetragonal prisms. Titration of the cyclam solution to the pH to a specific pH (and therefore a specific composition of molecular species) improves the homogeneity of the tetragonal prisms precipitated. The size of the tetragonal prisms was not significantly effected by changes in pH between 6.8 and 9. The tetragonal prism prepared at pH 9.5 where the KSiCat is not hydrolysing by adding acid was found to be significantly smaller. The increase in KSiCat concentration is thought to aid faster tetragonal prism formation causing a reduction in tetragonal prism size. The size of the tetragonal prisms reduced further in size at pH 10 which corresponds to a maximum concentration of $[cyclam]^+$, which indicated the formation of the tetragonal prisms might be through a two step mechanism involving the $[cyclam]^+$ species.

It has also been shown that this displacement reaction is not limited to dipotassium tris(1,2-benzenediolato-*O,O'*)silicate and tetragonal prisms utilising cyclam and dipotassium tris(1,2-benzenediolato-*O,O'*)germanate have been formed. Therefore we hypothesise that a range of other similar inorganic precursors such as iron could be used to generate a large array of inorganic materials with interesting morphologies.

There still remains a great deal of characterisation work to be carried out especially when using tertiary amines to precipitate SiCat. However, it was important to establish that the complexation of SiCat by cyclam was not a unique phenomenon and that this work does represent a new way of forming amorphous silica with controlled morphology using an organic template in an aqueous environment at 25 °C. The assembly of the organic template into tubular (in the case of cyclam and 4MEDAE) and plate-like structures (in the case of 4MEDAB) is not understood to date and work will continue to solve this problem. Furthermore work will continue to obtain the crystal structure of the materials precipitated using the tertiary amines. The key to

finding more amines that complex SiCat and other inorganic precursors to yield specific morphologies will be to understand the molecular interactions that enable a tertiary amine and cyclam to form a stable hydrogen bond with the catechol moiety in SiCat.

References

1. L. F. Lindoy, *The Chemistry of Macrocyclic Ligand Complexes*, Cambridge University Press, Cambridge, 1989.
2. P. D. Beer, *Acc. Chem. Res.*, 1998, **31**, 71-80.
3. H. Elias, *Coord. Chem. Rev.*, 1999, **187**, 37-73.
4. P. D. Beer, *Chem. Soc. Rev.*, 1989, **18**, 409-450.
5. S. G. Kang and S. J. Kim, *Bull. Korean Chem. Soc.*, 2003, **24**, 269-273.
6. I. Lukes, J. Kotek, P. Vojtisek and P. Hermann, *Coord. Chem. Rev.*, 2001, **216**, 287-312.
7. S. Aime, M. Botta, M. Fasano and E. Terreno, *Chem. Soc. Rev.*, 1998, **27**, 19-29.
8. D. S. Wragg, G. B. Hix and R. E. Morris, *J. Am. Chem. Soc.*, 1998, **120**, 6822-6823.
9. T. Wessels, L. B. McCusker, C. Baerlocher, P. Reinert and J. Patarin, *Microporous Mesoporous Mater.*, 1998, **23**, 67-77.
10. P. S. Wheatley and R. E. Morris, *J. Solid State Chem.*, 2002, **167**, 267-273.
11. V. Patinec, P. A. Wright, P. Lightfoot, R. A. Aitken and P. A. Cox, *J. Chem. Soc.Dalton Trans.*, 1999, 3909-3911.
12. D. S. Wragg, A. M. Z. Slawin and R. E. Morris, *J. Mater. Chem.*, 2001, **11**, 1850-1857.
13. P. A. Wright, M. J. Maple, A. M. Z. Slawin, V. Patinec, R. A. Aitken, S. Welsh and P. A. Cox, *J. Chem. Soc. Dalton Trans.*, 2000, **8**, 1243-1248.
14. M. J. Maple, E. F. Philp, A. M. Z. Slawin, P. Lightfoot, P. A. Cox and P. A. Wright, *J. Mater. Chem.*, 2001, **11**, 98-104.
15. F. Serpaggi, T. Loiseau, F. Taulelle and G. Ferey, *Microporous Mesoporous Mater.*, 1998, **20**, 197-206.
16. S. Mann and G. A. Ozin, *Nature*, 1996, **382**, 313-318.
17. M. Sumper and N. Kröger, *J. Mater. Chem.*, 2004, **14**, 2059-2065.
18. C. C. Perry and T. Keeling-Tucker, *Colloid Polym Sci*, 2003, **281**, 652-664.
19. S. Lorenz. N. Kröger, E. Brunner, M. Sumper, *Science*, 2002, **298**, 584-586.
20. N. Kröger, R. Deutzmann and M. Sumper, *Science*, 1999, **286**, 1129-1132.
21. M. R. Knecht and D. W. Wright, *Chem.Commun.*, 2003, 3038-3039.
22. M. Sumper and G. Lehmann, *Chembiochem*, 2006, **7**, 1419-1427.
23. S. V. Patwardhan, S. J. Clarson and C. C. Perry, *Chem. Commun.* 2005, 1113-1121.
24. P. J. Lopez, C. Gautier, J. Livage and T. Coradin, *Current Nanoscience*, 2005, **1**, 73-83.
25. D. Belton, G. Paine, S. V. Patwardhan and C. C. Perry, *J. Mater. Chem.*, 2004, **14**, 2231-2241.
26. D. Belton, S. V. Patwardhan and C. C. Perry, *Chem. Commun.*, 2005, 3475-3477.
27. D. J. P. Belton, Siddharth V.; Perry, Carole C., *J. Mater. Chem.*, 2005, **15**, 4629-4638.
28. V. V. Annenkov, S. V. Patwardhan, D. Belton, E. N. Danilovtseva and C. C. Perry, *Chem. Commun.*, 2006, 1521-1523.
29. S. V. Patwardhan and S. J. Clarson, *Silicon Chem.*, 2002, **1**, 207-214.
30. S. V. Patwardhan, N. Mukherjee and S. J. Clarson, *J. Inorg. Organomet. Polym.*, 2001, **11**, 117-121.
31. M. Sumper and E. Brunner, *Adv. Func. Mater.*, 2006, **16**, 17-26.
32. K. Lutz, C. Groger, M. Sumper and E. Brunner, *PCCP*, 2005, **7**, 2812-2815.

33. S. V. Patwardhan, N. Mukherjee, M. Steinitz-Kannan and S. J. Clarson, *Chem. Commun.*, 2003, 1122-1123.
34. S. V. Patwardhan, R. Maheshwari, N. Mukherjee, K. L. Kiick and S. J. Clarson, *Biomacromolecules*, 2006, **7**, 491-497.
35. J. J. Yuan, P. X. Zhu, N. Fukazawa and R. H. Jin, *Adv. Func. Mater.*, 2006, **16**, 2205-2212.
36. C. Gautier, P. J. Lopez, M. Hemadi, J. Livage and T. Coradin, *Langmuir*, 2006, **22**, 9092-9095.
37. J. J. E. Moreau, L. Vellutini, M. W. C. Man and C. Bied, *Chem. Eur. J.*, 2003, **9**, 1594-1599.
38. S.W. Karickhoff, L.A. Carreira and S. H. Hilal., *SPARC Preforms Automated Reasoning in Chemistry*, 3.01 edn., University of Georgia
39. S. Brunauer, P. H. Emmett and E. Teller, *J. Am. Chem. Soc.*, 1938, **60**, 309-319.
40. E. P. Barrett, L. G. Joyner and P. P. Halenda, *J. Am. Chem. Soc.*, 1951, **73**, 373-380.
41. D. Belton, The influence of small molecules on the precipitation of silica, Nottingham Trent University, 2005.
42. R. D. Hancock, R. J. Motekaitis, J. Mashishi, I. Cukrowski, J. H. Reibenspies and A. E. Martell, *J.Chem. Soc. Perkin Trans. 2*, 1996, 1925-1929.
43. G. E. Tilburey, S. V. Patwardhan, J. Huang, D. L. Kaplan, C. C. Perry, *J. Phys. Chem. B*, 2007, **111**, 4630-4638.
44. S. V. Patwardhan, C. Raab, N. Hüsing and S. J. Clarson, *Silicon Chem.*, 2003, 279-285.

Chapter 6 – Conclusions and Further work

6.1 Conclusions

In this thesis the intermolecular interactions that occur in the formation and dissolution of silica (that can be related to the bio-geochemical silicon cycle as shown in Chapter 1 Figure 1.1) have been investigated. In particular inspiration has been taken from biological organisms such as diatoms, sponges and plants in which silica is accumulated, stored and deposited in genetically controlled manor.[1, 2] Moreover, some of the hypotheses that have been made in the literature[3, 4] have been challenged by performing *in vitro* studies. The intermolecular interactions that were thought to govern the formation of intricately nano-patterned silica found in the diatom frustule were probed. Furthermore, new methods to investigate the formation of silica *in vitro* have been developed. Through these methods, a new class of additives has been investigated where novel silica based structures and mono dispersed spheres have been prepared.

Investigations into bioinspired and biomimetic silica *in vitro* have been dominated by studies involving tetramethoxysilane (TMOS) where additives have been inserted into a supersaturated solution containing silicic acid, and in most cases, authors investigate how the additive has controlled the structure of the silica formed. In this thesis some studies have been carried out the same way. However, the silicon species that additives interact with and the type of intermolecular interactions that govern the structure of the silica formed have also been investigated. In order to probe intermolecular interaction one must firstly completely understand the model silicifying system to be employed. The model system that is primarily employed in Professor Perry's lab utilises dipotassium tris(1,2-benzene-diolato-*O, O'*)silicate (KSiCat) which liberates a supersaturated solution of orthosilicic acid upon dissociation of the complex.[5] The overwhelming property for selection of this compound over any other silica precursor is the liberation of a "pure" solution of orthosilicic acid. Firstly, this gives confidence that the silica structures observed are

as a result of additive interactions with orthosilicic acid or a silicon species derived from orthosilicic acid. Secondly, orthosilicic acid is the aqueous soluble form of silicon found in nature and as such it would seem logical that biological organisms utilise this silicic acid or a silicon species derived from orthosilicic acid.[6] The disadvantage of this system as with all precursors to silica is the byproducts, in this case 3 molar equivalents of catechol and 2 molar equivalents of KCl. Previously, it was assumed that these by products have little effect outside their well documented roles in silica formation; catechol is known to aid the solubility of silicon[6-8] and potassium ion as with all cations acts as flocculating agent and direct silica formation towards gels as apposed to silica sols that are formed in the absence of salts.[6] In this thesis a procedure was established that allowed TMOS to be used as a precursor for silica formation where the function of the salts in the system (4.65 μM) was solely to adjust the pH of the system to 6.8 ±0.2. The kinetics of silica formation was monitored using the molybdenum blue assay, which showed a distinct difference in k_{3rd} which describes the rate at which trimers are formed. Using ^{29}Si it was possible to show that this increase in k_{3rd} was likely to be due to the presence of Q^1 species generated during the hydrolysis period when using TMOS. It was also suggested that the rapid equilibration of pH from an initial basic pH in the TMOS system may also partially account for the increase in k_{3rd} when compared to the KSiCat system. These results validated the primary concern with the TMOS system; there is not a single silicon species in solution after the hydrolysis period. The TMOS system did allow the role of catechol and KCl in silica formation to be investigated. As reported earlier in the literature, KCl was found to act as a flocculating agent and catechol also appeared to aid aggregation to some extent although this effect was insignificant when compared to KCl. When KCl and catechol were mixed together in the same molar ratio as present in the KSiCat system the aggregating characteristics were found to be faster in the TMOS system, perhaps indicating that the aggregation profile is influenced by the starting molecular species. In the unbuffered TMOS system no measurable particle size was observed in days. The effect of sodium phosphate buffer which is commonly used to buffer TMOS experiments was investigated.[9] This provided excellent evidence that even at a concentration of 100 mM the porosity of the silica was templated, as yet it is unclear whether this is due to the role of the sodium or the phosphate ions. Investigation into the role of buffers in silica formation

is crucial in determining the true role of an additive in silica formation. It is my opinion that the role of additives in silica formation cannot be fully understood until a complete understanding has been gained of the model system used to study the additives effect on silica formation. The development of the TMOS system in which silica is formed in the presence of a negligible amount of salt will allow scientists to develop new *in vitro* methods for silica formation where the interactions between a buffer and the forming siliceous phase can be minimised. Alternatively it is possible to conduct experiments involving TMOS in the absence of a buffer. This system will therefore facilitate investigation into the role of additives in silica formation where the role of counter ions is almost completely excluded.

The role of bioinspired and biomimetic additives in silica formation has been studied now for a significant period of time. Mechanisms have been proposed for the role of cationicially charged amine containing molecules where electrostatic interactions have been hypothesised to explain many of the effects observed *in vitro* from increases in rates of aggregation to catalysis of the condensation reaction.[10, 11] The effect of bioinspired and biomimetic additives on unsaturated solutions of orthosilicic acid was studied, which can be likened to the conditions found in the Earths aquatic reservoirs. A range of the most "active" bioinspired and biomimetic molecules studied in supersaturated solutions containing orthosilicic acid were investigated. None of the additives were found to induced condensation or aggregation of 1 mM solutions of orthosilicic acid generated from KSiCat. This was not especially surprising as electrostatic interactions have been proposed to cause the increases in the rate of condensation and aggregation and since orthosilicic acid has a pk_a of 9.8 at pH 6.8 it is almost completely uncharged. These results indicate that diatoms are unlikely to utilise orthosilicic acid as the precursor to frustule formation and instead as hypothesised by several researchers diatoms accumulate silicon in an as yet unknown form prior to cell division.[12] This hypothesis inspired investigations into the silicon species bioinspired and biomimetic additives act upon. Studies were preformed using precondensed solutions of orthosilicic acid which were then diluted to give globally unsaturated solutions of silicon. This enabled the study of a range of different silicon species at unsaturated concentrations which were all found to; firstly, dissolve back to a 1 mM solution of molybdenum blue active species (monomeric or dimeric silicon species) and secondly, the initial rate of dissolution was found to vary

in a non systematic manner which was hypothesised to be because of the introduction of charge onto the silicon species. In the presence of bioinspired and biomimetic additives at Si:N ratios of 1:6 it was found that only the bioinspired small molecules promoted the aggregation of silica particles with resulted in precipiatation. Even after the precipitation of silica, dissolution still occurred to give 1mM solutions of molybdenum blue active species. Bioinspired polyelectrolytes increased the initial rate of dissolution when compared to the blank for samples allowed to precondense for 60 mins prior to dilution. Further evidence was provided for the mechanism of catalysis proposed by Belton *et al.* between a silica surface and a molecule of orthosilicic acid by showing that the surface area of the precipitated silica varies in accordance with the expected activity of the additive, (*i.e.* TEPA > PEHA >N5 when comparing the surface area exhibited). PEHA was found to precipitate silica from solutions precondensed for ≥7 mins which coincided with the least stable silicon species when compared to the blank. This new way of studying bioinspired and biomimetic additives has revealed a substantial insight into the mechanism by which small molecules and polyelectrolytes aggregate and catalyse the formation of silica in supersaturated solutions of orthosilicic acid. It would appear that polyelectrolytes adopt a completely different orientation on the surface of a silica particle than small molecules, otherwise, one would expect to observed aggregation in the presence of polyelectrolytes in unsaturated solution of silica particles. It was hypothesised that the mechanism for particle aggregation using polyelectrolytes in supersaturated solutions containing orthosilicic acid may not be simply due to electrostatic interactions. What seemed to be an obvious mechanism for silica aggregation maybe over simplified.

The role of additives in silica formation dominates the second half of the thesis where the role of hydroxyl groups in silica formation was investigated. It is commonly believed that hydrogen bonding and the formation of Si-O-C bonds may play a role in the observed nano-patterned silica exhibited by diatoms in the form of their cell wall. The literature was reviewed in Chapter 4, principally it was Hecky *et al.* that proposed carbohydrate molcules might serve as a template for the formation of biosilica.[3] Lobel *et al.* suggested that this process was in fact energetically favourable on polyserine exhibiting a β-sheet conformation,[13, 14] but what, if any effect would hydrogen bonding have on the formation of silica *in vitro*? We investigated a number of

molecules that would enable the formation of Si-O-C bonds and the role hydrogen bonding to be investigated. Sericin a protein extracted from the cocoon of the silkworm *Bombyx mori* was studied because a large percentage of amino acids residues in the protein contained a hydroxyl group. Polyserine was also studied and alkanediols of carbon chain length 2-7 were also studied to investigate the role of hydroxyl containing additives on silica formation. Kinetic studies were undertaken where the effect of all of these molecules was not significantly different from the blank at a Si:OH ratio of 1:1. One intriguing result was the formation of structures in the native sericin and sericin precursor which then broke down as silica was formed. A similar effect was observed when the alkanediols were used at a Si:OH ratio of 1:4, these structures were also observed to form in the absence of silica. A trend of increasing k_{3rd} was observed when the alkanediols were studied at an Si:OH ratio of 1:4 with respect to the early stages of silica formation. This effect was proposed to be because of the hydrophobic effect as proposed by Belton *et al.*[10] In conclusion no evidence was found for the formation of Si-O-C bonds, and hydrogen bonding was also proposed to have no significant effect for additives that contain hydroxyl groups. The strongest hydrogen bonds known are those between two water molecules and if any effect were to be observed it would seem more likely that it would occur between water and a silicon species due to the large excess of water. It is important to note here that these are based on *in vitro* studies and not in biological organisms such as diatoms, where one might expect an effect if water were not the dominant species capable of hydrogen bonding. Furthermore, largely unexplored areas such as compartmentalisation may also have a significant effect.

Finally, in this thesis the role of amine architecture on the formation of silica *in vitro* was studied. In Chapter 5 the effect of azamacrocyclic molecules and tertiary amines on the formation of silica was investigated. Surprisingly a completely new area of silicon chemistry was discovered, crystalline inorganic-organic hybrid materials were formed where cyclam replaces the potassium ions in the KSiCat silica precursor to form needle-like tetragonal prisms. Single crystal X-ray diffraction showed that the structure of the tetragonal prisms can be likened to a layered structure, where when view along the a-axis a cyclam molecule can be visualised as being sandwiched between layers of SiCat molecules. The structure is formed by 2 hydrogen bonds between protonated amine groups in positions 4 and 11 on the cyclam molecule a

water, and the lone pairs of electrons on a 1, 2-benzenediolato *O,O'* silicate oxygen atom, where each cyclam molecule bridges two SiCat molecules in a 1:1 molecular ratio. This phenomena was shown to be specific to cyclam with regard to azamacrocyclic molecules, probably because derivatives of the cyclam structure (2MC and 4MC) are sterically strained such that the same conformation cannot be adopted. The bulky methyl groups are hypothesised to interact with the 1, 2-benzenediolato *O,O'* groups making complexation less energetically favourable. Changing the ring size will result in bond distances either too small or to large for hydrogen bonding to occur. Investigations into the pH range over which these structures could be formed showed that the formation of these tubes was solely dependent on the presence of $[cyclam]^+$ molecules and le Chatelier's principle was hypothesised to play an important role in the formation of more $[cyclam]^+$ to maintain the speciation equilibria. Tetragonal prism formation was not observed at pH values <6 because the stoichiometric excess of acid allowed rapid dissociation of the KSiCat complex which is vital for tetragonal prism formation. The size of the tetragonal prisms reduced significantly at pH 9.6, and still further at pH 10 size, which suggested a two step mechanism for the tetragonal prism formation. At pH 11 the tetragonal prisms became larger and finally at pH 12 the tetragonal prisms were heterogenous in size. It was found that the organic component of the tetragonal prism could be removed thermally which resulted in a size reduction but with retention overall tetragonal morphology. Similar structures were also formed in the presence of KGeCat. These results suggest that the formation of tetragonal prisms is independent of the inorganic atom and as such we hypothesise that where a tris (1, 2-benzenediolato *O,O'*) complex can be formed between an inorganic element we hypothesise tetragonal prisms can be formed. A similar phenomena also occurred when tertiary amines such as *N,N,N',N'*-tetramethylethylenediamine (4MEDAE) which precipitated crystalline hexagonal needle like prisms in the presence of SiCat and investigations into carbon chain length resulted in the formation of hexagonal plates when 4MEDAB was used and large structures with no specific morphology when 4MEDAH was used. These structures are yet to be fully characterised although changes in pH dramatically alter the structure and composition of the material precipitated. At low pH the formation of silica is favoured and at higher pH where KSiCat remains undissociated complexation is favoured. Removal of the organic template resulted in remarkable structural retention whilst amazingly there seemed to

be some retention of the organic component even after prolonged thermal treatment. It is believed that these structures form in a similar manner to cyclam where hydrogen bonds bridge between SiCat molecules, however it has not been possible to obtain any single crystal X-ray diffraction to confirm this.

The formation of inorganic-organic hybrid materials using tris (1,2-benzenediolato *O,O'*) inorganic complexes and cyclam and some tertiary amines shows remarkable control over structural morphology in an incredibly short synthesis time. This although interesting, has very little in common with controlling the formation of silica by understanding the intermolecular interactions. The synthesis of silica and other inorganic materials via this route is analogous to zeolite synthesis where an organic material acts as a template for the forming inorganic phase. The organic template is then removed through thermal degradation. However in the case of the tetragonal prisms formed using cyclam the inorganic content of the tetragonal prism is so low that removal of the organic phase causes a reduction in tetragonal prism size and some loss of structural homogeneity. The challenge that faces us now is to understand why the formation of an inorganic-organic hybrid material is so energetically favourable and furthermore, how these molecules stack to form such ornate structures.

The role of azamacrocyclic molecules and crown ethers was investigated in the formation of silica using KSiCat system and the TMOS derived in Chapter 2 Part II. The investigation included a kinetic study of the molecules at a Si:N ratio of 10:1, which showed a dramatic increase in k_{3rd} despite the incredible low ratio of Si:N. An empirical relationship was identified between the effective charge on a nitrogen atom situated in an azamacrocyclic ring with $\geq$ 14 atoms and the relative third order rate constant. Interestingly, smaller rings had a higher effective charge on a nitrogen atom but showed no enhancement of the k_{3rd}, which can be a likened to the results obtained in Chapter 2 Part II where the presence of KCl did not increase the k_{3rd}. This suggests that the mechanism proposed by Belton *et al.* where charge is accumulated on alternate nitrogen atoms is crucial to enhance the 3rd order rate constant, k_{3rd}.[11] The rate of aggregation in the KSiCat system and the TMOS system were comparable at pH 6.8 except in the case of 3NC where a stable particle size in the TMOS system was observed. Particle stabilisation was also observed in the other azamacrocyclic

molecules by increasing the pH. It has been shown for 4MC that increasing the pH increases the zeta potential which suggested cause the stabilisation of particles rather than gel formation. The materials from the KSiCat system and the TMOS system were characterised, it was shown that the porosity of the materials produced using KSiCat could be changed by altering the pH and thus the speciation in which the azamacrocyclic was added in. This chapter will play a large role in the further work section discussed next as much of the work associated with the azamacrocyclic molecules remains incomplete owing primarily to time constraints.

6.2 Further work

The opportunities for further work throughout this project are diverse due to the new techniques that have been developed to study the interaction of additives in a supersaturated unbuffered TMOS system and the use of the unsaturated system to study the interactions of an additive with different silicon species. The furtherwork section can be divided into:

- Studies that can be preformed relating to the data presented in this thesis.
- Studies that be carried out in the context of the field of biomimetic and bioinspired silica formation.

6.2.1 Further work related to the data presented in this thesis.

After an investigation has been carried out there are always opportunities for further work. In Chapter 3, a new method was presented for the study of the interactions of a particular additive with different silicon species. It has been shown that the stability and therefore type of silicon species present after different precondensation times varies. This was done by comparing the relative stabilities of each species by monitoring the rate of dissolution with respect to time. The initial rate of dissolution was calculated which was used to compare the stability of different silicon species. Truesdale *et al.* have proposed a different type of analysis which we are currently investigating with respect to our results.[15] This is not to say that either method is correct or incorrect as long as the scientific principles behind the analysis are correct either method of interpretation is equally valid.

The most obvious further work here is to find out what silicon species are present with respect to the precondensation time. This in principle could be carried out using mass spectrometry using an application called electrospray. However there are problems with first stabilising the system whilst maintaining the native silicon composition and ensuring that the silicon species composition remains unaffected by the elctrospray technique. Electrospray involves the removal of the solvent prior to entry into the mass spectrometer which might induce condensation. The technicalities involved in employing this technique mean that it will probably take a considerable amount of time to establish a reliable protocol. An alternative approach might be to

dilute the system in such a way as to effectively remove the water from the system. This would effectively quench the dissolution reaction, but one must be careful not to alter the silicon species whilst carrying out this procedure.

The unsaturated model system was used to study the silicon species that PEHA interacts with to form silica. Precipitation was found to coincide with the least stable or most reactive silicon species, which was hypothesised to be due to the introduction of charge to a silicon species. Our hypothesis could be investigated using zeta potential measurements, if the concentration of charged silicon species could be distinguished from the salts present in the solution which will also effect the solutions conductivity and ultimately the zeta potential of the system. Furthermore, it might then be possible to investigate how the zeta potential changes as the precipitate forms through the coordination of PEHA to the charged silicon species and from there to precipitation. The unsaturated system of course can be used to identify the silicon species that other additives act upon. Potentially the silicon species that polyelectrolytes interact with could be investigated by investigating the increase in the rate of dissolution at different precondensation times. It was surprising to find that polyelectrolytes increase the rate of dissolution in unsaturated silicon systems and this caused many problems in identifying the mechanism through which this occurs, and even now the scale of the molecular interactions are not fully understood. One fact is certain in that polyelectrolytes interact with silicon species in which the conformation of the polyelectrolyte must be such that a positive charge does not extend past the particle double layer. If this were not true then one would have expected to observe aggregation as has been seen in supersaturtaed systems and unsaturated systems using PEHA. This suggests that there is there is a change in molecular orientation in the unsaturated system or the positive charge of the polyelectrolyte is such that aggregation becomes unfavourable due to electrostatic repulsions between particles and dissolution is increased by the polyelectrolyte being associated with the silicon species. One thing that must remain in mind here is that the concentration studied was Si:N ratio of 1:6 which on a molecular scale equates to a small proportion of silicon species being associated with an individual polyelectrolyte molecule. More in depth calculations require knowledge of exactly how many silicon atoms are associated with a silicon species. Concentration studies with respect to an additive would also be interesting to study. This was investigated over a small range for

PEHA but it was found to have very little effect (data not presented). Changing the concentration of an additive could change its conformation on a surface as has been reported for proteins[16] which will undoubtedly change the additives effect on silica formation and dissolution.

The role of hydroxyl groups in silica formation was investigated where the effect of hydroxyl containing molecules on the formation of silica was investigated. An alternative approach could have employed, where these molecules could have been studied in a theoretical molecular interactions that could occur. The conclusion reached was that hydroxyl functionalised molecules do not play a significant role in silica formation. For this conclusion to be applied to biological organisms there are many other factors that we have not been considered to date. For instance, biological organisms have compartments in which silicon deposition occurs (SDV). In the SDV, scientist believe there maybe molecules containing hydroxyl groups. However, there undoubtably will be a "cocktail" of ions, glycoproteins, vesicles, membranes and many more factors that interact constructively to produce a molecular machine that produces the ornate biosilica exhibited by diatoms. In this environment perhaps hydroxyl containing molecules do have a role to play. To date these conditions have not yet been recreated in the laboratory, and as such it is simple wrong to conclude from the data presented, that hydroxyl containing molecules do not play a role *in vivo*. The most obvious further work which could be preformed would be to study monosaccharides and carbohydrates all of which contain hydroxyl groups and are present in biological organisms in the form of glycoproteins and in, or on membranes. With a view to compartmentalisation with respect to hydroxyl containing molecules, this is more difficult to study and understand. Simple studies have been conducted where changing the reaction vessel diameter has been shown to alter a materials morphology.[17] Some studies have recently been carried out with in more benign conditions where the pore structure of an onion and a polycarbonate membrane have been used to form silica.[18, 19] These results show that nano-confinement does have a role to play in silica formation *in vitro* which means almost certainly it will have a role *in vivo* too. Studying nano-confinement in a controlled manner for example by functionalising a nano-confined surface and identifying the intermolecular and interfacial interaction is by no means easy.

Finally in this section further work related to this thesis Chapter 5 will be considered, where azamacrocyclic molecules and tertiary amines have been used in the formation of inorganic-organic hybrid materials. We have shown that cyclam is present as $[cyclam]^{2+}$ in the tetragonal prisms and hypothesised that the mechanism for formation might initially be due to the $[cyclam]^{+}$ species. This mechanism is only supported by a size change of the tetragonal prisms at pH 9.6 and 10 and so there remains a lot of work to be carried out to prove this hypothesis. The mechanismn of formation could be investigated using ^{15}N doped cyclam and NMR to identify the coordination of nitrogen to the 1, 2-benzenediolato-*O,O'* moiety. The biggest problem will be the sensitivity of the technique and the transfer from solution to solid state and of course the reaction will need to be conducted under reduced temperature to slow the reaction down, which will be limited by the freezing point of water. Furthermore to confirm the hypothesis that: "any inorganic precursor involving the tris(1, 2-benzenediolato-*O,O'*) could be used to form tetragonal prisms" one must confirm the same or similar interactions are occurring using KGeCat. This will involve the synthesis of large crystals for single crystal x-ray diffraction studies. Following that, different inorganic precursors using tris(1, 2-benzenediolato-*O,O'*) could be synthesised and the formation of tetragonal prisms using these precursors could be investigated. Regarding the synthesis of tetragonal prisms, it would be extremely useful to synthesise or attach the tetragonal prisms to a surface in patterns. This might provide enough stability to control the reduction in size during thermal decomposition to form patterned arrays of silica columns. Furthermore, metal ions could be incorporated into the tetragonal prism structure, which once attached or synthesised on a surface may permit the formation of silica coated "nano-wires".

Tertiary amines have also been used to form similar structures as those templated by cyclam. However due to time constraints we have been unable to investigate these structures fully. Full charcaterisation should be carried out on these structures. The crystal structure of the hexagonal prisms and plates should be investigated. From our studies it has been shown that SiCat remains intact and that the tertiary amine is present as shown by FTIR. Amazingly, these structures retain their morphology better than the tetragonal prisms created using cyclam and some organic material seems to remain in the structure even after heating to 900 °C for 2 hours. How this is possible is, at this stage, extremely surprising. It has also been shown that these

molecules can be used to precipitate silica spheres of different sizes. Full characterisation should be carried out on the silica spheres produced including gas adsorption, FTIR and perhaps solid state NMR depending on presence or exclusion of azamacrocyclic molecules after synthesis. The unbuffered TMOS system can be used to investigate these structures in greater detail. For each of the molecules that form an inorganic-organic hybrid material we can conduct a similar study to that performed using cyclam and no doubt further studies will become clear once the initial results have been obtained. One interesting possibility to investigate would be to increase the amount of inorganic material associated with the structure. Perhaps the tetragonal prisms could act as a template for silica formation. The hybrid material could then be removed by acid addition which has been shown to dissolve the hybrid structures, leaving the deposited silica intact.

Mono-dispersed solution of different sized silica spheres were also precipitated using the azamacrocyclic molecules, time did not allow full characterisation of these structures. It has been hypothesised that the formation of silica spheres is through the formation of droplets. The molecular characteristic that allows an additive to form droplets and template silica spheres should be investigated. Several interesting observations have been made where the amount of organic material entrained in the silica spheres formed at pH 6.8 using 6NC was significantly higher than for the rest of the azamacrocyclic molecules and may indicate that these are in fact hollow spheres although this requires confirmation by TEM. It was also observed that 3NC might stabilise a silicon species and this observation also requires further investigation. Increasing the concentration of 3NC in the system might increase the stabilising effect. Investigating the reduction of k_{3rd} when using 3NC and 18C6 will need to focus on identifying an interaction between orthosilicic acid and the additive. NMR could be used to identify an interaction between orthosilicic acid and 3NC. Many of the problems associated with identifying such an interaction using NMR are associated with the low abundance of ^{29}Si NMR where one would observe a shift in the Q^0 peak if an interaction occurred between orthosilicic acid and 3NC. However, working at supersaturated orthosilicic acid concentrations would be required to obtain a ^{29}Si signal and at those concentrations condensation occurs, making it very hard to identify a specific interaction.

6.2.2 Further work related to the field of bioinspired and biomimetic silica formation *in vitro*.

The architecture of additives is thought to be very important when studying molecular interaction in the formation of bioinpired and biomimetic silica. The role of primary amines has been investigated previously[10] and in this thesis we have investigated the role of azamacrocyclic molecules which are an example of secondary amines. In Chapter 5 we showed that tertiary amines also have a profound effect on the formation of silica, where the formation of silica was preferred over complexation when KSiCat was used as a precursor to silica formation. However, we did not carry out any material characterisation or investigate the catalytic effect of tertiary amines on silica formation. Work into understanding the role of amine architecture may provide a useful insight into the role of specific alkylation in long chain polyamines extracted from diatoms. However, the formation of larger silica structure like those observed in biological organism will require molecules to organise on a larger length scale or the use of larger molecules. This was shown recently by Zollfrank where a rigid carbohydrate backbone was functionalised with a polyamine at a specific site and used to template silica formation.[20] One biomimetic approach might be to mix polyamines of different molecular weights where at a particular pH value the polyamines would self assemble into a droplet of a particular size. The arrangement of different sized droplets on a support might facilitate patterned silica formation. Another approach might be to functionalise small molecules such that molecular self assembly occurs in solution could occur. This would then act as a template for silica formation. Furthermore one might attempt to introduce complimentary functional groups into two different amine architectures which when mixed together could self assemble in a particular manner. Molecular self assembly has also been shown to occur in the formation of hexagonal plates using poly-(L-lysine).[21] The self assembly of a particular moiety could be used and further modified with other molecular functions to tailor the shape of the template for silica formation.

References

1. C. C. Perry and T. Keeling-Tucker, *Jbic*, 2000, **5**, 537-550.
2. R. Tacke, *Angew. Chem. Int. Ed.*, 1999, **38**, 3015-3018.
3. R. E. Hecky, K. Mopper, P. Kilham and E. T. Degens, *Mar. Biol.*, 1973, **19**, 323-331.
4. N. Kröger, Sumper, M., *The Biochemistry of Silica Formation in diatoms*, Wiley-VCH, Chichester, 2000.
5. D. Belton, The influence of small molecules on the precipitation of silica, Nottingham Trent University, 2005.
6. R. K. Iler, *The Chemistry of Silica* John Wiley & Sons, New York, 1979.
7. P. Bennett and D. I. Siegel, *Nature*, 1987, **326**, 684-686.
8. P. C. Bennett, *Geochim. Cosmochim. Acta*, 1991, **55**, 1781-1797.
9. S. V. Patwardhan, S. J. Clarson and C. C. Perry, *Chem. Commun.*, 2005, 1113-1121.
10. D. Belton, S. V. Patwardhan and C. C. Perry, *Chem. Commun.*, 2005, 3475-3477.
11. D. J. Belton, S. V. Patwardhan, C. C. Perry, *J. Mater. Chem.*, 2005, **15**, 4629-4638.
12. M. Hildebrand and R. Wetherbee, *Components and control of silicification in Diatoms*, Springer, New York, 2003.
13. K. D. Lobel, J. K. West and L. L. Hench, *Mar. Biol.*, 1996, **126**, 353-360.
14. K. D. Lobel, J. K. West and L. L. Hench, *J. Mater. Sci. Lett.*, 1996, **15**, 648-650.
15. V. W. Truesdale, J. E. Greenwood and A. R. Rendell, *Prog. Oceanogr.* 2005, **66**, 1-24.
16. P. Roach, D. Farrar and C. C. Perry, *J. Am. Chem. Soc.*, 2005, **127**, 8168-8173.
17. Y. Y. Wu, G. S. Cheng, K. Katsov, S. W. Sides, J. F. Wang, J. Tang, G. H. Fredrickson, M. Moskovits and G. D. Stucky, *Nat. Mater.*, 2004, **3**, 816-822.
18. C. Gautier, P. J. Lopez, M. Hemadi, J. Livage and T. Coradin, *Langmuir*, 2006, **22**, 9092-9095.
19. H. El Rassy, E. Belamie, J. Livage and T. Coradin, *Langmuir*, 2005, **21**, 8584-8587.
20. C. S. Zollfrank, H. Griel, P., *Adv. Mater.*, 2007, **19**, 984-987.
21. S. V. Patwardhan, R. Maheshwari, N. Mukherjee, K. L. Kiick and S. J. Clarson, *Biomacromolecules*, 2006, **7**, 491-497.

Publications

Tilburey, G. E.; Patwardhan, S. V.; Huang, J.; Kaplan, D. L.; Perry, C. C., Are hydroxyl containing biomolecules important in (bio)silicification? A model study. *J. Phys. Chem. B* **2007,** 111, (17), 4630-4638.

Oral Presentation

MRS 2007: Understanding molecular interactions in the precipitation and dissolution of silica and silicates under ambient conditions.

Poster Presentations

Junior Euromat 2004: Model studies of biosilicification showing controlled structure and form.

MC7 2006: The role of hydroxyl containing additives in bioinspired silicification.

Appendix 1

The Role of Organic Molecules in the Stability of Silicon Species in an Unsaturated System:

Implications for biological and bioinspired silicification.

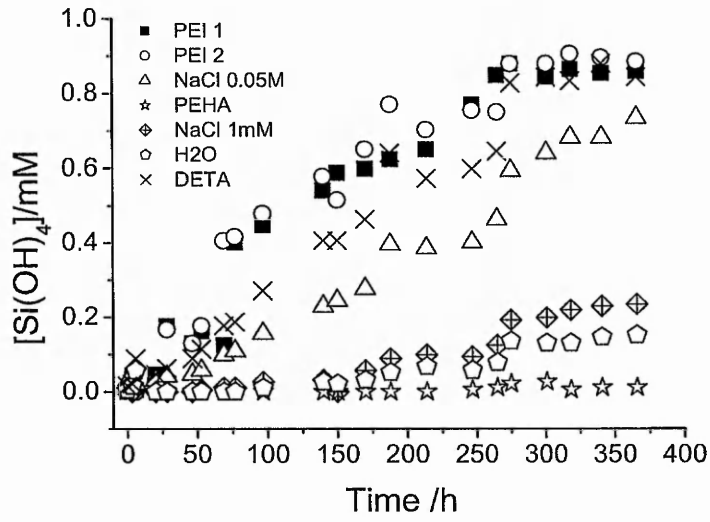

Figure 1 – Dissolution of Gasil 23D in the presence of bioinspired additives and NaCl, known to increase the dissolution of silica.

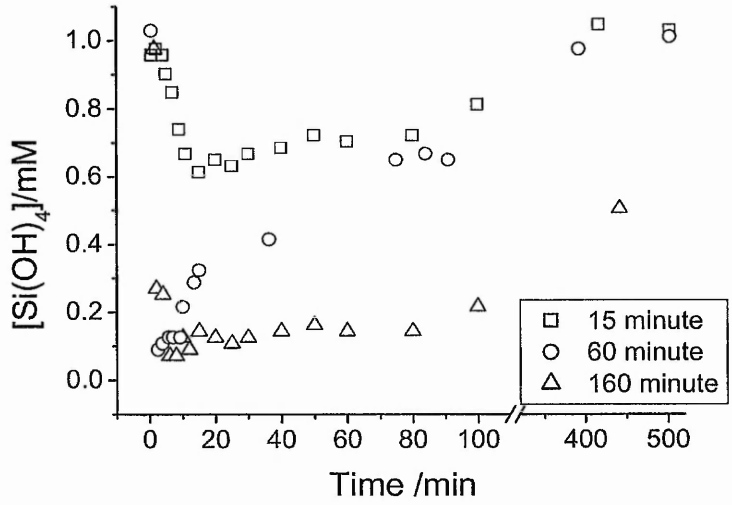

Figure 2 - NaOH digestion of supernatant in the presence of PEHA shows a decrease in the amount of silica remaining in solution from 15 to 60 and 160 minutes precondensing time. The amount of silicon species precipitated from solution is 89 and 93% for 60and 160 minutes respectively.

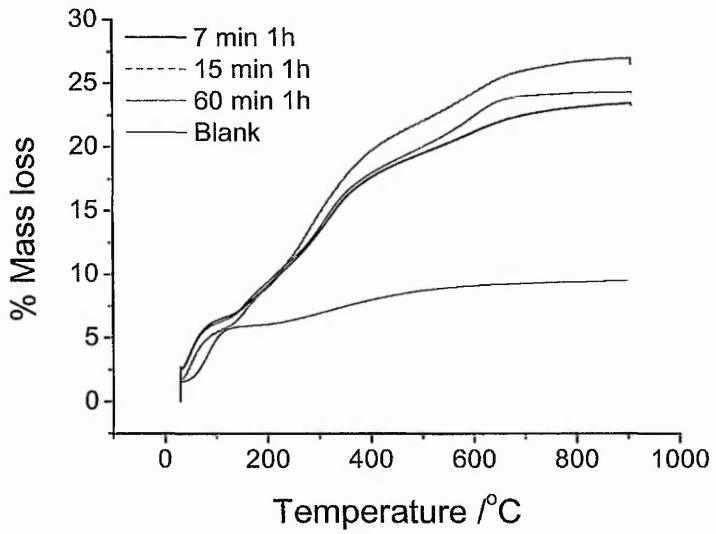

Figure 3 – Thermal gravimetric analysis of silicas isolated in the presence of PEHA formed from different precondensed silica systems and isolated after 1 hour. Blank silica is prepared from a 24h 30mM condensing system as no precipitate can be isolated in the absence of PEHA.

Appendix 2

Are hydroxyl containing biomolecules important in (bio)silicification? *A model study*

Samples	**Concentration***	**Relative rates**		
		k_{3rd}	k_+	k_-
Blank		1.00	1.00	1.00
Native Sericin	1%	1.42	0.98	0.82
	5%	1.58	1.08	1.08
	10%	1.32	1.01	1.01
Sericin precursor	1%	1.40	0.93	0.67
	5%	0.58	0.84	0.68
	10%	1.02	1.17	1.10
	200%	0.83	0.75	0.96
Polyserine	0.1	1.12	0.93	1.15
1,2 diol	1	0.94	1.11	1.65
	2	0.98	1.25	2.13
	4	0.79	1.03	1.31
	10	0.64	0.96	1.00
1,3 diol	1	0.97	1.05	1.32
	2	0.98	1.25	2.13
	4	0.85	0.99	1.22
	10	0.94	1.09	1.34
1,4 diol	1	0.91	1.15	1.49
	2	0.98	1.25	2.13
	4	1.07	0.90	1.11
	10	0.89	1.01	1.27
1,5 diol	1	0.88	1.19	1.59
	2	0.676	1.186	1.587
	4	1.16	1.006	1.282
	10	1.23	1.083	1.447
1,6 diol	1	0.91	1.22	1.51
	2	0.788	1.070	1.647
	4	1.19	1.010	1.246
	10	1.28	1.082	1.321
1,7 diol	1	0.88	1.24	1.84
	2	0.644	1.160	1.668
	4	1.35	1.020	1.259

10	1.12	0.796	0.972

* For sericin proteins, concentration is in wt%.

For diols and polyserine, concentration is the ratio of OH:Si

Table 1. A list of relative rate constants obtained from kinetic assays of silicification using a molybdosilicate method for silica samples prepared in the presence and absence of diols and sericin proteins.

Samples	Concentration*	Surface area	Pore volume	Pore size
Blank		1	1	1
Native Sericin[$]	1%	0.88		
	5%	0.75		
	10%	0.81		
Sericin precursor[$]	1%	0.87		
	5%	1		
1,2 diol	1	0.93	0.25	0.57
	2	0.98	0.84	0.85
	4	0.70	1.33	1.22
1,3 diol	1	0.94	0.30	0.57
	2	1.02	0.87	0.85
1,4 diol	1	0.99	0.33	0.57
	2	1.04	0.81	0.85
1,5 diol	1	0.95	0.44	0.57
	2	1.01	0.70	0.85
1,6 diol	1	0.98	0.46	0.75
	2	0.99	0.24	0.49
1,7 diol	1	0.95	0.35	0.57
	2	0.97	0.43	0.75
	4	0.75	1.70	1.58

* For sericin proteins, concentration is in wt%. For diols, concentration is the ratio of OH:Si.

[$] Due to small sample quantities generated with sericin proteins, pore volumes and pore sizes could not be determined accurately.

Table 2. A list of surface areas ($m^2\ g^{-1}$), pore volumes ($cc\ g^{-1}$) and pore sizes (Å) obtained for silica samples prepared in the presence and absence of diols and sericin proteins. Data presented relative to blank.

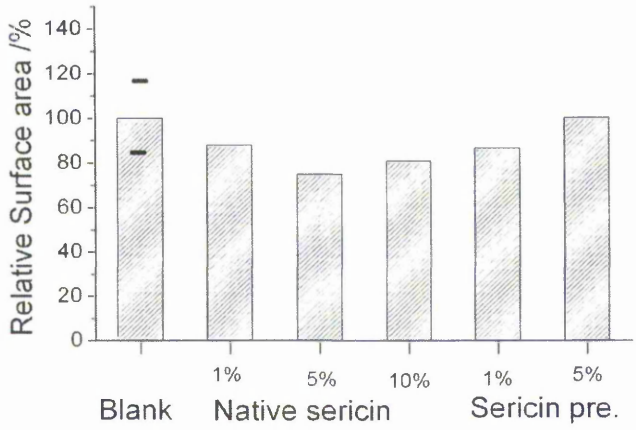

Figure 1. Surface area data obtained on silica samples prepared in the presence of sericin proteins. The horizontal lines over blank data show the 98% confidence limit envelop.

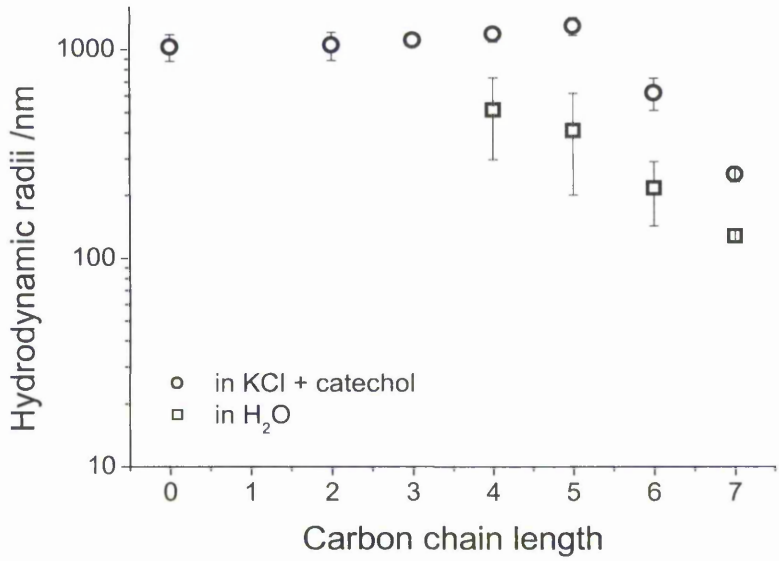

Figure 2. The formation of micelles in water and the model system in the absence of silicon. Error bars are one standard deviation from the mean. No particle/micelle formation was detected for 1,2 ethanediol and 1,3 propanediol in water.

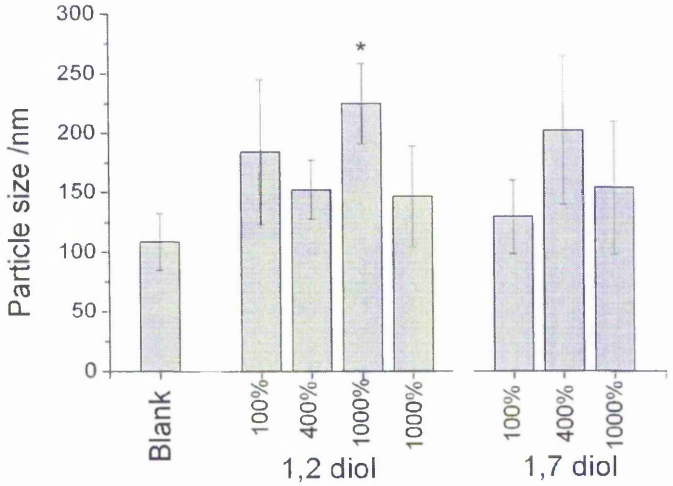

Figure 3. Particle sizes for silica samples produced in the presence and absence of alkanediols. Two data sets for 1,2 diol 1000% are shown due to bimodal particle sizes.

Appendix 3

Using Azamacrocyclic molecules to control the formation of silica

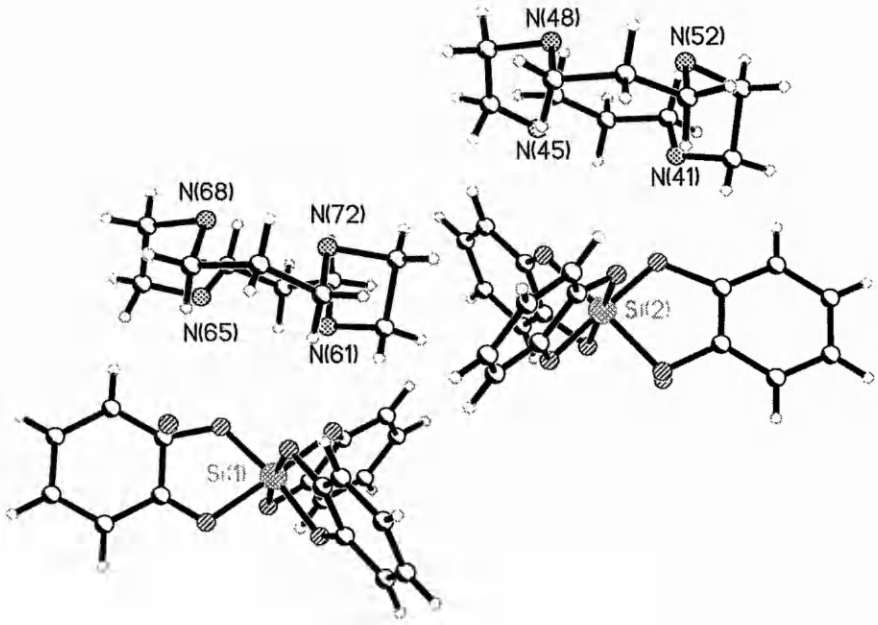

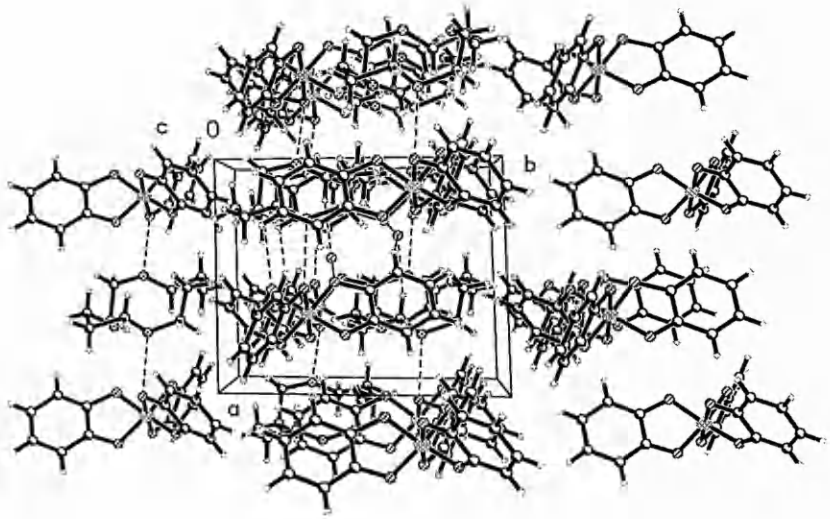

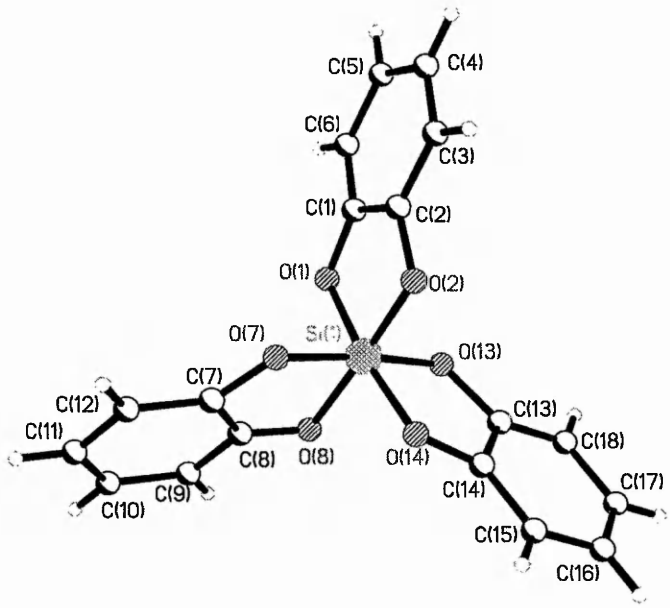
C(5)
C(4)
C(6)
C(3)
C(1)
C(2)
O(1)
O(2)
O(7)
Si(1)
O(13)
C(7)
C(12)
C(13)
C(11)
C(18)
C(8)
O(8)
O(14)
C(17)
C(9)
C(14)
C(10)
C(15)
C(16)

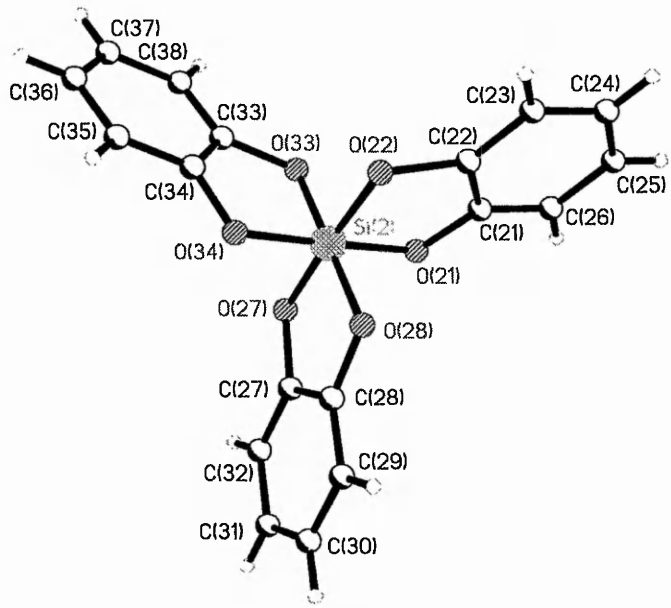
C(37)
C(38)
C(36)
C(23)
C(24)
C(33)
C(35)
O(33)
O(22)
C(22)
C(25)
C(34)
C(26)
Si(2)
C(21)
O(34)
O(21)
O(27)
O(28)
C(27)
C(28)
C(32)
C(29)
C(31)
C(30)

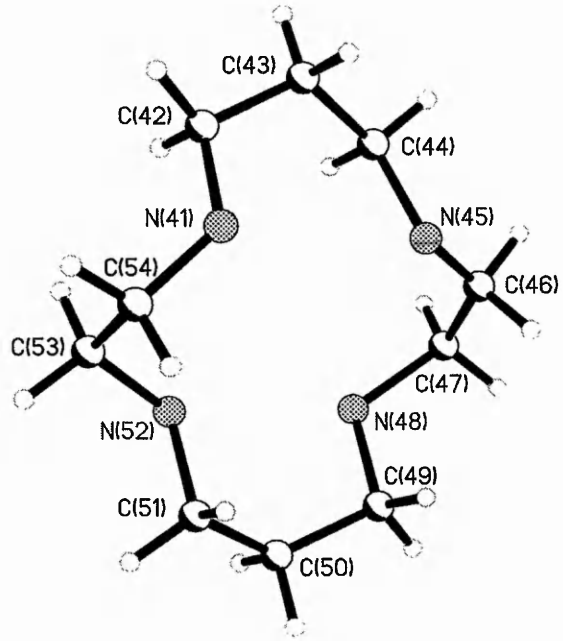
C(43)
C(42)
C(44)
N(41)
N(45)
C(54)
C(46)
C(53)
C(47)
N(52)
N(48)
C(49)
C(51)
C(50)

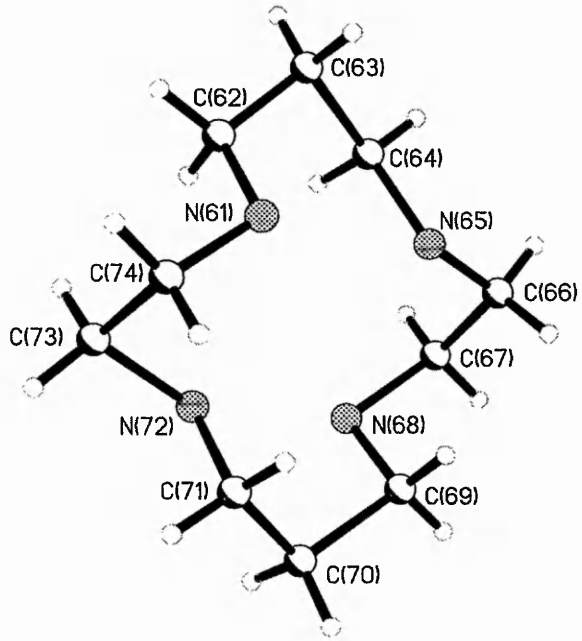
C(63)
C(62)
C(64)
N(61)
N(65)
C(74)
C(66)
C(73)
C(67)
N(72)
N(68)
C(71)
C(69)
C(70)

Table 1. Crystal data and structure refinement for Cyclam complex.

Identification code	Cyclam complex	
Empirical formula	C28 H40 N4 O7 Si	
Formula weight	572.73	
Temperature	93(2) K	
Wavelength	0.71073 Å	
Crystal system	Triclinic	
Space group	P1	
Unit cell dimensions	a = 9.953(3) Å	α= 77.209(19)°.
	b = 11.958(4) Å	β= 80.902(19)°.
	c = 12.250(4) Å	γ = 86.67(2)°.
Volume	1403.5(7) $Å^3$	
Z	2	
Density (calculated)	1.355 Mg/m^3	
Absorption coefficient	0.137 mm^{-1}	
F(000)	612	
Crystal size	0.200 x 0.200 x 0.030 mm^3	
Theta range for data collection	2.49 to 25.35°.	
Index ranges	-11<=h<=11, -14<=k<=13, -13<=l<=14	
Reflections collected	12565	
Independent reflections	7732 [R(int) = 0.1803]	
Completeness to theta = 00		
Largest diff. peak and hole	0.955 and -1.622 e.$Å^{-3}$25.00°	97.8 %
Absorption correction	Multiscan	
Max. and min. transmission	1.0000 and 0.8497	
Refinement method	Full-matrix least-squares on F^2	
Data / restraints / parameters	7732 / 3 / 245	
Goodness-of-fit on F^2	1.045	
Final R indices [I>2sigma(I)]	R1 = 0.2416, wR2 = 0.4948	
R indices (all data)	R1 = 0.3459, wR2 = 0.5661	
Absolute structure parameter	0.	

Table 2. Atomic coordinates (x 10^4) and equivalent isotropic displacement parameters ($Å^2$x 10^3) for Cyclam complex. U(eq) is defined as one third of the trace of the orthogonalized U^{ij} tensor.

	x	y	z	U(eq)
Si(1)	1411(10)	6904(8)	5363(8)	31(2)
O(1)	100(30)	7820(20)	4710(20)	39(6)
O(2)	2330(20)	6949(17)	3978(17)	19(4)
C(1)	478(18)	8024(17)	3574(11)	11(5)
C(2)	1748(18)	7609(19)	3166(15)	54(11)
C(3)	2146(16)	7720(20)	2007(16)	30
C(4)	1273(19)	8253(19)	1257(12)	30(8)
C(5)	2(18)	8668(17)	1665(13)	10(5)
C(6)	-395(15)	8553(16)	2823(14)	32(8)
O(7)	2200(30)	8010(20)	5550(20)	50(7)
O(8)	460(20)	6930(20)	6820(20)	34(6)
C(7)	1866(18)	8445(17)	6444(13)	22(6)
C(8)	783(19)	7789(14)	7068(16)	21(6)
C(9)	75(18)	8086(17)	8040(15)	26(7)
C(10)	450(20)	9038(19)	8388(15)	28(7)
C(11)	1530(20)	9694(17)	7764(19)	43(10)
C(12)	2240(19)	9398(17)	6792(17)	39(9)
O(13)	400(20)	5750(20)	5360(20)	31(6)
O(14)	2621(19)	5869(17)	5911(16)	17(4)
C(13)	1003(19)	4663(11)	5796(18)	30
C(14)	2230(20)	4786(14)	6150(20)	30
C(15)	2957(18)	3822(19)	6630(20)	41(9)
C(16)	2450(20)	2735(15)	6760(20)	89(18)
C(17)	1223(18)	2611(11)	6397(16)	9(5)
C(18)	498(14)	3576(13)	5917(15)	3(4)
Si(2)	6551(9)	3253(7)	1390(7)	19(2)
O(21)	5557(18)	2015(15)	1239(15)	11(4)
O(22)	7603(19)	3253(16)	66(16)	15(4)
C(21)	6265(17)	1633(15)	261(12)	9(5)
C(22)	7312(18)	2272(14)	-445(15)	24(7)
C(23)	7892(18)	1963(16)	-1448(15)	28(7)
C(24)	7430(20)	1015(18)	-1746(14)	27(7)
C(25)	6380(20)	376(15)	-1041(16)	22(7)
C(26)	5798(17)	685(15)	-38(15)	30(8)
O(27)	5510(20)	3180(20)	2690(20)	32(6)
O(28)	7790(20)	2331(19)	2100(20)	27(5)
C(27)	6265(18)	2553(17)	3608(14)	17(6)
C(28)	7541(19)	2100(18)	3267(12)	40(9)
C(29)	8295(16)	1477(17)	4071(16)	18(6)
C(30)	7770(20)	1306(18)	5215(15)	33(8)
C(31)	6500(20)	1760(20)	5556(12)	33(8)
C(32)	5743(17)	2380(20)	4752(16)	38(8)
O(33)	5250(30)	4160(20)	720(20)	39(6)
O(34)	7420(20)	4489(17)	1518(17)	23(5)
C(33)	5600(20)	5337(13)	590(20)	33(7)
C(34)	6830(20)	5464(18)	940(20)	34(7)
C(35)	7340(20)	6550(20)	810(30)	100(20)
C(36)	6610(20)	7514(16)	320(30)	95(19)
C(37)	5380(20)	7387(14)	-29(18)	11(5)
C(38)	4875(18)	6298(17)	100(20)	34(9)
N(41)	10250(20)	2900(20)	140(20)	18(5)

C(42)	10790(30)	3910(20)	-770(30)	23(7)
C(43)	10410(30)	5010(20)	-480(20)	16(6)
C(44)	10910(30)	5270(20)	540(20)	17(6)
N(45)	10390(30)	4550(20)	1670(20)	26(6)
C(46)	10860(30)	4810(30)	2520(30)	34(8)
C(47)	12150(30)	4550(20)	2870(20)	14(5)
N(48)	12660(20)	3330(18)	2714(18)	12(5)
C(49)	12130(30)	2370(30)	3650(30)	28(7)
C(50)	12560(30)	1260(30)	3290(30)	24(7)
C(51)	12190(30)	880(20)	2310(20)	20(6)
N(52)	12660(20)	1807(18)	1320(18)	12(5)
C(53)	12170(40)	1560(40)	250(40)	49(11)
C(54)	10550(30)	1710(30)	190(30)	27(7)
N(61)	5090(30)	6710(30)	4290(30)	43(8)
C(62)	5760(40)	7690(40)	3310(30)	48(10)
C(63)	5150(40)	8860(30)	3390(30)	39(9)
C(64)	5740(40)	9010(30)	4490(30)	45(10)
N(65)	5330(30)	8260(20)	5690(20)	38(7)
C(66)	5590(30)	8630(30)	6630(30)	26(7)
C(67)	7040(30)	8360(30)	6690(30)	23(7)
N(68)	7600(30)	7110(20)	6480(20)	23(6)
C(69)	6890(30)	6350(20)	7430(20)	19(6)
C(70)	7400(70)	5000(50)	7200(60)	100(20)
C(71)	6740(40)	4750(40)	6160(30)	51(11)
N(72)	7410(20)	5670(20)	5210(20)	18(5)
C(73)	7170(30)	5360(20)	4010(20)	21(6)
C(74)	5500(40)	5530(40)	4120(40)	55(11)
O(81)	4260(40)	4020(30)	-1120(40)	100
O(82)	3300(40)	6360(30)	7980(30)	100

Table 3. Bond lengths [Å] and angles [°] for Cyclam complex.

Si(1)-O(7)	1.66(3)
Si(1)-O(14)	1.77(2)
Si(1)-O(13)	1.75(3)
Si(1)-O(1)	1.82(3)
Si(1)-O(2)	1.79(2)
Si(1)-O(8)	1.89(3)
O(1)-C(1)	1.35(3)
O(2)-C(2)	1.31(2)
C(1)-C(2)	1.3900
C(1)-C(6)	1.3900
C(2)-C(3)	1.3900
C(3)-C(4)	1.3900
C(3)-H(3A)	0.9500
C(4)-C(5)	1.3900
C(4)-H(4A)	0.9500
C(5)-C(6)	1.3900
C(5)-H(5A)	0.9500
C(6)-H(6A)	0.9500
O(7)-C(7)	1.30(3)
O(8)-C(8)	1.21(3)
C(7)-C(8)	1.3900
C(7)-C(12)	1.3900
C(8)-C(9)	1.3900
C(9)-C(10)	1.3900
C(9)-H(9A)	0.9500
C(10)-C(11)	1.3900
C(10)-H(10A)	0.9500
C(11)-C(12)	1.3900
C(11)-H(11A)	0.9500
C(12)-H(12A)	0.9500
O(13)-C(13)	1.43(3)
O(14)-C(14)	1.33(2)
C(13)-C(14)	1.3900
C(13)-C(18)	1.3900
C(14)-C(15)	1.3900
C(15)-C(16)	1.3900
C(15)-H(15A)	0.9500
C(16)-C(17)	1.3900
C(16)-H(16A)	0.9500
C(17)-C(18)	1.3900
C(17)-H(17A)	0.9500
C(18)-H(18A)	0.9500
Si(2)-O(27)	1.75(3)
Si(2)-O(34)	1.80(2)
Si(2)-O(22)	1.78(2)
Si(2)-O(28)	1.81(2)
Si(2)-O(33)	1.81(3)
Si(2)-O(21)	1.88(2)
O(21)-C(21)	1.44(2)
O(22)-C(22)	1.51(2)
C(21)-C(22)	1.3900
C(21)-C(26)	1.3900
C(22)-C(23)	1.3900
C(23)-C(24)	1.3900
C(23)-H(23A)	0.9500
C(24)-C(25)	1.3900
C(24)-H(24A)	0.9500
C(25)-C(26)	1.3900
C(25)-H(25A)	0.9500
C(26)-H(26A)	0.9500
O(27)-C(27)	1.49(3)
O(28)-C(28)	1.37(3)
C(27)-C(28)	1.3900
C(27)-C(32)	1.3900
C(28)-C(29)	1.3900
C(29)-C(30)	1.3900
C(29)-H(29A)	0.9500
C(30)-C(31)	1.3900
C(30)-H(30A)	0.9500
C(31)-C(32)	1.3900
C(31)-H(31A)	0.9500
C(32)-H(32A)	0.9500
O(33)-C(33)	1.44(3)
O(34)-C(34)	1.37(2)
C(33)-C(34)	1.3900
C(33)-C(38)	1.3900
C(34)-C(35)	1.3900
C(35)-C(36)	1.3900
C(35)-H(35A)	0.9500
C(36)-C(37)	1.3900
C(36)-H(36A)	0.9500
C(37)-C(38)	1.3900
C(37)-H(37A)	0.9500
C(38)-H(38A)	0.9500
N(41)-C(54)	1.43(4)
N(41)-C(42)	1.51(4)
C(42)-C(43)	1.46(4)
C(42)-H(42A)	0.9900
C(42)-H(42B)	0.9900
C(43)-C(44)	1.53(4)
C(43)-H(43A)	0.9900
C(43)-H(43B)	0.9900
C(44)-N(45)	1.49(4)
C(44)-H(44A)	0.9900
C(44)-H(44B)	0.9900
N(45)-C(46)	1.30(4)
C(46)-C(47)	1.42(4)
C(46)-H(46A)	0.9900
C(46)-H(46B)	0.9900
C(47)-N(48)	1.56(3)
C(47)-H(47A)	0.9900
C(47)-H(47B)	0.9900
N(48)-C(49)	1.49(4)
C(49)-C(50)	1.52(4)
C(49)-H(49A)	0.9900
C(49)-H(49B)	0.9900
C(50)-C(51)	1.48(4)

C(50)-H(50A)	0.9900
C(50)-H(50B)	0.9900
C(51)-N(52)	1.49(4)
C(51)-H(51A)	0.9900
C(51)-H(51B)	0.9900
N(52)-C(53)	1.56(5)
C(53)-C(54)	1.62(5)
C(53)-H(53A)	0.9900
C(53)-H(53B)	0.9900
C(54)-H(54A)	0.9900
C(54)-H(54B)	0.9900
N(61)-C(74)	1.50(5)
N(61)-C(62)	1.57(5)
C(62)-C(63)	1.51(5)
C(62)-H(62A)	0.9900
C(62)-H(62B)	0.9900
C(63)-C(64)	1.60(5)
C(63)-H(63A)	0.9900
C(63)-H(63B)	0.9900
C(64)-N(65)	1.56(5)
C(64)-H(64A)	0.9900
C(64)-H(64B)	0.9900
N(65)-C(66)	1.38(4)
C(66)-C(67)	1.47(4)
C(66)-H(66A)	0.9900
C(66)-H(66B)	0.9900
C(67)-N(68)	1.63(4)
C(67)-H(67A)	0.9900
C(67)-H(67B)	0.9900
N(68)-C(69)	1.42(4)
C(69)-C(70)	1.73(7)
C(69)-H(69A)	0.9900
C(69)-H(69B)	0.9900
C(70)-C(71)	1.61(7)
C(70)-H(70A)	0.9900
C(70)-H(70B)	0.9900
C(71)-N(72)	1.51(5)
C(71)-H(71A)	0.9900
C(71)-H(71B)	0.9900
N(72)-C(73)	1.65(3)
C(73)-C(74)	1.65(5)
C(73)-H(73A)	0.9900
C(73)-H(73B)	0.9900
C(74)-H(74A)	0.9900
C(74)-H(74B)	0.9900
O(7)-Si(1)-O(14)	94.8(12)
O(7)-Si(1)-O(13)	170.9(14)
O(14)-Si(1)-O(13)	87.1(11)
O(7)-Si(1)-O(1)	92.6(13)
O(14)-Si(1)-O(1)	172.2(12)
O(13)-Si(1)-O(1)	86.1(12)
O(7)-Si(1)-O(2)	93.7(13)
O(14)-Si(1)-O(2)	88.6(10)
O(13)-Si(1)-O(2)	95.3(11)
O(1)-Si(1)-O(2)	88.4(11)
O(7)-Si(1)-O(8)	83.8(13)
O(14)-Si(1)-O(8)	92.8(10)
O(13)-Si(1)-O(8)	87.2(11)
O(1)-Si(1)-O(8)	90.6(12)
O(2)-Si(1)-O(8)	177.2(12)
C(1)-O(1)-Si(1)	108.0(17)
C(2)-O(2)-Si(1)	113.7(15)
O(1)-C(1)-C(2)	117.5(16)
O(1)-C(1)-C(6)	122.3(16)
C(2)-C(1)-C(6)	120.0
O(2)-C(2)-C(3)	126.8(15)
O(2)-C(2)-C(1)	111.9(16)
C(3)-C(2)-C(1)	120.0
C(2)-C(3)-C(4)	120.0
C(2)-C(3)-H(3A)	120.0
C(4)-C(3)-H(3A)	120.0
C(3)-C(4)-C(5)	120.0
C(3)-C(4)-H(4A)	120.0
C(5)-C(4)-H(4A)	120.0
C(6)-C(5)-C(4)	120.0
C(6)-C(5)-H(5A)	120.0
C(4)-C(5)-H(5A)	120.0
C(5)-C(6)-C(1)	120.0
C(5)-C(6)-H(6A)	120.0
C(1)-C(6)-H(6A)	120.0
C(7)-O(7)-Si(1)	122(2)
C(8)-O(8)-Si(1)	107.1(18)
O(7)-C(7)-C(8)	104.4(18)
O(7)-C(7)-C(12)	135.2(18)
C(8)-C(7)-C(12)	120.0
O(8)-C(8)-C(7)	121.9(17)
O(8)-C(8)-C(9)	118.0(18)
C(7)-C(8)-C(9)	120.0
C(10)-C(9)-C(8)	120.0
C(10)-C(9)-H(9A)	120.0
C(8)-C(9)-H(9A)	120.0
C(9)-C(10)-C(11)	120.0
C(9)-C(10)-H(10A)	120.0
C(11)-C(10)-H(10A)	120.0
C(10)-C(11)-C(12)	120.0
C(10)-C(11)-H(11A)	120.0
C(12)-C(11)-H(11A)	120.0
C(11)-C(12)-C(7)	120.0
C(11)-C(12)-H(12A)	120.0
C(7)-C(12)-H(12A)	120.0
C(13)-O(13)-Si(1)	112.9(16)
C(14)-O(14)-Si(1)	115.6(16)
C(14)-C(13)-C(18)	120.0
C(14)-C(13)-O(13)	111.3(16)
C(18)-C(13)-O(13)	128.7(16)
O(14)-C(14)-C(13)	112.7(16)
O(14)-C(14)-C(15)	127.1(16)
C(13)-C(14)-C(15)	120.0
C(14)-C(15)-C(16)	120.0
C(14)-C(15)-H(15A)	120.0
C(16)-C(15)-H(15A)	120.0

C(17)-C(16)-C(15)	120.0	C(29)-C(30)-H(30A)	120.0
C(17)-C(16)-H(16A)	120.0	C(31)-C(30)-H(30A)	120.0
C(15)-C(16)-H(16A)	120.0	C(30)-C(31)-C(32)	120.0
C(16)-C(17)-C(18)	120.0	C(30)-C(31)-H(31A)	120.0
C(16)-C(17)-H(17A)	120.0	C(32)-C(31)-H(31A)	120.0
C(18)-C(17)-H(17A)	120.0	C(31)-C(32)-C(27)	120.0
C(17)-C(18)-C(13)	120.0	C(31)-C(32)-H(32A)	120.0
C(17)-C(18)-H(18A)	120.0	C(27)-C(32)-H(32A)	120.0
C(13)-C(18)-H(18A)	120.0	C(33)-O(33)-Si(2)	108.3(17)
O(27)-Si(2)-O(34)	92.8(11)	C(34)-O(34)-Si(2)	109.2(16)
O(27)-Si(2)-O(22)	177.2(12)	C(34)-C(33)-C(38)	120.0
O(34)-Si(2)-O(22)	89.7(10)	C(34)-C(33)-O(33)	113.4(17)
O(27)-Si(2)-O(28)	89.3(12)	C(38)-C(33)-O(33)	126.5(17)
O(34)-Si(2)-O(28)	89.6(10)	O(34)-C(34)-C(33)	116.6(19)
O(22)-Si(2)-O(28)	89.5(10)	O(34)-C(34)-C(35)	123.0(19)
O(27)-Si(2)-O(33)	88.6(12)	C(33)-C(34)-C(35)	120.0
O(34)-Si(2)-O(33)	91.4(11)	C(34)-C(35)-C(36)	120.0
O(22)-Si(2)-O(33)	92.5(11)	C(34)-C(35)-H(35A)	120.0
O(28)-Si(2)-O(33)	177.7(13)	C(36)-C(35)-H(35A)	120.0
O(27)-Si(2)-O(21)	86.3(11)	C(37)-C(36)-C(35)	120.0
O(34)-Si(2)-O(21)	176.8(10)	C(37)-C(36)-H(36A)	120.0
O(22)-Si(2)-O(21)	91.3(9)	C(35)-C(36)-H(36A)	120.0
O(28)-Si(2)-O(21)	93.5(10)	C(38)-C(37)-C(36)	120.0
O(33)-Si(2)-O(21)	85.5(10)	C(38)-C(37)-H(37A)	120.0
C(21)-O(21)-Si(2)	105.9(13)	C(36)-C(37)-H(37A)	120.0
C(22)-O(22)-Si(2)	112.5(13)	C(37)-C(38)-C(33)	120.0
C(22)-C(21)-C(26)	120.0	C(37)-C(38)-H(38A)	120.0
C(22)-C(21)-O(21)	120.4(13)	C(33)-C(38)-H(38A)	120.0
C(26)-C(21)-O(21)	119.3(13)	C(54)-N(41)-C(42)	127(2)
C(23)-C(22)-C(21)	120.0	C(43)-C(42)-N(41)	113(2)
C(23)-C(22)-O(22)	130.9(13)	C(43)-C(42)-H(42A)	108.8
C(21)-C(22)-O(22)	109.1(13)	N(41)-C(42)-H(42A)	108.6
C(22)-C(23)-C(24)	120.0	C(43)-C(42)-H(42B)	109.2
C(22)-C(23)-H(23A)	120.0	N(41)-C(42)-H(42B)	109.1
C(24)-C(23)-H(23A)	120.0	H(42A)-C(42)-H(42B)	107.7
C(25)-C(24)-C(23)	120.0	C(42)-C(43)-C(44)	118(2)
C(25)-C(24)-H(24A)	120.0	C(42)-C(43)-H(43A)	108.0
C(23)-C(24)-H(24A)	120.0	C(44)-C(43)-H(43A)	108.1
C(24)-C(25)-C(26)	120.0	C(42)-C(43)-H(43B)	107.8
C(24)-C(25)-H(25A)	120.0	C(44)-C(43)-H(43B)	107.7
C(26)-C(25)-H(25A)	120.0	H(43A)-C(43)-H(43B)	107.3
C(25)-C(26)-C(21)	120.0	N(45)-C(44)-C(43)	117(2)
C(25)-C(26)-H(26A)	120.0	N(45)-C(44)-H(44A)	107.8
C(21)-C(26)-H(26A)	120.0	C(43)-C(44)-H(44A)	108.0
C(27)-O(27)-Si(2)	108.7(16)	N(45)-C(44)-H(44B)	108.0
C(28)-O(28)-Si(2)	115.9(16)	C(43)-C(44)-H(44B)	108.3
C(28)-C(27)-C(32)	120.0	H(44A)-C(44)-H(44B)	107.2
C(28)-C(27)-O(27)	116.6(15)	C(46)-N(45)-C(44)	114(3)
C(32)-C(27)-O(27)	123.4(15)	N(45)-C(46)-C(47)	129(3)
O(28)-C(28)-C(29)	131.1(15)	N(45)-C(46)-H(46A)	105.1
O(28)-C(28)-C(27)	108.8(15)	C(47)-C(46)-H(46A)	105.7
C(29)-C(28)-C(27)	120.0	N(45)-C(46)-H(46B)	104.8
C(28)-C(29)-C(30)	120.0	C(47)-C(46)-H(46B)	104.5
C(28)-C(29)-H(29A)	120.0	H(46A)-C(46)-H(46B)	105.9
C(30)-C(29)-H(29A)	120.0	C(46)-C(47)-N(48)	111(2)
C(29)-C(30)-C(31)	120.0	C(46)-C(47)-H(47A)	109.0

N(48)-C(47)-H(47A)	109.2
C(46)-C(47)-H(47B)	110.2
N(48)-C(47)-H(47B)	109.7
H(47A)-C(47)-H(47B)	108.0
C(49)-N(48)-C(47)	115(2)
N(48)-C(49)-C(50)	108(3)
N(48)-C(49)-H(49A)	110.1
C(50)-C(49)-H(49A)	110.3
N(48)-C(49)-H(49B)	110.0
C(50)-C(49)-H(49B)	110.2
H(49A)-C(49)-H(49B)	108.5
C(51)-C(50)-C(49)	127(3)
C(51)-C(50)-H(50A)	105.9
C(49)-C(50)-H(50A)	105.8
C(51)-C(50)-H(50B)	105.4
C(49)-C(50)-H(50B)	105.6
H(50A)-C(50)-H(50B)	106.2
N(52)-C(51)-C(50)	105(2)
N(52)-C(51)-H(51A)	110.8
C(50)-C(51)-H(51A)	110.9
N(52)-C(51)-H(51B)	110.7
C(50)-C(51)-H(51B)	110.9
H(51A)-C(51)-H(51B)	108.8
C(51)-N(52)-C(53)	109(2)
C(54)-C(53)-N(52)	117(3)
C(54)-C(53)-H(53A)	108.0
N(52)-C(53)-H(53A)	107.9
C(54)-C(53)-H(53B)	108.1
N(52)-C(53)-H(53B)	107.9
H(53A)-C(53)-H(53B)	107.3
N(41)-C(54)-C(53)	105(3)
N(41)-C(54)-H(54A)	111.0
C(53)-C(54)-H(54A)	110.7
N(41)-C(54)-H(54B)	110.6
C(53)-C(54)-H(54B)	110.7
H(54A)-C(54)-H(54B)	108.8
C(74)-N(61)-C(62)	113(3)
N(61)-C(62)-C(63)	112(3)
N(61)-C(62)-H(62A)	109.3
C(63)-C(62)-H(62A)	109.0
N(61)-C(62)-H(62B)	109.2
C(63)-C(62)-H(62B)	108.9
H(62A)-C(62)-H(62B)	107.8
C(62)-C(63)-C(64)	99(3)
C(62)-C(63)-H(63A)	111.8
C(64)-C(63)-H(63A)	111.8
C(62)-C(63)-H(63B)	112.4
C(64)-C(63)-H(63B)	112.2
H(63A)-C(63)-H(63B)	109.7
N(65)-C(64)-C(63)	124(3)
N(65)-C(64)-H(64A)	106.2
C(63)-C(64)-H(64A)	106.1
N(65)-C(64)-H(64B)	106.5
C(63)-C(64)-H(64B)	106.5
H(64A)-C(64)-H(64B)	106.4
C(66)-N(65)-C(64)	120(3)
N(65)-C(66)-C(67)	105(3)
N(65)-C(66)-H(66A)	110.8
C(67)-C(66)-H(66A)	110.7
N(65)-C(66)-H(66B)	110.6
C(67)-C(66)-H(66B)	110.7
H(66A)-C(66)-H(66B)	108.8
C(66)-C(67)-N(68)	117(2)
C(66)-C(67)-H(67A)	108.1
N(68)-C(67)-H(67A)	108.0
C(66)-C(67)-H(67B)	108.2
N(68)-C(67)-H(67B)	108.1
H(67A)-C(67)-H(67B)	107.3
C(69)-N(68)-C(67)	102(2)
N(68)-C(69)-C(70)	104(3)
N(68)-C(69)-H(69A)	111.2
C(70)-C(69)-H(69A)	111.2
N(68)-C(69)-H(69B)	111.0
C(70)-C(69)-H(69B)	110.6
H(69A)-C(69)-H(69B)	109.0
C(71)-C(70)-C(69)	110(4)
C(71)-C(70)-H(70A)	109.6
C(69)-C(70)-H(70A)	109.5
C(71)-C(70)-H(70B)	109.8
C(69)-C(70)-H(70B)	109.6
H(70A)-C(70)-H(70B)	108.0
C(70)-C(71)-N(72)	100(4)
C(70)-C(71)-H(71A)	112.1
N(72)-C(71)-H(71A)	112.3
C(70)-C(71)-H(71B)	111.0
N(72)-C(71)-H(71B)	111.7
H(71A)-C(71)-H(71B)	109.5
C(71)-N(72)-C(73)	107(2)
N(72)-C(73)-C(74)	100(2)
N(72)-C(73)-H(73A)	112.0
C(74)-C(73)-H(73A)	112.2
N(72)-C(73)-H(73B)	111.6
C(74)-C(73)-H(73B)	111.4
H(73A)-C(73)-H(73B)	109.6
N(61)-C(74)-C(73)	110(3)
N(61)-C(74)-H(74A)	109.7
C(73)-C(74)-H(74A)	109.9
N(61)-C(74)-H(74B)	109.7
C(73)-C(74)-H(74B)	109.5
H(74A)-C(74)-H(74B)	108.3

Symmetry transformations used to generate equivalent atoms:

Table 4. Hydrogen coordinates (x 10^4) and isotropic displacement parameters ($Å^2$x 10^3) for Cyclam complex.

	x	y	z	U(eq)
H(3A)	3015	7441	1729	36
H(4A)	1545	8332	465	36
H(5A)	-594	9029	1152	12
H(6A)	-1264	8836	3102	39
H(9A)	-664	7638	8466	31
H(10A)	-34	9241	9052	33
H(11A)	1788	10345	8002	51
H(12A)	2980	9846	6366	46
H(15A)	3797	3906	6880	49
H(16A)	2947	2076	7084	107
H(17A)	878	1868	6480	11
H(18A)	-342	3491	5672	4
H(23A)	8608	2400	-1930	34
H(24A)	7822	805	-2432	32
H(25A)	6059	-272	-1245	27
H(26A)	5083	248	445	36
H(29A)	9167	1167	3838	22
H(30A)	8288	880	5765	39
H(31A)	6140	1642	6338	39
H(32A)	4871	2692	4985	46
H(35A)	8182	6640	1048	121
H(36A)	6959	8258	234	114
H(37A)	4884	8043	-359	13
H(38A)	4033	6210	-138	41
H(42A)	11800	3837	-909	28
H(42B)	10455	3877	-1480	28
H(43A)	9401	5075	-362	19
H(43B)	10735	5620	-1151	19
H(44A)	11919	5195	431	20
H(44B)	10680	6085	565	20
H(46A)	10193	4506	3192	40
H(46B)	10757	5660	2393	40
H(47A)	12093	4590	3671	16
H(47B)	12814	5125	2412	16
H(49A)	11123	2435	3815	34
H(49B)	12502	2406	4349	34
H(50A)	13569	1240	3186	29
H(50B)	12268	643	3960	29
H(51A)	12645	141	2235	24
H(51B)	11192	797	2397	24
H(53A)	12654	2072	-425	59
H(53B)	12449	761	199	59
H(54A)	10342	1485	-498	33
H(54B)	10024	1227	863	33
H(62A)	5638	7524	2573	58
H(62B)	6746	7689	3335	58
H(63A)	4139	8863	3507	46
H(63B)	5478	9455	2710	46
H(64A)	6743	8933	4310	54
H(64B)	5539	9815	4551	54
H(66A)	5016	8215	7323	31
H(66B)	5396	9459	6542	31
H(67A)	7222	8426	7440	28
H(67B)	7576	8950	6116	28
H(69A)	5898	6471	7457	23
H(69B)	7154	6463	8144	23
H(70A)	8403	4950	7033	125

H(70B)	7100	4413	7893	125
H(71A)	5741	4851	6272	62
H(71B)	6994	3975	6024	62
H(73A)	7471	4567	3968	25
H(73B)	7639	5903	3342	25
H(74A)	5193	5411	3427	66
H(74B)	5067	4951	4771	66

Table 5. Torsion angles [°] for Cyclam complex.

O(7)-Si(1)-O(1)-C(1)	95(2)	C(26)-C(21)-C(22)-O(22)	179.2(16)
O(14)-Si(1)-O(1)-C(1)	-65(10)	O(21)-C(21)-C(22)-O(22)	5.9(18)
O(13)-Si(1)-O(1)-C(1)	-94.2(19)	Si(2)-O(22)-C(22)-C(23)	-179.9(12)
O(2)-Si(1)-O(1)-C(1)	1.2(19)	Si(2)-O(22)-C(22)-C(21)	1.0(16)
O(8)-Si(1)-O(1)-C(1)	178.6(18)	C(21)-C(22)-C(23)-C(24)	0
O(7)-Si(1)-O(2)-C(2)	-90(2)	O(22)-C(22)-C(23)-C(24)	-179(2)
O(14)-Si(1)-O(2)-C(2)	175.8(18)	C(22)-C(23)-C(24)-C(25)	0
O(13)-Si(1)-O(2)-C(2)	88.9(19)	C(23)-C(24)-C(25)-C(26)	0
O(1)-Si(1)-O(2)-C(2)	2.9(19)	C(24)-C(25)-C(26)-C(21)	0
O(8)-Si(1)-O(2)-C(2)	-64(24)	C(22)-C(21)-C(26)-C(25)	0
Si(1)-O(1)-C(1)-C(2)	-5(2)	O(21)-C(21)-C(26)-C(25)	173.3(18)
Si(1)-O(1)-C(1)-C(6)	170.2(12)	O(34)-Si(2)-O(27)-C(27)	-83.2(17)
Si(1)-O(2)-C(2)-C(3)	-173.1(12)	O(22)-Si(2)-O(27)-C(27)	71(25)
Si(1)-O(2)-C(2)-C(1)	-6(2)	O(28)-Si(2)-O(27)-C(27)	6.3(18)
O(1)-C(1)-C(2)-O(2)	8(2)	O(33)-Si(2)-O(27)-C(27)	-174.6(18)
C(6)-C(1)-C(2)-O(2)	-168(2)	O(21)-Si(2)-O(27)-C(27)	99.9(17)
O(1)-C(1)-C(2)-C(3)	175(2)	O(27)-Si(2)-O(28)-C(28)	-8(2)
C(6)-C(1)-C(2)-C(3)	0	O(34)-Si(2)-O(28)-C(28)	84.7(19)
O(2)-C(2)-C(3)-C(4)	166(2)	O(22)-Si(2)-O(28)-C(28)	174.5(19)
C(1)-C(2)-C(3)-C(4)	0	O(33)-Si(2)-O(28)-C(28)	-32(33)
C(2)-C(3)-C(4)-C(5)	0	O(21)-Si(2)-O(28)-C(28)	-94.3(19)
C(3)-C(4)-C(5)-C(6)	0	Si(2)-O(27)-C(27)-C(28)	-4(2)
C(4)-C(5)-C(6)-C(1)	0	Si(2)-O(27)-C(27)-C(32)	177.5(13)
O(1)-C(1)-C(6)-C(5)	-175(2)	Si(2)-O(28)-C(28)-C(29)	-176.9(13)
C(2)-C(1)-C(6)-C(5)	0	Si(2)-O(28)-C(28)-C(27)	7(2)
O(14)-Si(1)-O(7)-C(7)	-96(2)	C(32)-C(27)-C(28)-O(28)	177(2)
O(13)-Si(1)-O(7)-C(7)	5(11)	O(27)-C(27)-C(28)-O(28)	-2(2)
O(1)-Si(1)-O(7)-C(7)	87(2)	C(32)-C(27)-C(28)-C(29)	0
O(2)-Si(1)-O(7)-C(7)	175(2)	O(27)-C(27)-C(28)-C(29)	-178(2)
O(8)-Si(1)-O(7)-C(7)	-3(2)	O(28)-C(28)-C(29)-C(30)	-176(3)
O(7)-Si(1)-O(8)-C(8)	7.6(19)	C(27)-C(28)-C(29)-C(30)	0
O(14)-Si(1)-O(8)-C(8)	102.1(18)	C(28)-C(29)-C(30)-C(31)	0
O(13)-Si(1)-O(8)-C(8)	-171.0(19)	C(29)-C(30)-C(31)-C(32)	0
O(1)-Si(1)-O(8)-C(8)	-84.9(19)	C(30)-C(31)-C(32)-C(27)	0
O(2)-Si(1)-O(8)-C(8)	-17(25)	C(28)-C(27)-C(32)-C(31)	0
Si(1)-O(7)-C(7)-C(8)	-1(3)	O(27)-C(27)-C(32)-C(31)	178(2)
Si(1)-O(7)-C(7)-C(12)	-173.6(15)	O(27)-Si(2)-O(33)-C(33)	95.5(19)
Si(1)-O(8)-C(8)-C(7)	-11(2)	O(34)-Si(2)-O(33)-C(33)	2.7(19)
Si(1)-O(8)-C(8)-C(9)	171.4(11)	O(22)-Si(2)-O(33)-C(33)	-87.1(18)
O(7)-C(7)-C(8)-O(8)	9(2)	O(28)-Si(2)-O(33)-C(33)	119(32)
C(12)-C(7)-C(8)-O(8)	-177(2)	O(21)-Si(2)-O(33)-C(33)	-178.2(18)
O(7)-C(7)-C(8)-C(9)	-174(2)	O(27)-Si(2)-O(34)-C(34)	-96.7(19)
C(12)-C(7)-C(8)-C(9)	0	O(22)-Si(2)-O(34)-C(34)	84.5(18)
O(8)-C(8)-C(9)-C(10)	177(2)	O(28)-Si(2)-O(34)-C(34)	174.0(19)
C(7)-C(8)-C(9)-C(10)	0	O(33)-Si(2)-O(34)-C(34)	-8.0(19)
C(8)-C(9)-C(10)-C(11)	0	O(21)-Si(2)-O(34)-C(34)	-24(19)
C(9)-C(10)-C(11)-C(12)	0	Si(2)-O(33)-C(33)-C(34)	3(2)
C(10)-C(11)-C(12)-C(7)	0	Si(2)-O(33)-C(33)-C(38)	179.6(14)
O(7)-C(7)-C(12)-C(11)	171(3)	Si(2)-O(34)-C(34)-C(33)	12(2)
C(8)-C(7)-C(12)-C(11)	0	Si(2)-O(34)-C(34)-C(35)	-175.1(13)
O(7)-Si(1)-O(13)-C(13)	-100(9)	C(38)-C(33)-C(34)-O(34)	173(2)
O(14)-Si(1)-O(13)-C(13)	1.3(18)	O(33)-C(33)-C(34)-O(34)	-10(3)
O(1)-Si(1)-O(13)-C(13)	177.6(19)	C(38)-C(33)-C(34)-C(35)	0
O(2)-Si(1)-O(13)-C(13)	89.6(18)	O(33)-C(33)-C(34)-C(35)	177(2)
O(8)-Si(1)-O(13)-C(13)	-91.6(18)	O(34)-C(34)-C(35)-C(36)	-173(3)
O(7)-Si(1)-O(14)-C(14)	165.9(19)	C(33)-C(34)-C(35)-C(36)	0
O(13)-Si(1)-O(14)-C(14)	-5.1(19)	C(34)-C(35)-C(36)-C(37)	0
O(1)-Si(1)-O(14)-C(14)	-34(10)	C(35)-C(36)-C(37)-C(38)	0

O(2)-Si(1)-O(14)-C(14)	-100.5(18)	C(36)-C(37)-C(38)-C(33)	0
O(8)-Si(1)-O(14)-C(14)	81.9(18)	C(34)-C(33)-C(38)-C(37)	0
Si(1)-O(13)-C(13)-C(14)	2(2)	O(33)-C(33)-C(38)-C(37)	-176(3)
Si(1)-O(13)-C(13)-C(18)	-179.8(13)	C(54)-N(41)-C(42)-C(43)	-173(3)
Si(1)-O(14)-C(14)-C(13)	8(2)	N(41)-C(42)-C(43)-C(44)	63(3)
Si(1)-O(14)-C(14)-C(15)	-177.1(13)	C(42)-C(43)-C(44)-N(45)	-66(3)
C(18)-C(13)-C(14)-O(14)	176(2)	C(43)-C(44)-N(45)-C(46)	180(3)
O(13)-C(13)-C(14)-O(14)	-6.3(19)	C(44)-N(45)-C(46)-C(47)	-77(4)
C(18)-C(13)-C(14)-C(15)	0	N(45)-C(46)-C(47)-N(48)	-37(5)
O(13)-C(13)-C(14)-C(15)	178(2)	C(46)-C(47)-N(48)-C(49)	-83(3)
O(14)-C(14)-C(15)-C(16)	-175(2)	C(47)-N(48)-C(49)-C(50)	172(2)
C(13)-C(14)-C(15)-C(16)	0	N(48)-C(49)-C(50)-C(51)	-61(4)
C(14)-C(15)-C(16)-C(17)	0	C(49)-C(50)-C(51)-N(52)	57(4)
C(15)-C(16)-C(17)-C(18)	0	C(50)-C(51)-N(52)-C(53)	-174(2)
C(16)-C(17)-C(18)-C(13)	0	C(51)-N(52)-C(53)-C(54)	70(4)
C(14)-C(13)-C(18)-C(17)	0	C(42)-N(41)-C(54)-C(53)	63(4)
O(13)-C(13)-C(18)-C(17)	-178(3)	N(52)-C(53)-C(54)-N(41)	64(4)
O(27)-Si(2)-O(21)-C(21)	-170.9(15)	C(74)-N(61)-C(62)-C(63)	170(3)
O(34)-Si(2)-O(21)-C(21)	116(18)	N(61)-C(62)-C(63)-C(64)	70(4)
O(22)-Si(2)-O(21)-C(21)	7.8(13)	C(62)-C(63)-C(64)-N(65)	-66(4)
O(28)-Si(2)-O(21)-C(21)	-81.8(14)	C(63)-C(64)-N(65)-C(66)	-162(3)
O(33)-Si(2)-O(21)-C(21)	100.2(15)	C(64)-N(65)-C(66)-C(67)	-79(3)
O(27)-Si(2)-O(22)-C(22)	24(25)	N(65)-C(66)-C(67)-N(68)	-44(4)
O(34)-Si(2)-O(22)-C(22)	177.8(14)	C(66)-C(67)-N(68)-C(69)	-65(3)
O(28)-Si(2)-O(22)-C(22)	88.2(15)	C(67)-N(68)-C(69)-C(70)	177(3)
O(33)-Si(2)-O(22)-C(22)	-90.8(15)	N(68)-C(69)-C(70)-C(71)	-71(5)
O(21)-Si(2)-O(22)-C(22)	-5.2(14)	C(69)-C(70)-C(71)-N(72)	63(5)
Si(2)-O(21)-C(21)-C(22)	-9.5(17)	C(70)-C(71)-N(72)-C(73)	166(3)
Si(2)-O(21)-C(21)-C(26)	177.2(10)	C(71)-N(72)-C(73)-C(74)	66(3)
C(26)-C(21)-C(22)-C(23)	0	C(62)-N(61)-C(74)-C(73)	58(4)
O(21)-C(21)-C(22)-C(23)	-173.3(18)	N(72)-C(73)-C(74)-N(61)	56(3)

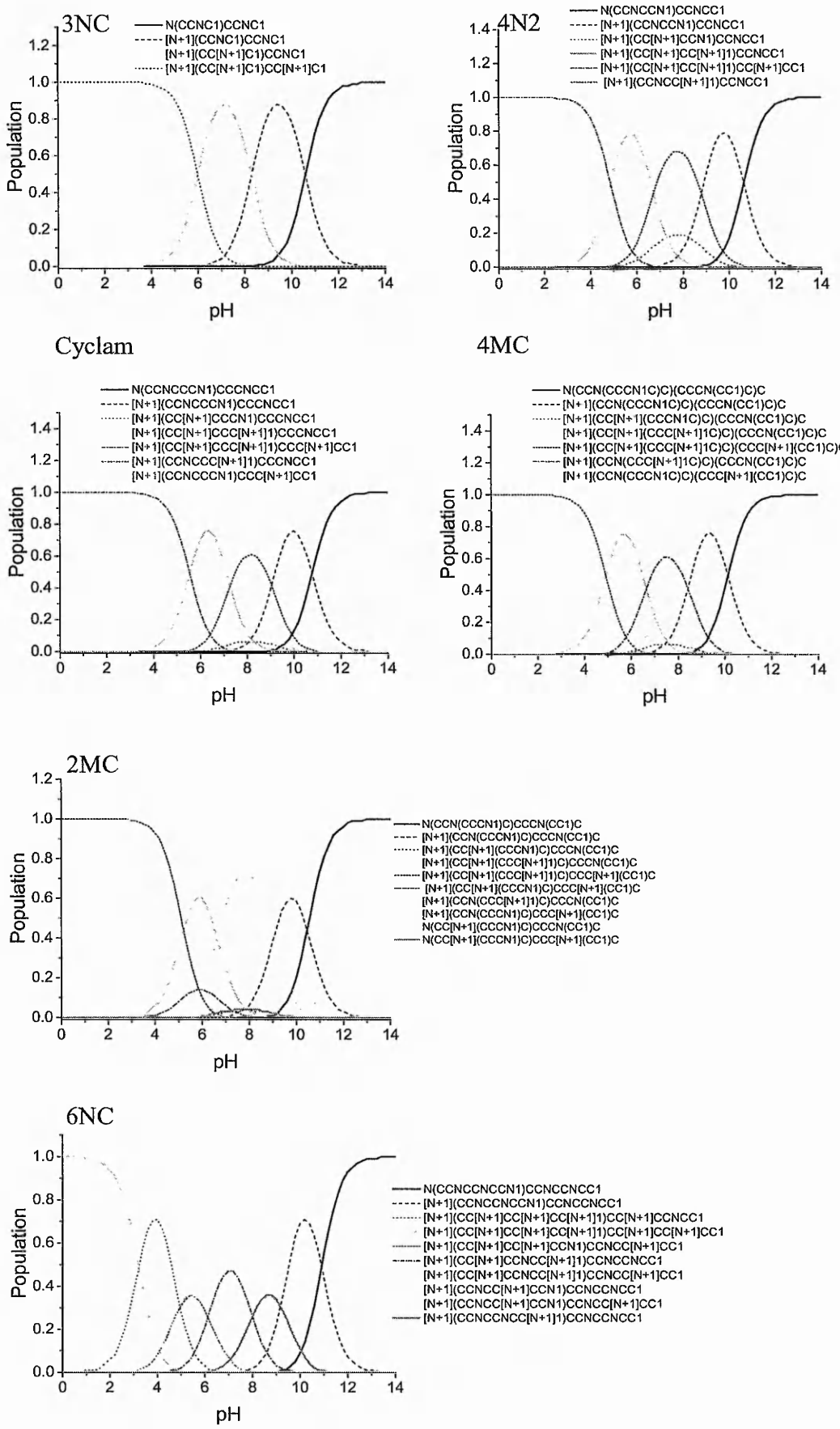

Figure 1 – The speciation diagrams for the azamacrocyclic molecules investigated generated from SPARC[38].

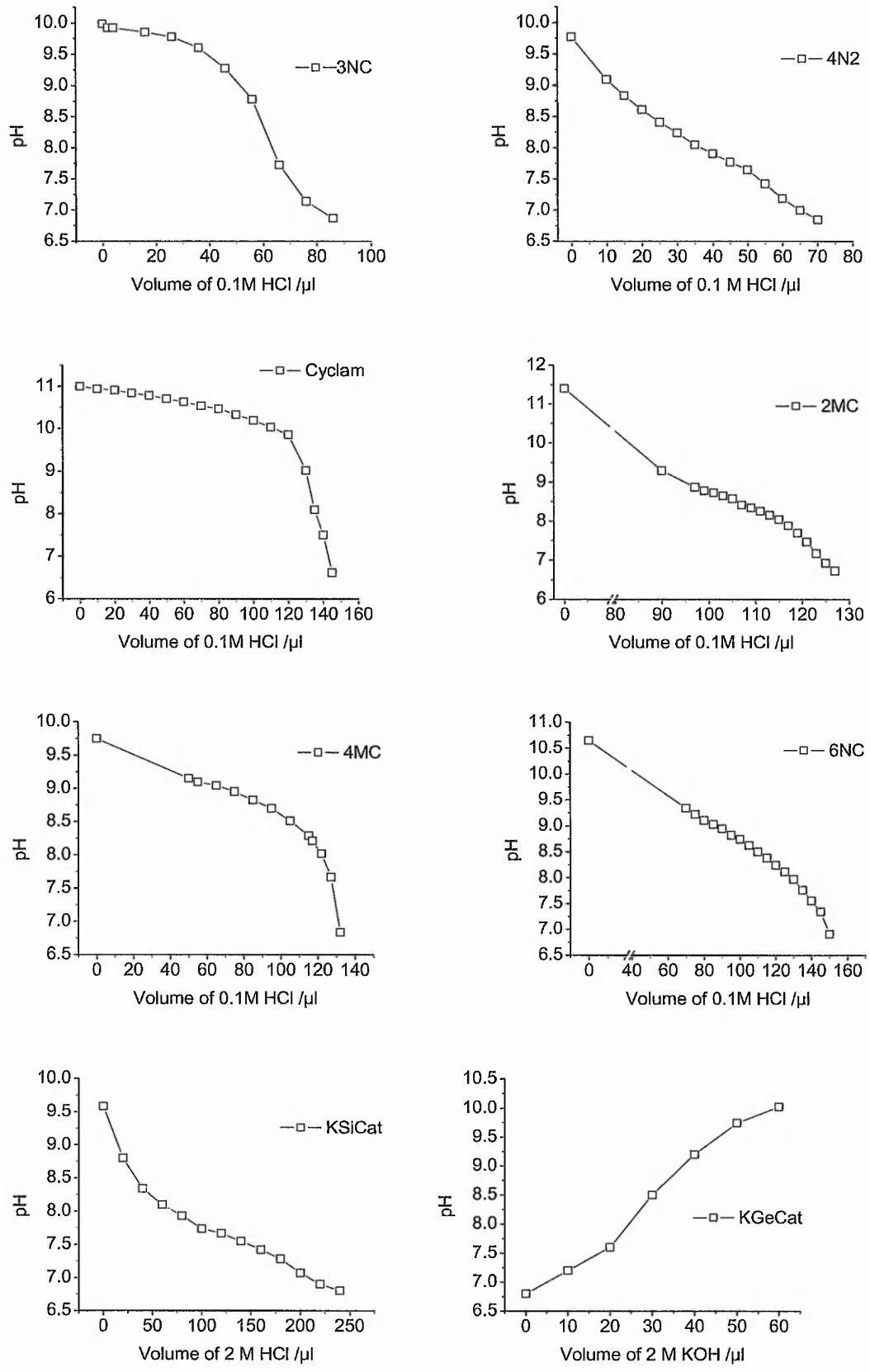

Figure 2 – Titration curves for the azamacrocyclic molecules, KSiCat and KGeCat used to study pH to calculate the amount of acid/base required to achieve the desired pH at a Si/Ge:N ratio 10:1.

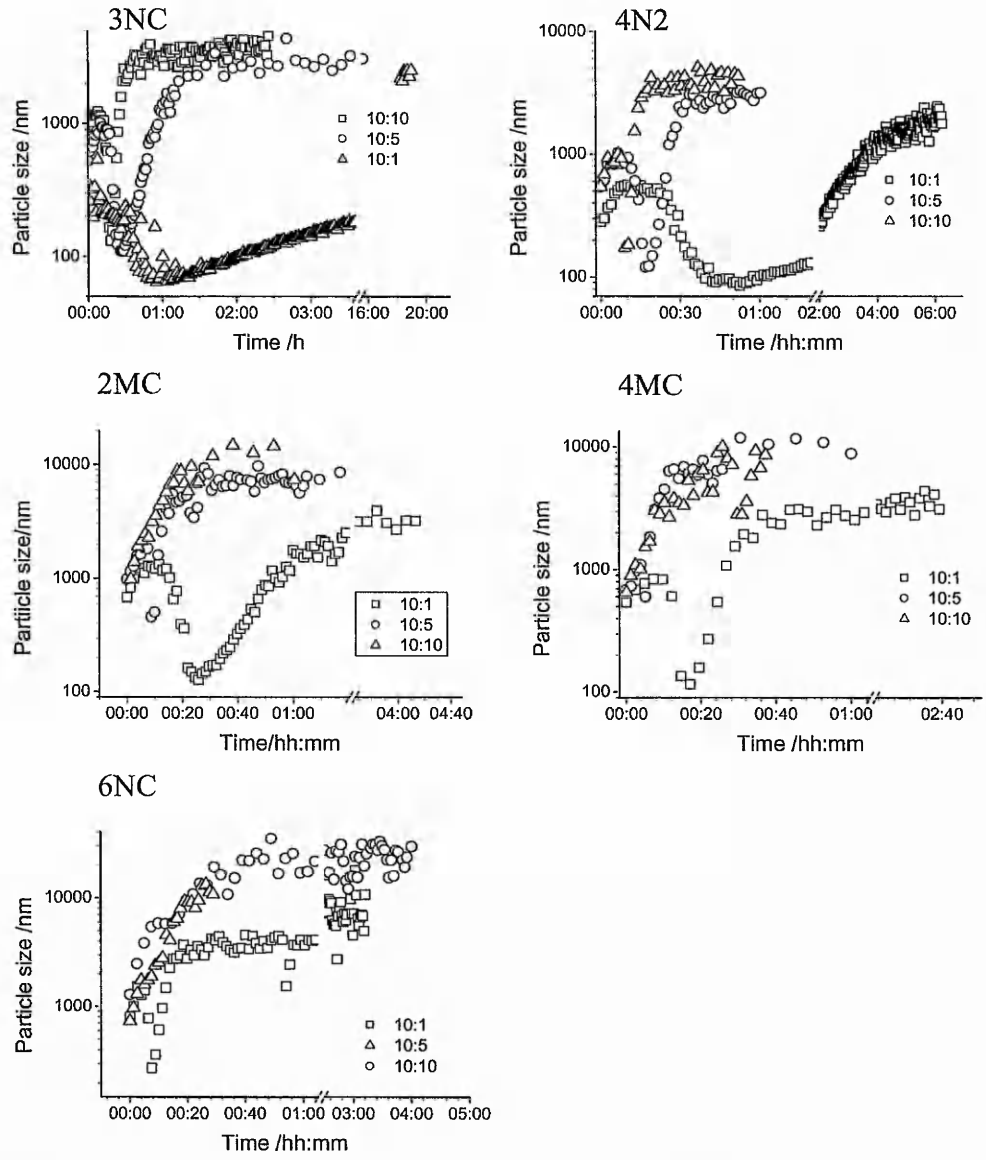

Figure 2 – Dynamic light scattering of azamacrocyclic molecules in KSiCat using the protonated method.

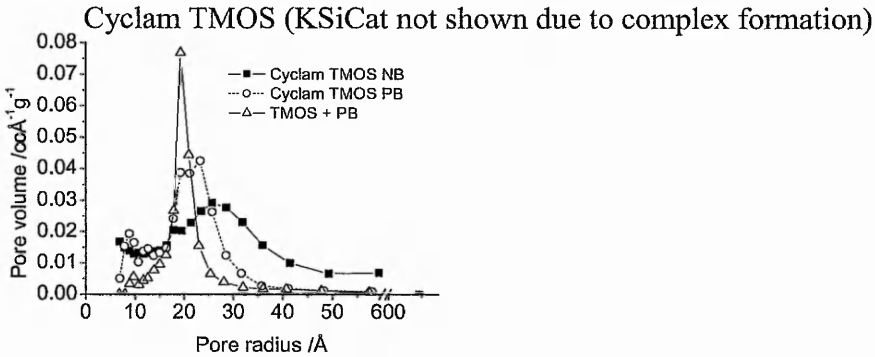

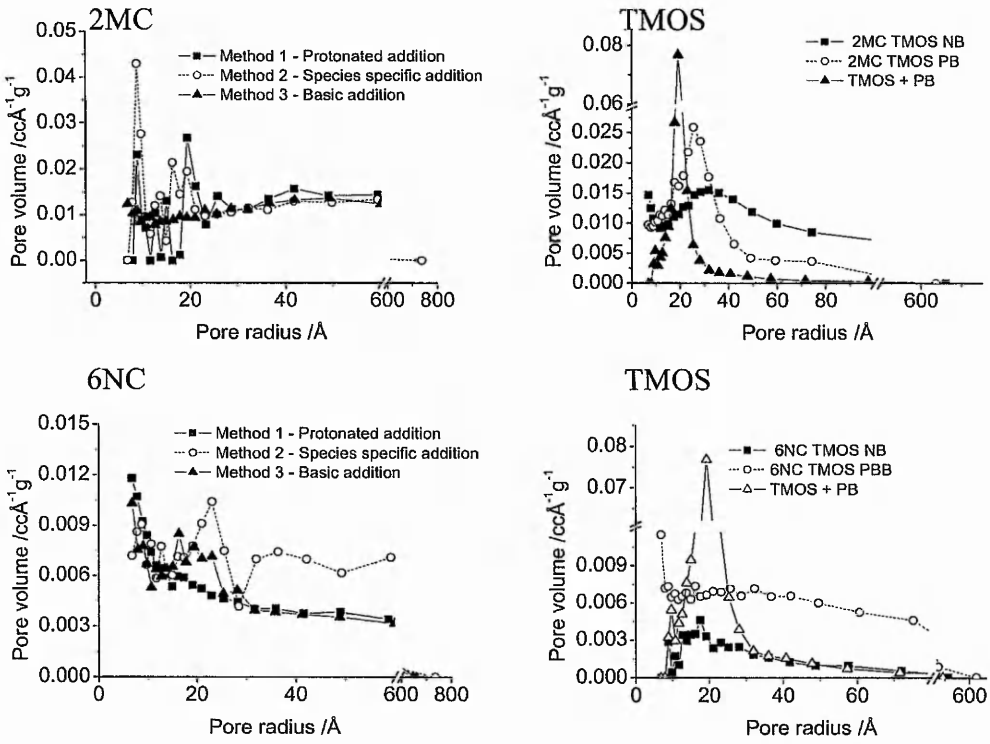

Figure 3 – The porosity data for the remaining azamacrocyclic molecules in the KSiCat system prepared using the 3 different methods of preparation.